Report on the cross border effects of the continuation of lignite mining in Turów (Poland) on water in Germany

Sylwester Kraśnicki, Ph. D.

Summary

This report analyzes the most important trends in the impact on groundwater and surface waters of lignite mining by the Turów opencast mine. The Turów mine is located in south-western Poland, near the border with Germany and the Czech Republic, in the Zittau basin. The mine area is drained by the Nysa Łużycka and its right tributaries, including the Miedzianka. The mining of lignite using the opencast method necessitates the drainage of the coal deposit and of the aquifers present in the overburden. The Turów mine drains the Quaternary aquifer: GWL 1 and the Neogene aquifers: GWL OO, GWL HM, GWL OU, GWL ZiC and GWL ZU. Some of them are connected with the aquifers on the Polish side: Quaternary, Nwg, Nwd, Mw and Pw.

The heaviest impact of the mine on water resources is the depression cone, which developed both in the Quaternary and Neogene aquifers. The depression cone extends beyond the borders of Poland and has a negative impact on water resources in the Czech Republic and Germany. In the German part of the Zittau basin, the depression cone includes the aquifers of GWL ZiC and GWL ZU, in which a continuous lowering of the groundwater table is observed. This trend continued in 2020-2022, which is consistent with the conclusions of the Krupp report (Krupp 2020). Thus, there is a negative impact on the resources of the Groundwater Body DESN_NE 2. The area where such drainage of these aquifers is not observed is the northern part of the city of Zittau and the area between this town and the village of Drausendorf. They are located behind the sealing wall built by the Turów mine in 1997 along the Nysa Łużycka River. On the one hand, it proves the effectiveness of the constructed sealing wall; on the other hand, it indicates its drawback, which is its insufficient length. In order to eliminate groundwater drainage in Germany completely, the sealing wall must be extended at both ends.

Another threat to water resources is acid mining drainage, which causes the oxidation of coal seams and the sulfur they contain. This causes the release of the pollutants such as heavy metals. An increase of the concentrations of sulphates, iron, and manganese and changes in parameters such as total dissolved solids, electrolytic conductivity and pH are also observed. Waters with such a changed chemical composition flow into the mine excavation and are pumped out of it, and after partial pre-treatment, discharged into the surface waters of the Miedzianka and Nysa Łużycka rivers. In the chemical analyzes of the waters of the Nysa Łużycka, an increase in the concentrations of sulphates and calcium, as well as an increase in the electrolytic conductivity below the discharge of underground waters from the Turów mine to Nysa Łużycka, is visible. Underground waters additionally deteriorate the chemical status of the waters of the Nysa Łużycka.

Introduction

The Turów lignite mine is located in the Bogatynia commune of the Lower Silesia Voivodship near the border with the Czech Republic and Germany. Exploitation of lignite near Bogatynia was started using the underground method in the first half of the 18th century and the open-cast method in 1904. The average annual lignite exploitation from this deposit in the years 2011-2021 was about 8,3 million tons, but in recent years the output has been declining. Geological resources of this deposit at the end of 2021 amounted to approximately 299,9 million tons, and industrial resources to approximately 270,8 million tons and they allow for the continuation of exploitation until 2044. For this purpose, the exploitation of the south-eastern part of the deposit in the area of Opolno Zdrój is started under the prolonged license (Badura, Cymerman 2009a and b, Badura, Cymerman 2016, PIG-PIB 2021).

This report aims to analyze the negative impacts of the exploitation of the deposit on water resources in the adjacent area of Germany. The subject of the survey will be the impact of the Turów mine on the quantitative status of surface and groundwater bodies, as well as its impact on their quality status. All aquifers in the German part of the Zittau basin will be analyzed. The basic methodology is is the GIS analysis. The Geographic Information System (GIS) analysis is widely applied to illustrate different issues on maps. In this review the analysis concentrated on overlaying layers with different sorts of information: topography, hydrology (rivers, springs, watershed), hydrogeology (aquifers), functioning investment (the mine and its drainage area) and its monitoring system of hydrological wells and points of collecting samples of surface water. The overlaying helped to make maps illustrating extent of the impact of the Turów mine on groundwater and surface water. The supplementary method is a diagram analysis used to assess the trends of the drainage effects and the impact o pollutants release to surface water.

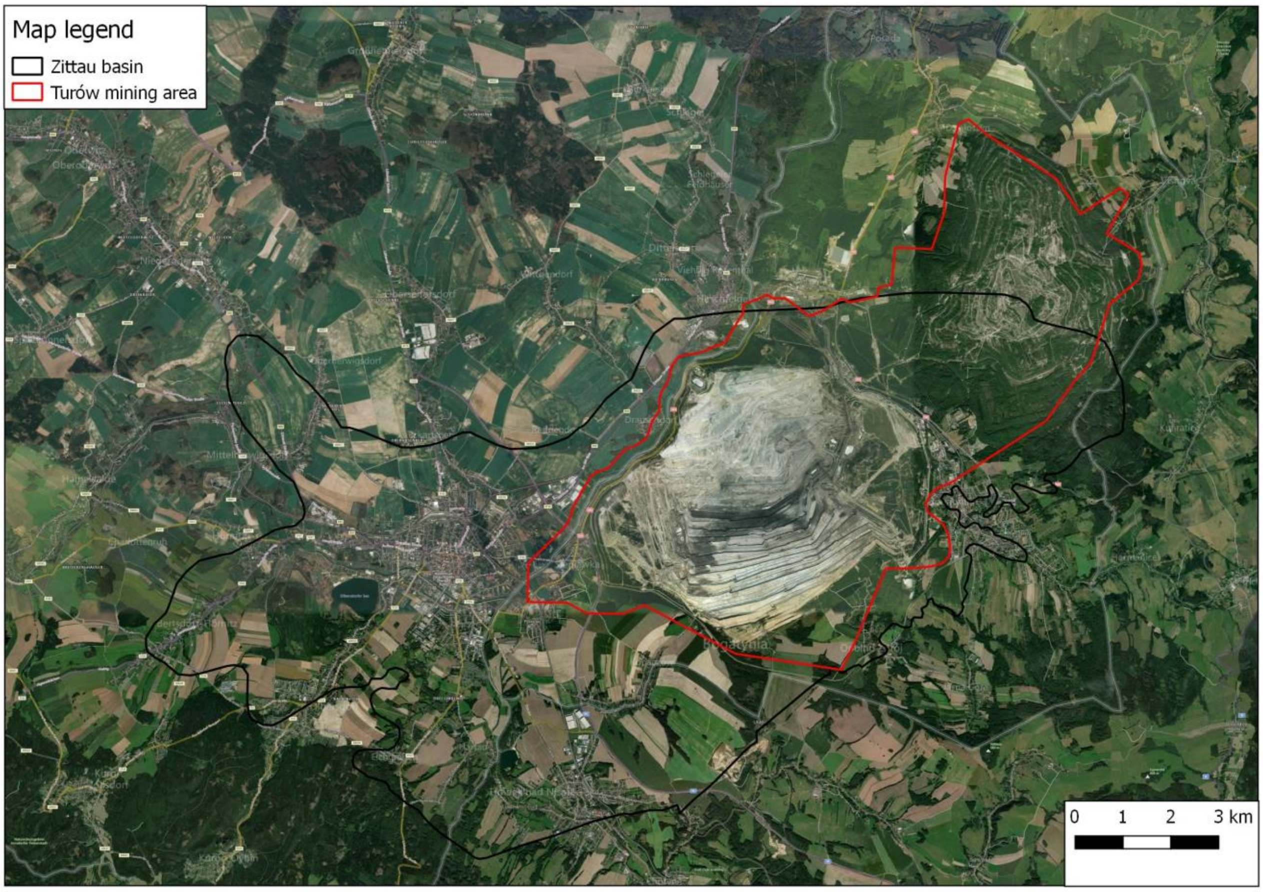

Fig. 1. Location of the Turów lignite mine in the Zittau basin.

Geologic settings

The open pit lignite mine Turów is located within the Zittau basin divided between three countries: Czech Republic, Poland and Germany. The base of this tectonic basin is composed mainly of crystalline rocks: granitoids, gneisses, greywack sandstones, sericite-quartzite slates and phyllites. The entire rock complex is cut locally by diabase and quartz veins. During the Variscan orogeny in the Carboniferous faults were formed distinguishing the Zittau basin and the horsts of Działoszyn, Opolno Zdrój and Markocice (Badura, Cymerman 2009a and b, Badura, Cymerman 2016).

The bottom of the Zittau basin is filled with the Cenozoic sediments with a thickness of up to 400 m north of Hrádek nad Nisou. The oldest are the dusty clays - regoliths of the Eocene-Oligocene age. There are effusive rocks of similar age: basalts, trachytes and their tuffs. While basalts occur both in the basin and in its surroundings, trachites occur only south of it (Badura, Cymerman 2009a and b, Badura, Cymerman 2016, Kasiński et al 2015).

In the Zittau basin, the lower and middle Miocene deposits are covered with lignite. These are: conglomerates, silts and clays of the lower Miocene, and middle Miocene loam with gravel. They form 4-5 sedimentation cycles. The lignite exploited by the mine is located on the sediments of the following cycles: the second (seam I) and the fourth (seam II). Coal seams occur in both fragments of the Zittau basin. The gravels of the Upper Miocene do not contain lignite (Badura, Cymerman 2009a and b, Badura, Cymerman 2016).

In the area of interest, the Pleistocene sediments cover the older ones only partially. The Mindel and Riss glaciations sediments are glacial till and glaciofluvial sands. The Würm glaciation left loesses and river terraces, 5-7 meters above the present river level. The youngest Holocene sediments include alluvial sands, gravels and silts of the floodplain terraces 0.5-1.5 meters above the present river level and of the valley bottoms (Badura, Cymerman 2009a and b, Badura, Cymerman 2016).

Hydrogeologic and hydrologic settings

The following aquifers are distinguished in the area. The aquifers of the German part of the Zittau basin are illustrated in Figure 2 (Dziedziak, Woźniak 2002a and b, Fiszer, Sadowska 2019, Krupp 2020):

1. Proterozoic-paleozoic. groundwater occur within the cracks and faults of crystalline rocks. Its utility as water resource is low due to poor filtration coefficient values. Mineral waters were found in this aquifer. In the health resort of Opolno-Zdrój ferrous waters of the sulfate-calcium-magnesium type occur with an increased content of carbon dioxide (10-130 mg/dm^3) and iron (up to 25 mg/dm^3). Within the KWB Turów opencast there is an outflow of mineral water from the fault gap. These are bicarbonate-sodium waters with mineralization of 4.2 g/dm^3 and temperature 24-27 ° C (Dowgiałło, Fistek 2007).

2. Paleogene-Neogene. Groundwaters are found within sands and gravels, occurring as interbedding among clays and silts. There are aquifers: under coal seam (podwęglowy - Pw), between coal seams (międzywęglowy - Mw), overburden lower (nadkładowy dolny - Nd), overburden upper (nadkładowy góny - Ng). The thickness of the aquifer of this complex is from a few to more than a hundred meters. The water table is confined. Groundwater is fresh and slightly acidic, with mineralization up to 500 mg/dm3. In the German part of the Zittau basin, there are other aquifers: Zittauer Unterflöz (GWL ZU), Zittau C (GWL ZiC), Oberflöz-Unterbank (GWL OU), Hauptmittel (GWL HM), Oberflöz-Oberbank (GWL OO). The aquifers of the Polish and German parts of the Zittau basin

correlate with each other. The podwęglowy aquifer correlates with Zittauer Unterflöz, międzywęglowy with Zittau C, nadwęglowy dolny with Oberflöz-Unterbank and nadwęglowy górny with Oberflöz-Oberbank.

3. Quaternary (Q). The aquifer consists of sands and gravel, and the groundwater table is unconfined or slightly confined. Its thickness varies from a few to 20 meters. The filtration coefficient is usually 5-25 m/d but sometimes exceeds 100 m/d (Staśko, Michniewicz 2007). The groundwater is freshwater, with hardness from medium-hard to hard and slightly acidic. Sometimes its mineralization may exceed 1000 mg/dm3. This aquifer is correlated with Grundwasserleiter 1 (GWL 1) in Germany.

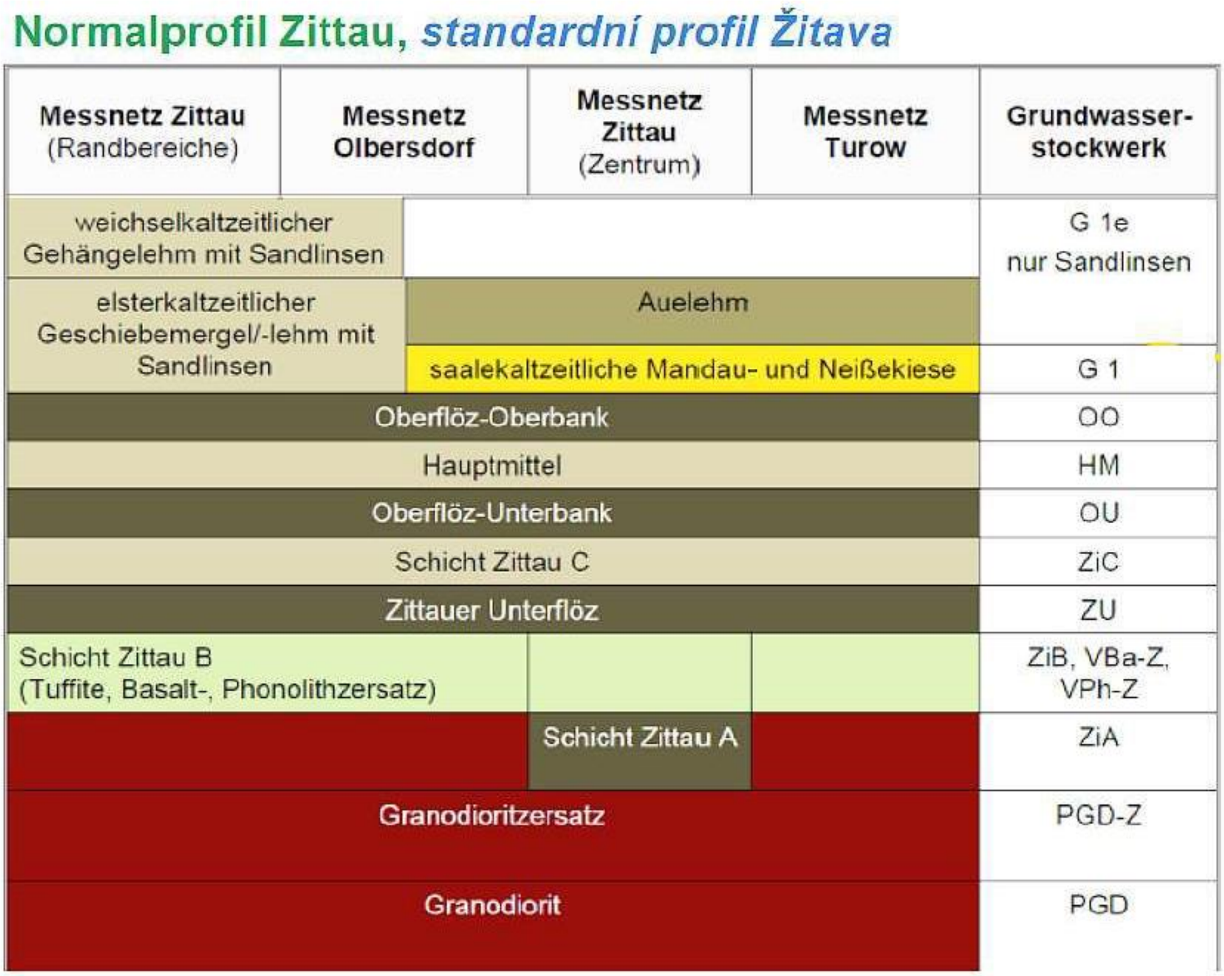

Fig. 2. The aquifers of the German part of the Zittau basin (Börke 2018).

The Grounwater Bodies of this area of are also divided by the three countires: Czech Republic, Poland and Germany. In Poland where the Turów mine is located the area belongs to the Groundwater Body PLGW6000105 with an area of 332.8 km^2 and covering the Polish part of the upper Nysa Łużycka catchment. Its quantitative status was described as bad due to the drainage by Turów mine. According to the Water Framework Directive, the achievement of a good quantitative status was identified as endangered. On the other hand, its chemical state was defined as good and achieving the goal (good chemical status) is not compromised. In Germany the adjacent area belongs to the Groundwater Body DESN_NE 2 with an area of 507,8 km^2. Its quantitative and chemical status is assessed as good.

According to the hydrographic division, the mine area is entirely located within the Nysa Łużycka catchment and its right tributaries: Miedzianka and Nowa Biedrzychówka. In addition, the Turów opencast mine has its own catchment of anthropogenic origin. The German part of Zittau basin also belongs to the Nysa Łużycka catchment and its tributaries: Mandau, Pfaffenbach Hartau, Eichgrabener Pfaffenbach, Eckartsbach and Wittgendorfer Wasser. The surface water bodies are described in the Table 1.

Table 1. Ecological and chemical status od surface water bodies in Polish and German part of Zittau basin (BFG 2022, ISOK 2022).

Water body name	**Water body number in Poland and Germany**	**Length [km]**	**Current and final ecological status**	**Current and final chemical status**
Lausitzer Neisse-3	DERW_DESN_674-3	2,45	Bad Good after 2027	Not good Good after 2045
Nysa Łużycka from Mandau to Miedzianka	PLRW60008174159 DERW_DESN_674-4	8,45	Poor Good	Not good Good
Miedzianka from state border to Nysa Łużycka	PLRW60004174169	18,36	Poor Good	Good Good
The inflow from the Turoszów excavation	PLRW60000174156	2,52	Bad Good	Not good Good
Nysa Łużycka from Miedzianka to Pliessnitz	PLRW60001017431 DERW_DESN_674-5	21,08	Moderate Good	Good Good
Pfaffenbach Hartau	DERW_DESN_674132	5,4	Moderate Good after 2027	Not good Good after 2045
Mandau-3	DERW_DESN_67414-3	5,07	Poor Good after 2027	Not good Good after 2045
Goldbach	DERW_DESN_674148	9,27	Poor Good after 2027	Not good Good after 2045
Eckartsbach	DERW_DESN_674154	9,13	Bad Good after 2027	Not good Good after 2045
Wittgendorfer Wasser	DERW_DESN_674158	6,32	Poor Good after 2027	Not good Good after 2045

The Turów mine impact groundwater and surface water

Groundwater monitoring results

The groundwater table in the German part of the Zittau basin has been observed in 57 hydrogeological wells (piezometers, wells and hydrogeological nodes) since 1986 in all aquifers described above (LULGS 2022). In relation to this network of monitoring points, observations are also carried out in the Polish part of the Zittau basin in 38 hydrogeological wells located along the Nysa Łużycka River. Their distribution is shown on the map (Fig.2).

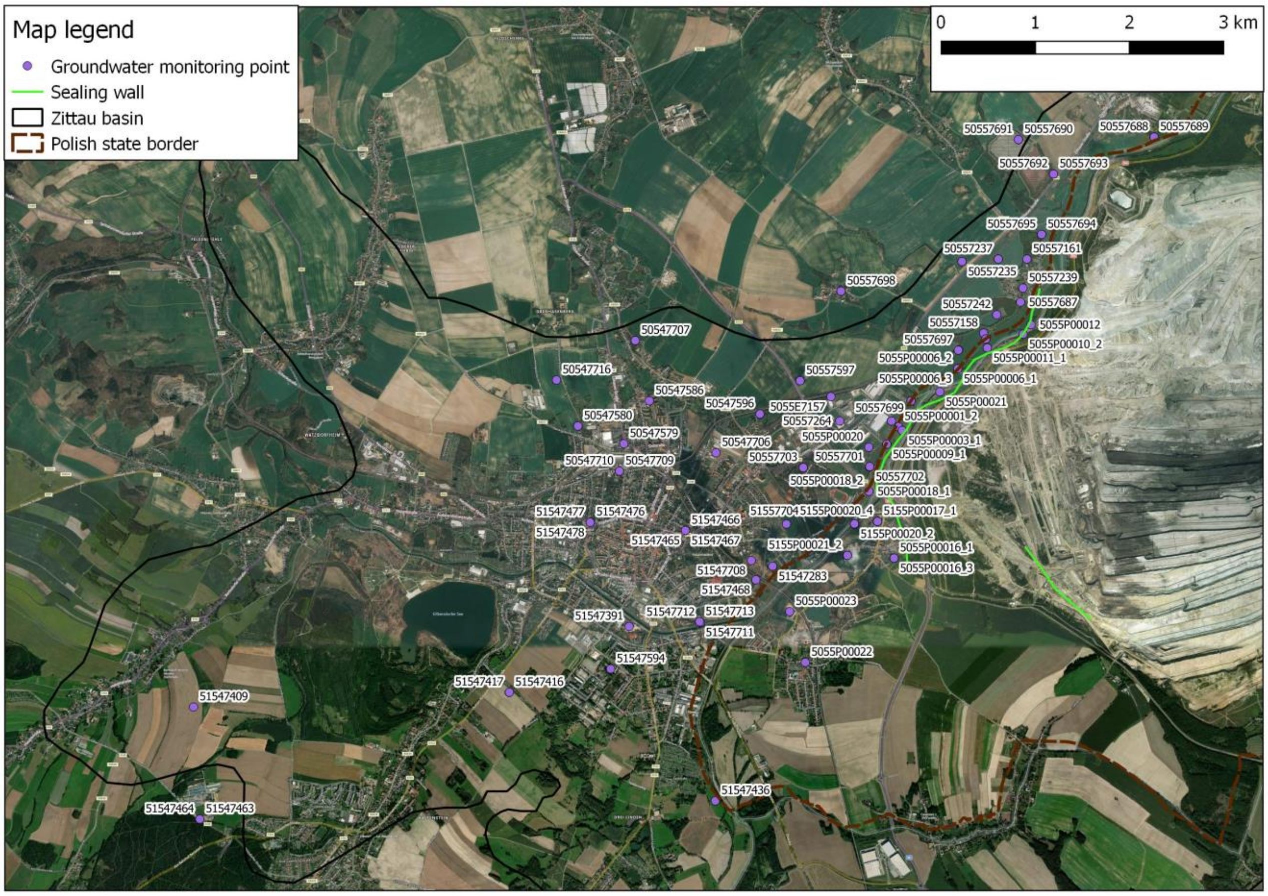

Fig. 2. Location of the groundwater wells monitoring the Zittau basin aquifers.

The number of hydrogeological wells in each aquifer is presented in the Table 2 Three hydrogeological wells monitor two aquifers each. The well No. 5055P00003_1 monitors the GWL 1 and GWL OO aquifers, the well No. 50557698 monitors the GWL ZiB and GWL VBaZ aquifers, and the well No. 5055P00012 monitors the GWL ZiA and GWL PGDZ aquifers.

Table 2. Amount of groundwater wells monitoring each aquifer.

Aquifer	**Amount of monitoring wells**
GWL 1e	1
GWL 1	20
GWL1+OO	1
GWL OO	21
GWL HM	6
GWL OU	12
GWL ZiC	21
GWL ZU	9
GWL ZiB+VBaZ	1
GWL VBaZ	1
GWL ZiA+PGDZ	1
GWL PGDZ	1

The monitoring results of the groundwater table are presented in this report from the shallowest to the deepest aquifers. The aquifers monitored by one borehole are described at the end in a separate subsection. Graphs of the position of the groundwater table in all of the monitoring points mentioned are presented in Annex 1.

Aquifer GWL 1

The above map shows that most of the monitoring points are located in the Nysa Łużycka valley (Fig 3.).

Fig. 3. Location of the groundwater wells monitoring the GWL 1 aquifer.

The amplitude of groundwater table fluctuations throughout the observation period was 1.5-50 meters, and in the period 2020-2022, it was 0.25-8 m. If in 2020-2022, a water table changes its position by at least 1 meter, the change can be considered an important trend. In three hydrogeological wells (50557158, 50557161 and 5055P00011_1), the groundwater table rise by more than 1 meter was observed (Fig.4).

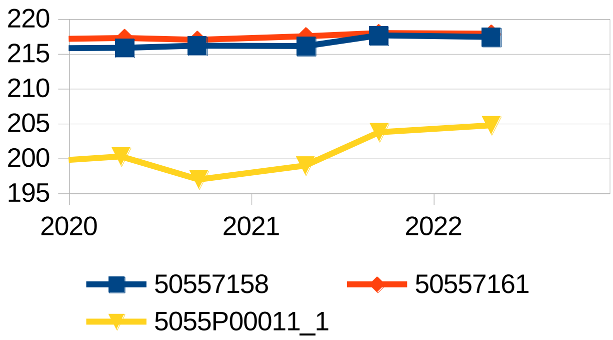

Fig. 4. The water table rise in the monitoring wells no.: 50557158, 50557161 and 5055P00011_1.

No groundwater table drop was observed in any of the boreholes. In the remaining 17 wells, no significant trend of changing the position of the groundwater table was observed (Fig 5) or this trend was ambiguous, and there was observed its rise and drop (Fig 6).

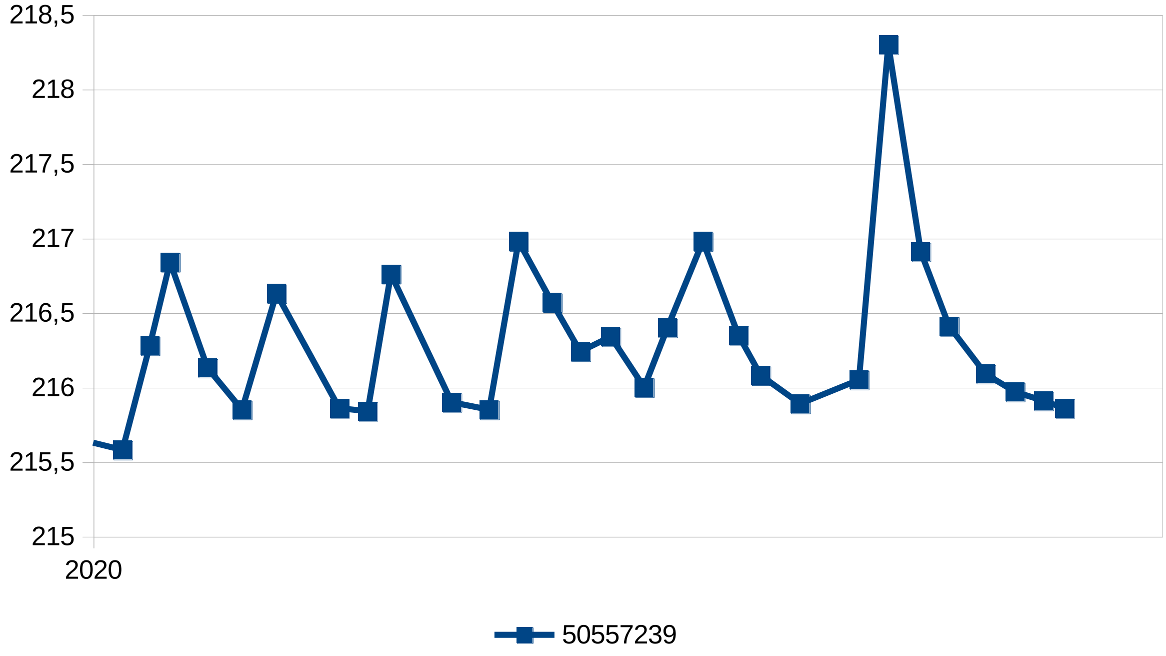

Fig. 5. The water table changes in the monitoring well No. 50557239.

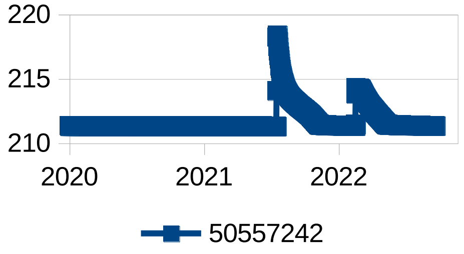

Fig. 6. The water table changes in the monitoring well No. 50557242.

Aquifer GWL OO

The location of the hydrogeological monitoring points for the GWL OO aquifer is illustrated on the map (Fig.7).

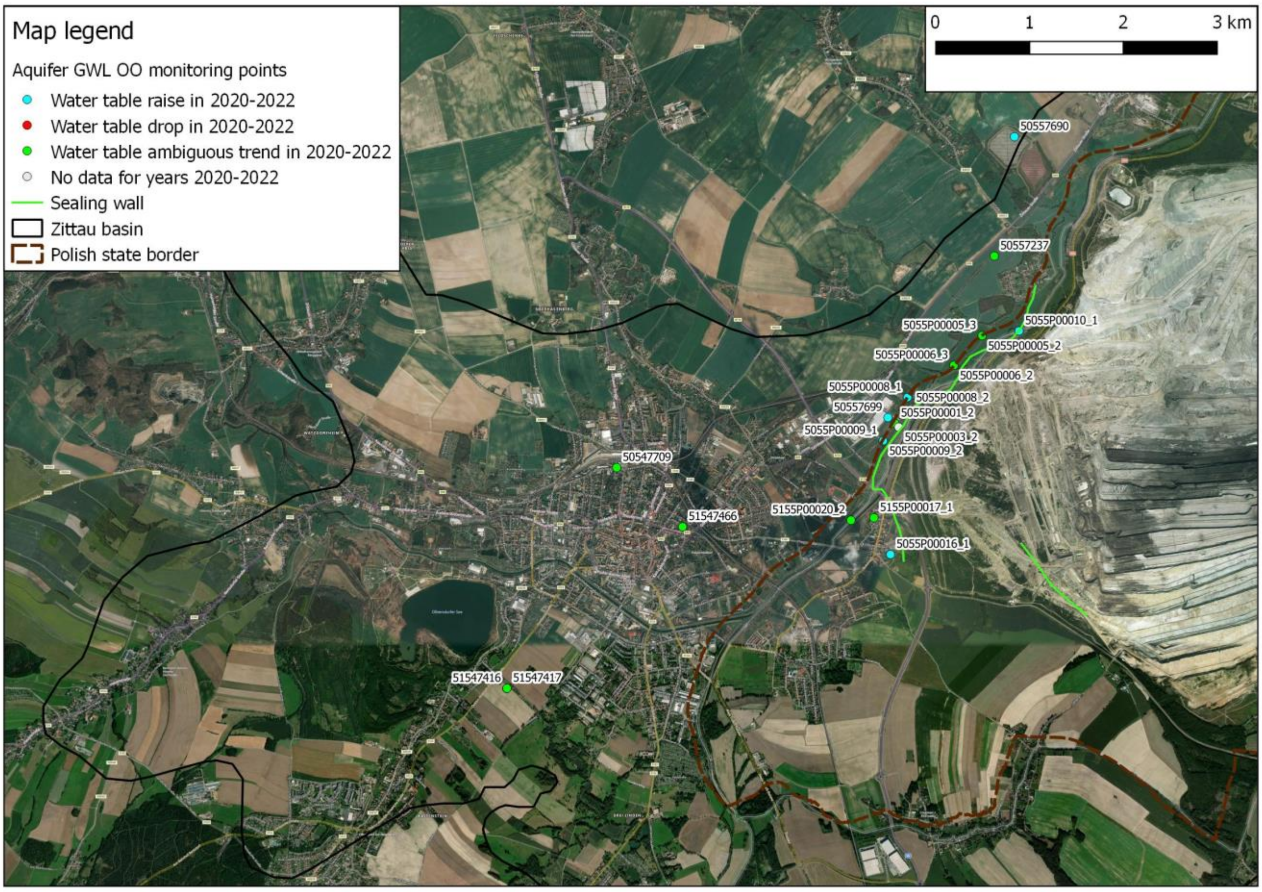

Fig. 7. Location of the groundwater wells monitoring the GWL OO aquifer.

Most of the monitoring points are located in the Nysa Łużycka valley, but several points are located in other parts of the described area. The amplitude of water table fluctuations during the entire observation period was 2.5-30 meters, and in the years 2020-2022, it was 0.2-15 m. In many points, a large rise of the water table is observed throughout the entire observation period. In the period 2020-2022, the rise of the groundwater table by more than 1 meter was observed in 7 hydrogeological wells (Fig.8).

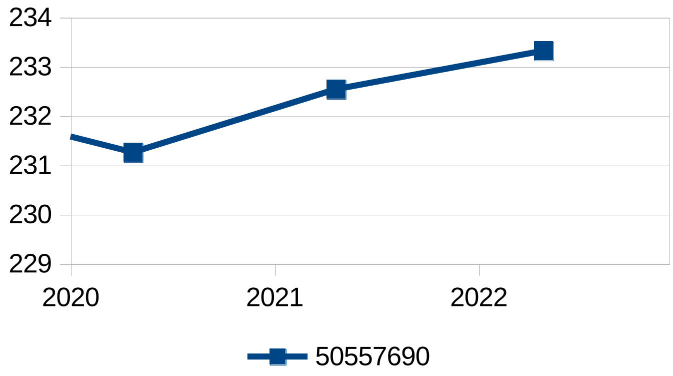

Fig. 8. The water table changes in the monitoring well No. 50557690.

The groundwater table drop was observed in well no. 5055P00008_1. In this well, the groundwater table rise was also observed throughout the observation period, and its drop was observed in 2021. In this hydrogeological node, there are three wells (5055P00008_1, 5055P00008_2 and 5055P00008_3), of which only in the first one the lowering of the groundwater table was observed. The well 5055P00008_2 monitors another groundwater layer in this aquifer, but this, in turn, has experienced a groundwater table rise.

On the other hand, the well 5055P00008_3 monitors the aquifer GWL OU, and there the trends were ambiguous in 2020-2022. In this situation, it is difficult at present to ascribe the lowering of the groundwater table in the borehole 5055P00008_1 to the drainage of the lignite deposit exploited by the Turów mine since, in the remaining two wells, such drop is not observed, but its observations should be continued (Fig.9 -11). According to the author of the report, the reason may be a leakage of the insulating layer built of clays between the wells 5055P00008_1 and 5055P00008_2 because, at the same time, in the second well, the groundwater table rises.

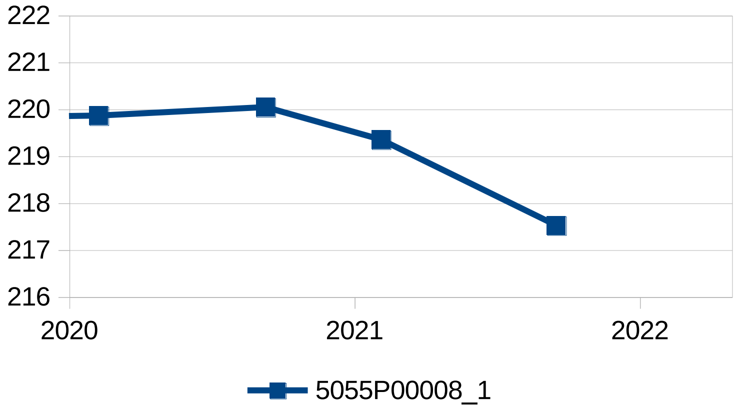

Fig. 9. The water table changes in the monitoring well No. 5055P00008_1.

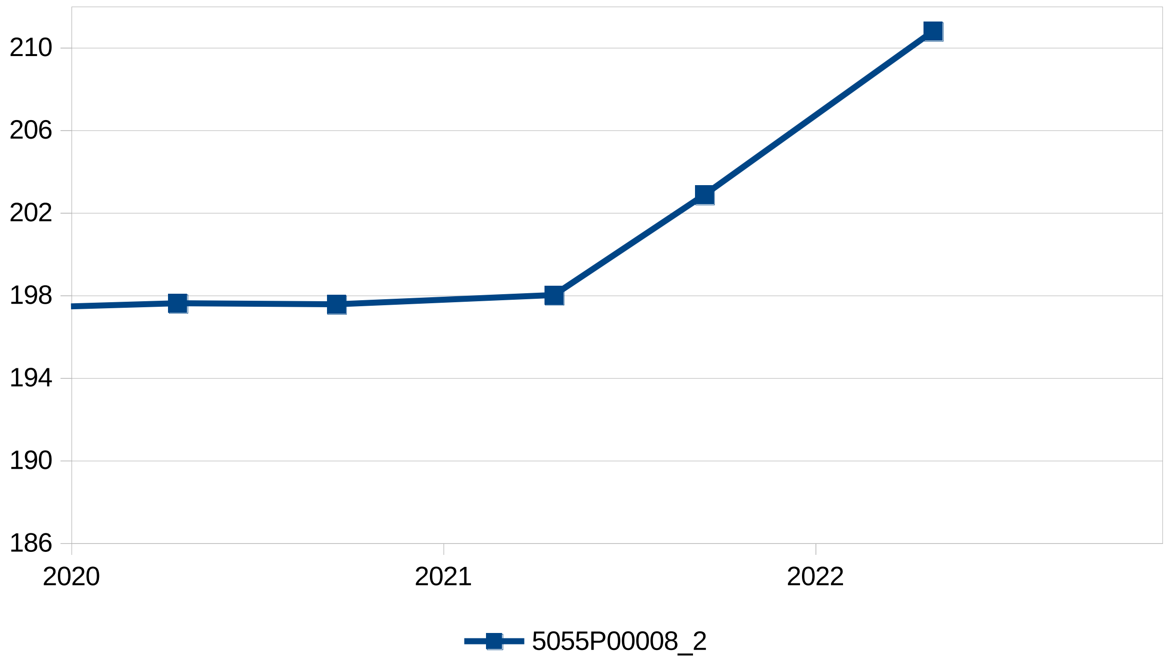

Fig. 10. The water table changes in the monitoring well No. 5055P00008_2.

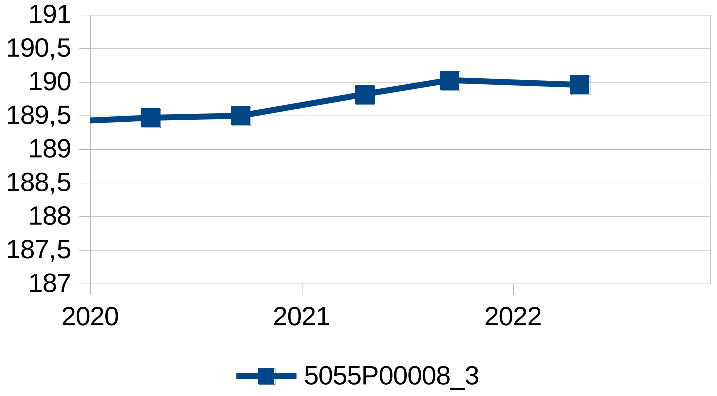

Fig. 11. The water table changes in the monitoring well No. 5055P00008_3.

In the remaining boreholes, no significant trend of changing the position of the groundwater table was observed (Fig. 12) Or this trend was ambiguous, and there was a rise and drop of the groundwater table (Fig. 13).

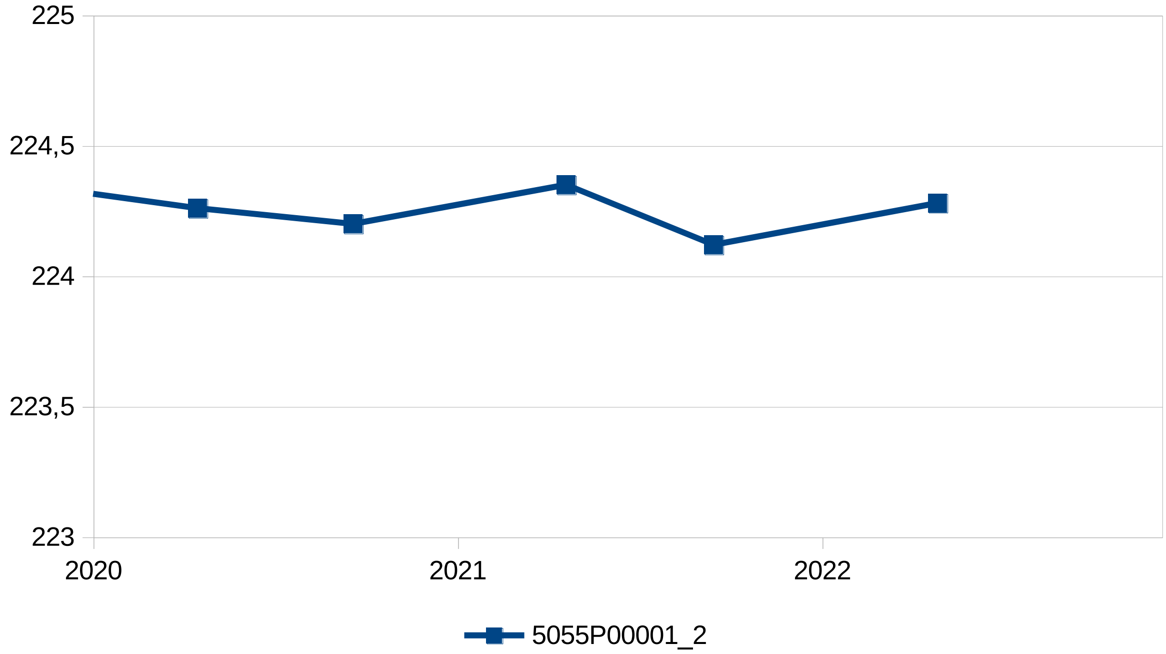

Fig. 12. The water table changes in the monitoring well No. 5055P00001_2.

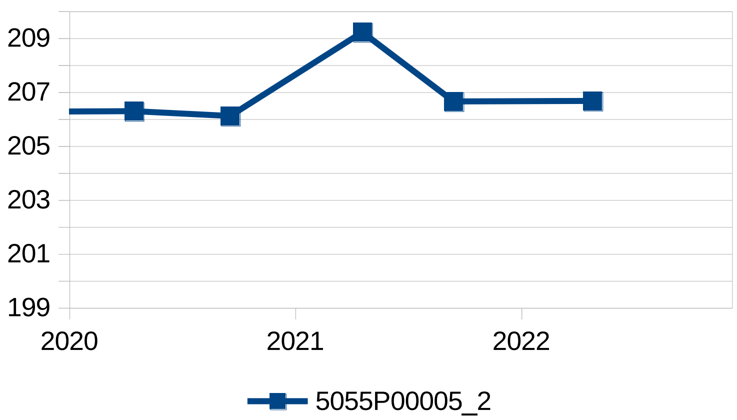

Fig. 13. The water table changes in the monitoring well No. 5055P00005_2.

Aquifer GWL HM

The location of the hydrogeological monitoring points of the HM aquifer GWL is illustrated on the map (Fig. 14).

Fig. 14. Location of the groundwater wells monitoring the GWL HM aquifer.

Most of the monitoring points are located in the Nysa Łużycka valley on the Polish side. The amplitude of the groundwater table fluctuations throughout the observation period was 2-20 meters, and in the years 2020-2022, it was 0.2-3.5 m. In the period 2020-2022, only in the hydrogeological well No. 5055P00016_2, the groundwater table rise by more than 1 meter was observed (Fig. 15). No groundwater table drop was observed in this aquifer.

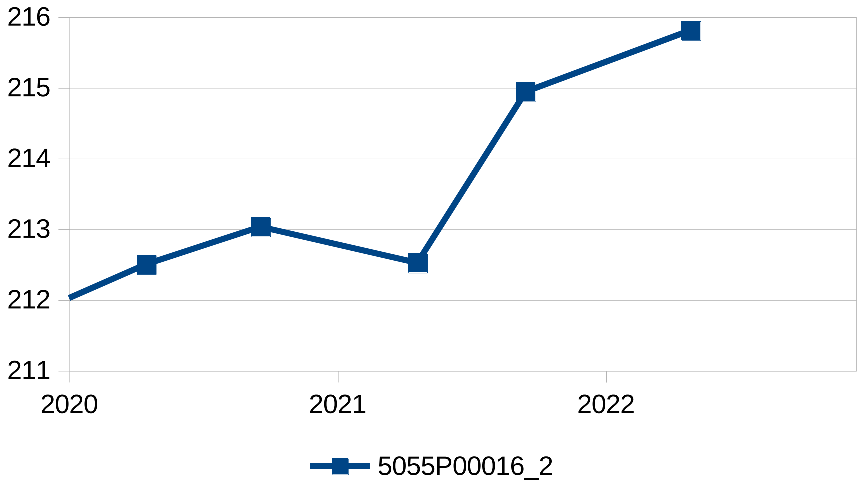

Fig. 15. The water table changes in the monitoring well No. 5055P00016_2.

In the remaining wells, no significant trend of changing the position of the groundwater table was observed (Fig. 16).

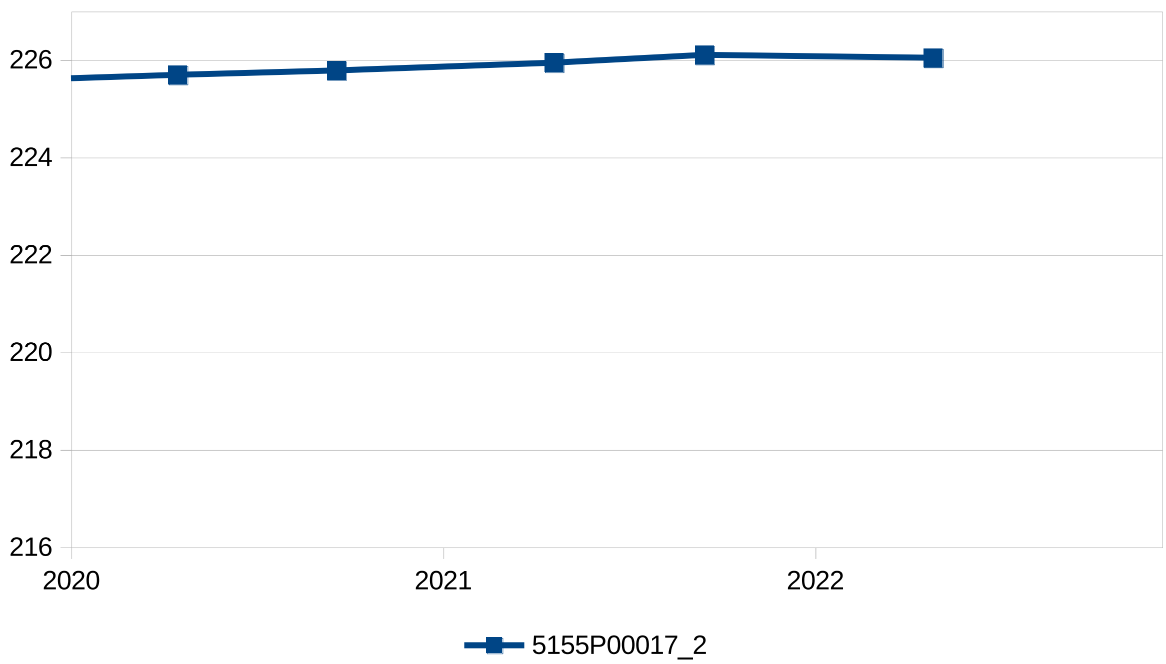

Fig. 16. The water table changes in the monitoring well No. 5155P00017_2.

Aquifer GWL OU

The location of the hydrogeological monitoring points for the GWL OU aquifer is illustrated on the map (Fig. 17).

Fig. 17. Location of the groundwater wells monitoring the GWL OU aquifer.

Most of the monitoring points are located in the Nysa Łużycka valley. The amplitude of groundwater table fluctuations throughout the observation period was 4.5-50 meters, and in the years 2020-2022, it was 0.2-45 m. A record-high groundwater table rise took place in well no. 50547579 in 2021, reaching maximum values throughout the entire observation period. (Fig.18) In the period 2020-2022, the rise of the groundwater table by more than 1 meter was observed in 5 hydrogeological wells (Fig.19). No groundwater table drop was observed at this aquifer.

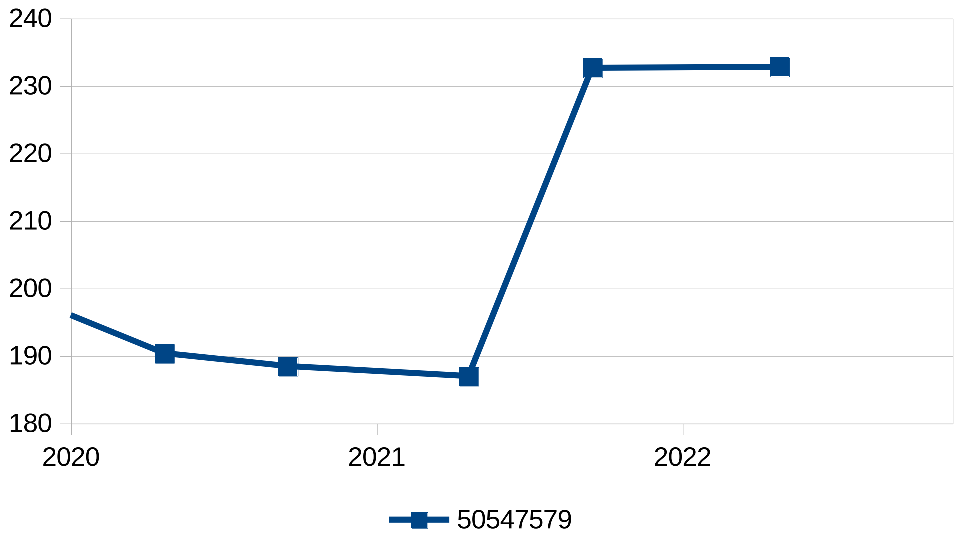

Fig. 18. The water table changes in the monitoring well No. 50547579.

In the remaining wells, no significant trend of changing the position of the groundwater table was observed or this trend was ambiguous, and there was a rise and drop of the groundwater table (Fig. 19).

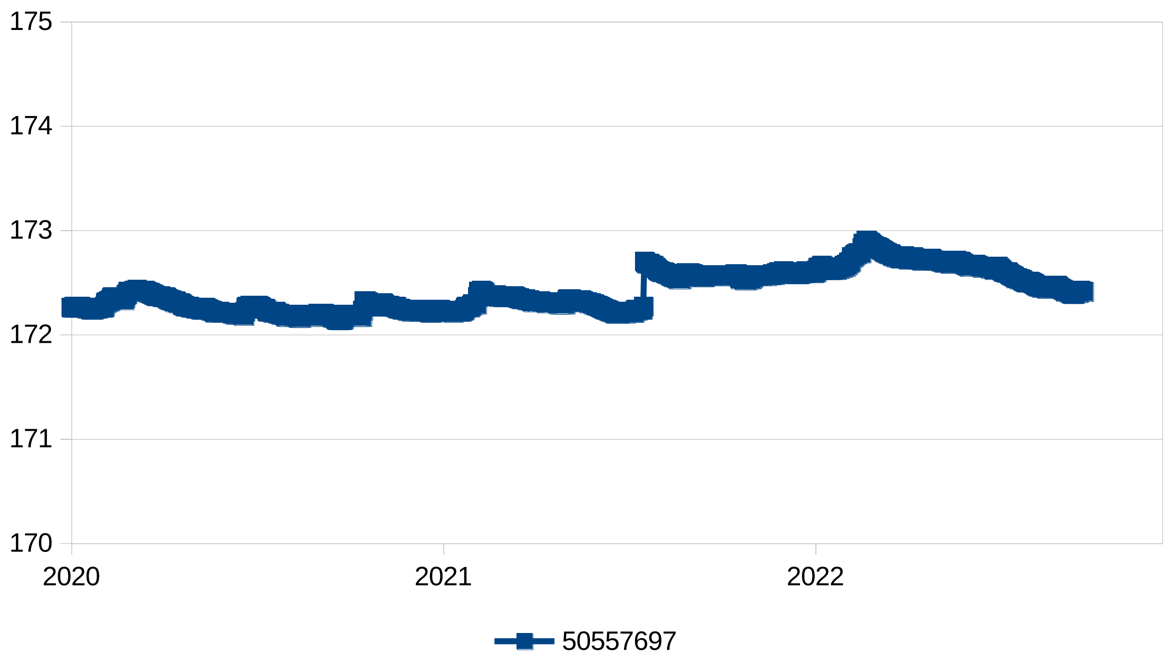

Fig. 19. The water table changes in the monitoring well No. 50557697.

Aquifer GWL ZiC

The location of the hydrogeological monitoring points for the aquifer ZiC aquifer is illustrated on the map (Fig. 20).

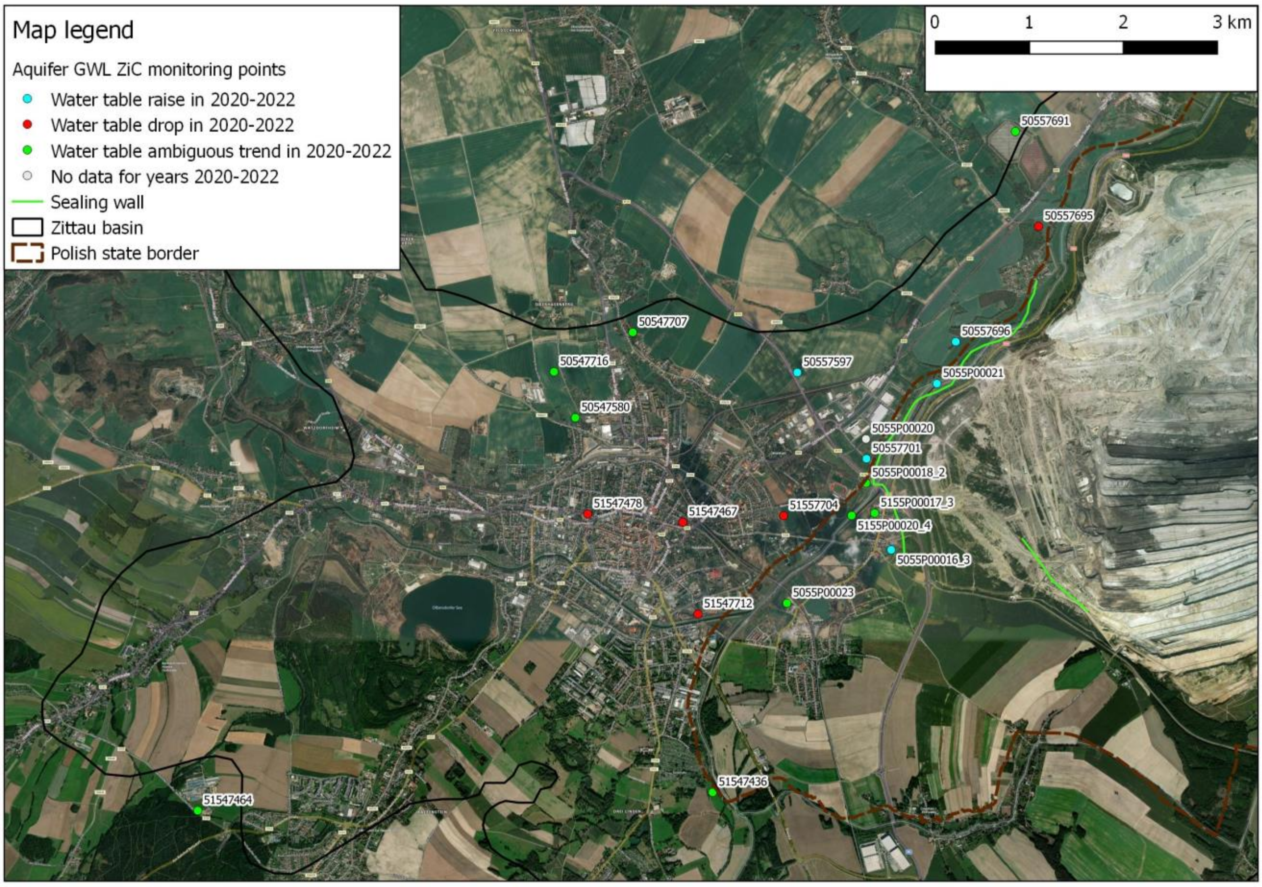

Fig. 20. Location of the groundwater wells monitoring the GWL ZiC aquifer.

Most of the monitoring wells are located in the Nysa Łużycka valley, but numerous wells are also located in the area of the town Zittau. The amplitude of groundwater table fluctuations throughout the observation period was 2.5-75 meters, and in the years 2020-2022, it was 0.3-18 m reaching minimal values over the entire observation period. (Fig. 21). In the period 2020-2022, the rise of the groundwater table by more than 1 meter was observed in 5 hydrogeological wells (Fig. 22).

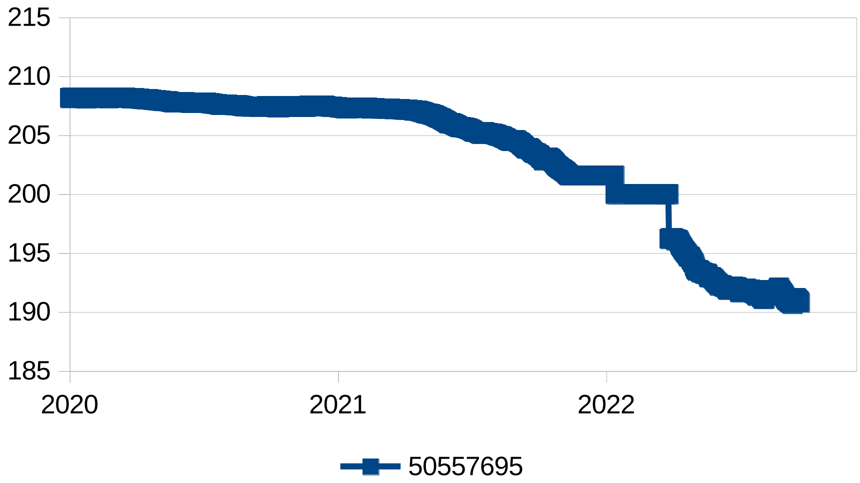

Fig. 21. The water table changes in the monitoring well No. 50557695.

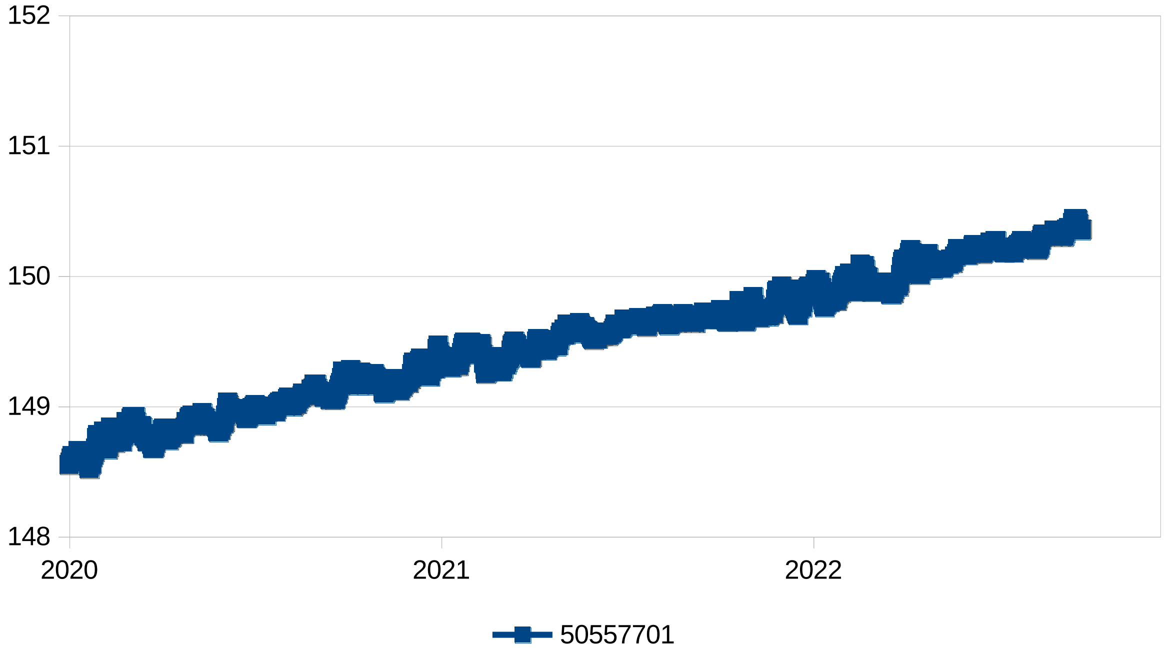

Fig. 22. The water table changes in the monitoring well No. 50557701.

On the other hand, in 5 hydrogeological wells, a groundwater table drop was observed. One of them is located in the village of Drausendorf, and the rest in Zittau. Therefore, the unfavourable trends described in the Krupp report (Krupp 2020) continue. Hydrogeological wells in which the groundwater table rises are located between those in which it is dropped and behind the sealing wall built by KWB Turów in 1997 between Nysa Łużycka and the border of the opencast mine (Fiszer, Sadowska 2019). Thus, the groundwater monitoring points in this area confirm that the sealing wall prevents further drainage of this aquifer. However, since there is a further decline in the groundwater table of this level in the Zittau and Drausendorf areas, it may mean that the sealing wall length is insufficient. In the remaining boreholes, no significant trend of changing the position of the groundwater table was observed or this trend was ambiguous, and the groundwater table rose and dropped (Fig. 23).

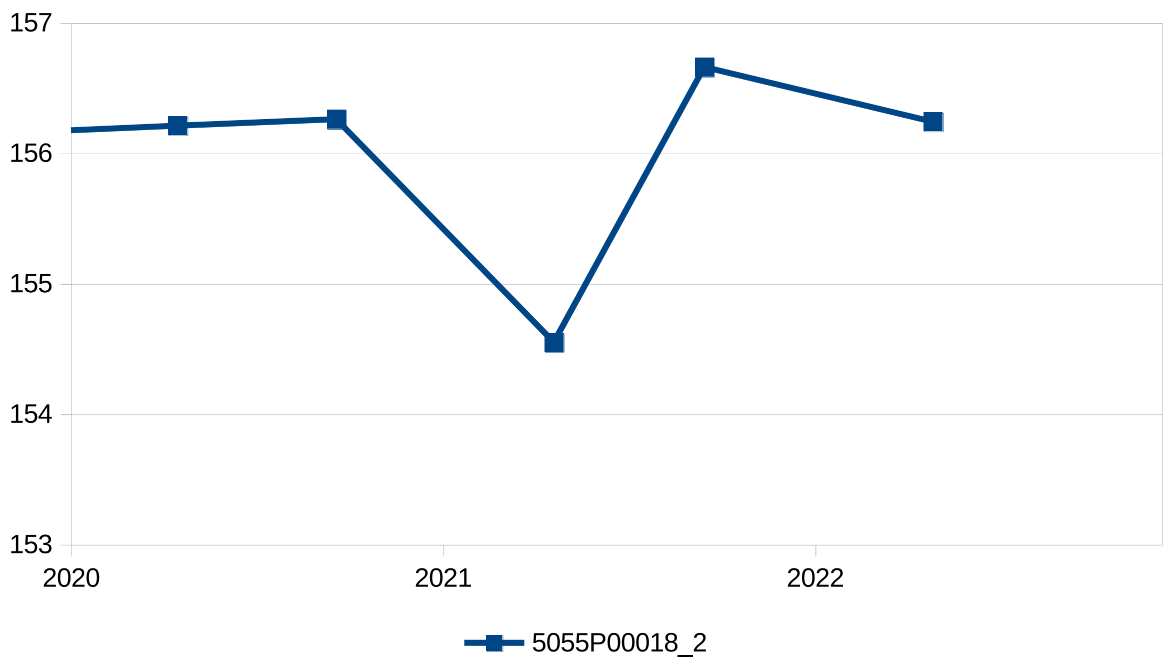

Fig. 23. The water table changes in the monitoring well No. 5055P00018_2.

Aquifer GWL ZU

The map illustrates the location of the hydrogeological monitoring points for the GWL ZU aquifer (Fig. 24).

Fig. 24. Location of the groundwater wells monitoring the GWL ZU aquifer.

All monitoring wells of this aquifer are located in the German part of the Zittau basin. The amplitude of the groundwater table fluctuations during the entire observation period was 4-90 meters, and in the years 2020-2022, it was 0.3-14 m. In this aquifer, the most significant drop of the groundwater table is observed. A record-breaking lowering of the groundwater table took place in well no. 50557689, from 2020, it dropped by 14 meters (Fig. 25).

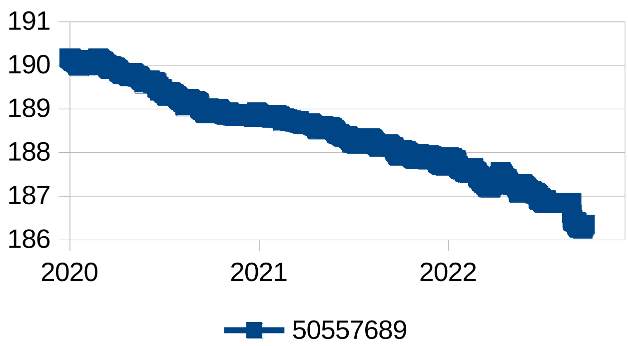

Fig. 25. The water table changes in the monitoring well No. 50557689.

In the period 2020-2022, in two hydrogeological wells (50557700 and 50547710), the groundwater table rise by more than 1 meter was observed (Fig. 26). On the other hand, in two hydrogeological wells (50557689 and 51547708), the groundwater table drop was observed (Fig.?).

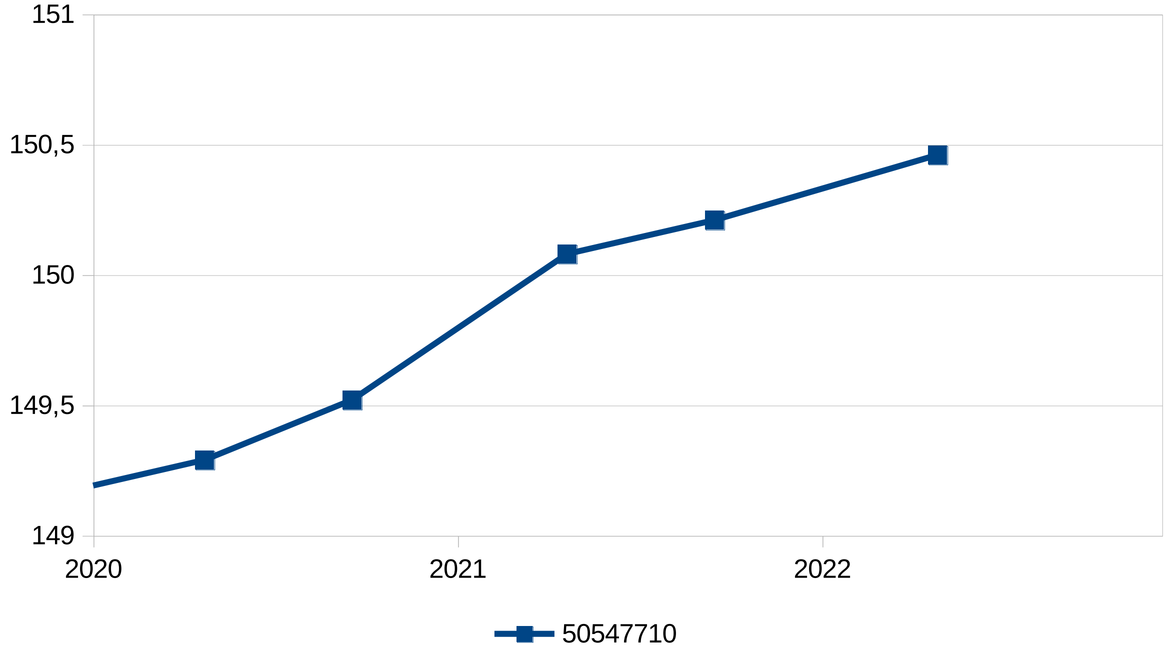

Fig. 26. The water table changes in the monitoring well No. 50547710.

This is a continuation of the unfavourable trends described in the Krupp report (Krupp 2020). As in the case of the ZiC aquifer drainage, the groundwater table drop in 2020-2022 is observed in Zittau and south of Hirschfelde, i.e. south and north of the anti-filtration screen built along the Łużycka Nysa. On the other hand, the rising of the groundwater table was observed in the wells behind the screen. In the remaining boreholes, no significant trend of changing the position of the groundwater table was observed or this trend was ambiguous, and the groundwater table rose and dropped (Fig. 27).

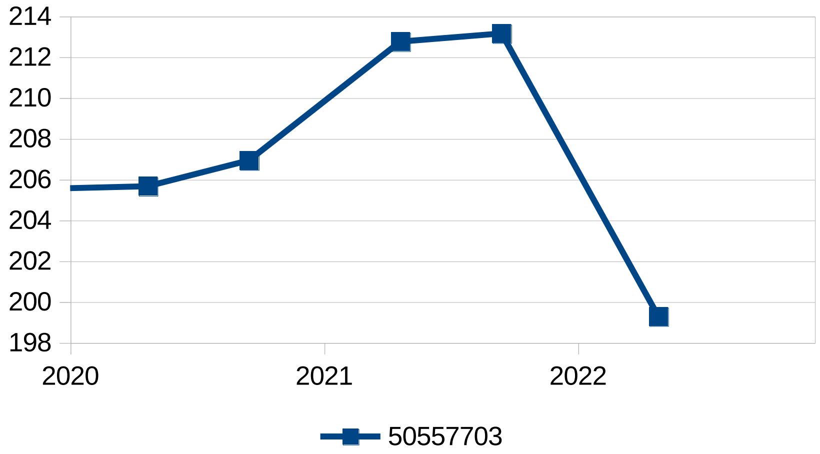

Fig. 27. The water table changes in the monitoring well No. 50557703.

Other aquifers

The map below illustrates the location of the monitoring wells in the following aquifers: GWL 1e (50557688), GWL 1 + OO (5055P00003_1), GWL ZiB + VBaZ (50557698), GWL VbaZ (5055P00022), GWL ZiA + PGDZ (5055LP00012) (51547711) (Fig. 28).

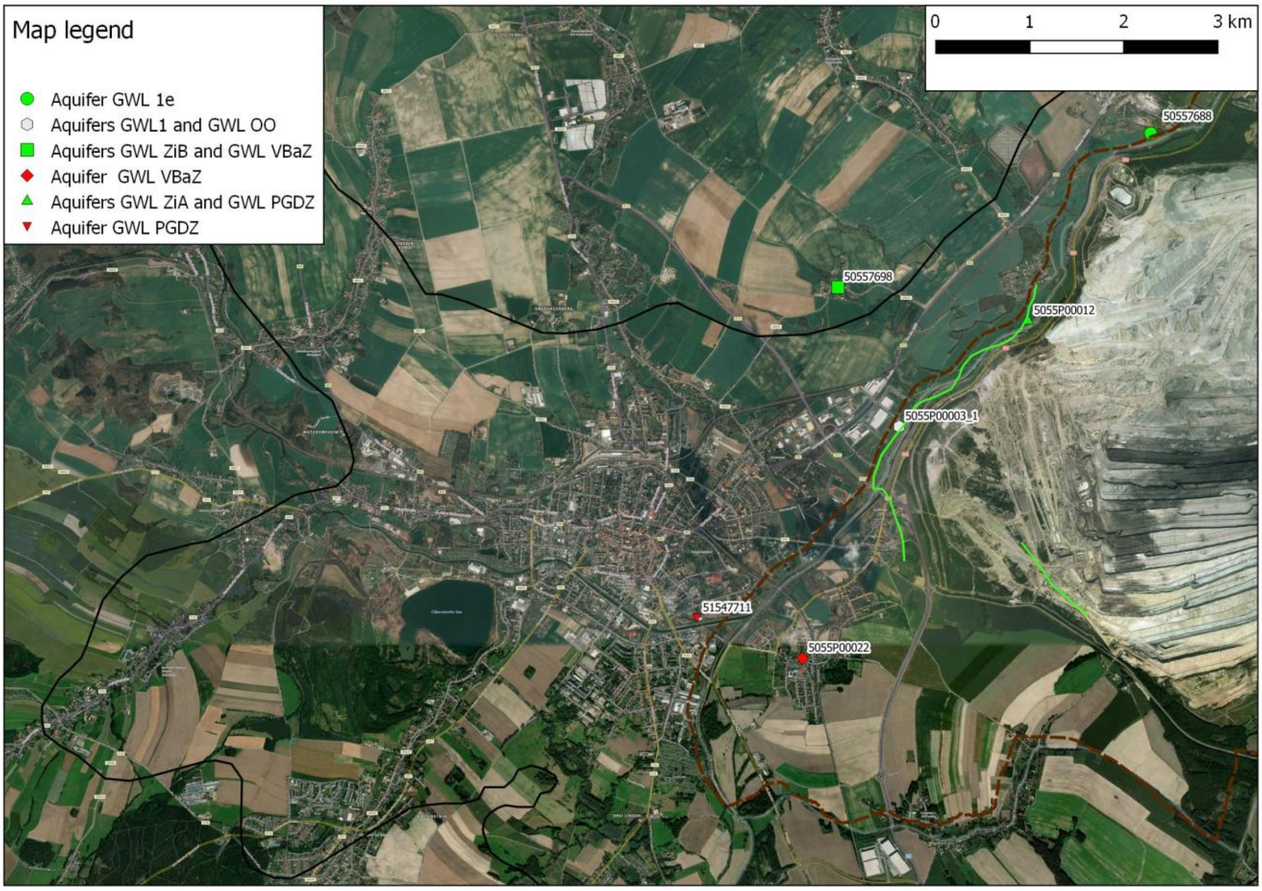

Fig. 28. Location of the groundwater wells monitoring the aquifers: GWL 1e, GWL1 and OO, GWL ZiB and VBaZ, GWL VBaZ, GWL ZiA and PGDZ, GWL PGDZ.

In the wells located in the northern part of the Zittau basin area (50557688, 50557698 and 5055P00003_1), a rise of the groundwater table was observed in 2020-2022. During the entire observation period, no clear trends in changes in the position of the groundwater table in these wells were found because it was both dropping and rising. In turn, in the wells located south of them (51547711 and 5055P00022) (Fig. 29), the groundwater table drop was observed during this period, and this is a continuation of the downward trend of the groundwater table throughout the observation period. They monitor deep aquifers (GWL VBaZ and GWL PGDZ) in the southern part of Zittau and are located in an area where the aquifers of GWL ZiC and GWL ZU are also drained (Fig. 30). In well No. 5055P00003_1, no observations were carried out in the years 2020-2022, while in the entire observation period (1990-2013), a weak trend of rising groundwater table was observed.

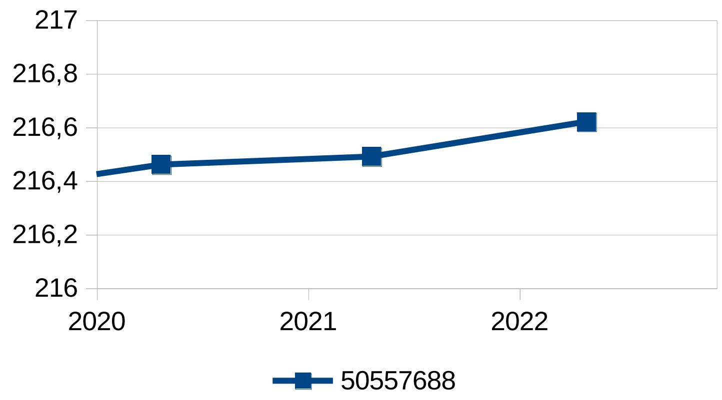

Fig. 29. The water table changes in the monitoring well No. 50557688.

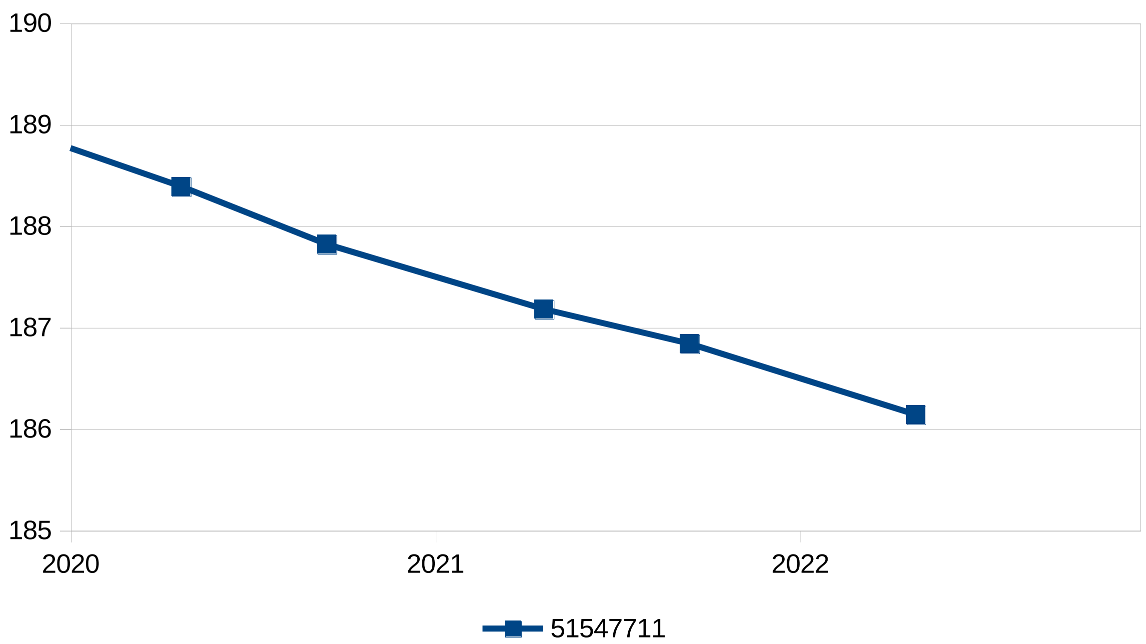

Fig. 30. The water table changes in the monitoring well No. 50557711.

Summing up, it can be concluded that the most heavily drained aquifers throughout the observation period were GWL ZiC and GWL ZU, and this trend has continued over the last two years. The levels of GWL VbaZ and GWL PGDZ may be drained to a similar extent, and the groundwater table drop by 20-35 meters is also observed, but each of these aquifers are observed only by one hydrogeological well, and it is difficult to say whether this trend applies to the whole extent of the aquifers. Groundwater table rise was often observed in aquifers GWL OO and GWL OU during the observation period and in the last two years. In most monitoring wells, the aquifers GWL 1 and GWL HM did not show unequivocal trends, and the groundwater table was often subject to strong fluctuations.

Hydrogeological monitoring data show that the effectiveness of the sealing wall built along the Nysa Łużycka and the opencast lignite mine is appropriate. It protects the water resources of the Neogene and Quaternary aquifers properly in the area from the northern part of Zittau to the vicinity of the village of Drausendorf. This confirms the rising of the groundwater table in the aquifers of GWL ZiC and GWL ZU, which is a continuation of the trend observed before 2020. On the other hand, in the southern part of Zittau and between the villages of Drausendorf and Hirschfelde, which are not protected by a sealing wall from the impact of the Turów mine, dewatering of aquifers still takes place: GWL ZiC, GWL ZU, GWL VbaZ and GWL PGDZ. Pursuant to the license granted for the exploitation of the Turów deposit, further exploitation of its south-eastern part is planned, which, however, is located deeper and requires increasing the depth of the deposit's drainage. This entails a deepening of the depression cone and an increase in its range. This means that the drainage of the abovementioned aquifers will continue as it did in 2022-2022 and earlier. In order to limit the inflow of water from Germany, it would be necessary to extend the existing sealing wall both to the north along the Nysa Łużycka and to the south-east towards the other sealing wall, limiting the inflow of groundwater from the territory of the Czech Republic. A numerical hydrogeological model should provide more precise data about the proposed extention of the sealing wall and its depth.

The continuous, long-term drainage of the deep aquifers of the GWL ZiC and GWL ZU in the central and southern parts of the city of Zittau also resulted in the lowering of the land surface. According to the Krupp study (Krupp 2021), this is particularly visible in the area limited by the following tectonic faults: the Zittau fault, called the southern fault (uskok Południowy) on the Polish side and the Pethau fault. In this area, especially along the Mandau River, the lowering of the land surface in 2014-2019 locally exceeded 5 mm per year. With the continuation of the exploitation of the lignite deposit, the gradual deepening of the open-pit mine, and increasing the drainage depth, the groundwater table of these aquifers will continue to drop. It may result in further lowering of the land surface in this area. In order to minimize this threat, the existing sealing wall should be extended to the southeast.

Water bodies

Many years of lignite mining in Turów and drainage of the deposit resulted in a significant loss of groundwater in the Zittau Basin. The Polish Groundwater Body No. PLGW6000105 has a good chemical state, and the quantitative goal is less stringent and is to protect the quantitative state from further deterioration from the present poor state. In the case of deepening of the depression cone during the exploitation of the remaining part of the deposit, it will not be possible for the quantitative condition of this JCWPd to avoid deterioration. On the German side, there is the Groundwater Body DESN_NE 2. The area of the depression cone draining the GWL ZiC and ZU aquifers in Germany is 19.2 km^2, which is 3.8% of the surface area of the Groundwater Body DESN_NE 2 (507,8 km^2). In case of further deepening of the depression cone, the groundwater outflow from the Groundwater Body to the Turów mine will intensify (LULGS 2022, ISOK 2022).

Turów lignite mining has an impact on the chemical state of the Surface Water Bodies. This applies in particular to the Miedzianka River. The data available so far on the impact of mine water discharge on the waters of Miedzianka suggest that the Acid Mine Drainage is taking place now. In Miedzianka waters below the discharge of mine waters from the Turów mine, the concentration of sulphates is 11 times higher than above the discharge site (389.6 and 33.7 mg/dm^3, respectively). The amount of suspension in water also increases six times (from 5 to 30 mg/dm^3) (Błachuta, Mazurek 2018).

A Turów lignite mine is particularly predisposed to acid mine drainage (AMD). Exposing the exploited lignite seams leads to their oxidation, during which the sulfur present in sulphide minerals and organic matter will oxidize (total sulfur on average 1%, and combustible sulfur on average 0.73%). Similar phenomena will occur in the artificially created aeration zone within the depression cone. The product of sulfur oxidation is, among others, sulfuric acid by reaction:

$$\mathbf{4FeS_2 + 15O_2 + 14H_2O \longrightarrow 4Fe(OH)_3 + 8H_2SO_4}$$

The resulting sulfuric acid lowers the pH (even to 2.0-2.5) of groundwater and increases its aggressiveness towards minerals present in the surrounding rocks. It increases the total hardness of water, oxidation of iron and manganese compounds and the leaching of a number of elements (metals, metalloids and radionuclides) from the deposit and rocks. These processes significantly change the chemical composition of water and their basic physicochemical parameters, such as: pH, redox potential, electrolytic conductivity and dry residue.

On the other hand, the area of Nysa Łużycka River catchment below the estuary of Miedzianka is 851 km2, and along this river there are such cities and towns as Zittau, Hradek nad Nisou, Liberec, Jablonec nad Nisou and numerous villages. Pollutants such as heavy metals, iron and manganese compounds or increased total mineralization may come from groundwater drained by the Turów mine and urbanized areas. In order to capture the mine's influence on the waters of Nysa Łużycka, the author compared the results of chemical analyzes of this river at the Drausendorf and Kloster Marienthal stations. The following parameters were compared: electrical conductivity, calcium and sulphates from 2015 (Fig. 31 -33) (LULGS 2022).

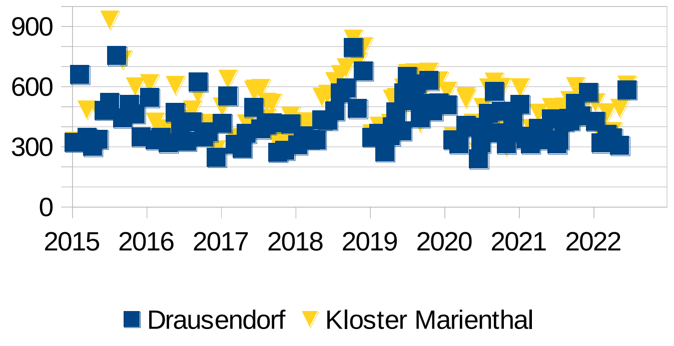

Fig. 31. Electrical conductivity (µS/cm) of Nysa Łużycka water measured in Drausendorf and Kloster Marienthal in 2015-2022.

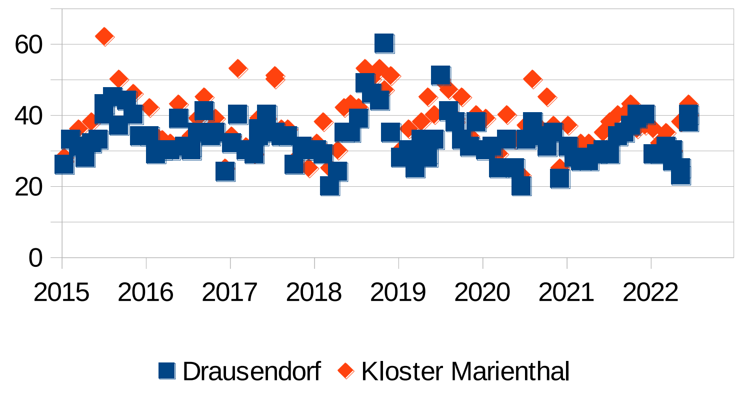

Fig. 32. Calcium concentration (mg/dm^3) of Nysa Łużycka water measured in Drausendorf and Kloster Marienthal in 2015-2022.

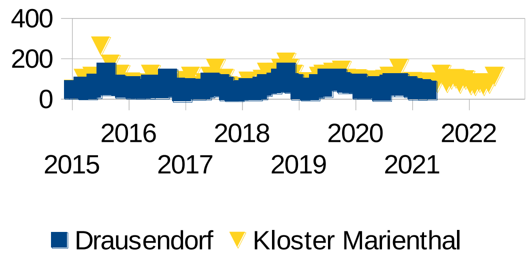

Fig. 33. Sulphate concentration (mg/dm^3) of Nysa Łużycka water measured in Drausendorf and Kloster Marienthal in 2015-2022.

In all the series of measurements, it is visible that usually, at the given time of the analysis, the parameter values were higher in the waters sampled in Kloster Marienthal than in Drausendorf. Typically, these are 10-30% higher. This suggests that the Turów mine, together with the catchments of watercourses flowing between Drausendorf and Kloster Marienthal, contributes to the general anthropopression exerted on the quality of the waters of the Nysa Łużycka River. The longer the mine operates, the longer its negative impact on the waters of the Nysa Łużycka River will be. However, the concentrations of heavy metals show a different image. Concentrations of arsenic, lead, and nickel in Drausendorf and Kloster Marienthal since 2015 are illustrated below (Fig. 34-36).

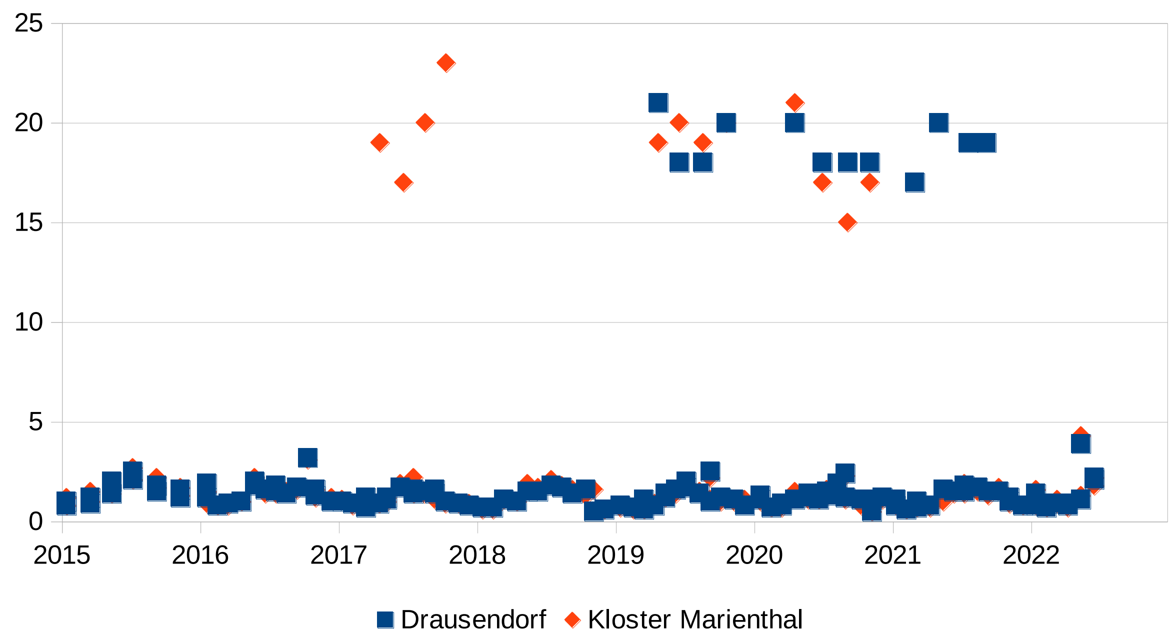

Fig. 34. Arsenic concentration (µg/dm^3) of Nysa Łużycka water measured in Drausendorf and Kloster Marienthal in 2015-2022.

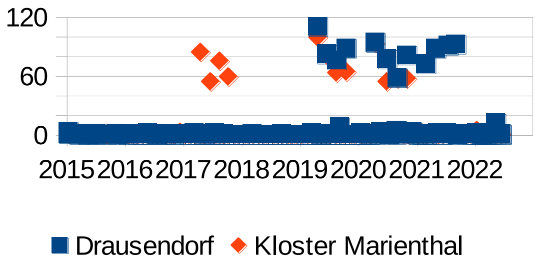

Fig. 35. Lead concentration (µg/dm^3) of Nysa Łużycka water measured in Drausendorf and Kloster Marienthal in 2015-2022.

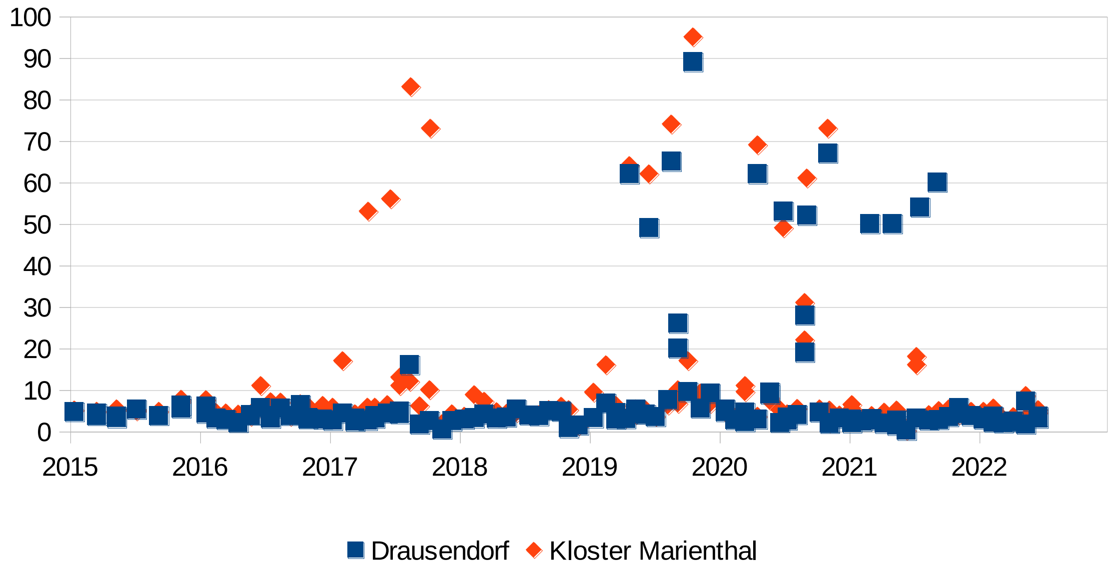

Fig. 36. Nickel concentration (µg/dm^3) of Nysa Łużycka water measured in Drausendorf and Kloster Marienthal in 2015-2022.

The concentrations of arsenic and lead measured on the same day in Drausendorf are often higher than in Kloster Marienthal despite the other point being located below the discharge wastewater from Turów mine or power station. The nickel concentrations are usually higher in Kloster Marienthal. This may suggest that the Turów mine or power station wastewater pollutes the Nysa Łużycka river only with some heavy metals like nickel while the others like arsenic and lead don't show such impact.

Conclusions

The above considerations lead to the following conclusions:

1. Monitoring groundwater in the German part of the Zittau basin in 2020-2022 shows that in the shallower aquifers (GWL 1, GWL OO, GWL HM, GWL OU), there is no lowering of the groundwater table that the impact of KWB Turów could cause.
2. Groundwater monitoring of deeper aquifers (GWL ZiC and GWL ZU) shows progressive groundwater drainage in the southern part of Zittau and between Drausendorf and Hirschfelde. While between these areas, there is the groundwater table rise in these aquifers. These dependencies, described in the Krupp report (Krupp 2020), remain valid.
3. The sealing wall built by the Turów mine in 1997 serves its purpose to a limited extent, and to eliminate groundwater drainage from Germany, it would have to be extended both to the north and southeast. A numerical hydrogeological model should provide more precise data about the proposed extention of the sealing wall and its depth.
4. The deepening of the Turów mine drainage will increase and deepen the depression cone and will result in a greater inflow of groundwater from both Polish and German Groundwater bodies.
5. Drainage of groundwater from deep aquifers (GWL ZiC and GWL ZU) leads to the lowering of the land surface. Further drainage of the Turów lignite mine will intensify this phenomenon.
6. The acid mine drainage causes the release of many pollutants, including sulphates, iron, manganese, and heavy metals, to groundwater within the depression cone. The Turów mine drainage causes an inflow of the pollutants with the groundwater to the mine. The mine discharges them later to the surface water of Miedzianka and Nysa Łużycka rivers.
7. The Turów mine contributes to the increase of the concentration of the pollutants. The concentration of pollutants in the waters of the Nysa Łużycka River is visible in the increase in electrolytic conductivity and the concentration of calcium and sulphates, measured above and below the point of the pollutants discharge.
8. The Turów mine or power station wastewater might also pollute the Nysa Łużycka water with some heavy metals like nickel because its concentration is usually higher in the monitoring point located below the discharge point of the Turów mine water.

References

1. Badura J., Cymerman Z., 2009a, Szczegółowa Mapa Geologiczna Polski w skali 1:50000. Arkusz Bogatynia (792). Państwowy Instytut Geologiczny, Warszawa.

2. Badura J., Cymerman Z., 2009b, Szczegółowa Mapa Geologiczna Polski w skali 1:50000. Arkusz Grabiszyce Górne (793). Państwowy Instytut Geologiczny, Warszawa.

3. Badura J., Cymerman Z., 2016, Objaśnienia do Szczegółowa Mapa Geologiczna Polski w skali 1:50000. Arkusze: Bogatynia (792) i Grabiszyce Górne (793). Państwowy Instytut Geologiczny, Warszawa.

4. BFG, 2022, Bundesanstalt für Gewässerkunde. Karten zum 3. WRRL-Bewirtschaftungsplan. URL address: https://geoportal.bafg.de/karten/wfdmaps2022/#
5. Błachuta J., Mazurek M., 2018, Oddziaływanie na wody powierzchniowe przedsięwzięcia. Kontynuacja eksploatacji złoża węgla brunatnego Turow. Raport o oddziaływaniu na środowisko. PGE GIEK S.A., Bogatynia.
6. Börke, P., 2018, Wasserwirtschaftliche Besonderheiten des Zittauer Beckens (Vodohospodářské zvláštnosti Žitavské pánve). Konferenz Zittau 16.05.2018 BfN (2020, 23. August) Schutzgebiete in Deutschland. https://geodienste.bfn.de/schutzgebiete?lang=de
7. Dowgiałło J., Fistek J., 2007, Prowincja sudecka. [w:] Hydrogeologia regionalna Polski t. II, Państwowy Instytut Geologiczny, Warszawa.
8. Dziedziak J, Woźniak M., 2002a - Mapa hydrogeologiczna Polski w skali 1:50 000, arkusz Bogatynia (792). CAG, Warszawa.
9. Dziedziak J, Woźniak M., 2002b - Mapa hydrogeologiczna Polski w skali 1:50 000, arkusz Grabiszyce Górne (793). CAG, Warszawa.
10. Fiszer J., Sadowska M., 2019, Oddziaływanie na wody podziemne przedsięwzięcia. Kontynuacja eksploatacji złoża węgla brunatnego Turów. Raport o oddziaływaniu na środowisko. PGE GIEK S.A., Bogatynia.
11. ISOK, 2022, Charakterystyki JCWP oraz JCWPd obszaru polskiej części zlewni Nysy Łużyckiej. Adres URL: https://wody.isok.gov.pl/index.html
12. Kasiński J., Badura J., Pańczyk M., Pecskay Z., Saternus A., Słodkowska B., Urbański P., 2015, Osady paleogeńskie w polskiej części niecki żytawskiej – nowe światło na problem wieku zapadliska tektonicznego. [w:] Biuletyn Państwowego Instytutu Geologicznego 461 ss 295-324. Warszawa.

13. Krupp R., 2020, Gutachten zu den grenzüberschreitenden Auswirkungen einer Fortführung des Abbaus der Braunkohlelagerstätte Turów (Polen) auf die Gewässer in Deutschland. Burgdorf.
14. Krupp R., 2021, Geologisches Gutachten zu Bauschäden im Stadtgebiet Zittau, Sachsen Burgdorf.
15. LULGS (Landesamt für Umwelt, Landwirtschaft und Geologie Sachsen), 2022, Groundwater and surface water data online. URL address: https://www.umwelt.sachsen.de/umwelt/infosysteme/ida/
16. PIG-PIB, 2021, Karta informacyjna złoża kopaliny stałej, o którym mowa w art. 22 ust. 2 ustawy - prawo geologiczne i górnicze. Turów. Stan na 2021-12-31. Warszawa.
17. Staśko S., Michniewicz M., 2007, Subregion Sudetów [w:] Hydrogeologia regionalna Polski t. II, Państwowy Instytut Geologiczny, Warszawa.

Annex 1. Groundwater monitoring results of the western part of Zittau basin.

GWL 1

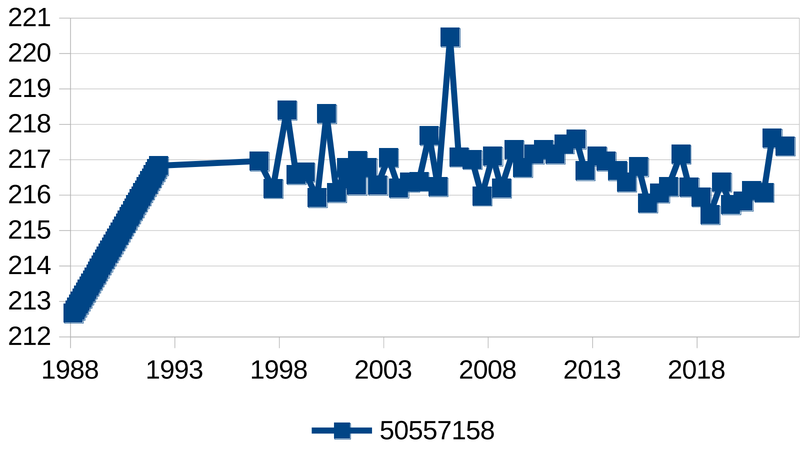

Fig. 37. The water table changes in the monitoring well No. 50557158.

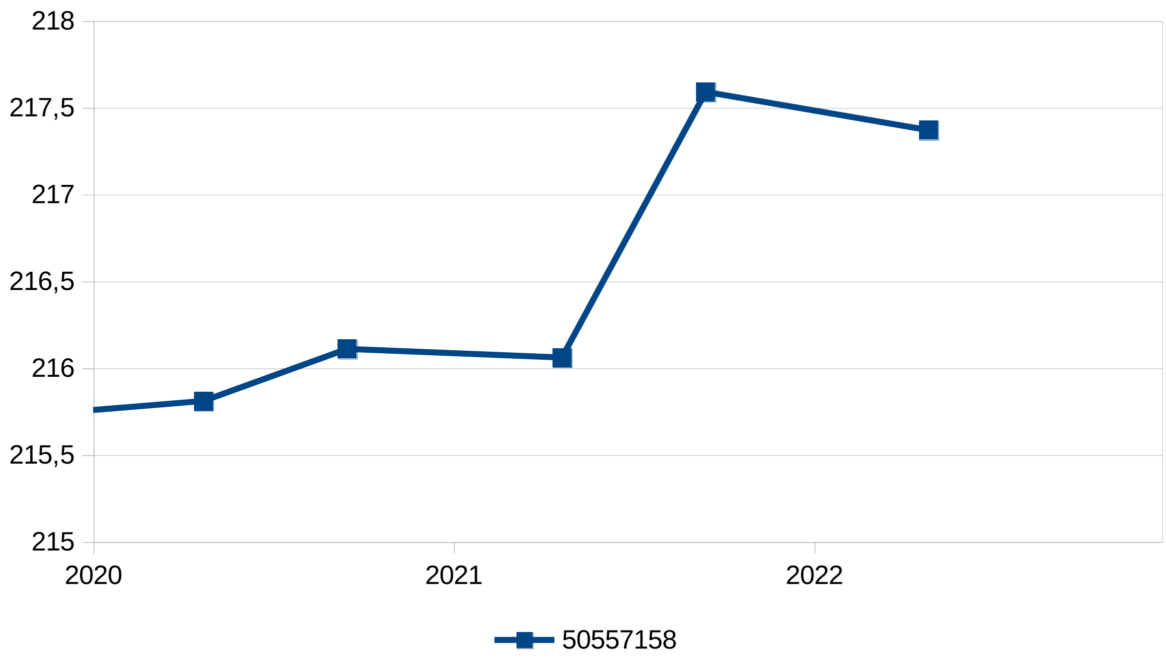

Fig. 38. The water table changes in the monitoring well No. 50557158

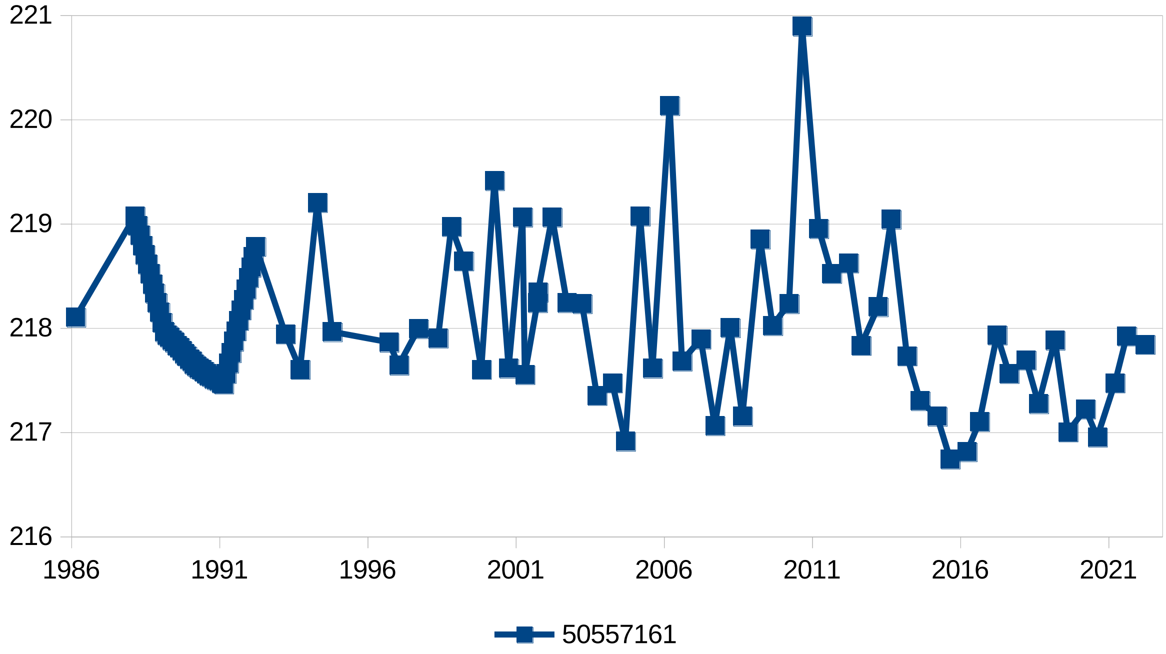

Fig. 39. The water table changes in the monitoring well No. 50557161

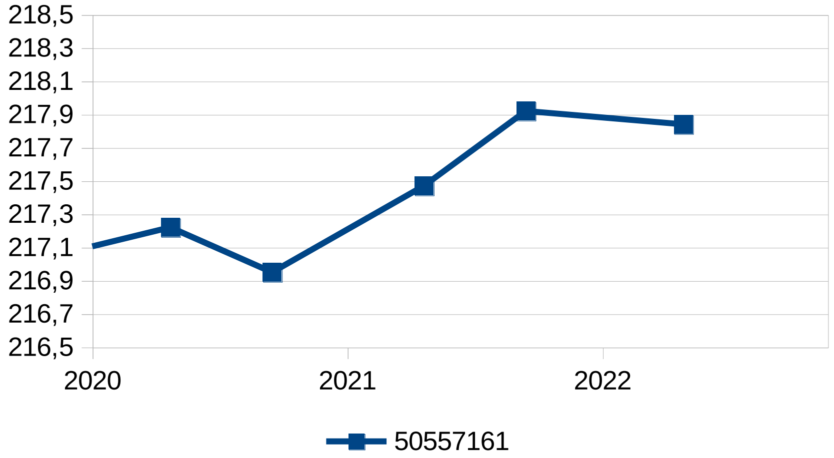

Fig. 40 The water table changes in the monitoring well No. 50557161

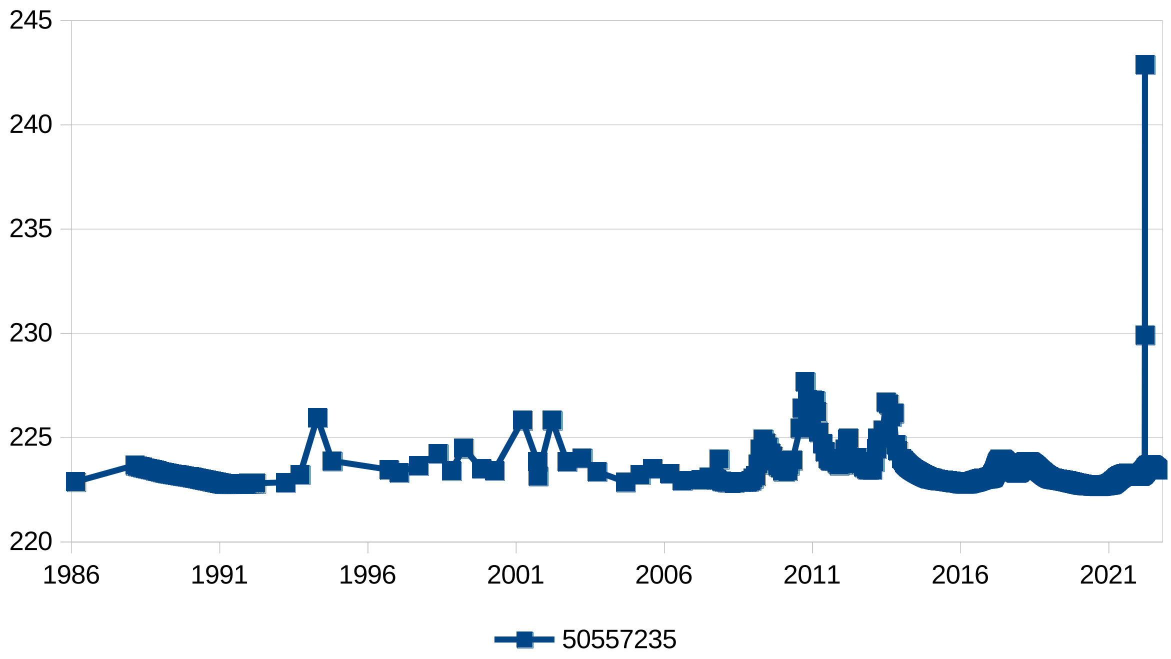

Fig. 41. The water table changes in the monitoring well No. 50557235

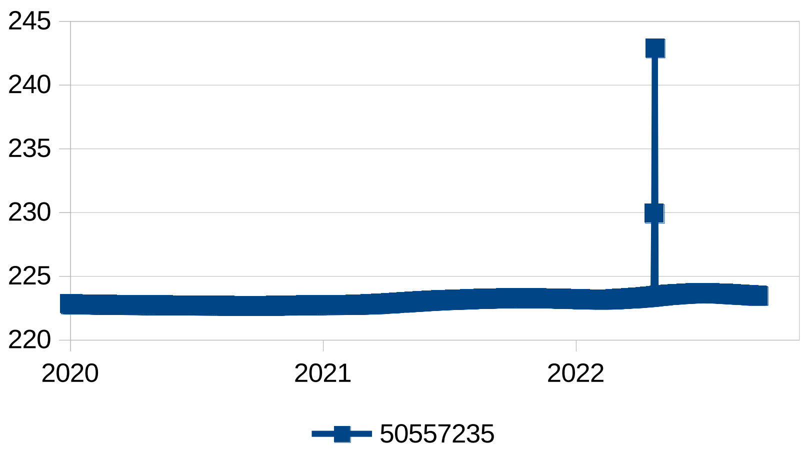

Fig. 42. The water table changes in the monitoring well No. 50557235

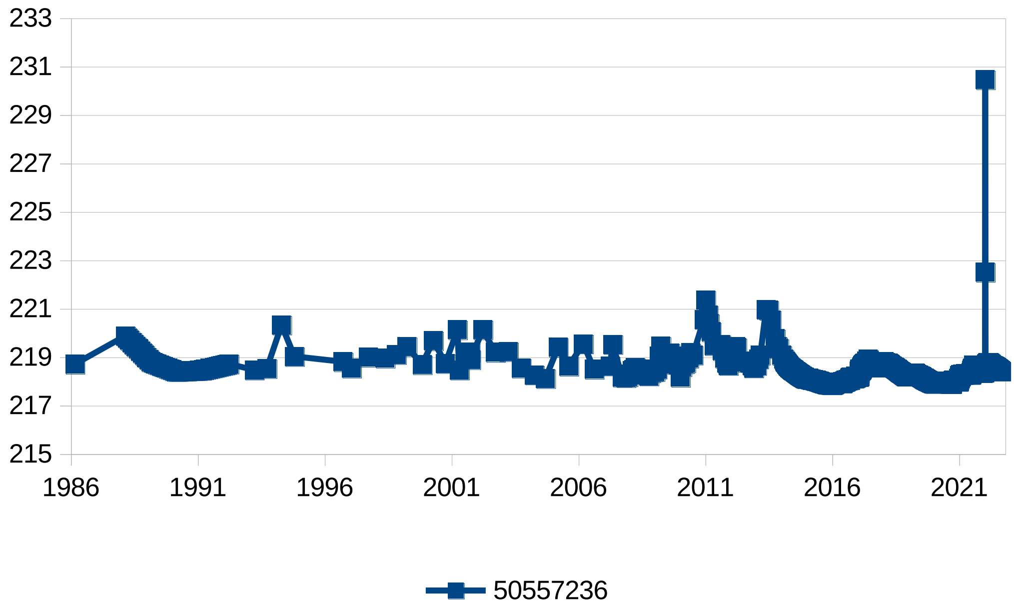

Fig. 43. The water table changes in the monitoring well No. 50557236

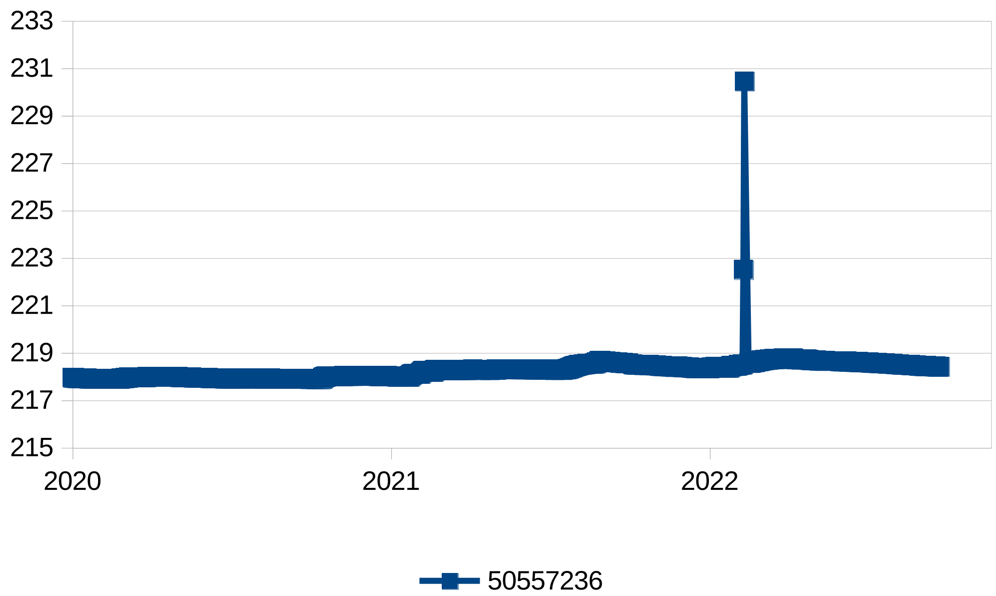

Fig. 44. The water table changes in the monitoring well No. 50557236

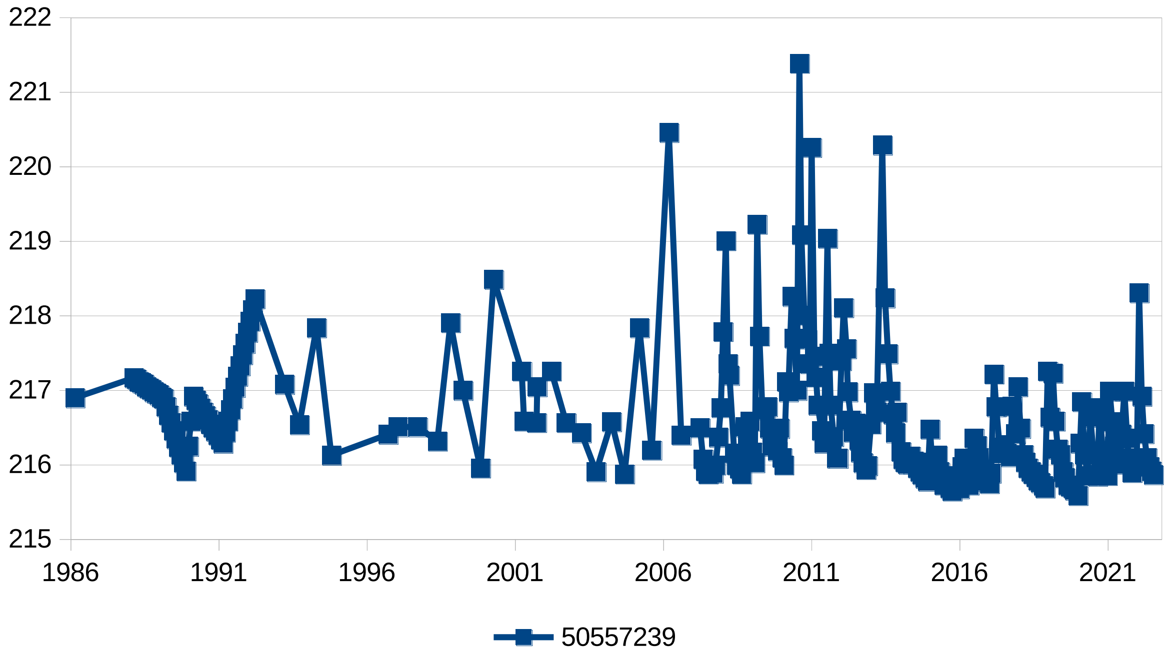

Fig. 45. The water table changes in the monitoring well No. 50557239

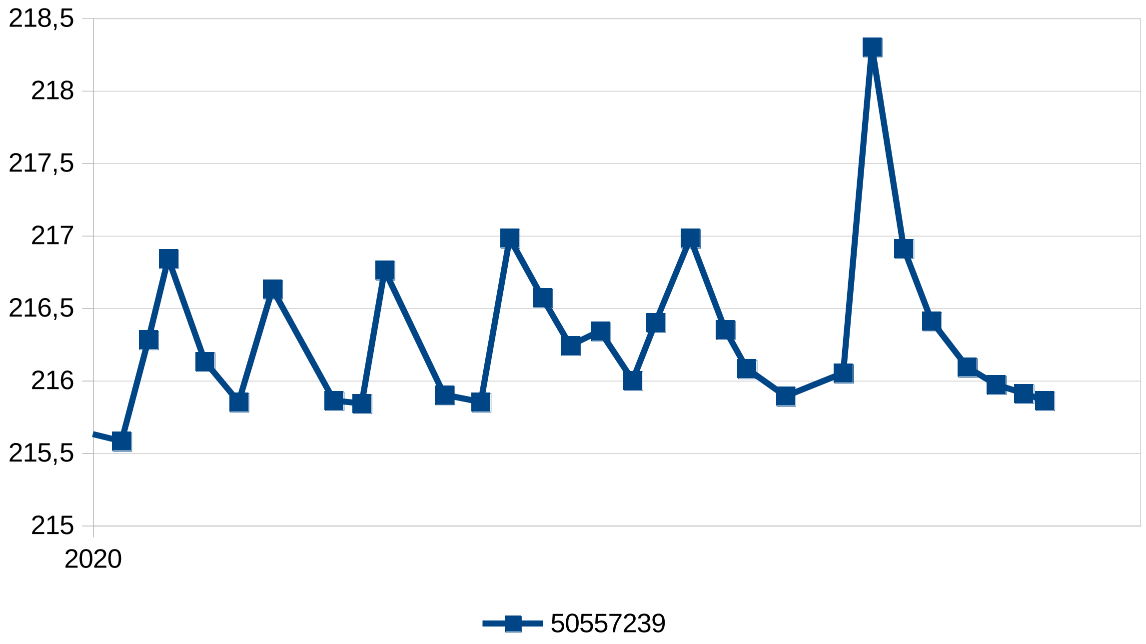

Fig. 46. The water table changes in the monitoring well No. 50557239

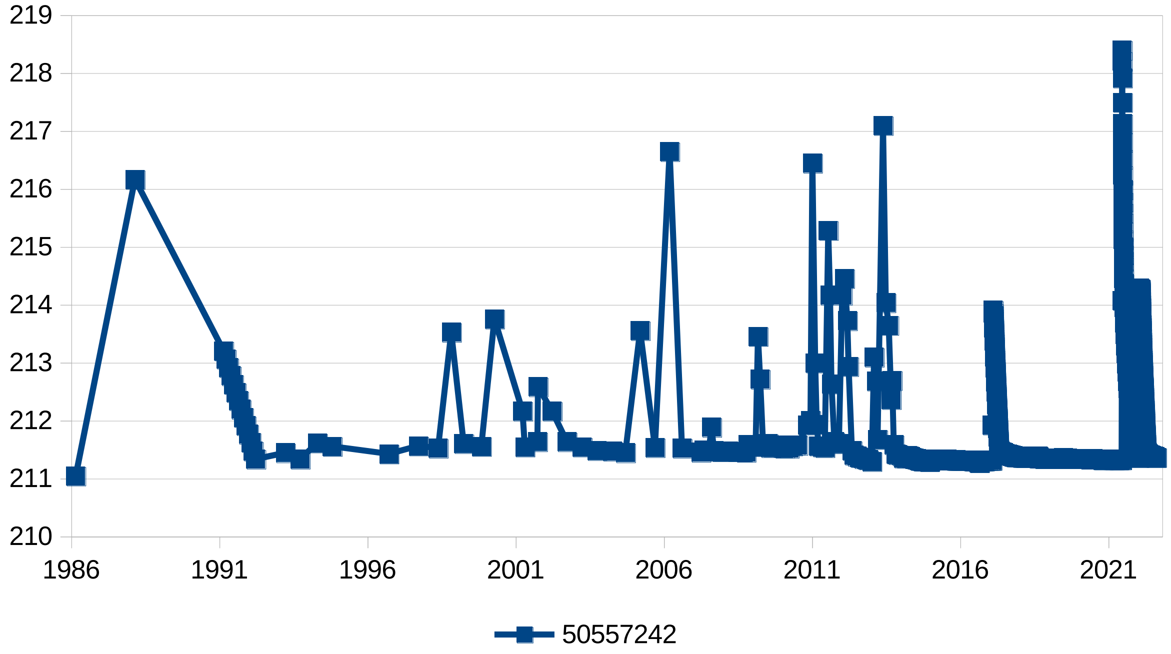

Fig. 47. The water table changes in the monitoring well No. 50557242

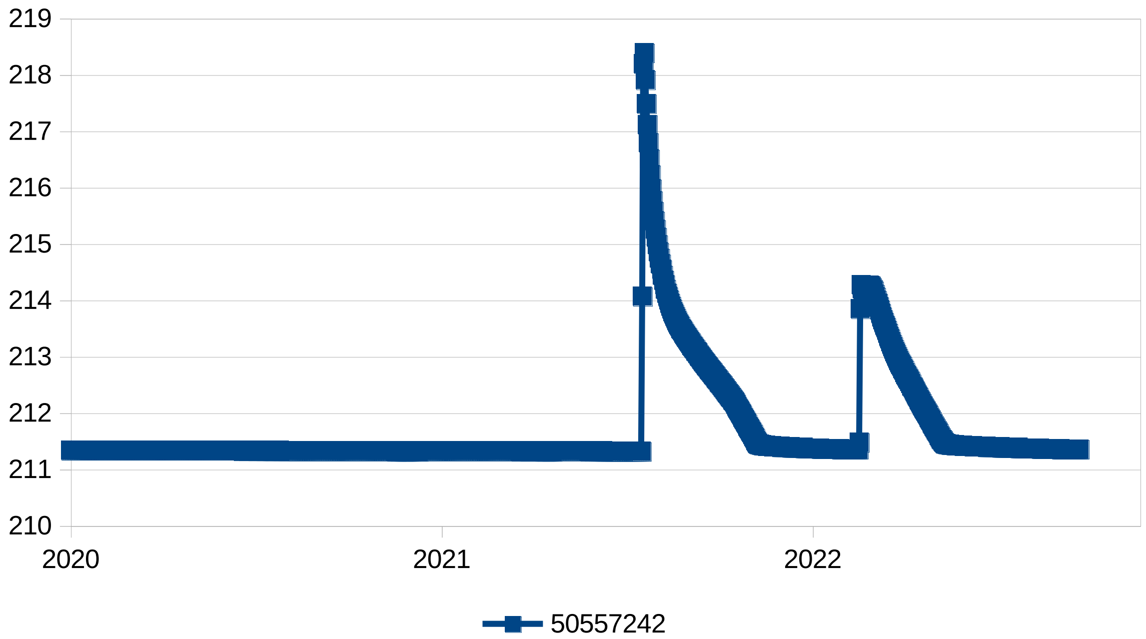

Fig. 48. The water table changes in the monitoring well No. 50557242

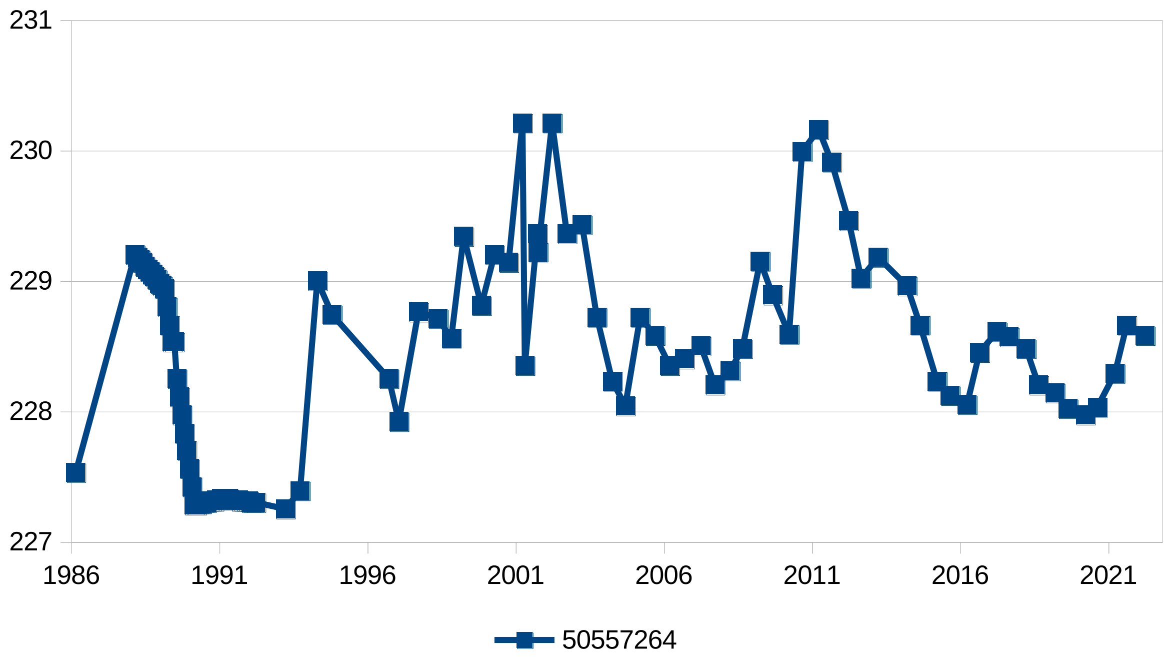

Fig. 49. The water table changes in the monitoring well No. 50557264

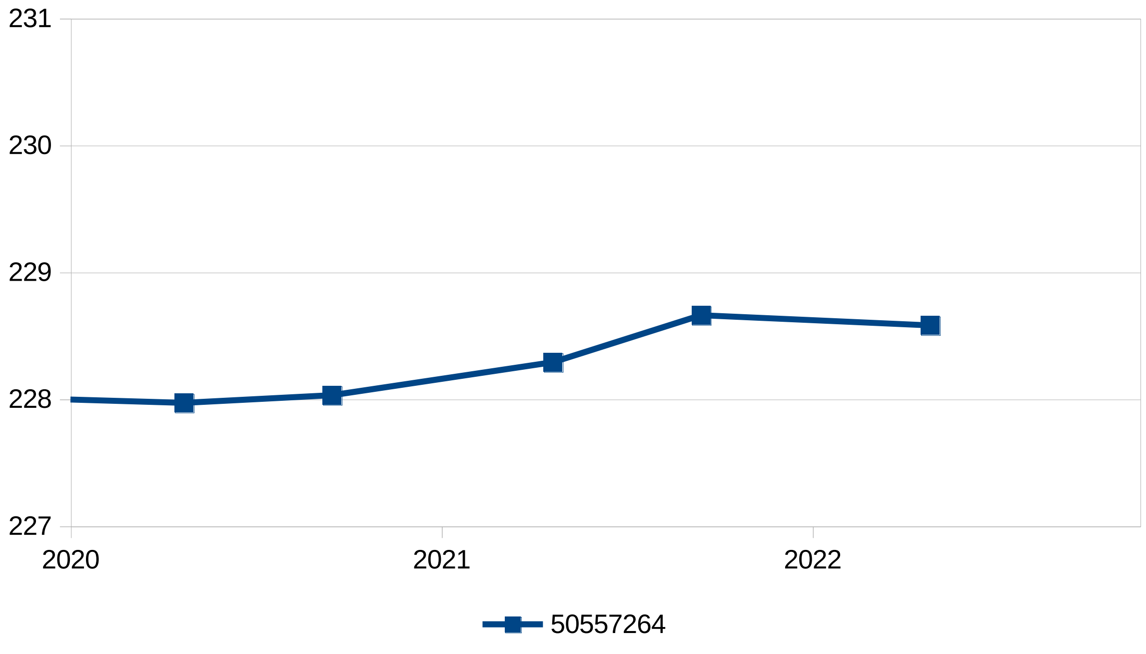

Fig. 50. The water table changes in the monitoring well No. 50557264

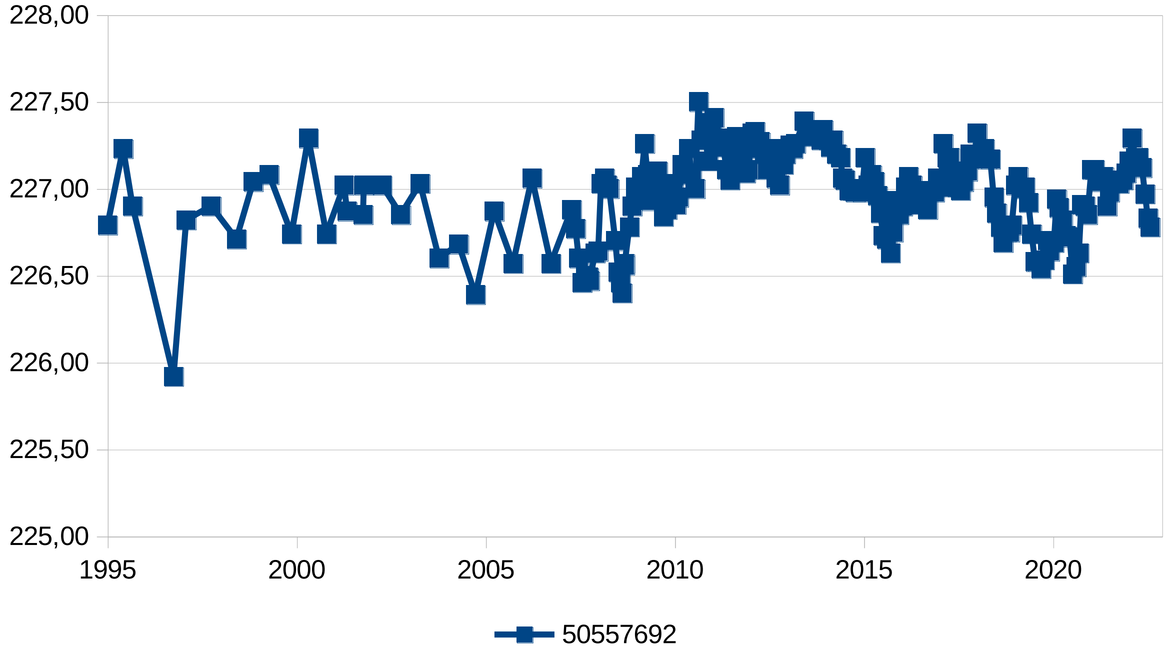

Fig. 51. The water table changes in the monitoring well No. 50557692

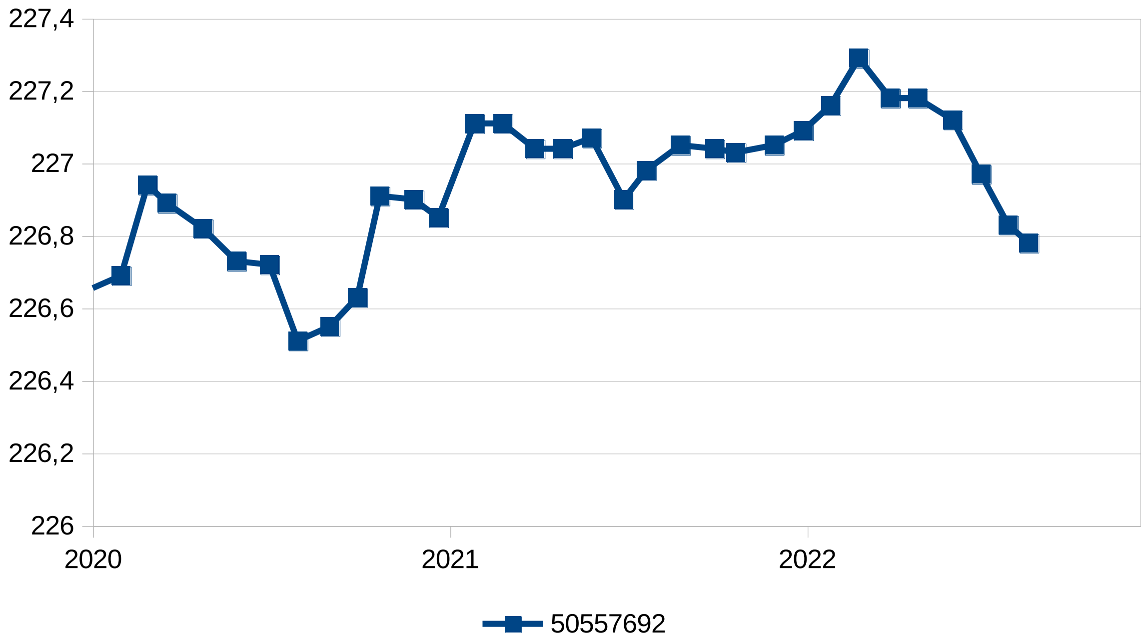

Fig. 52. The water table changes in the monitoring well No. 50557692

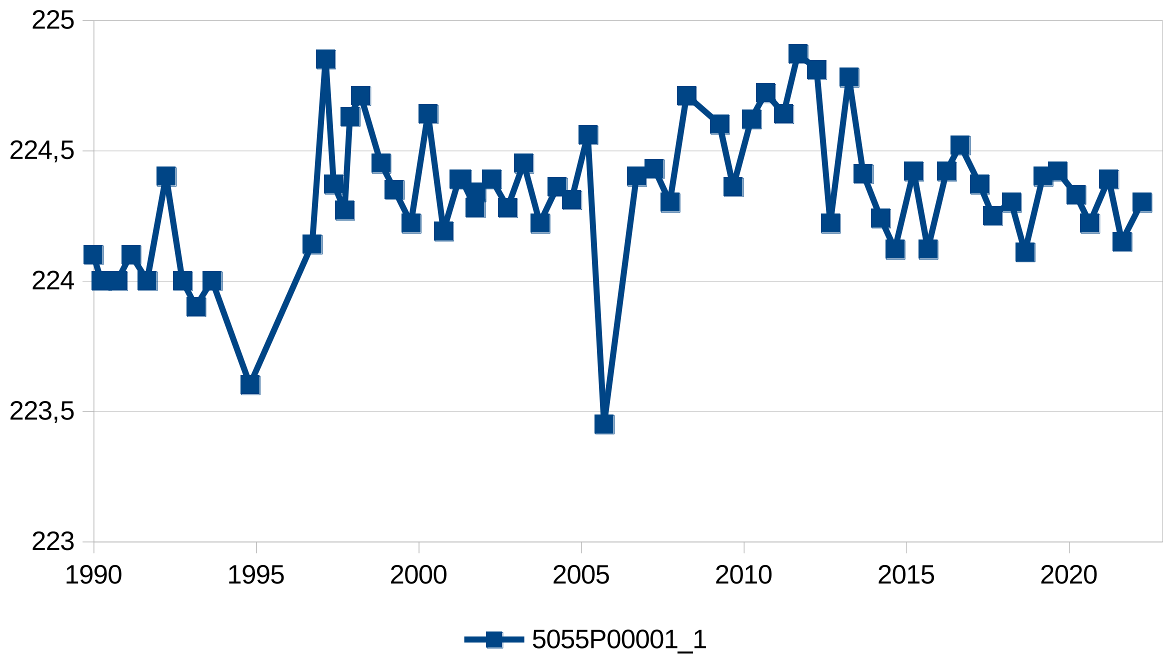

Fig. 53. The water table changes in the monitoring well No. 5055P00001_1

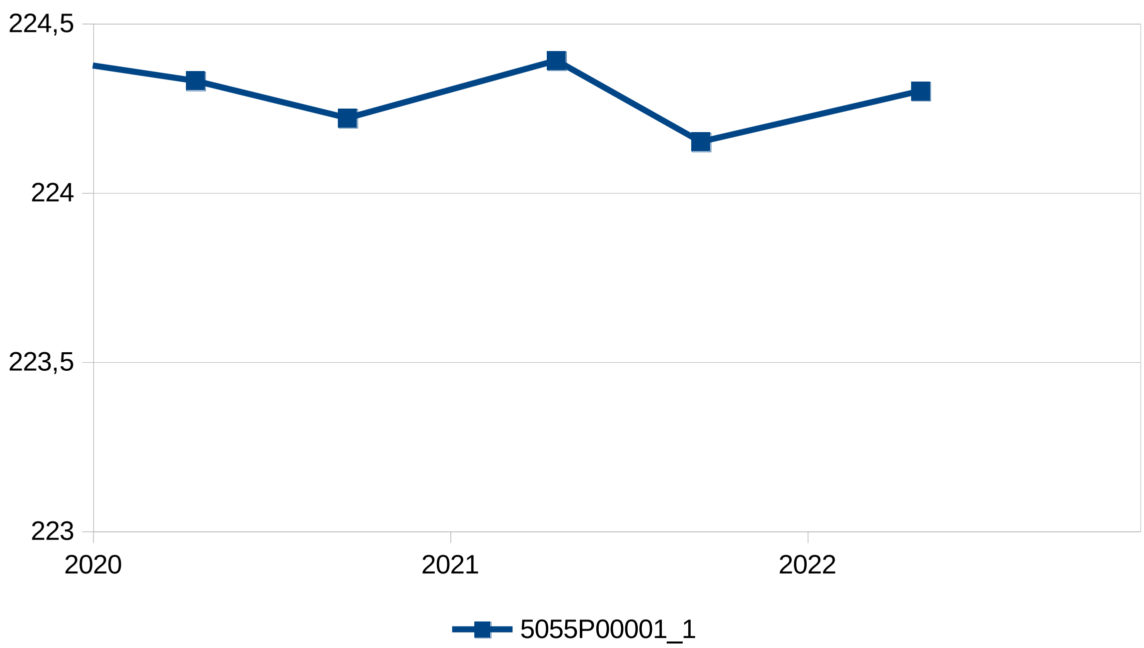

Fig. 54. The water table changes in the monitoring well No. 5055P00001_1

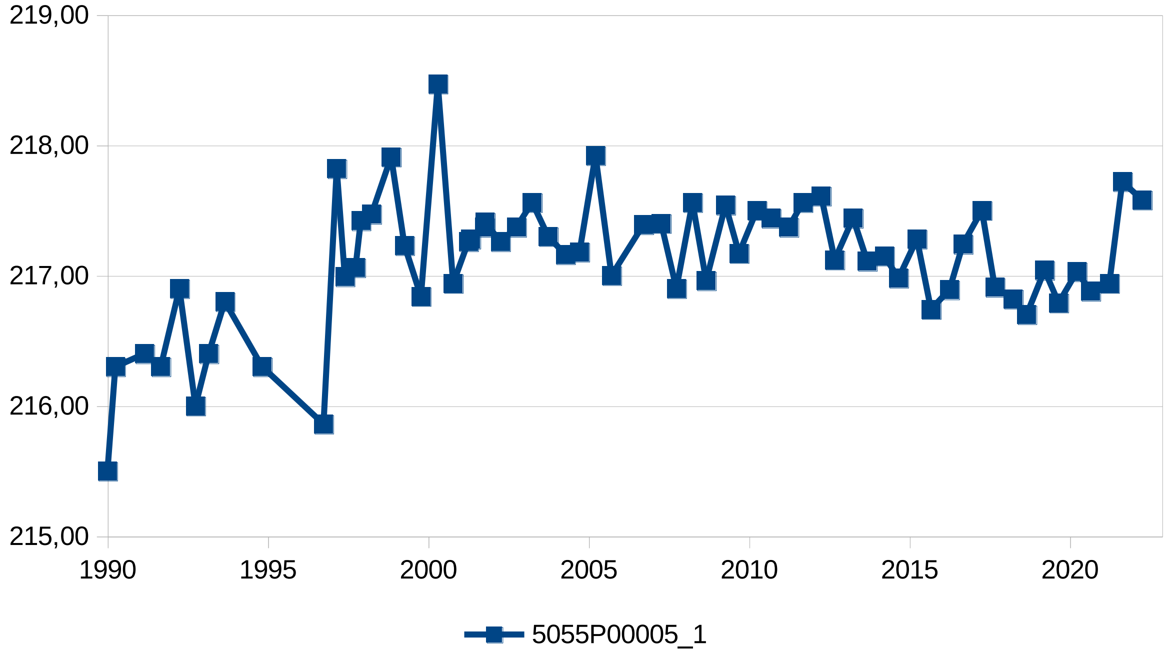

Fig. 55. The water table changes in the monitoring well No. 5055P00005_1

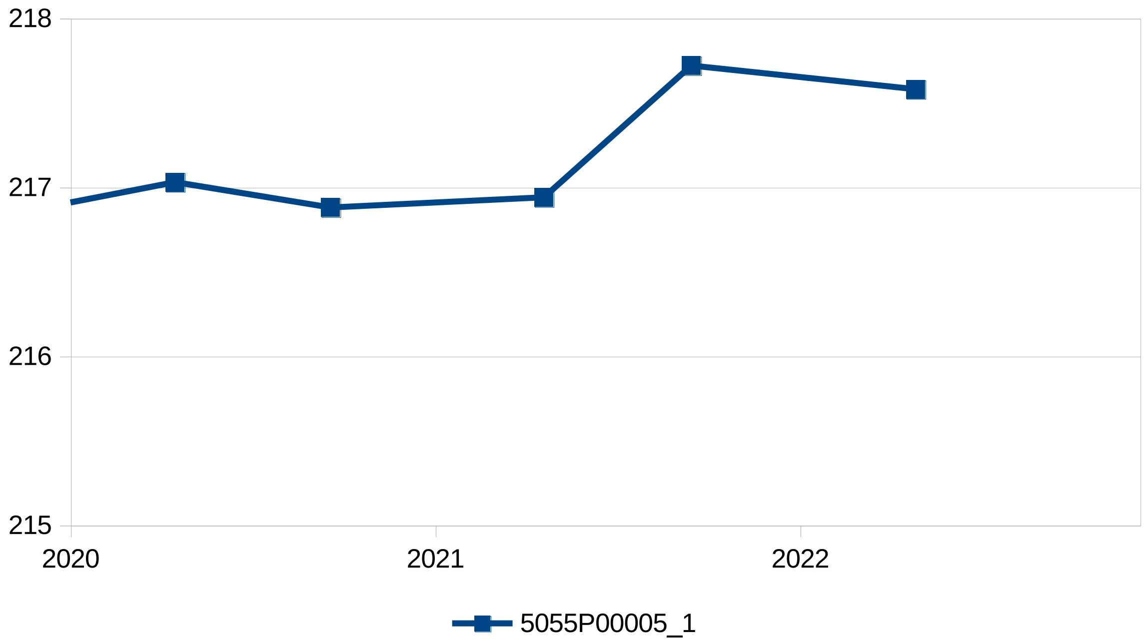

Fig. 56. The water table changes in the monitoring well No. 5055P00005_1

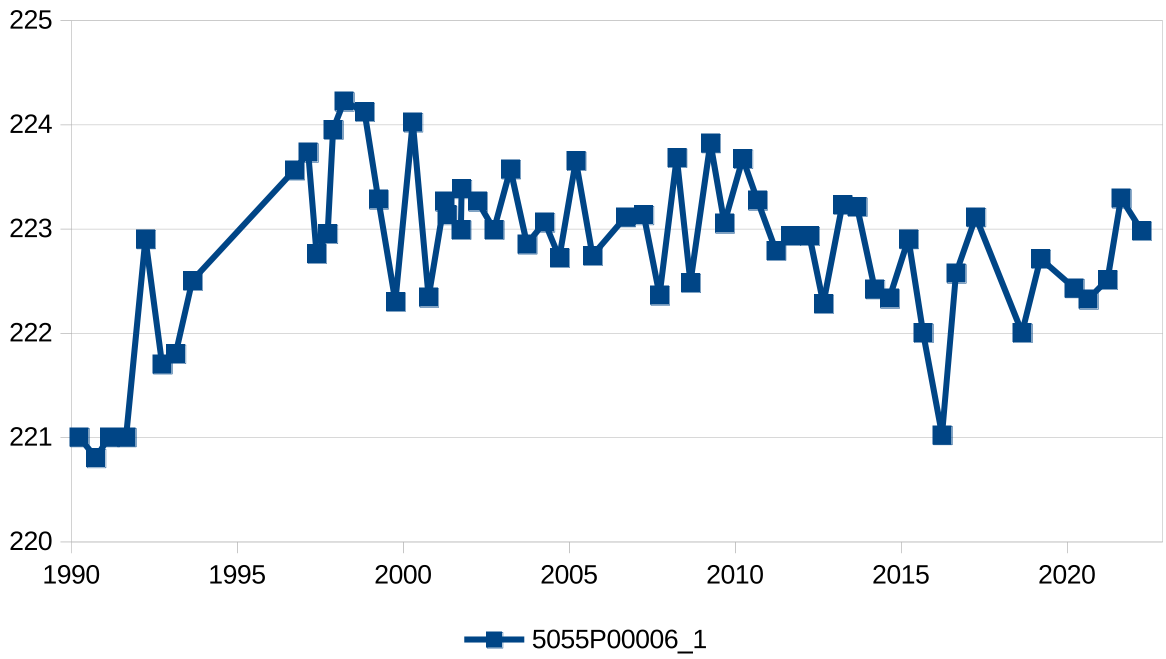

Fig. 57. The water table changes in the monitoring well No. 5055P00006_1

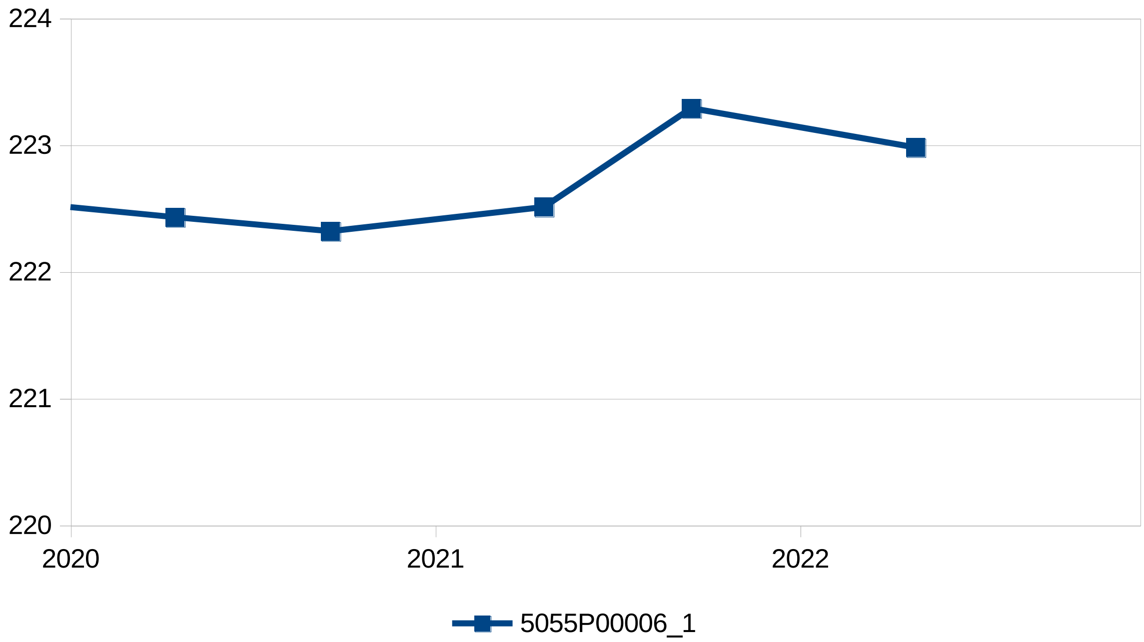

Fig. 58. The water table changes in the monitoring well No. 5055P00006_1

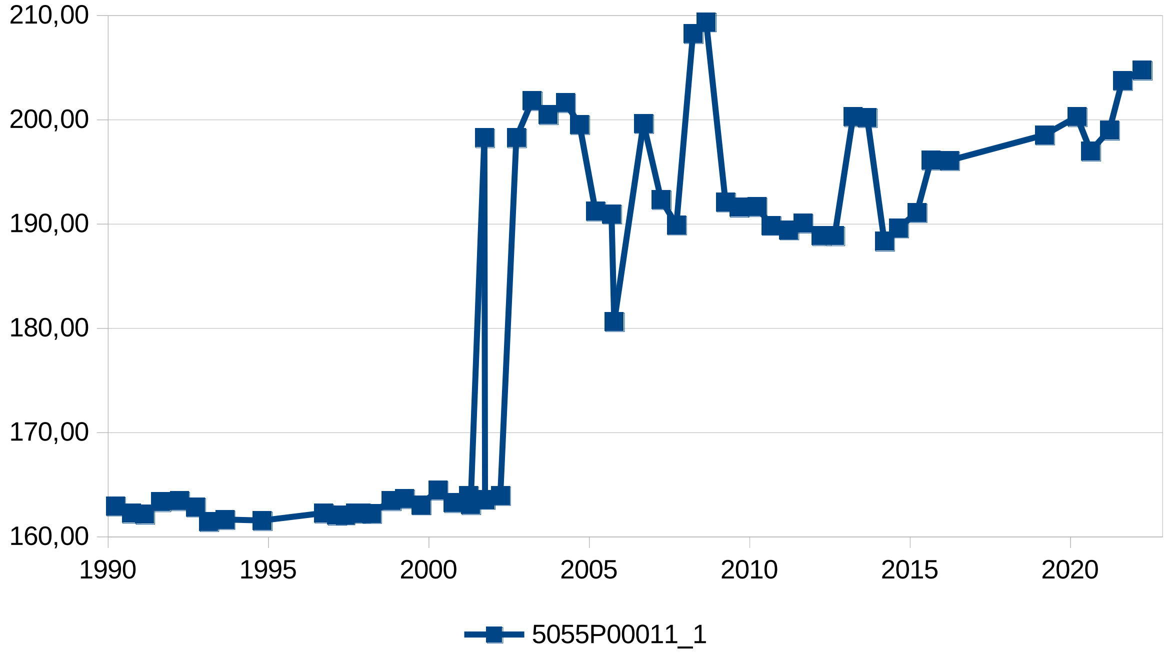

Fig. 59. The water table changes in the monitoring well No. 5055P00011_1

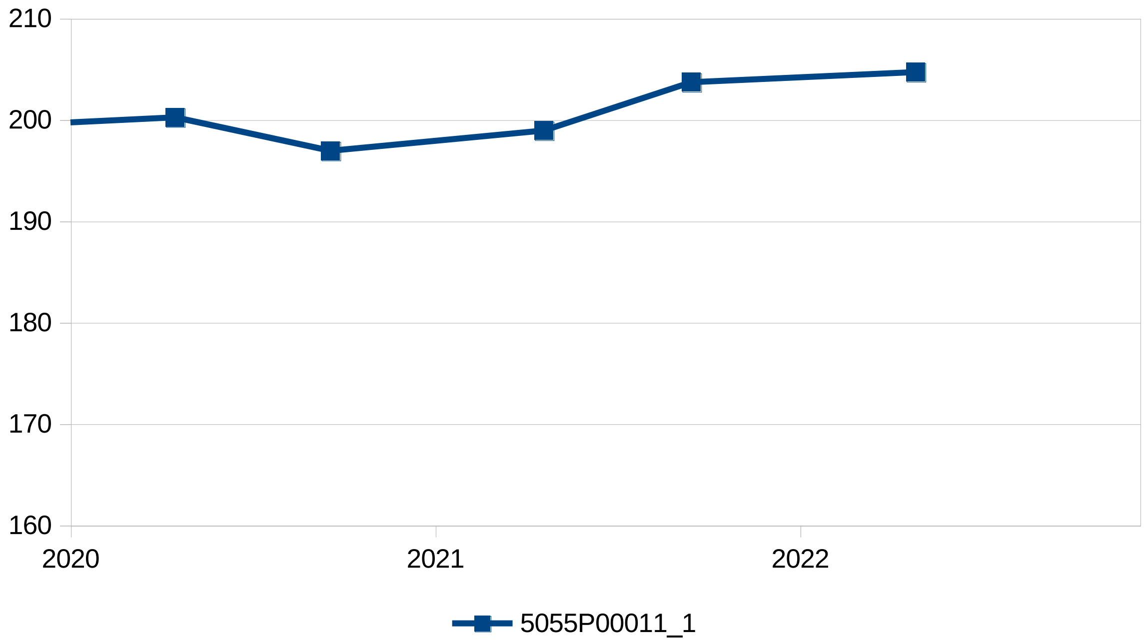

Fig. 60. The water table changes in the monitoring well No. 5055P00011_1

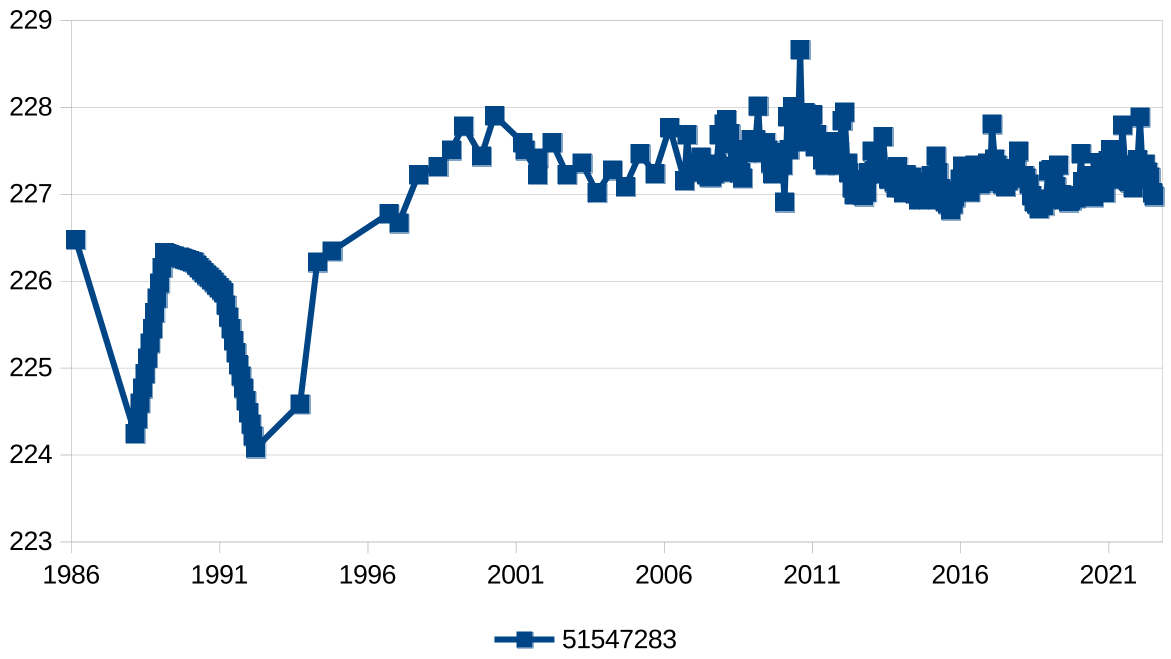

Fig. 61. The water table changes in the monitoring well No. 51547283

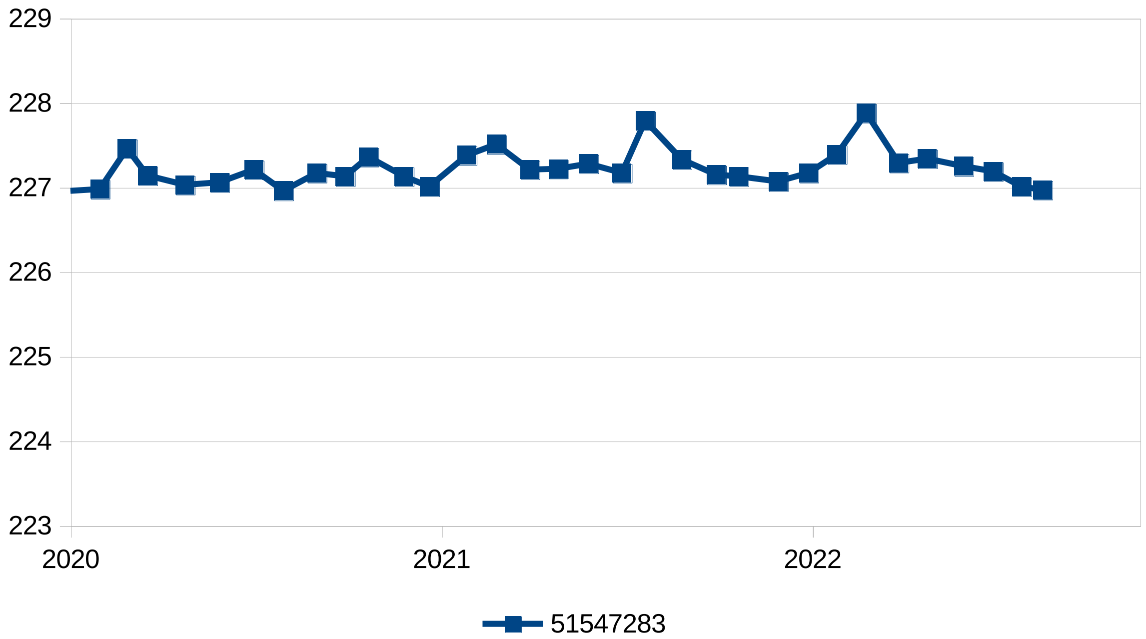

Fig. 62. The water table changes in the monitoring well No. 51547283

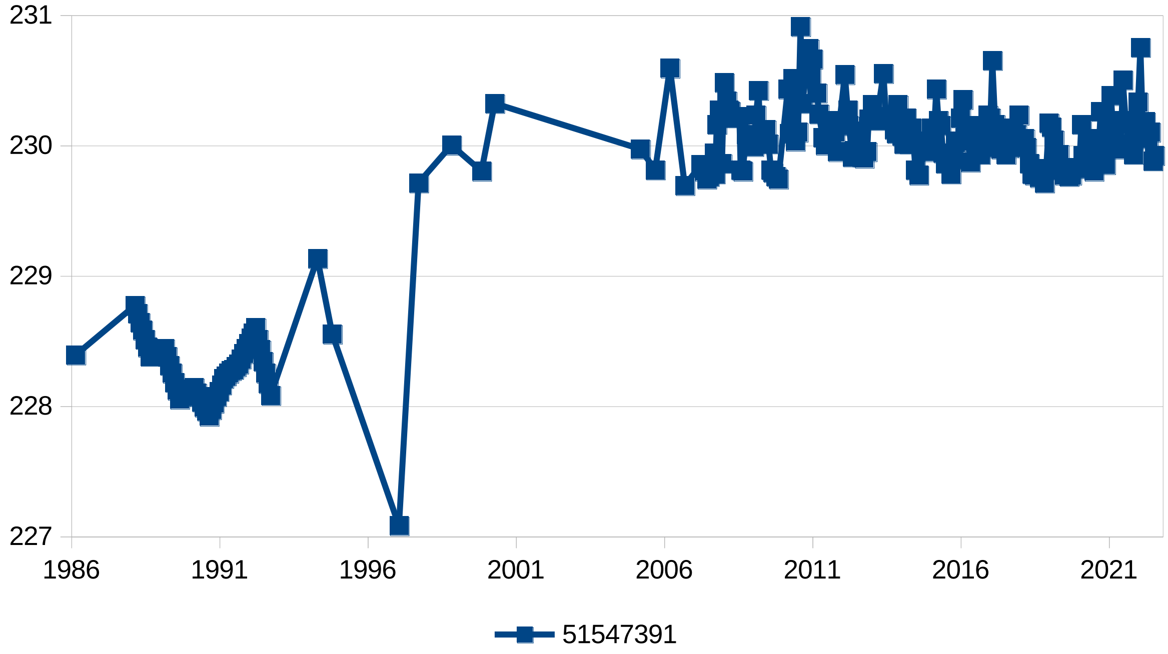

Fig. 63. The water table changes in the monitoring well No. 51547391

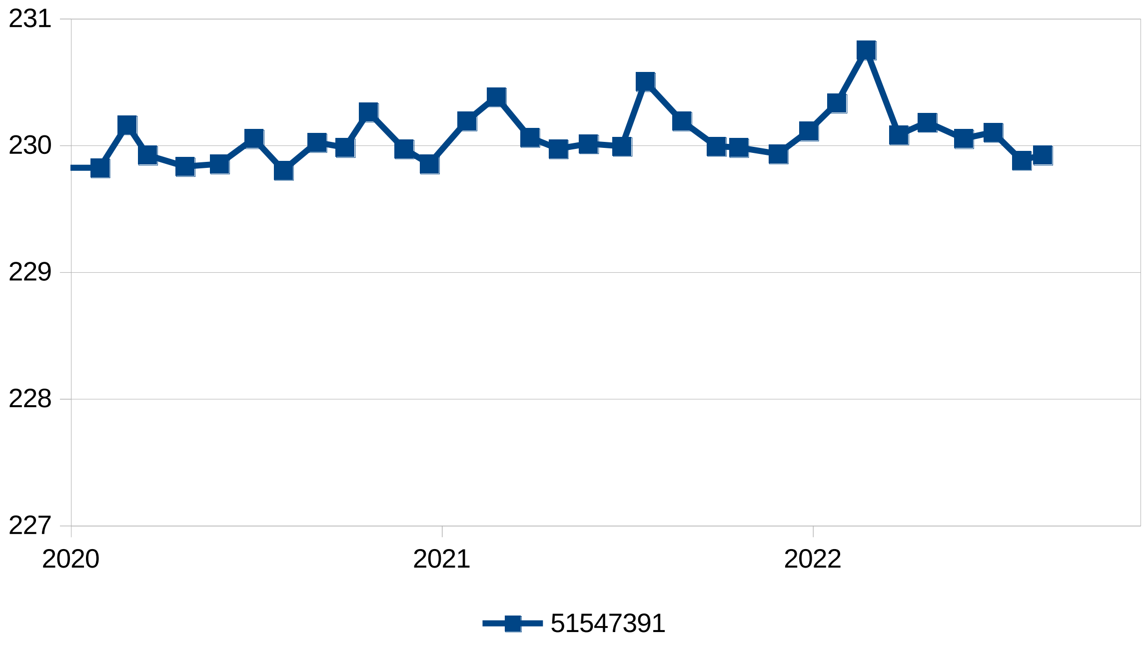

Fig. 64. The water table changes in the monitoring well No. 51547391

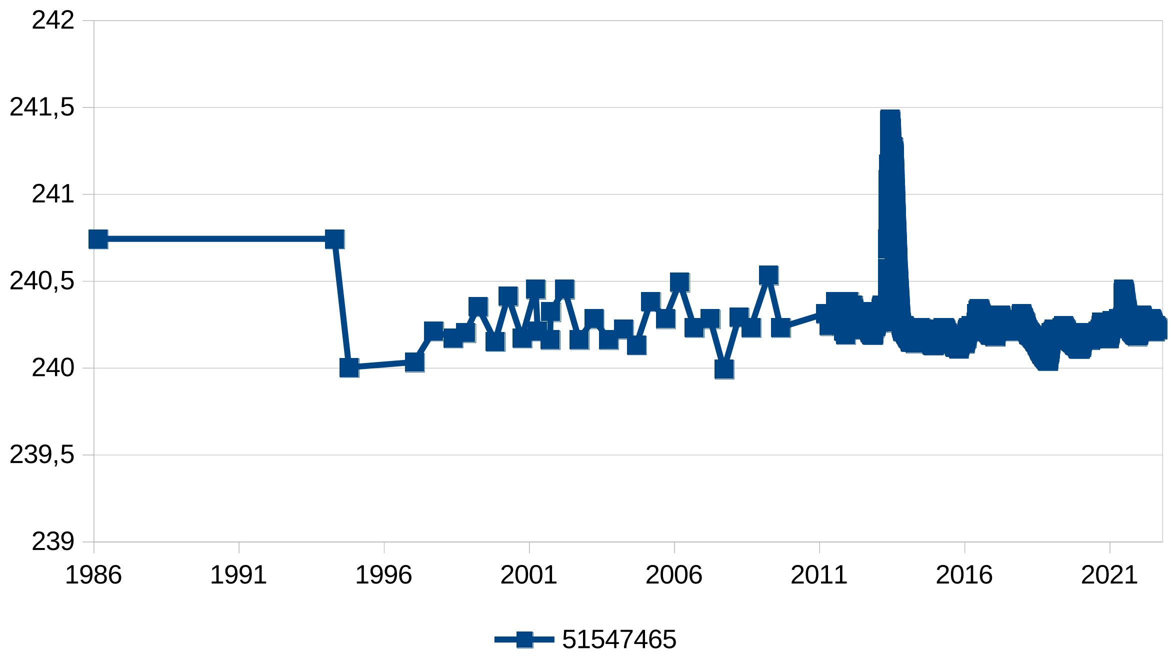

Fig. 65. The water table changes in the monitoring well No. 51547465

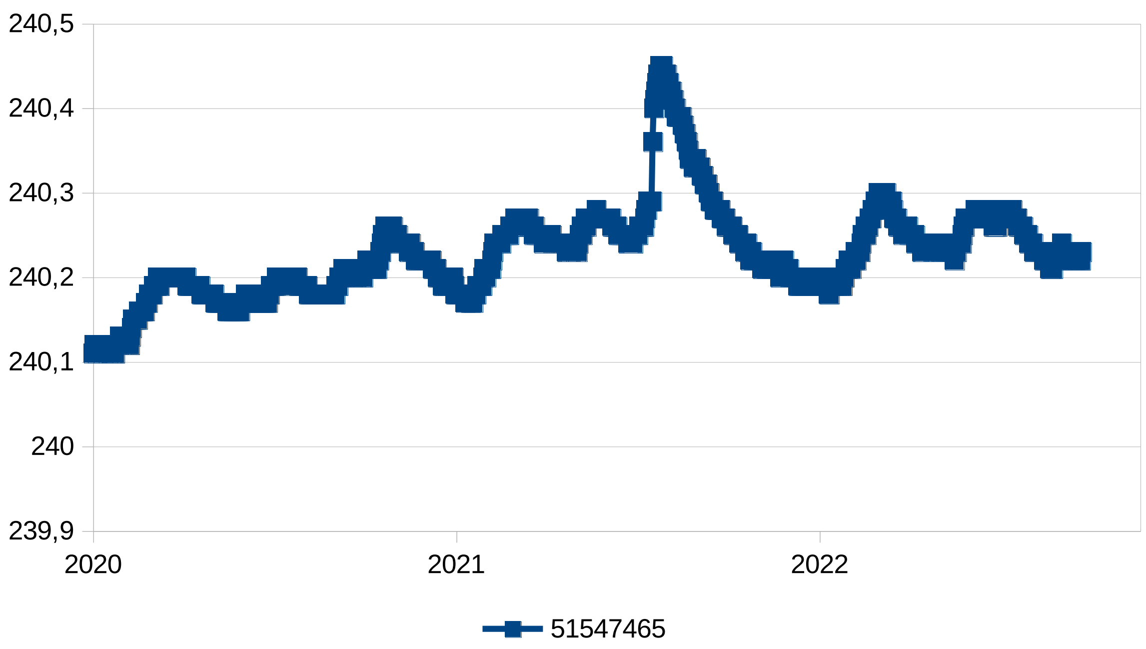

Fig. 66. The water table changes in the monitoring well No. 51547465

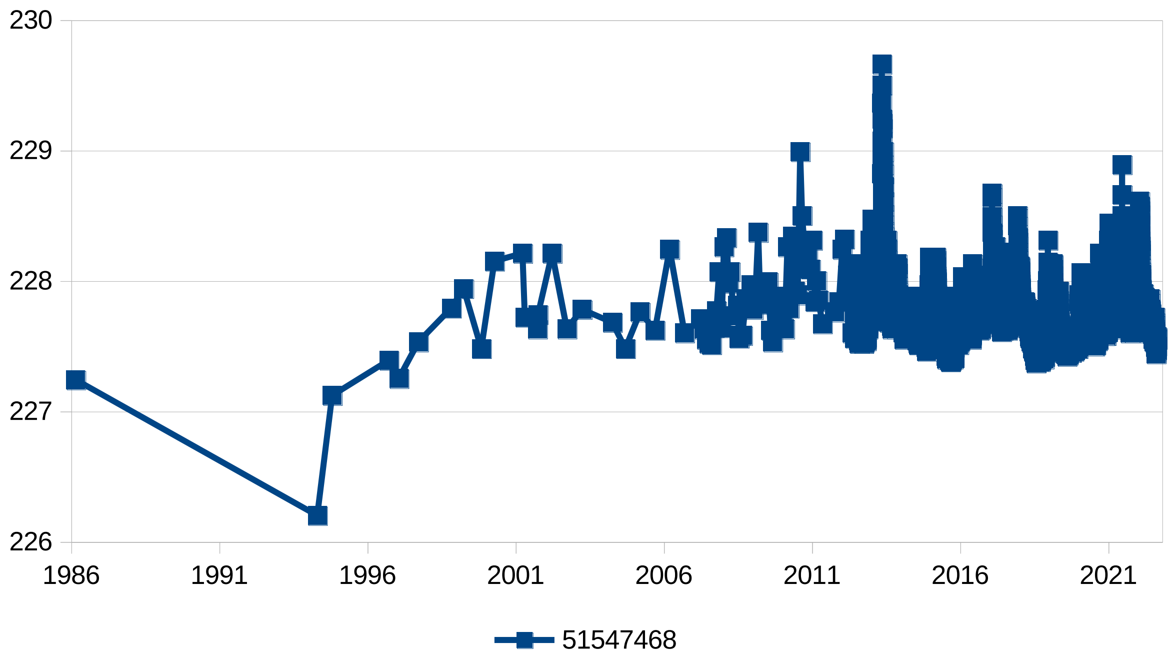

Fig. 67. The water table changes in the monitoring well No. 51547468

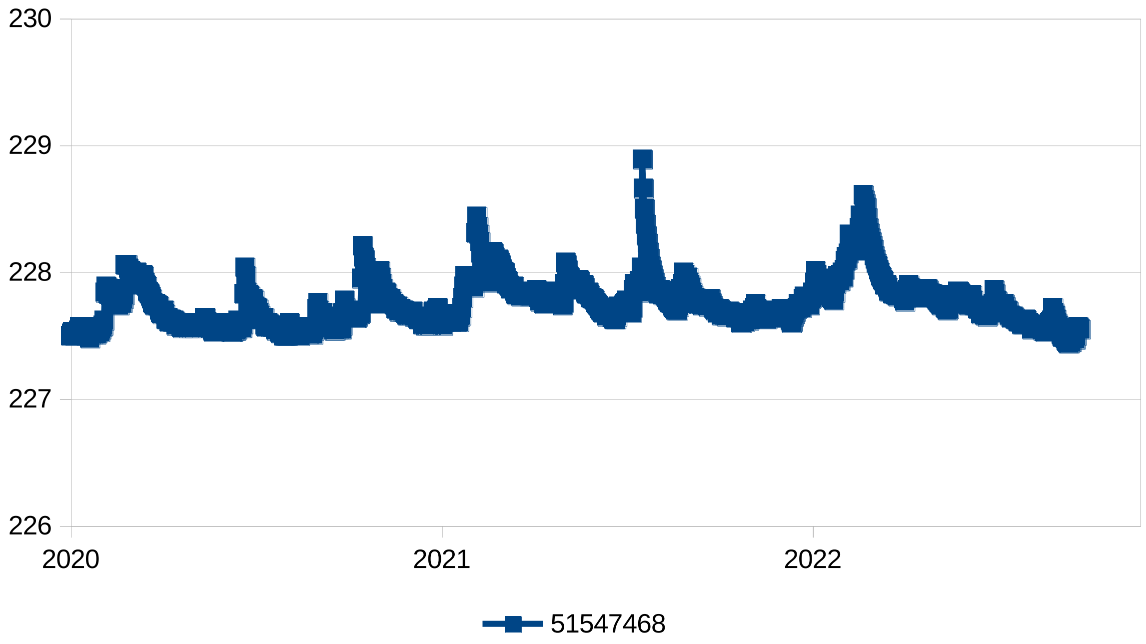

Fig. 68. The water table changes in the monitoring well No. 51547468

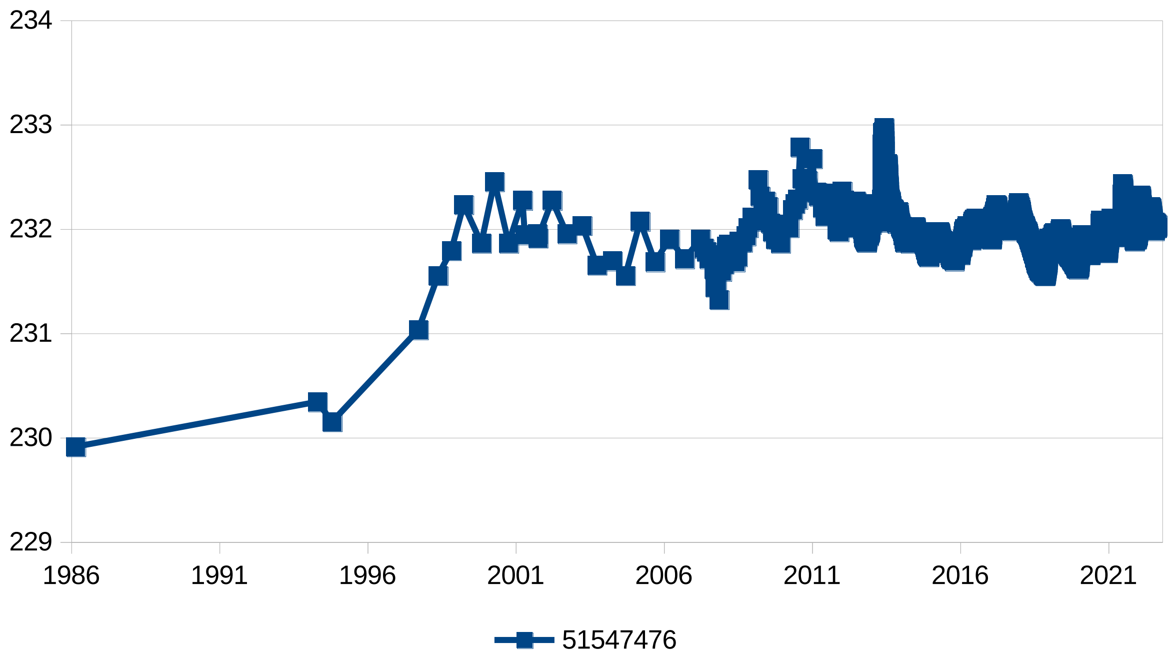

Fig. 69. The water table changes in the monitoring well No. 51547476

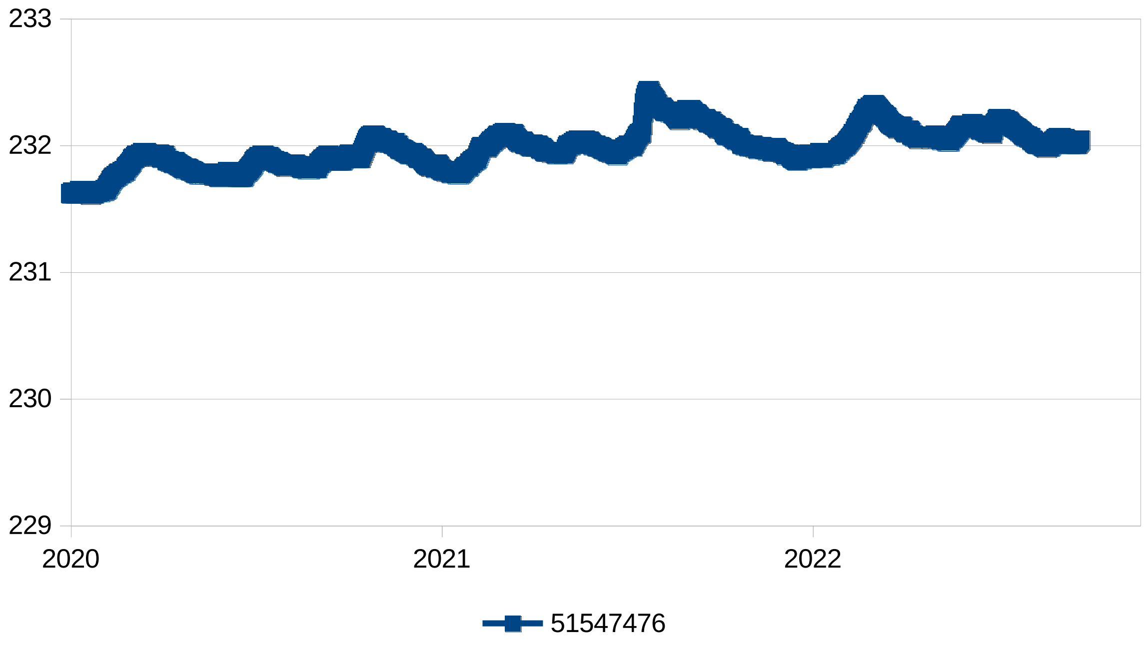

Fig. 70. The water table changes in the monitoring well No. 51547476

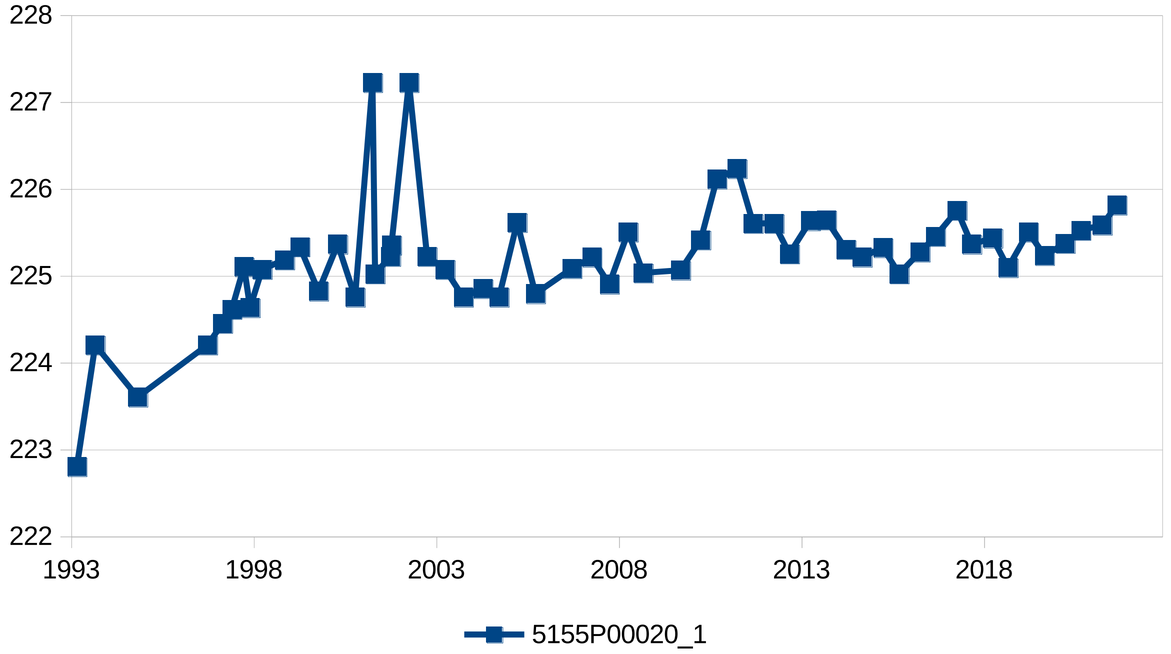

Fig. 71. The water table changes in the monitoring well No. 5155P00020_1

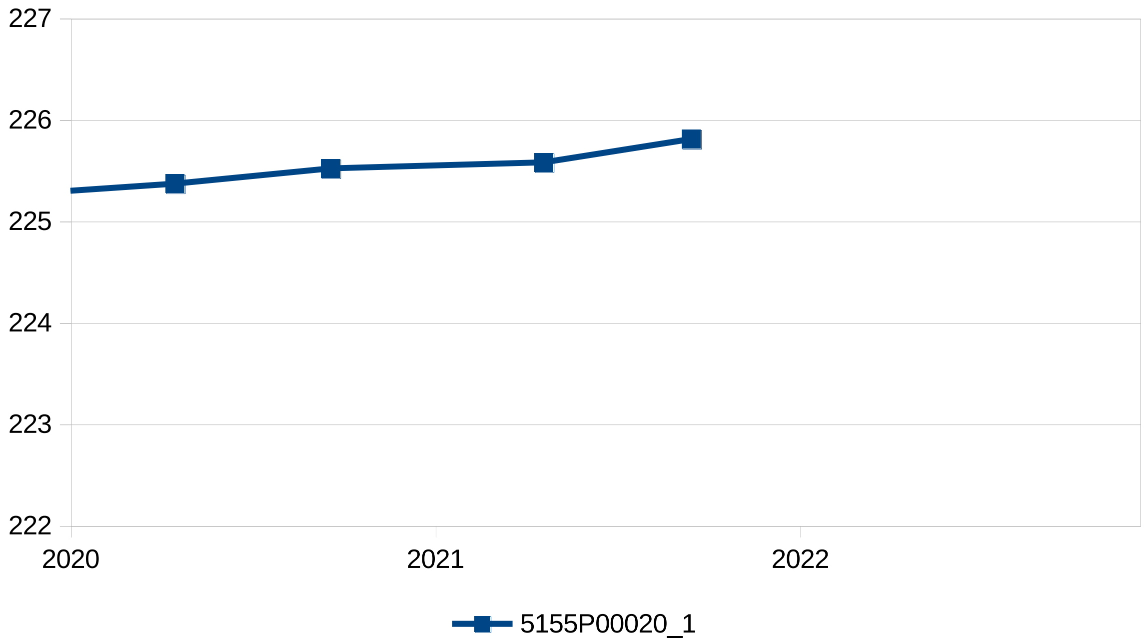

Fig. 72. The water table changes in the monitoring well No. 5155P00020_1

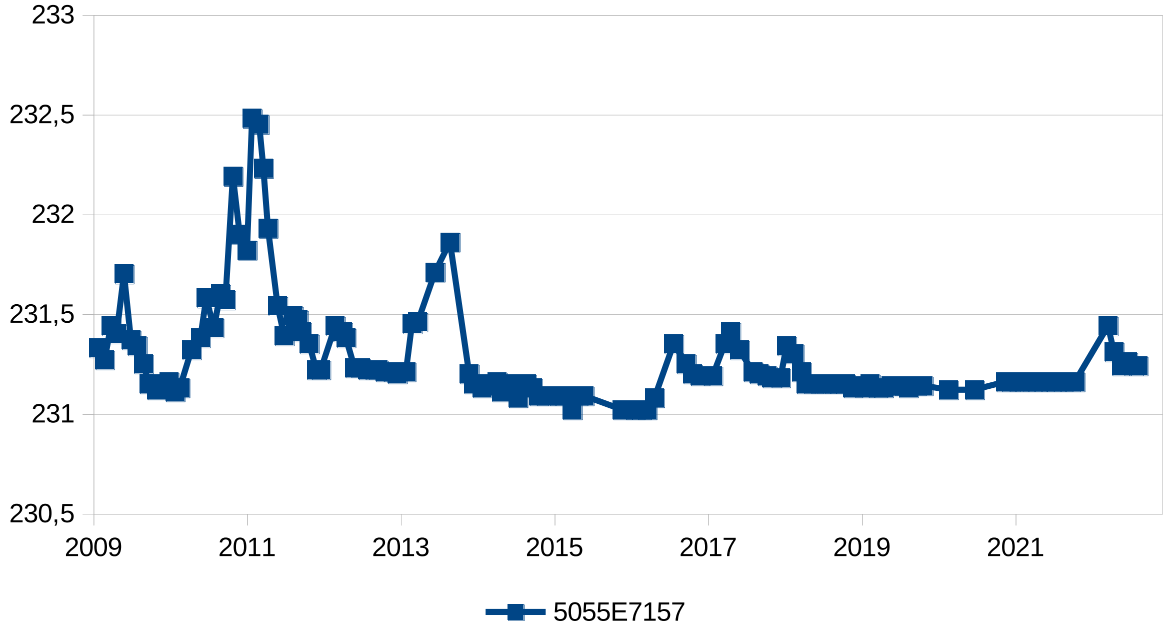

Fig. 73. The water table changes in the monitoring well No. 5055E7157

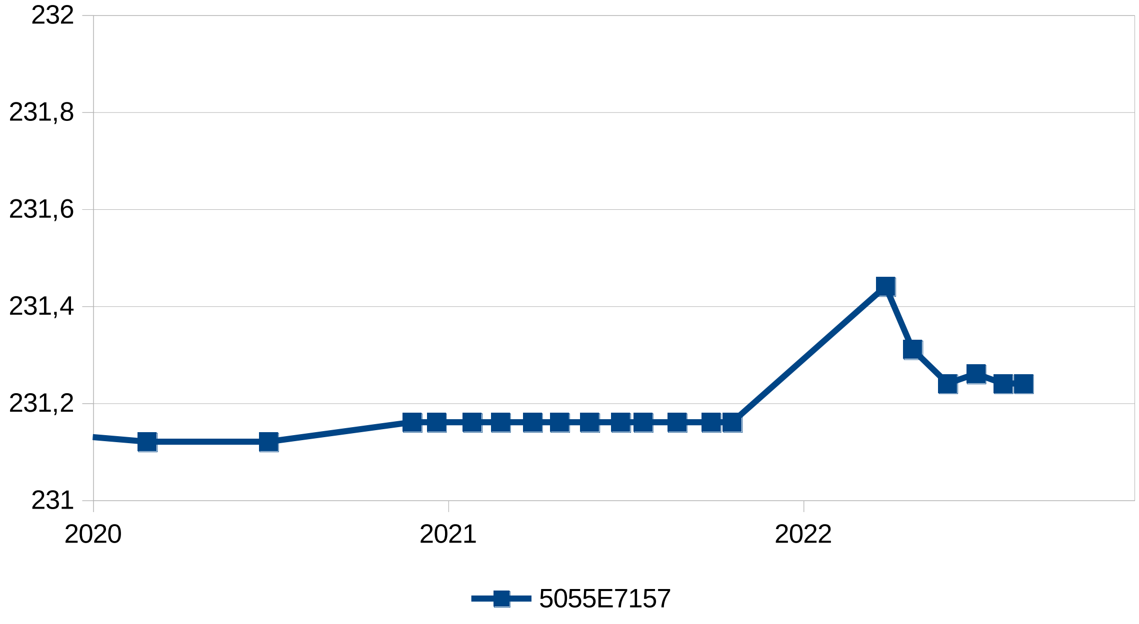

Fig. 74. The water table changes in the monitoring well No. 5055E7157

GWL 00

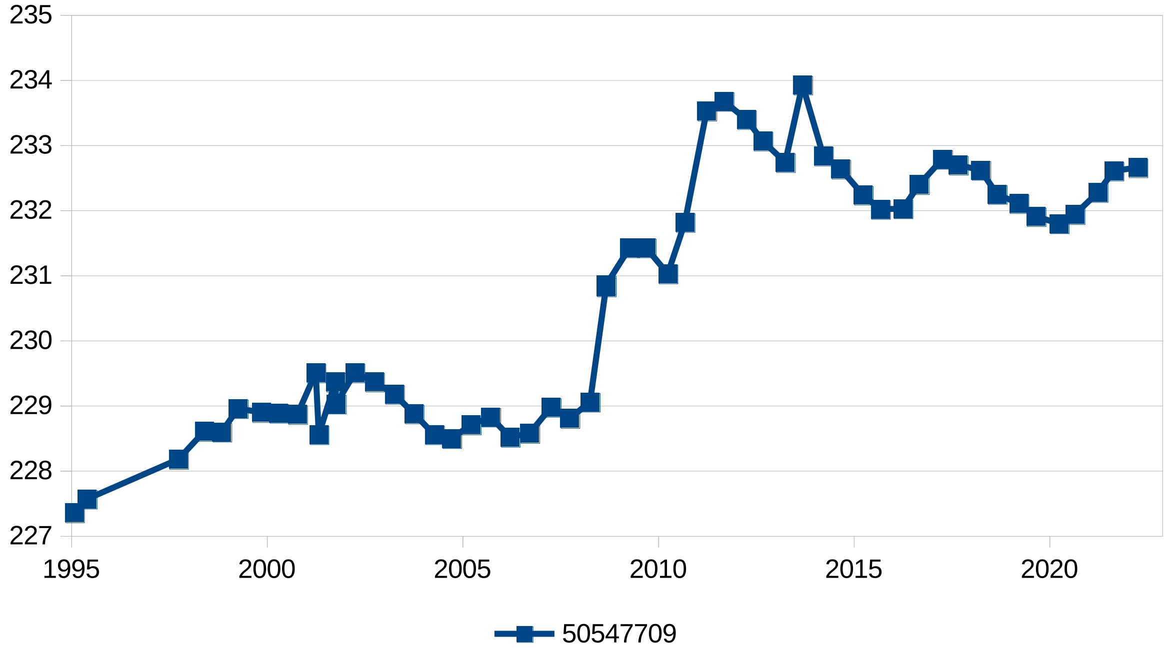

Fig. 75. The water table changes in the monitoring well No. 50547709

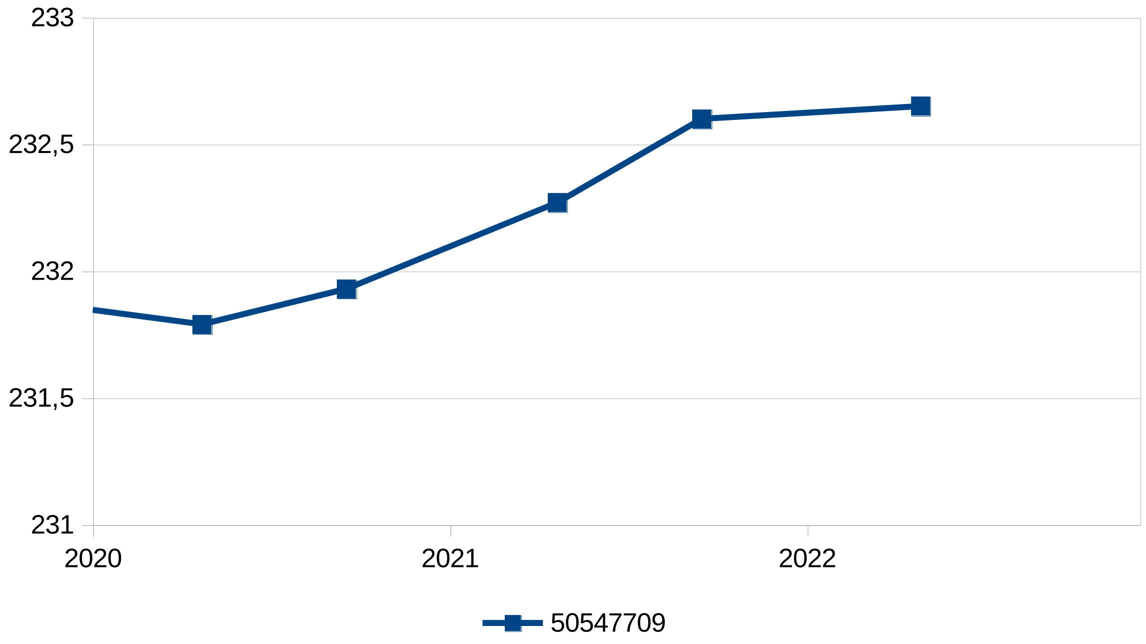

Fig. 76. The water table changes in the monitoring well No. 50547709

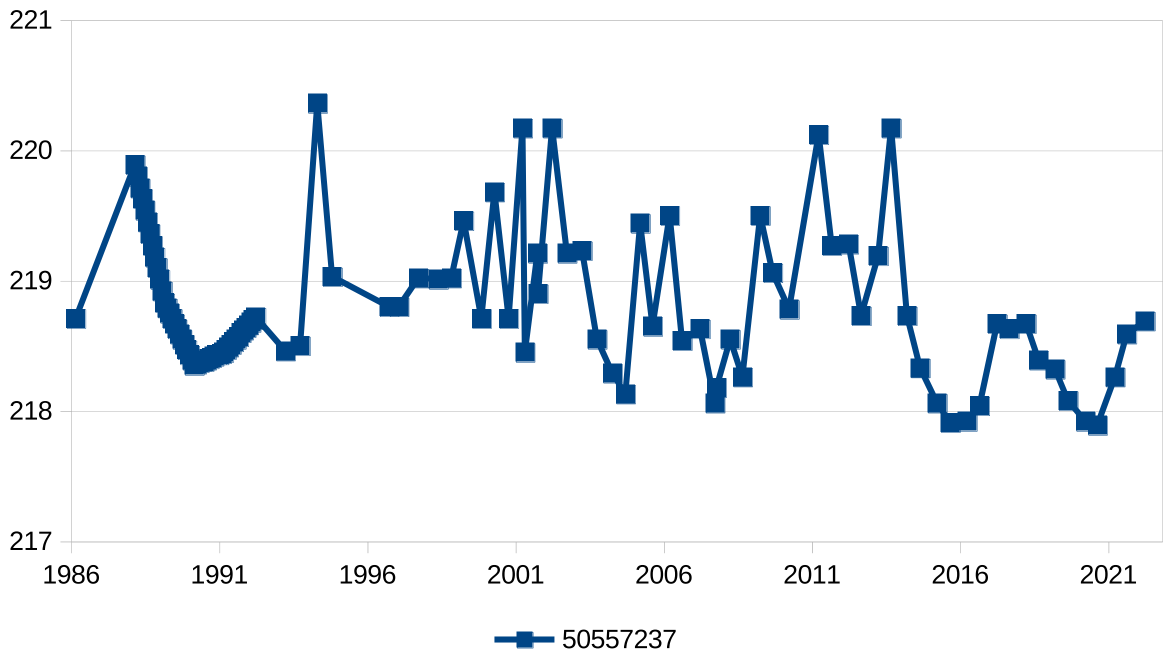

Fig. 77. The water table changes in the monitoring well No. 50557237

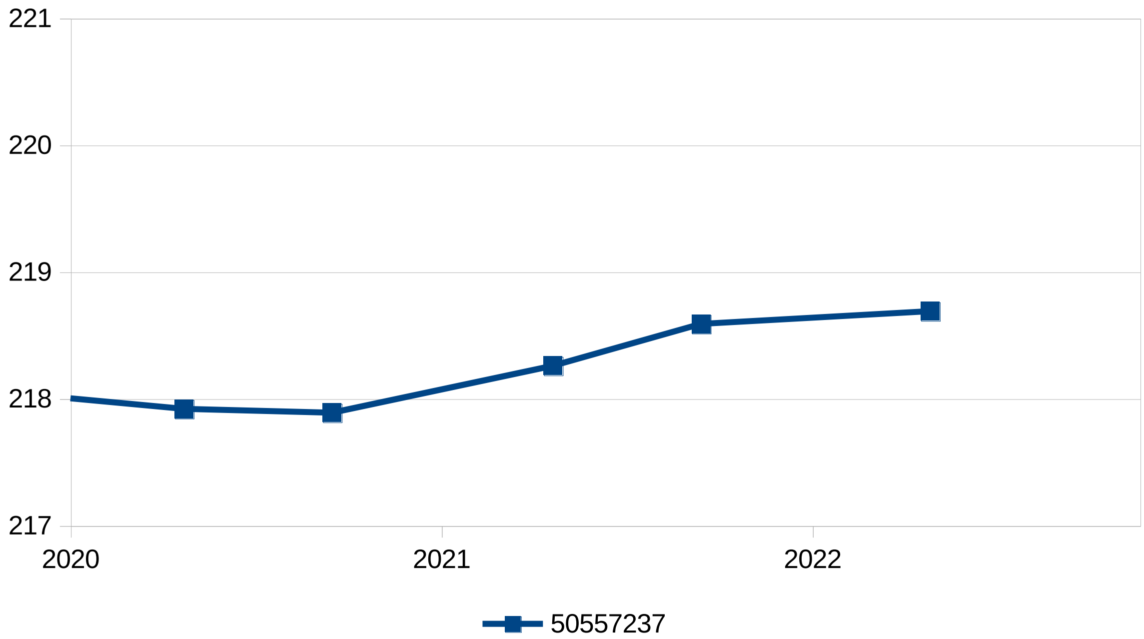

Fig. 78. The water table changes in the monitoring well No. 50557237

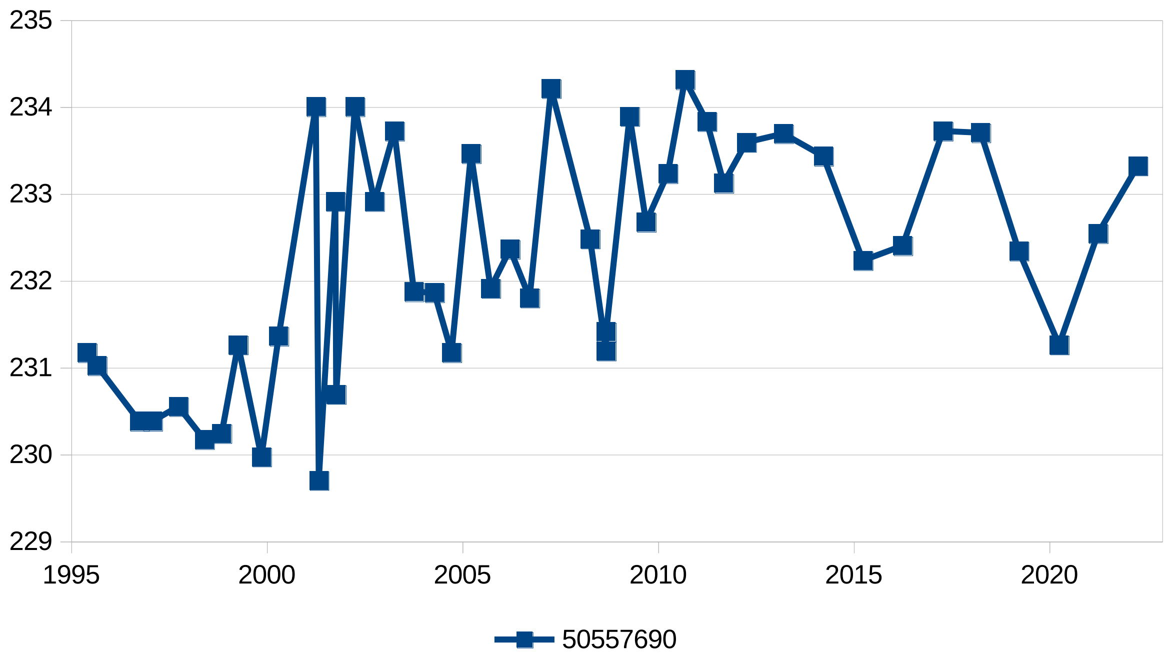

Fig. 79. The water table changes in the monitoring well No. 50557690

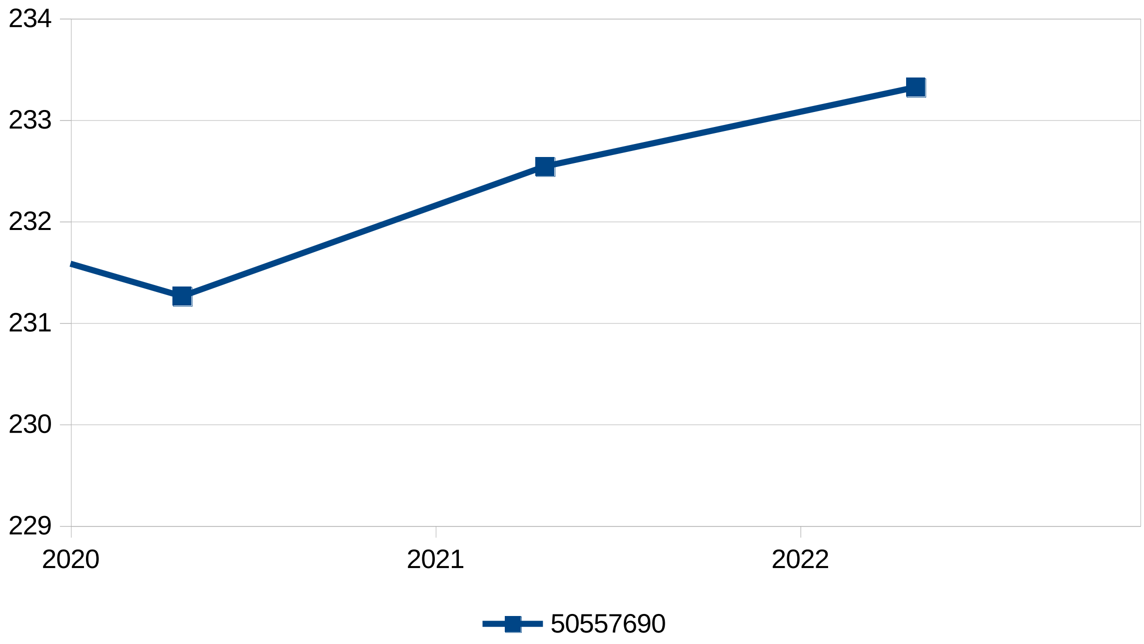

Fig. 80. The water table changes in the monitoring well No. 50557690

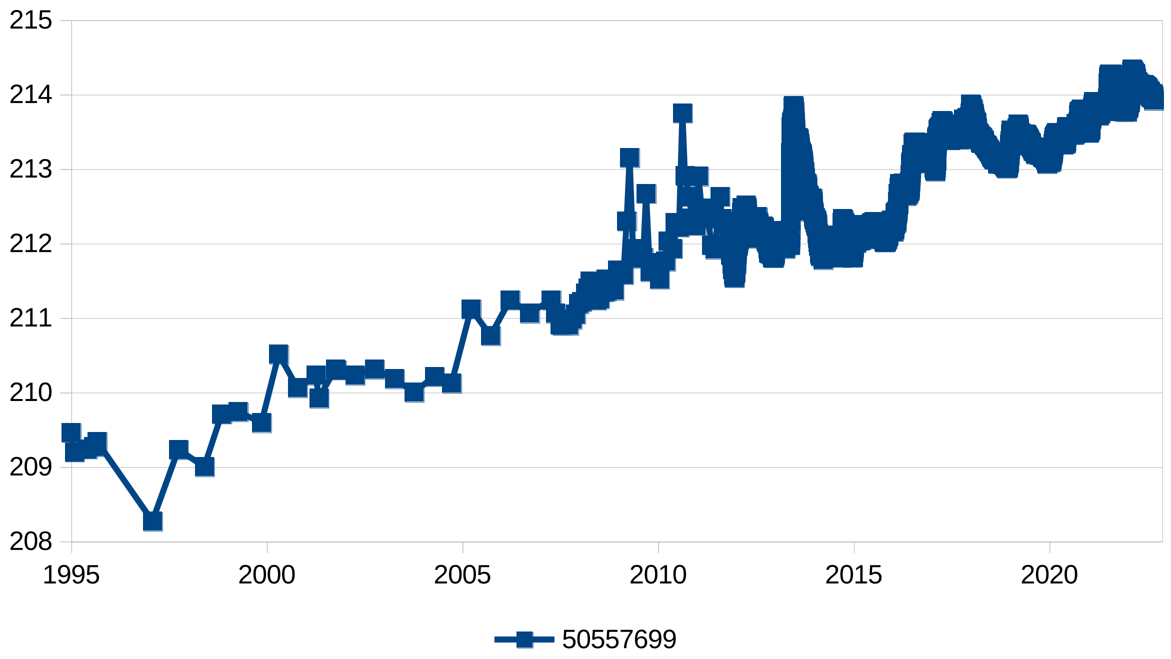

Fig. 81. The water table changes in the monitoring well No. 50557699

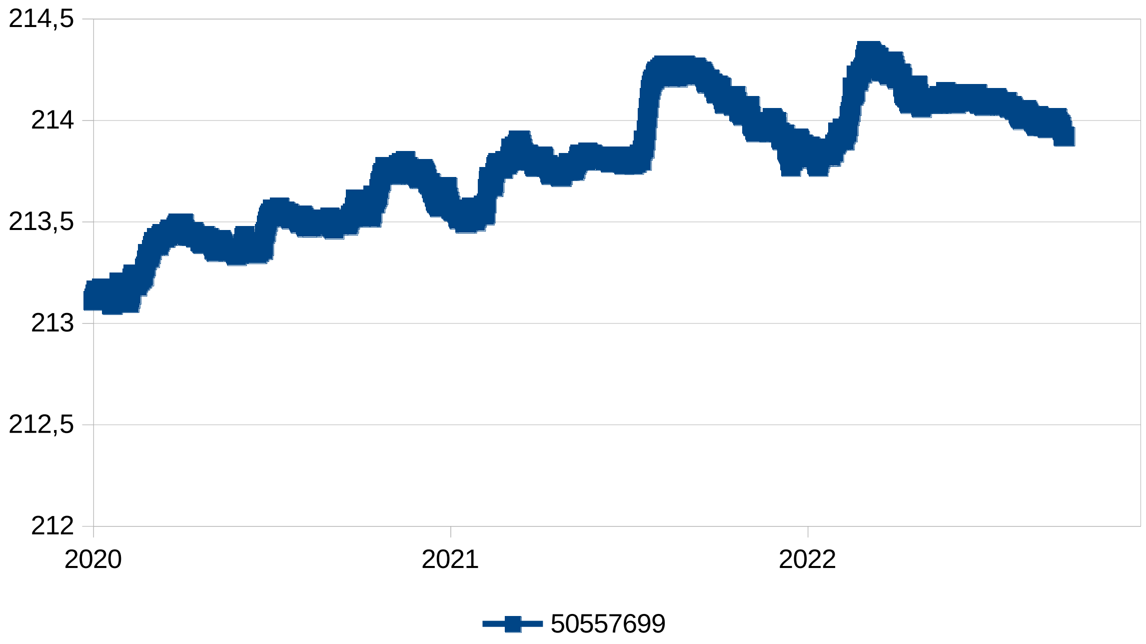

Fig. 82. The water table changes in the monitoring well No. 50557699

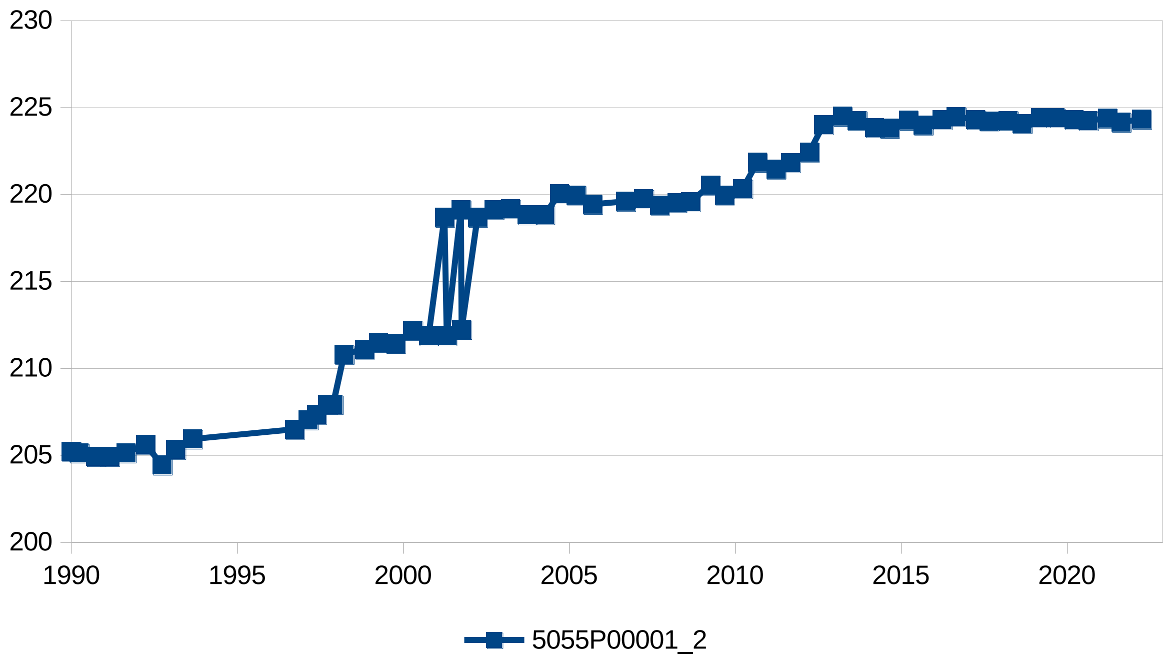

Fig. 83. The water table changes in the monitoring well No. 5055P00001_2

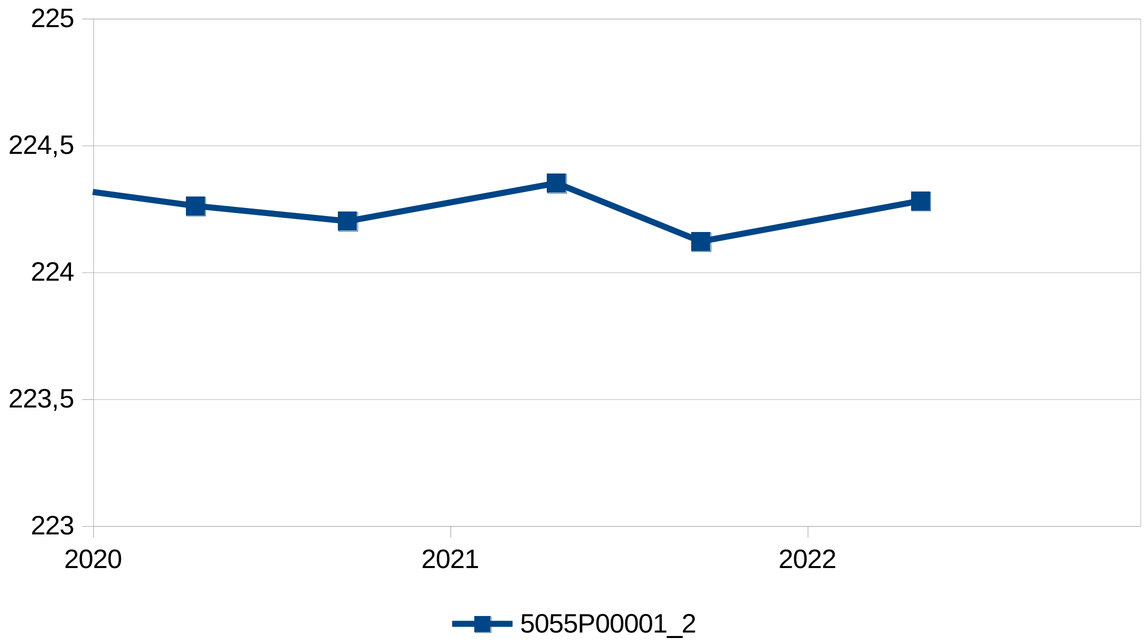

Fig. 84. The water table changes in the monitoring well No. 5055P00001_2

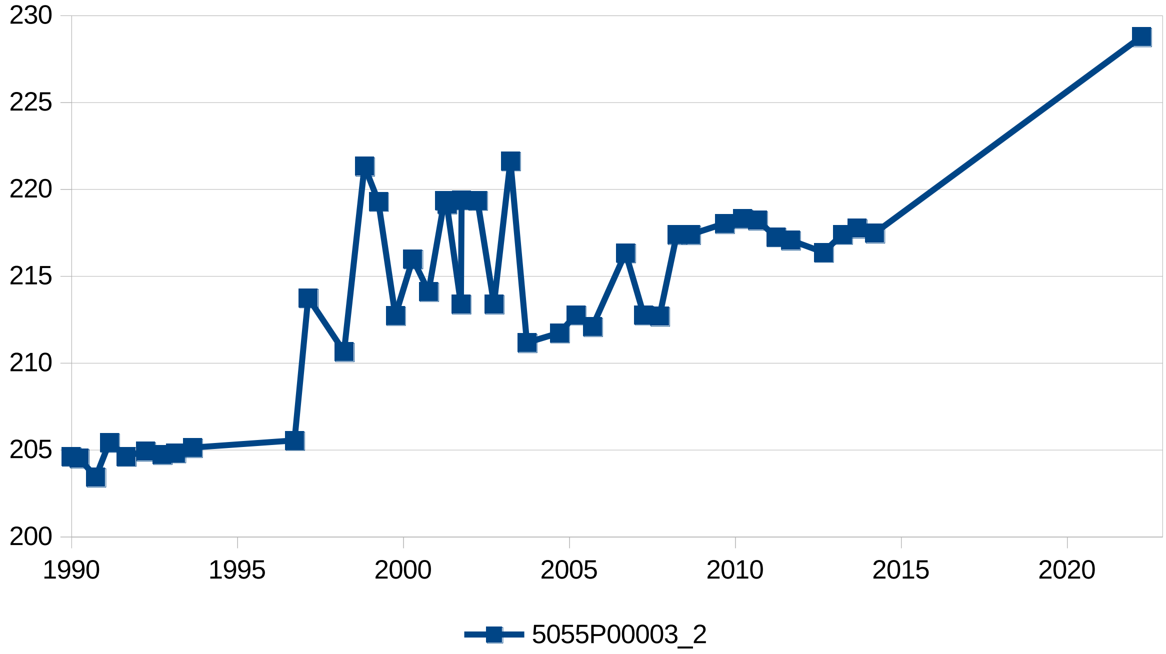

Fig. 85. The water table changes in the monitoring well No. 5055P00003_2

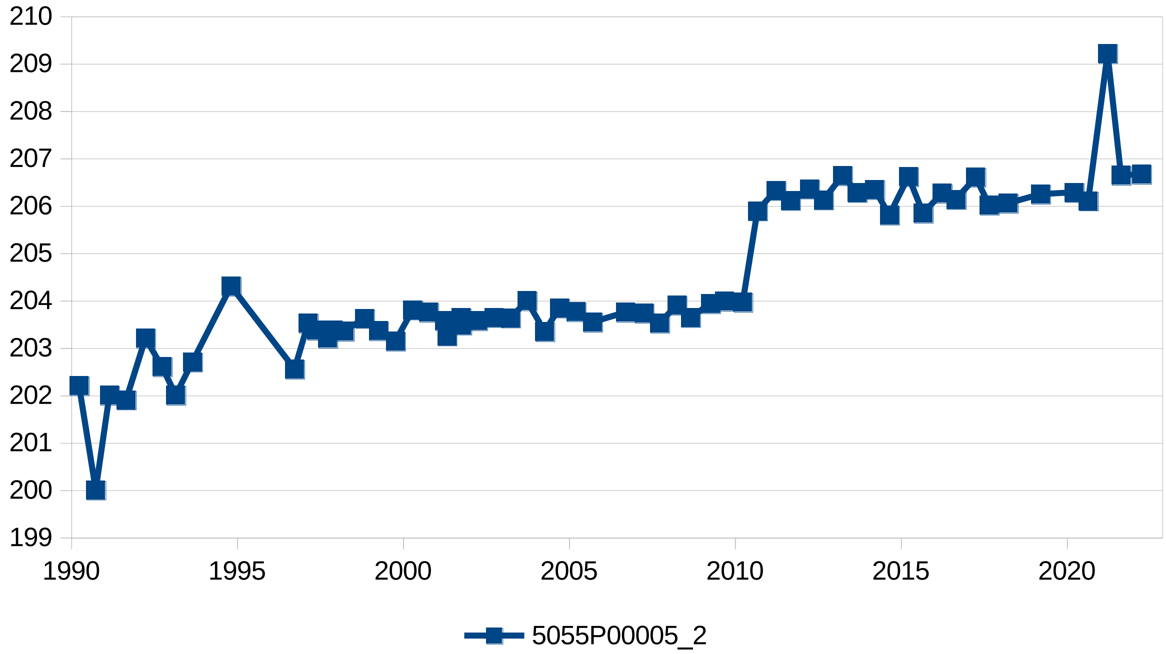

Fig. 86. The water table changes in the monitoring well No. 5055P00005_2

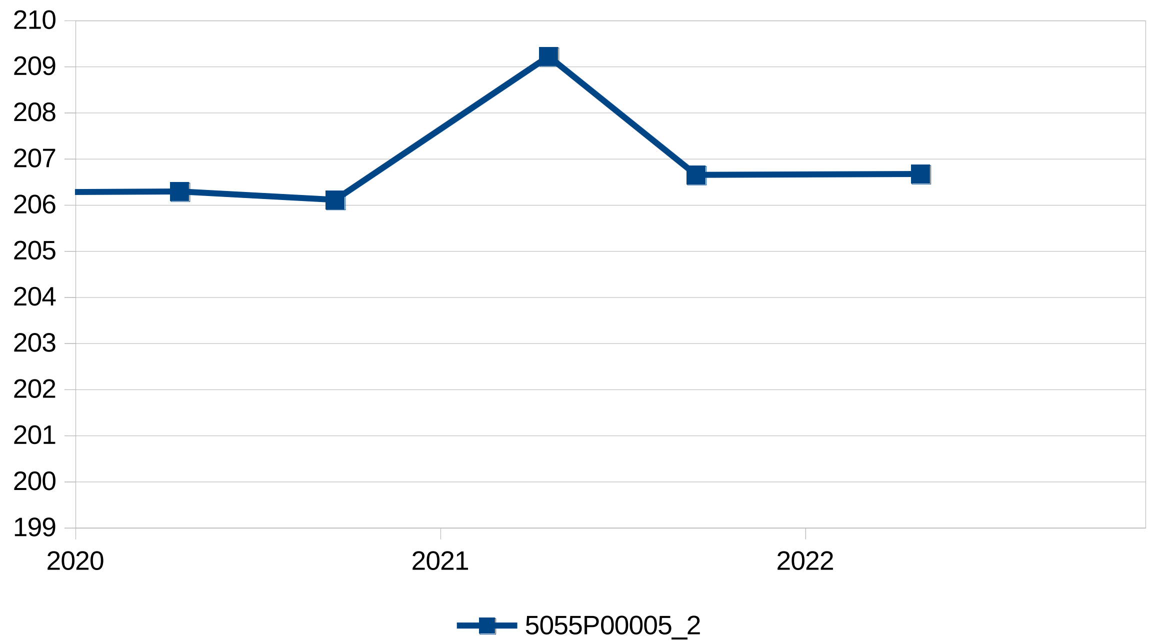

Fig. 87. The water table changes in the monitoring well No. 5055P00005_2

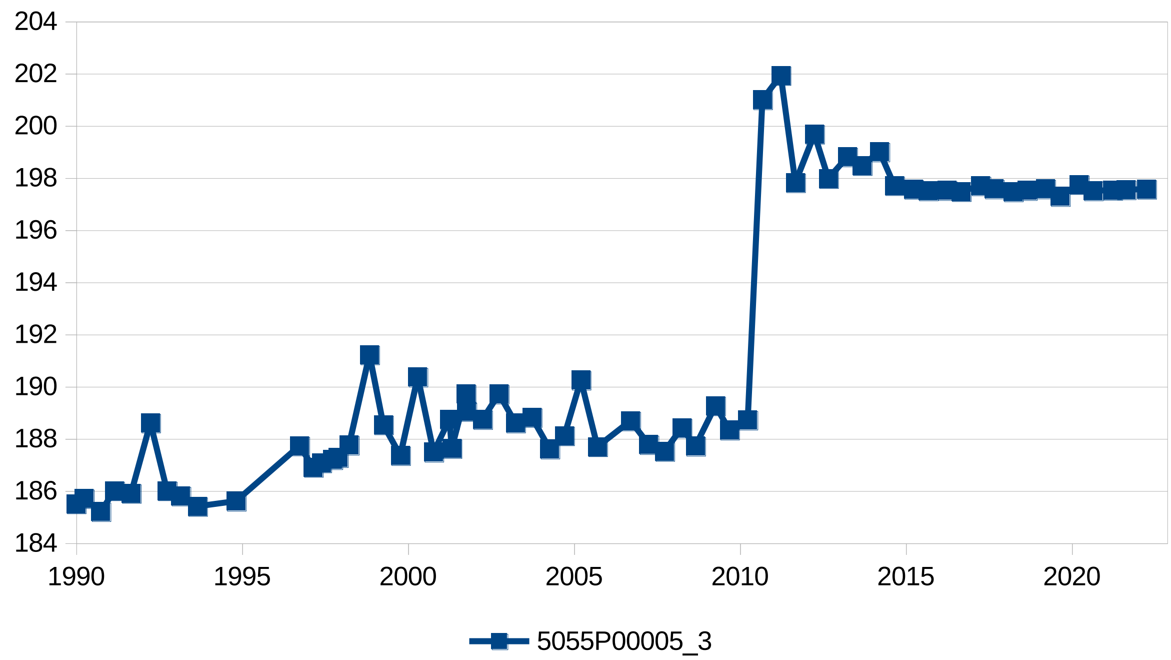

Fig. 88. The water table changes in the monitoring well No. 5055P00005_3

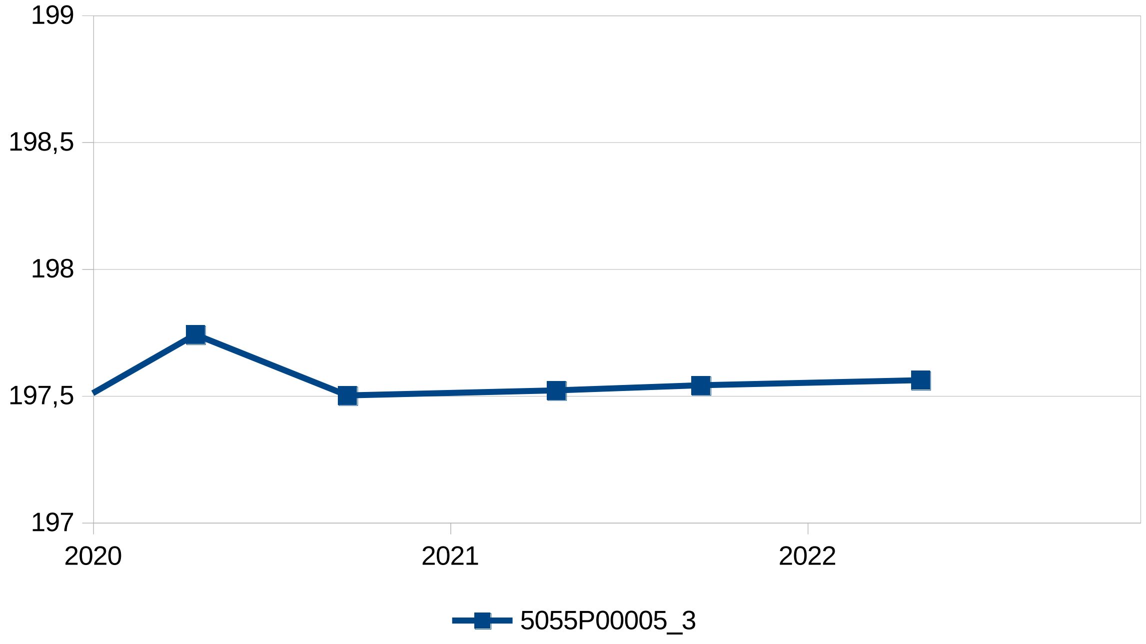

Fig. 89. The water table changes in the monitoring well No. 5055P00005_3

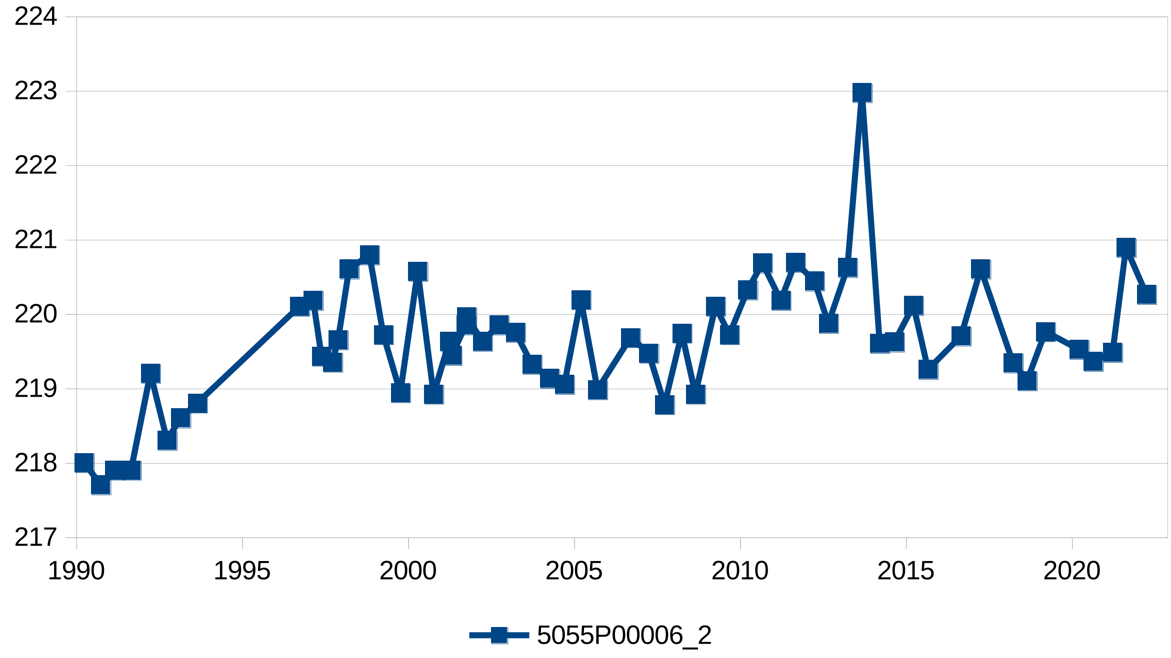

Fig. 90. The water table changes in the monitoring well No. 5055P00006_2

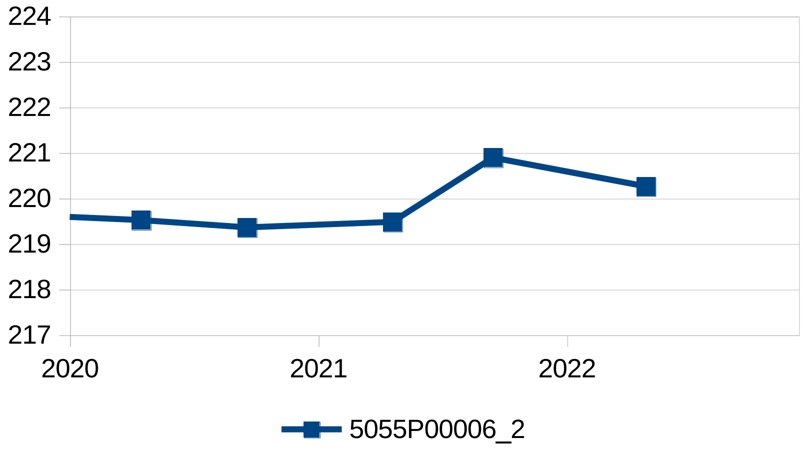

Fig. 91. The water table changes in the monitoring well No. 5055P00006_2

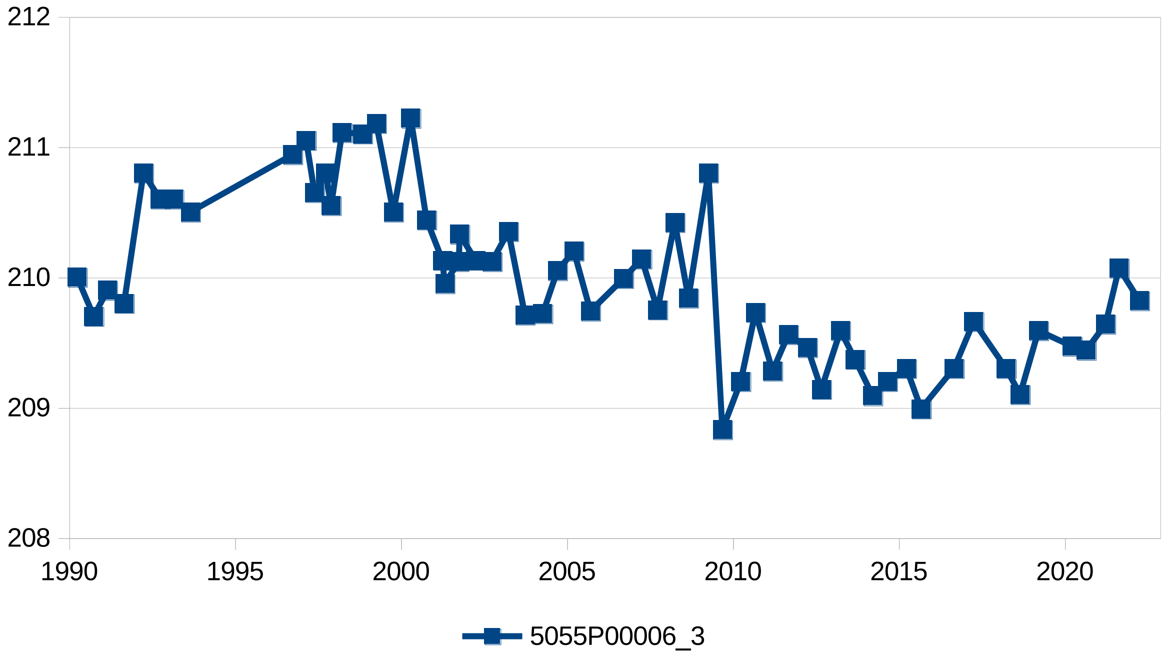

Fig. 92. The water table changes in the monitoring well No. 5055P00006_3

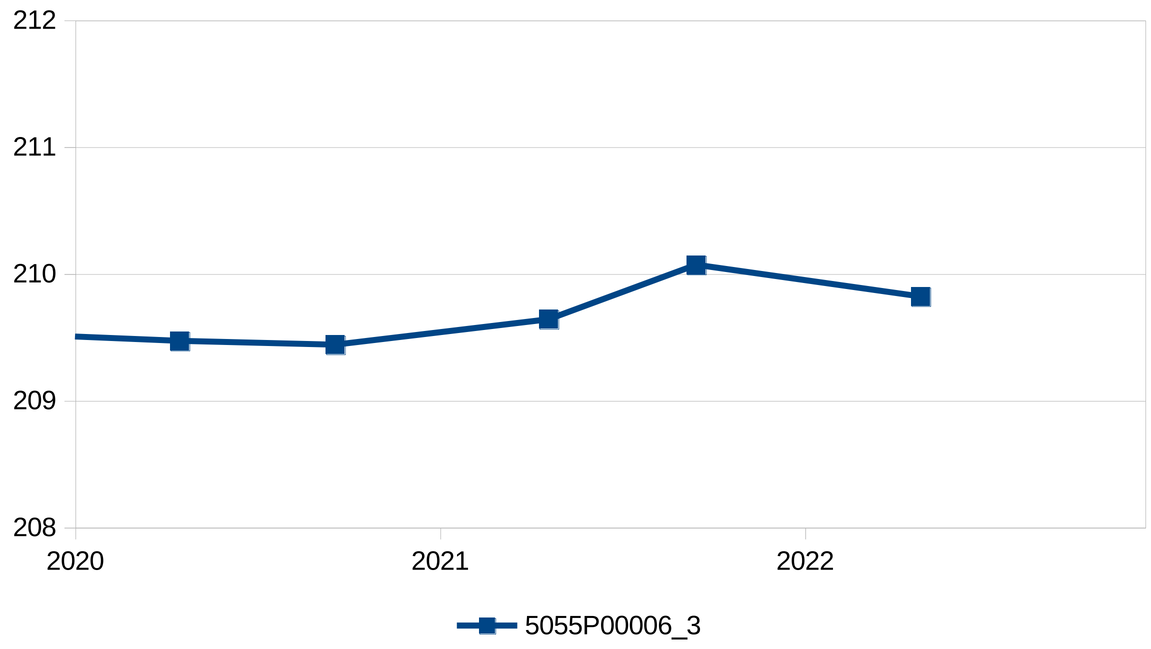

Fig. 93. The water table changes in the monitoring well No. 5055P00006_3

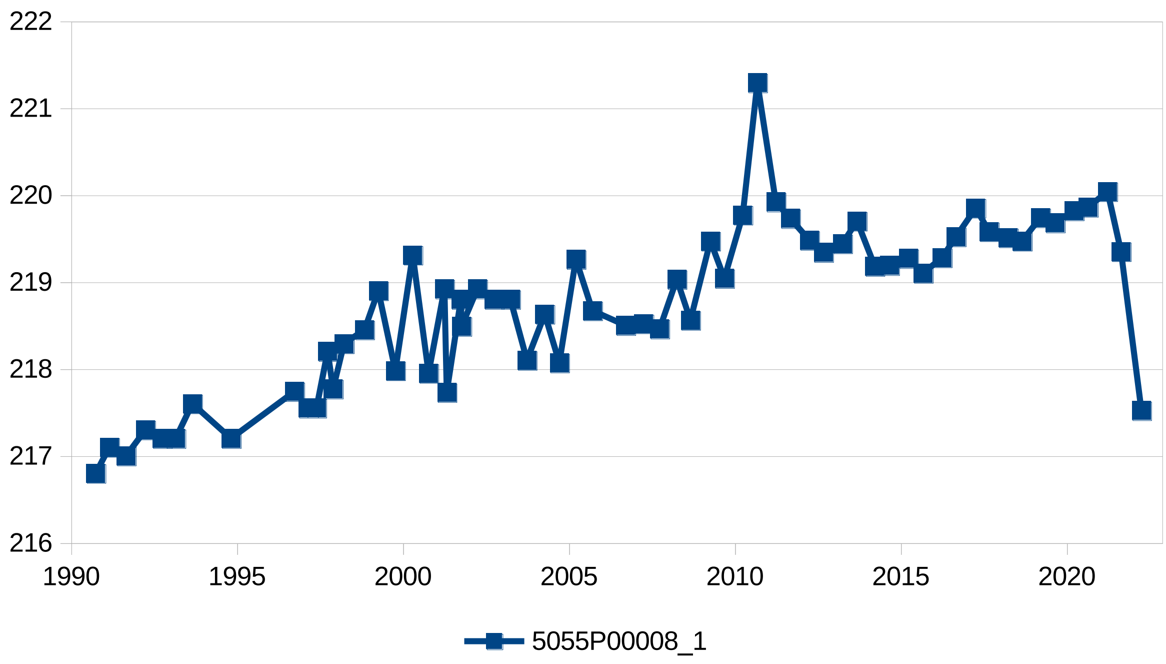

Fig. 94. The water table changes in the monitoring well No. 5055P00008_1

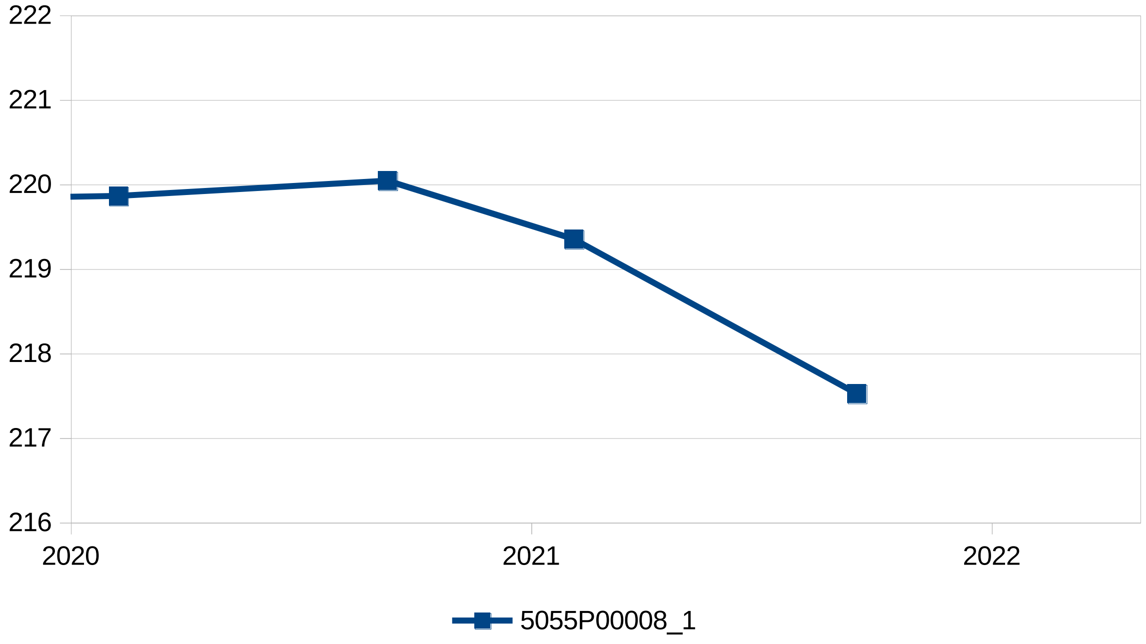

Fig. 95. The water table changes in the monitoring well No. 5055P00008_1

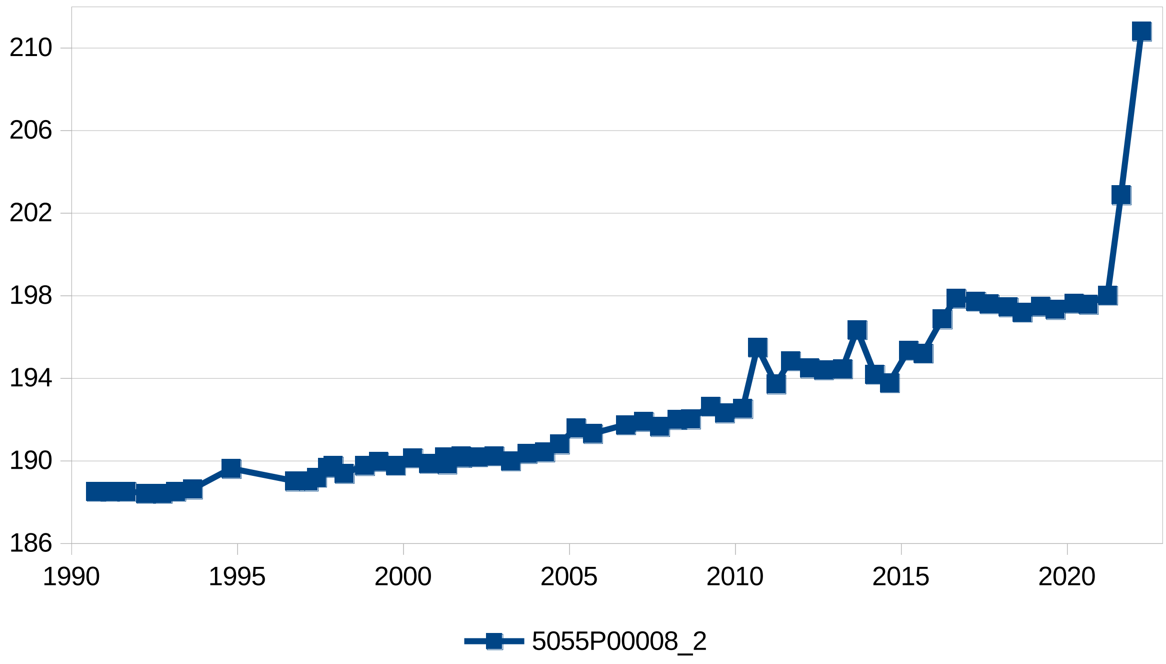

Fig. 96. The water table changes in the monitoring well No. 5055P00008_2

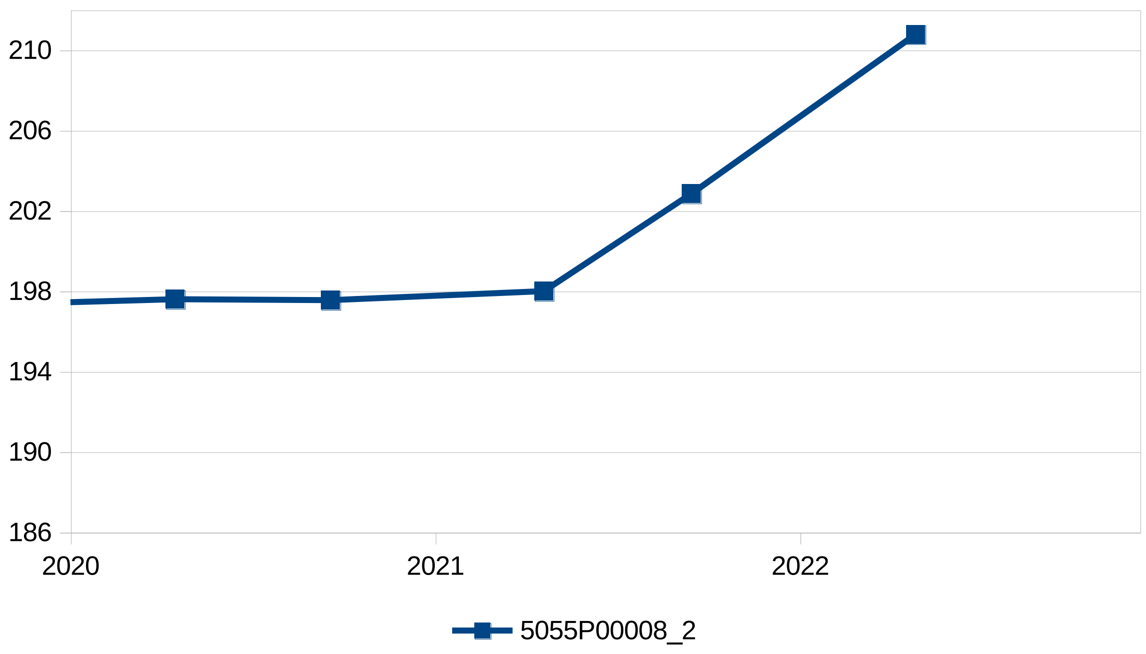

Fig. 97. The water table changes in the monitoring well No. 5055P00008_2

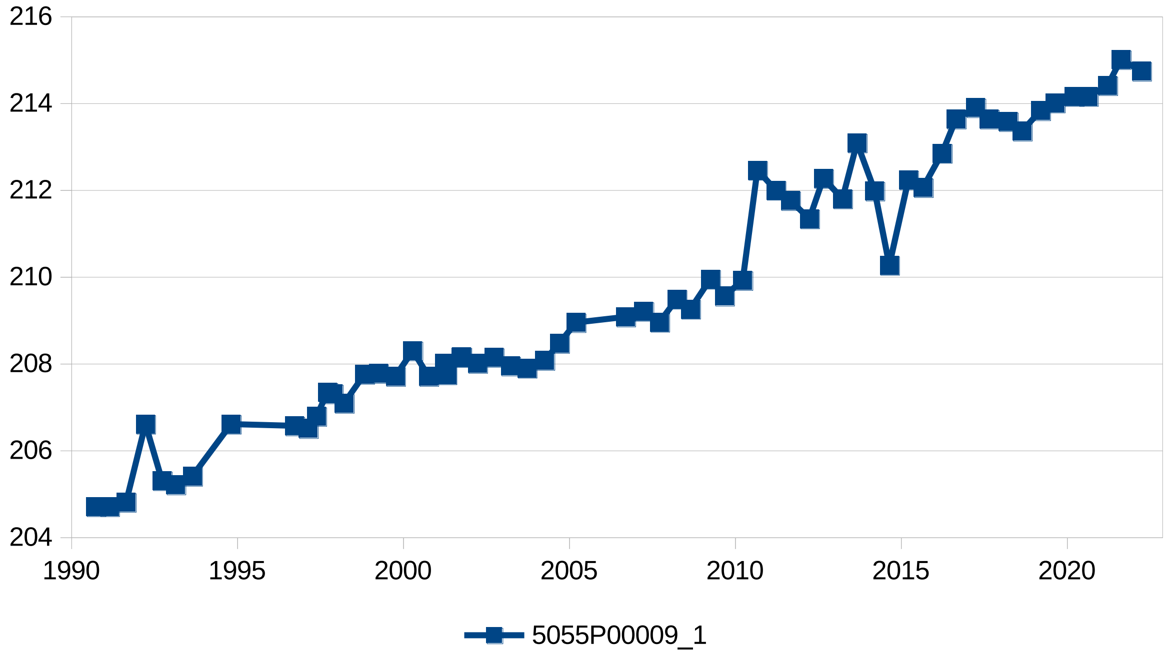

Fig. 98. The water table changes in the monitoring well No. 5055P00009_1

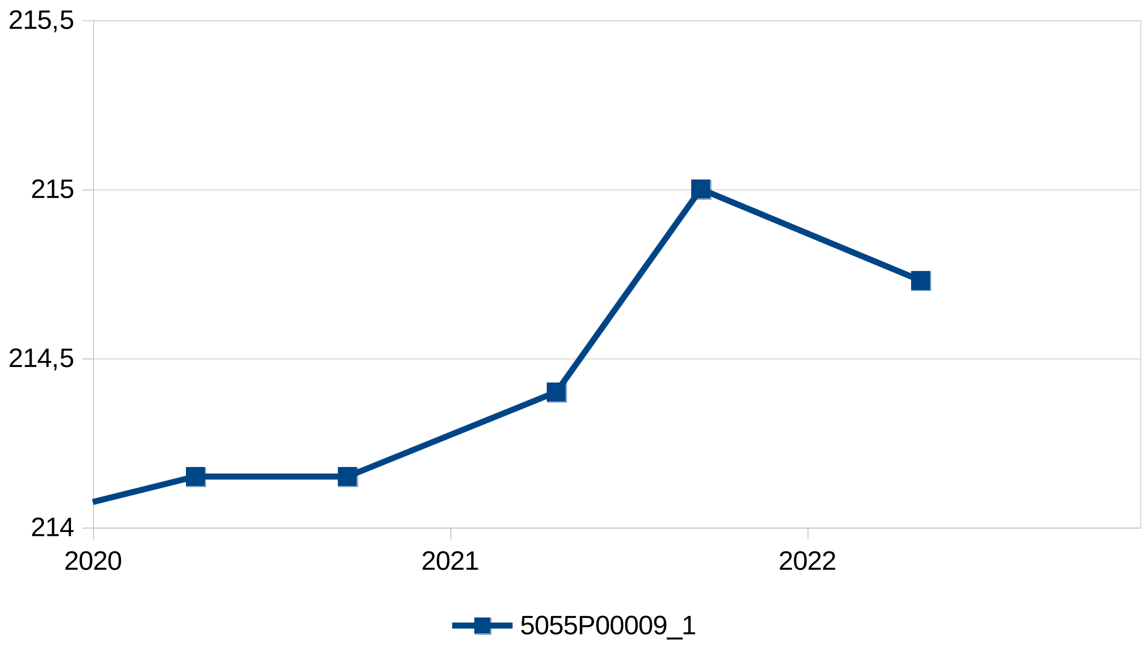

Fig. 99. The water table changes in the monitoring well No. 5055P00009_1

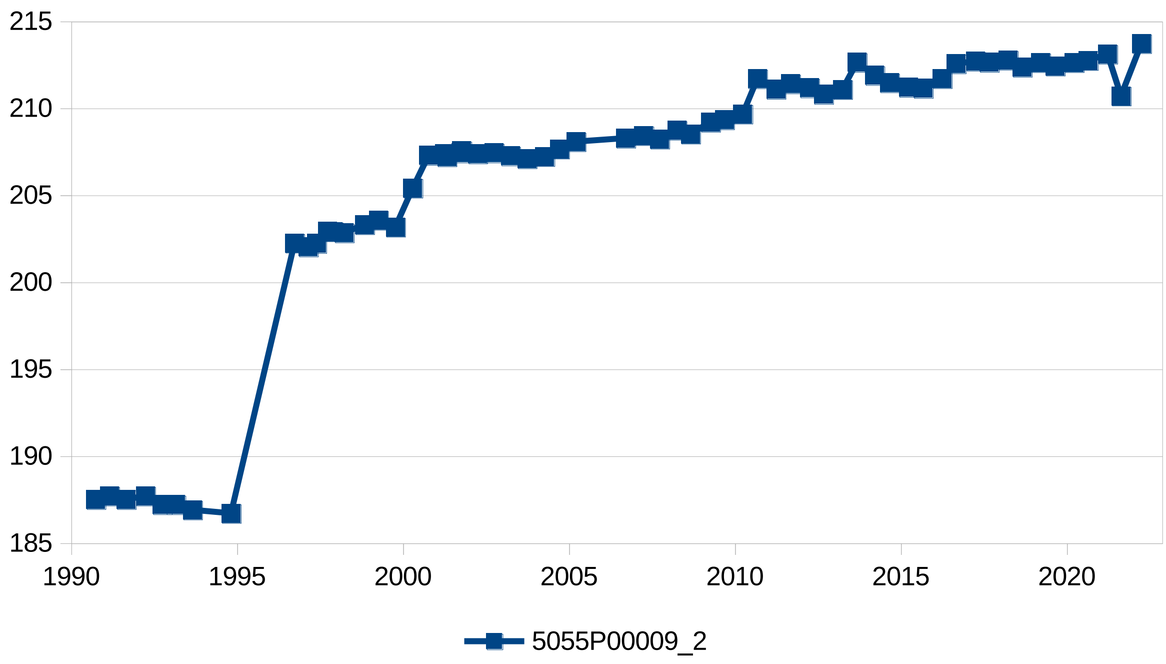

Fig. 100. The water table changes in the monitoring well No. 5055P00009_2

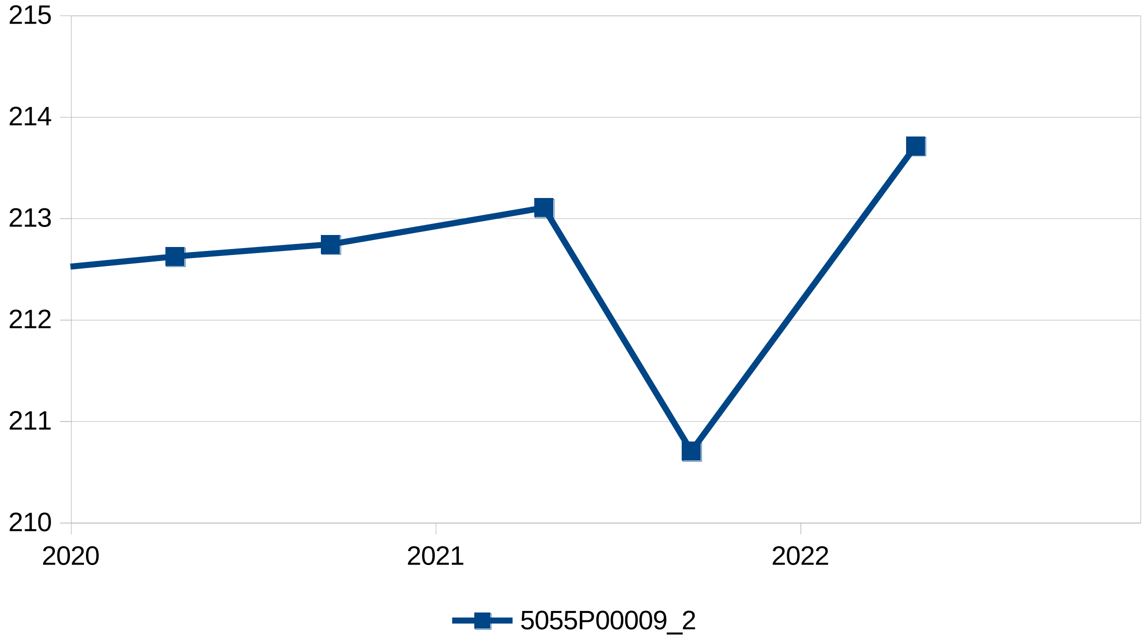

Fig. 101. The water table changes in the monitoring well No. 5055P00009_2

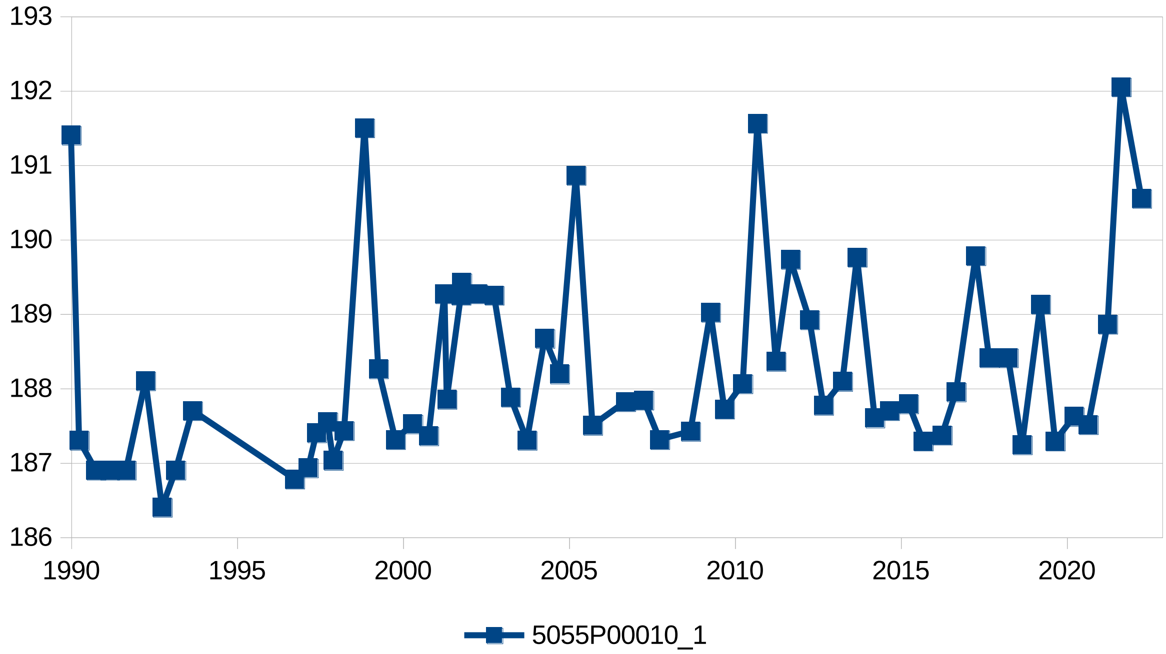

Fig. 102. The water table changes in the monitoring well No. 5055P00010_1

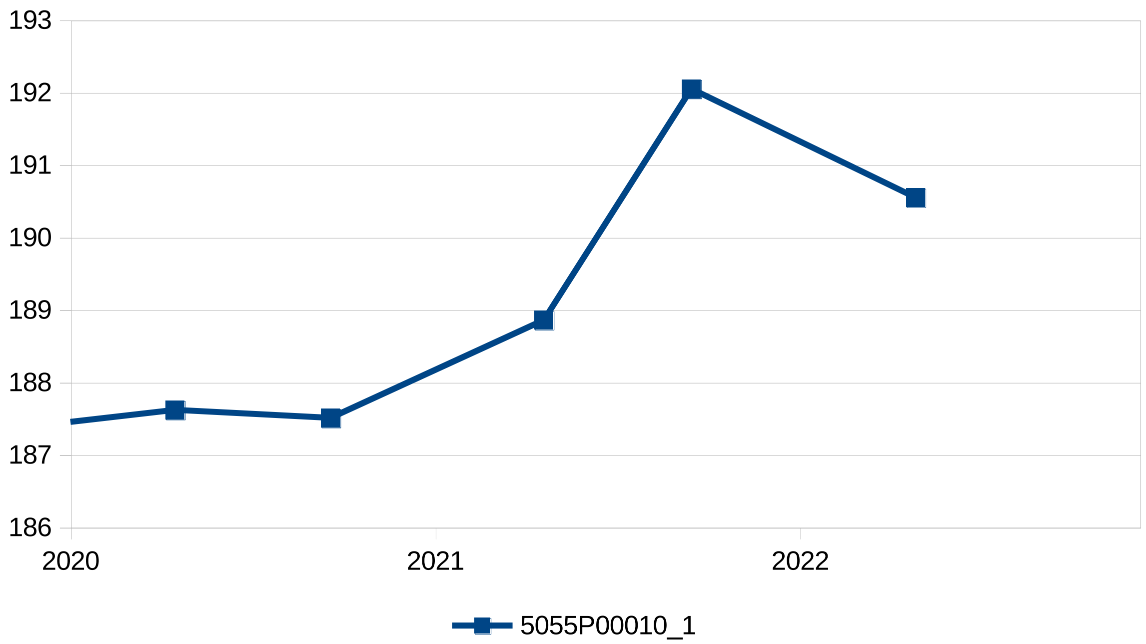

Fig. 103. The water table changes in the monitoring well No. 5055P00010_1

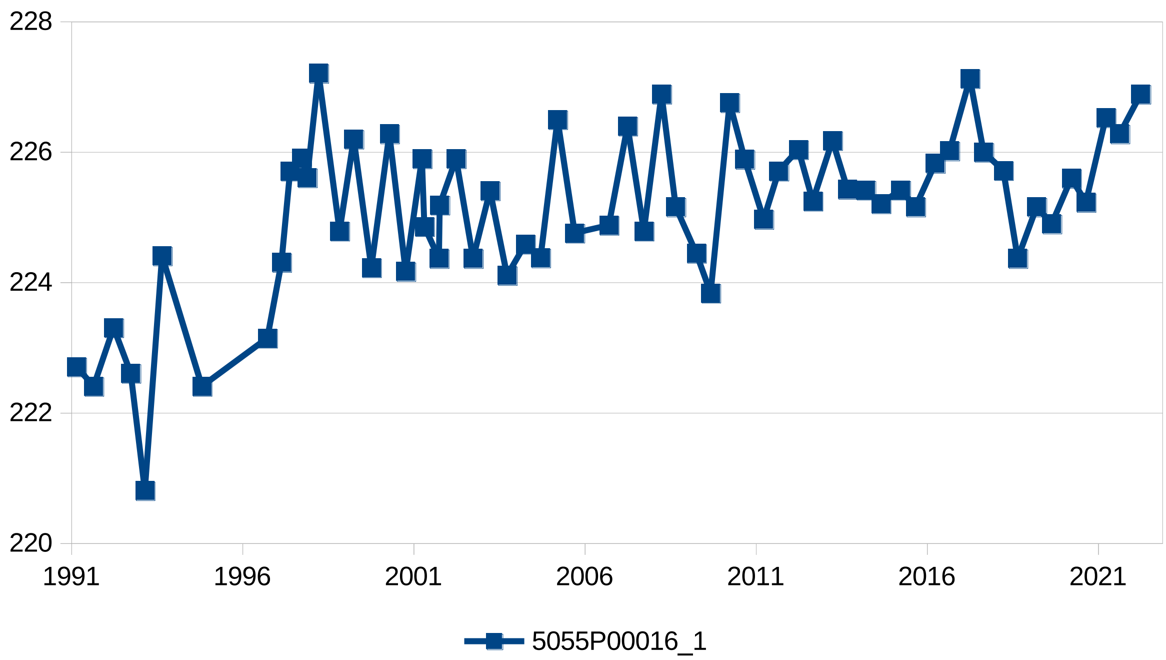

Fig. 104. The water table changes in the monitoring well No. 5055P00016_1

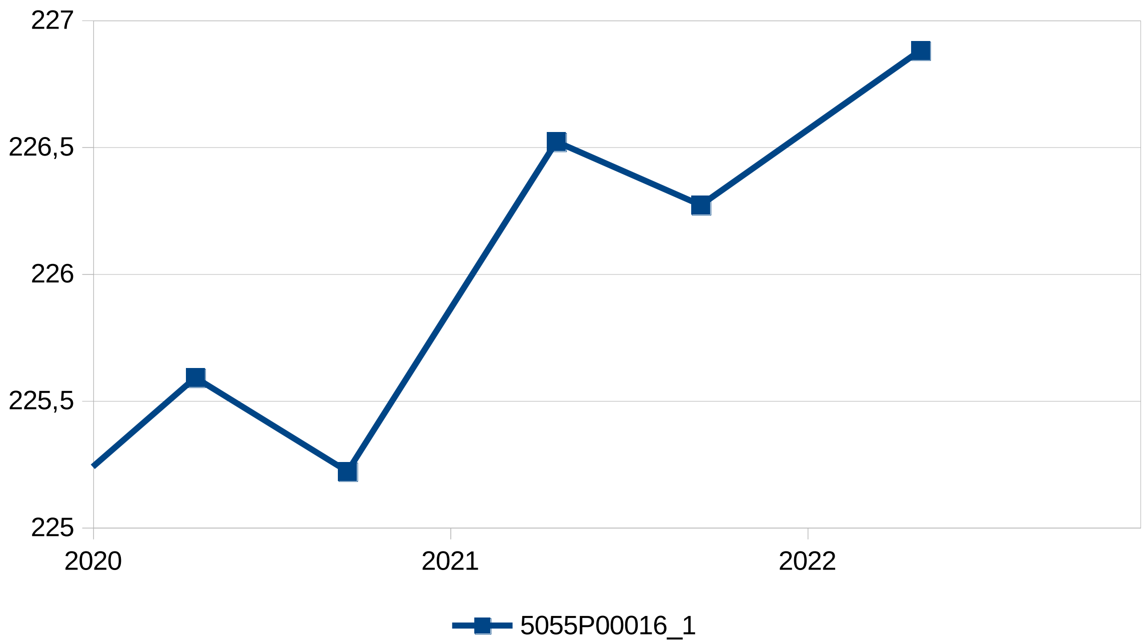

Fig. 105. The water table changes in the monitoring well No. 5055P00016_1

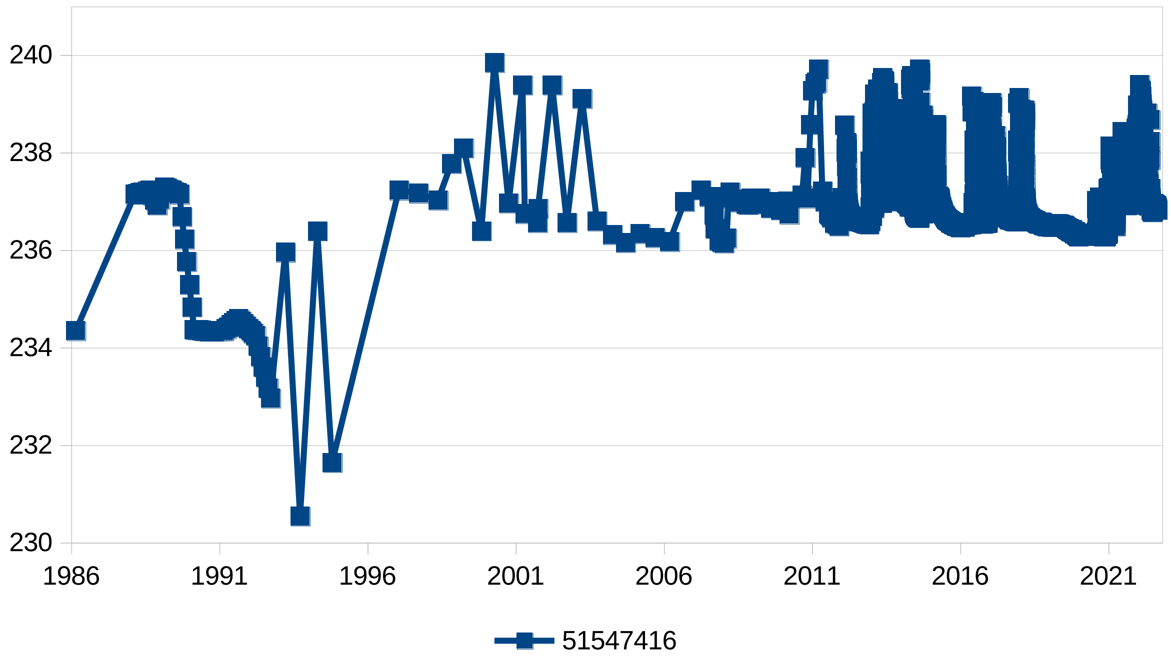

Fig. 106. The water table changes in the monitoring well No. 51547416

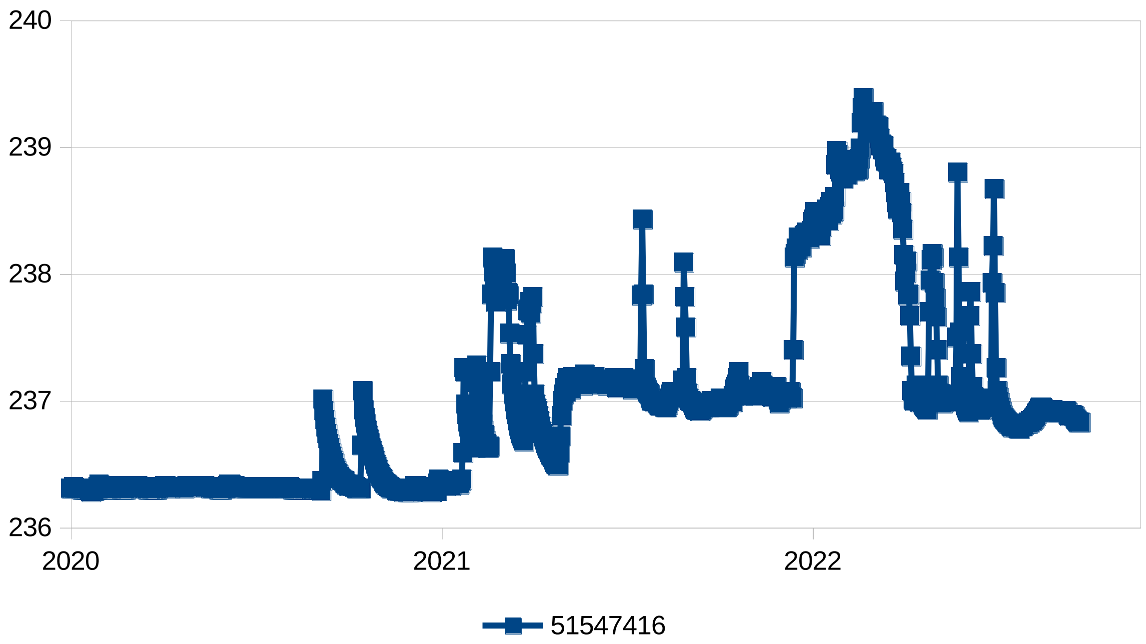

Fig. 107. The water table changes in the monitoring well No. 51547416

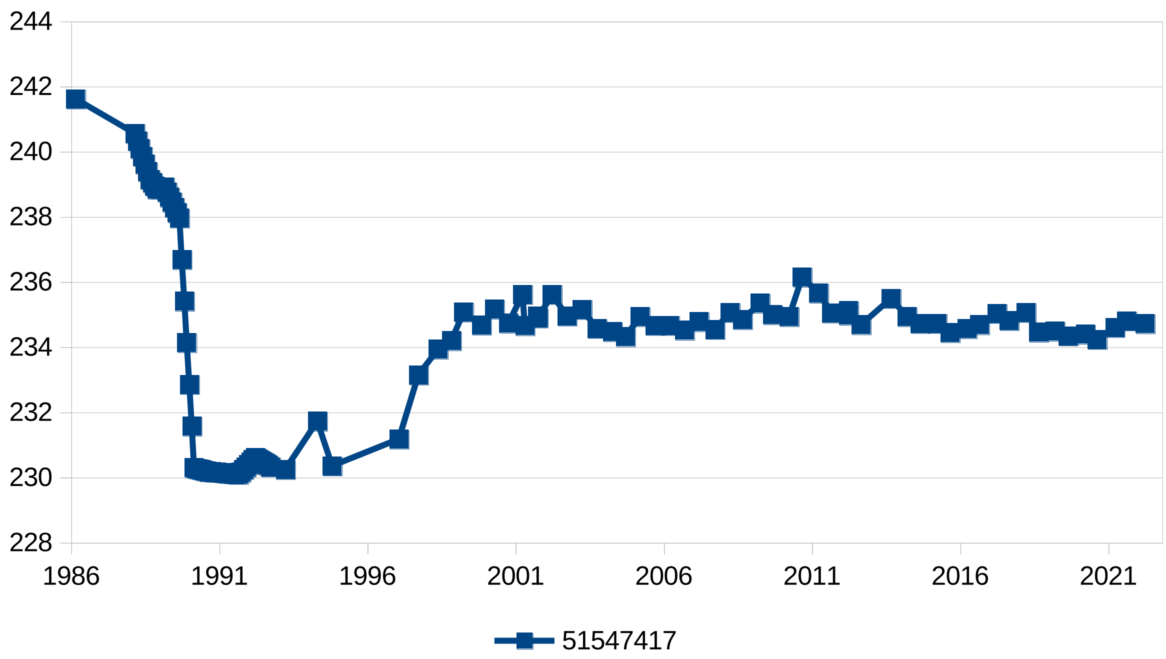

Fig. 108. The water table changes in the monitoring well No. 51547417

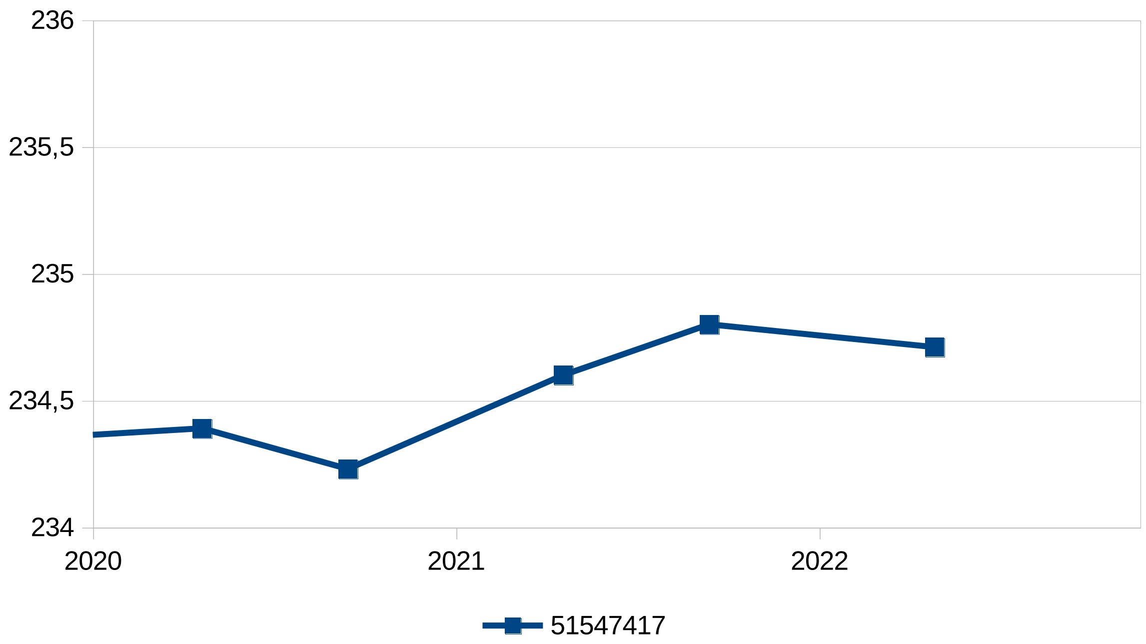

Fig. 109. The water table changes in the monitoring well No. 51547417

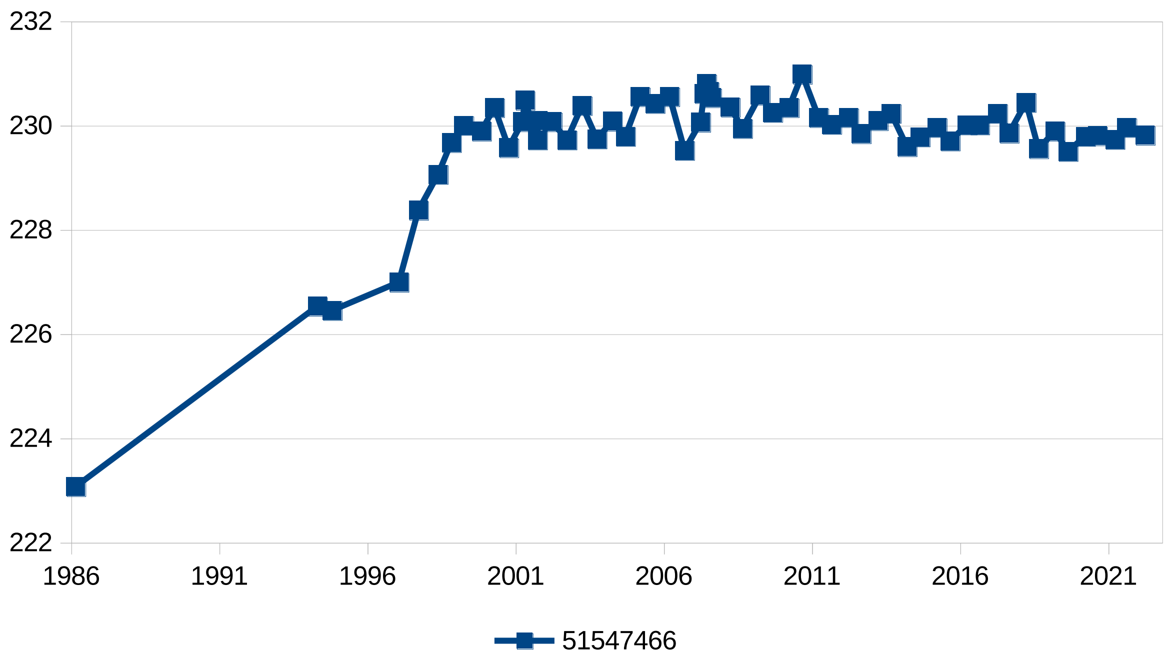

Fig. 110. The water table changes in the monitoring well No. 51547466

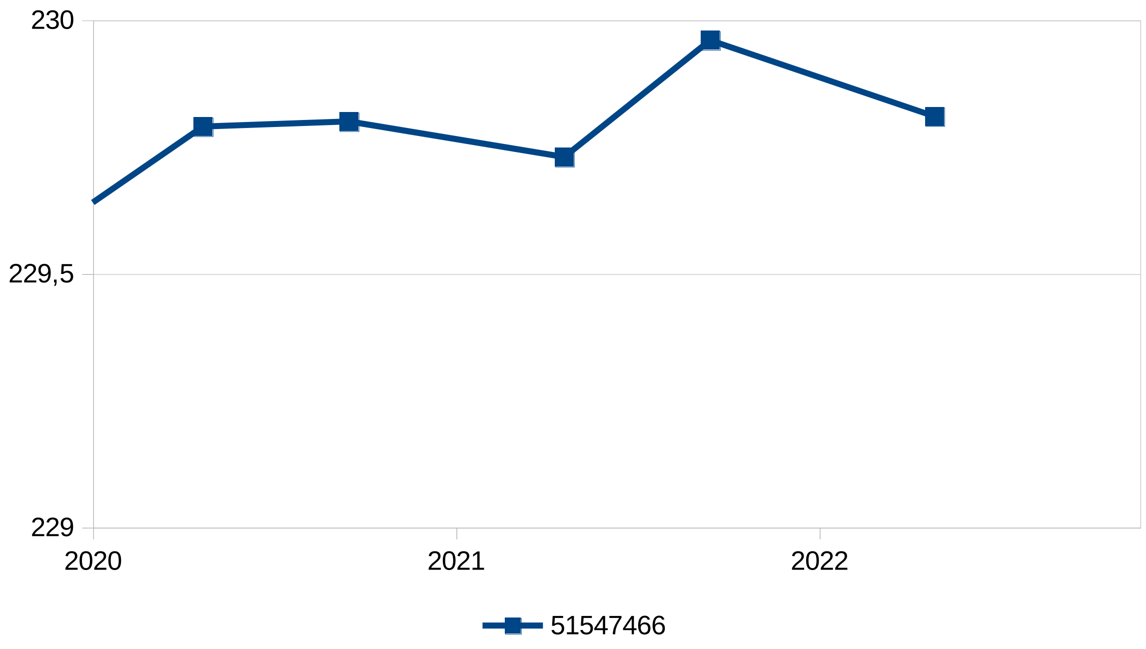

Fig. 111. The water table changes in the monitoring well No. 51547466

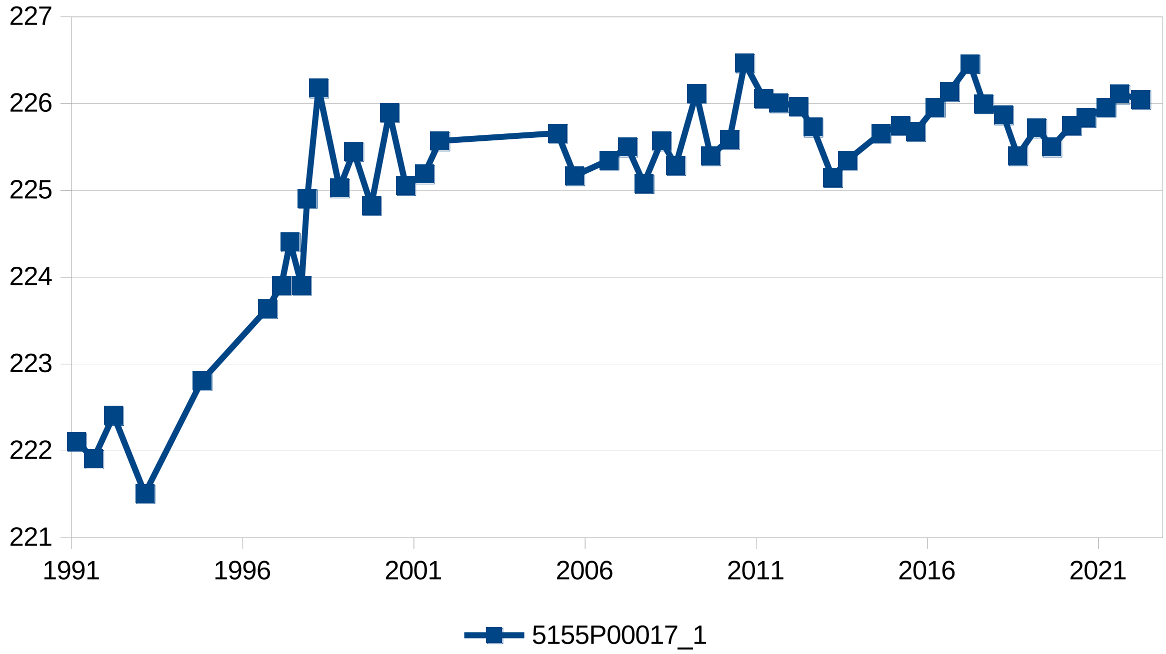

Fig. 112. The water table changes in the monitoring well No. 5155P00017_1

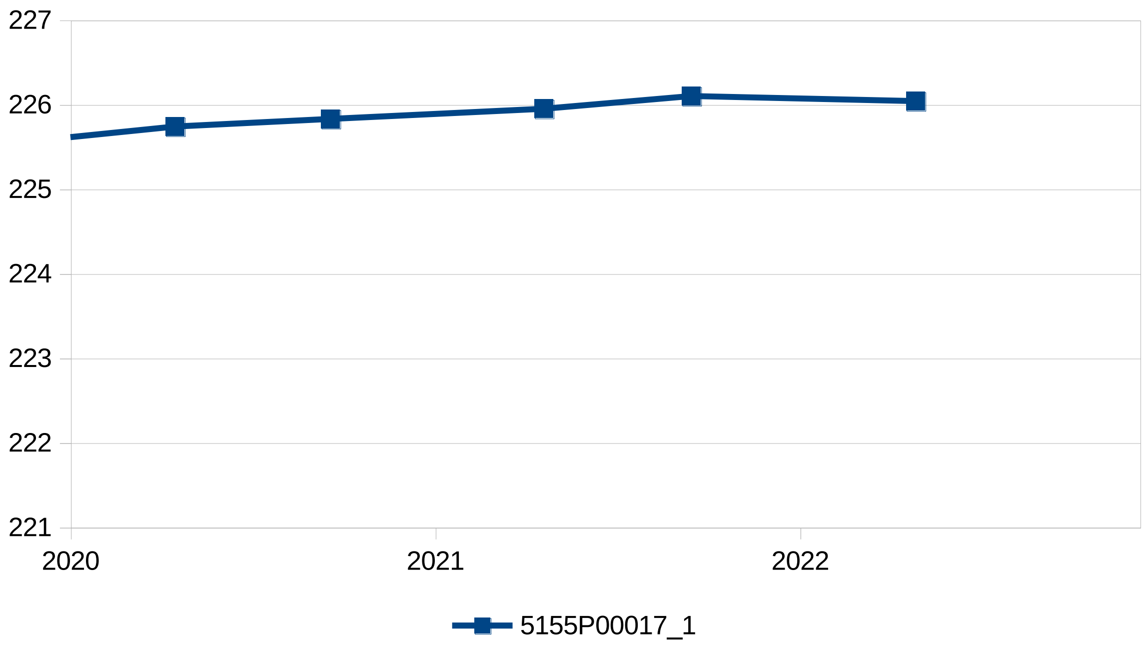

Fig. 113. The water table changes in the monitoring well No. 5155P00017_1

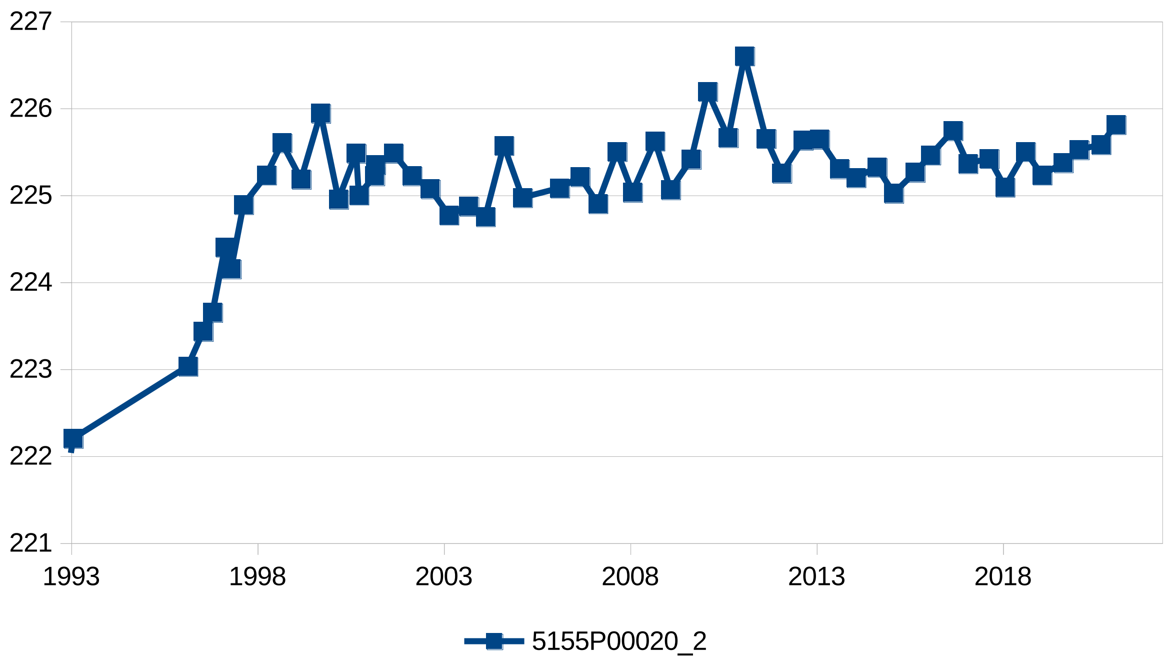

Fig. 114. The water table changes in the monitoring well No. 5155P00020_2

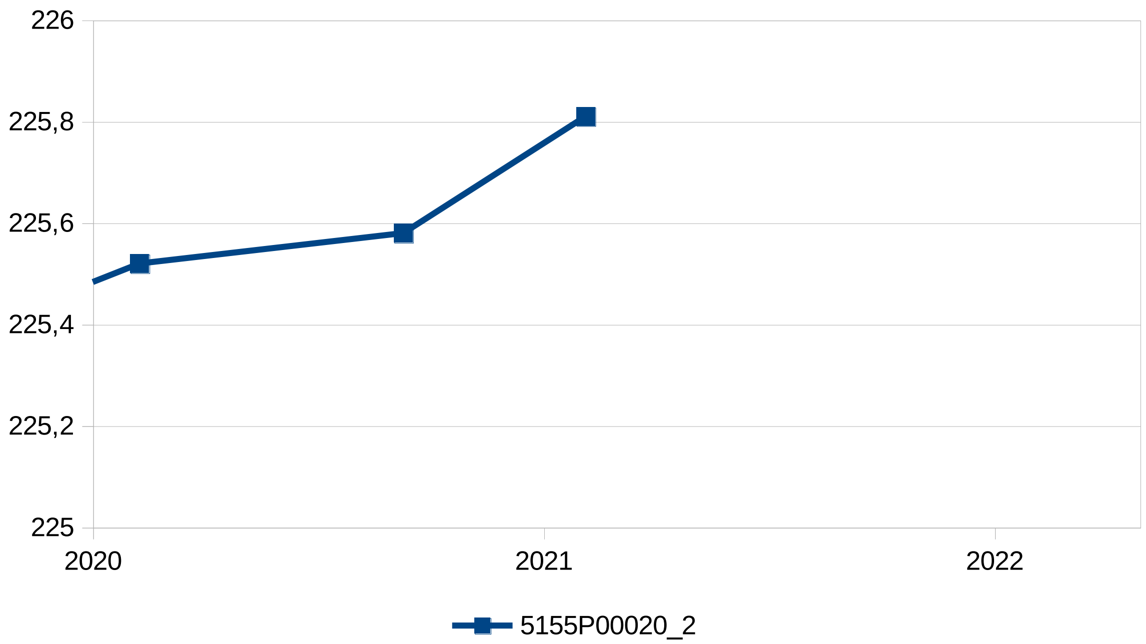

Fig. 115. The water table changes in the monitoring well No. 5155P00020_2

WL HM

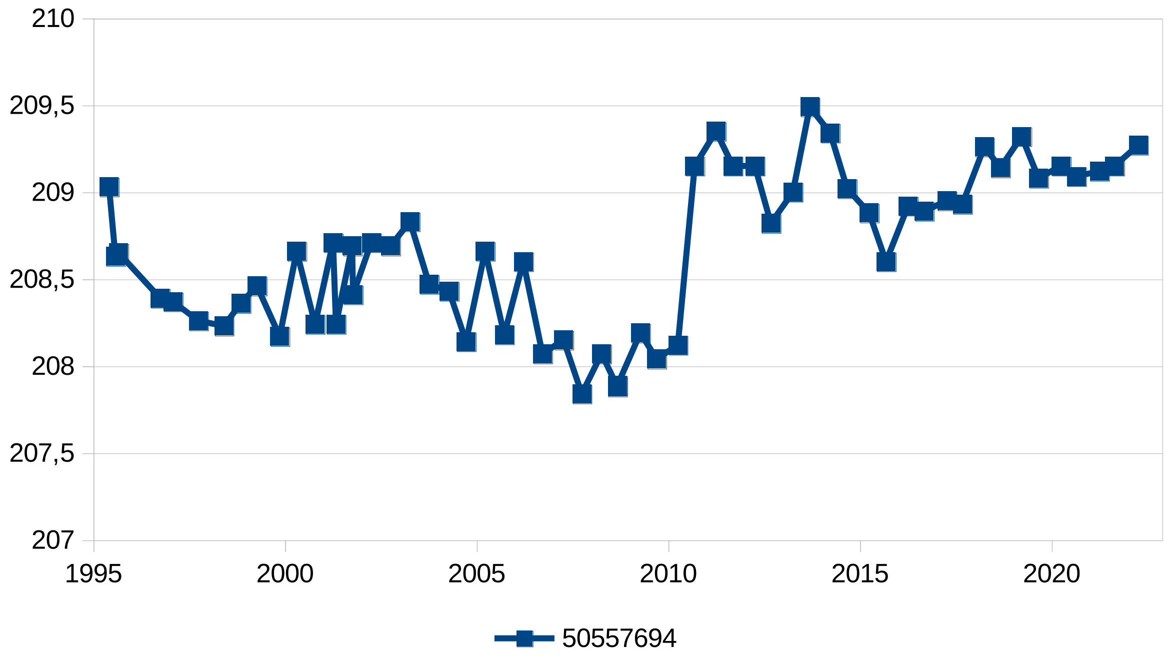

Fig. 116. The water table changes in the monitoring well No. 50557694

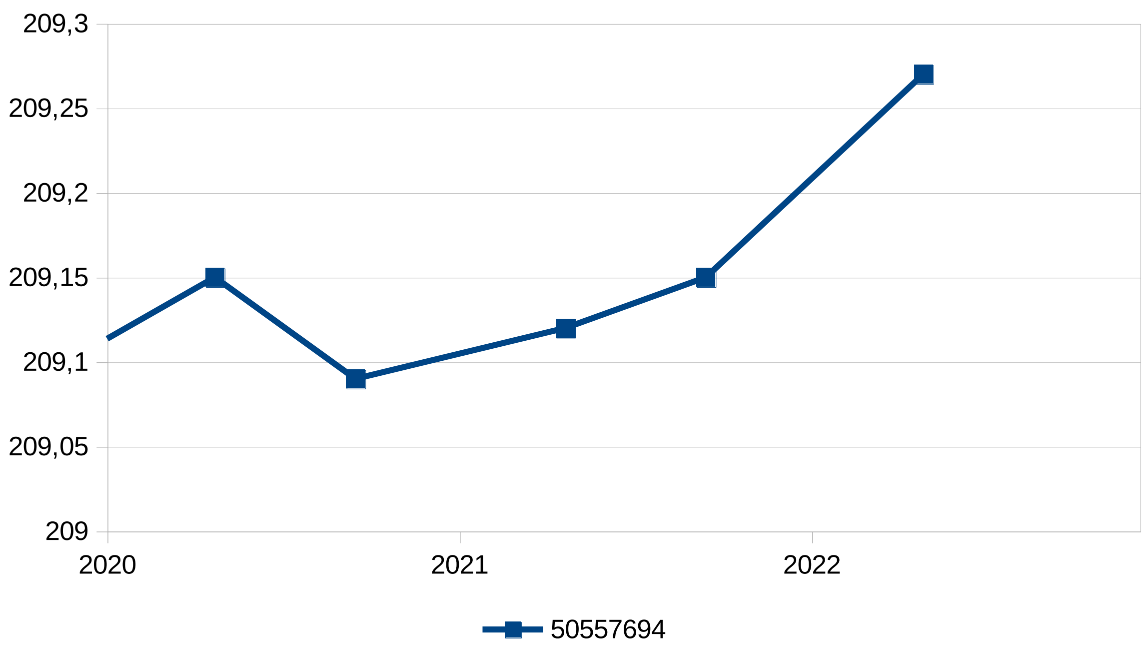

Fig. 117. The water table changes in the monitoring well No. 50557694

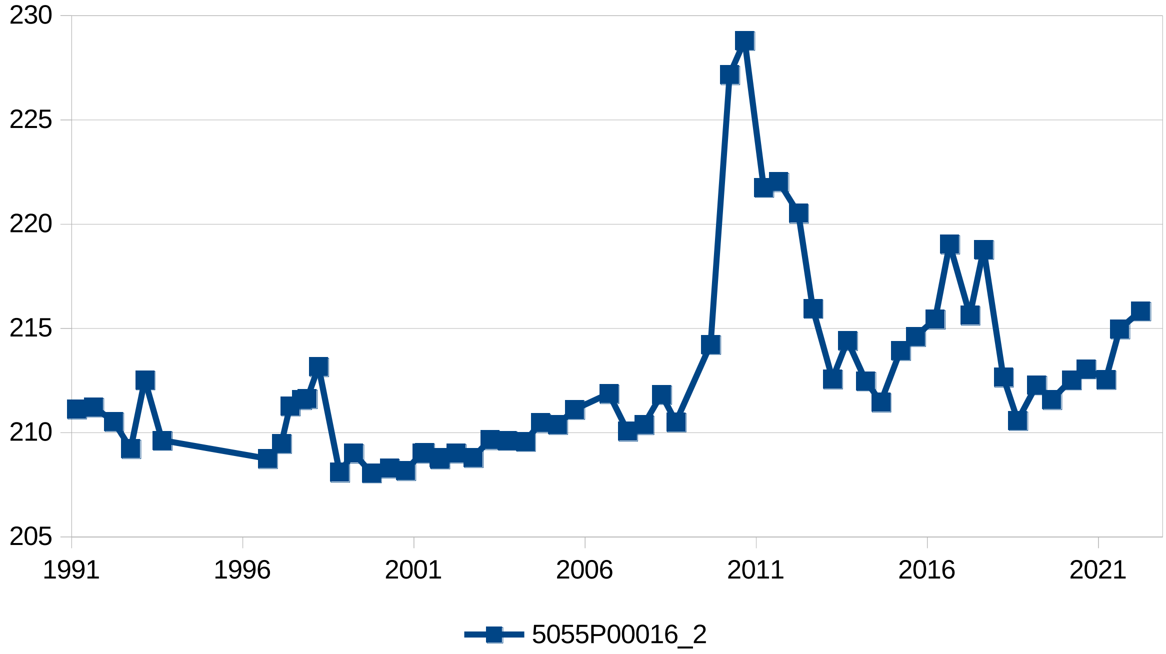

Fig. 118. The water table changes in the monitoring well No. 5055P00016_2

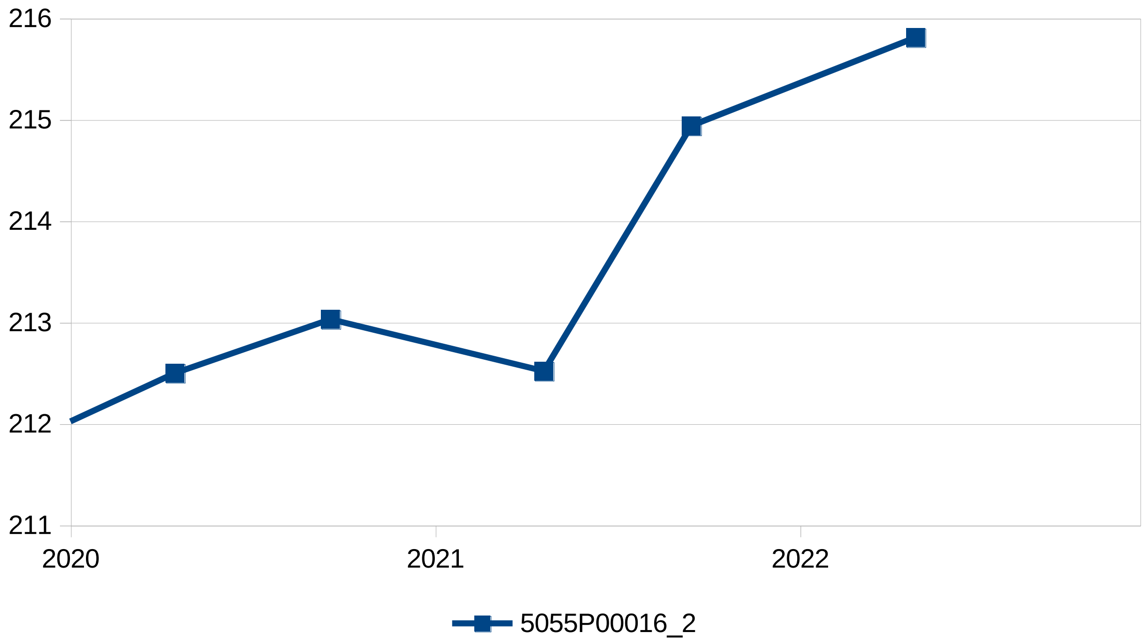

Fig. 119. The water table changes in the monitoring well No. 5055P00016_2

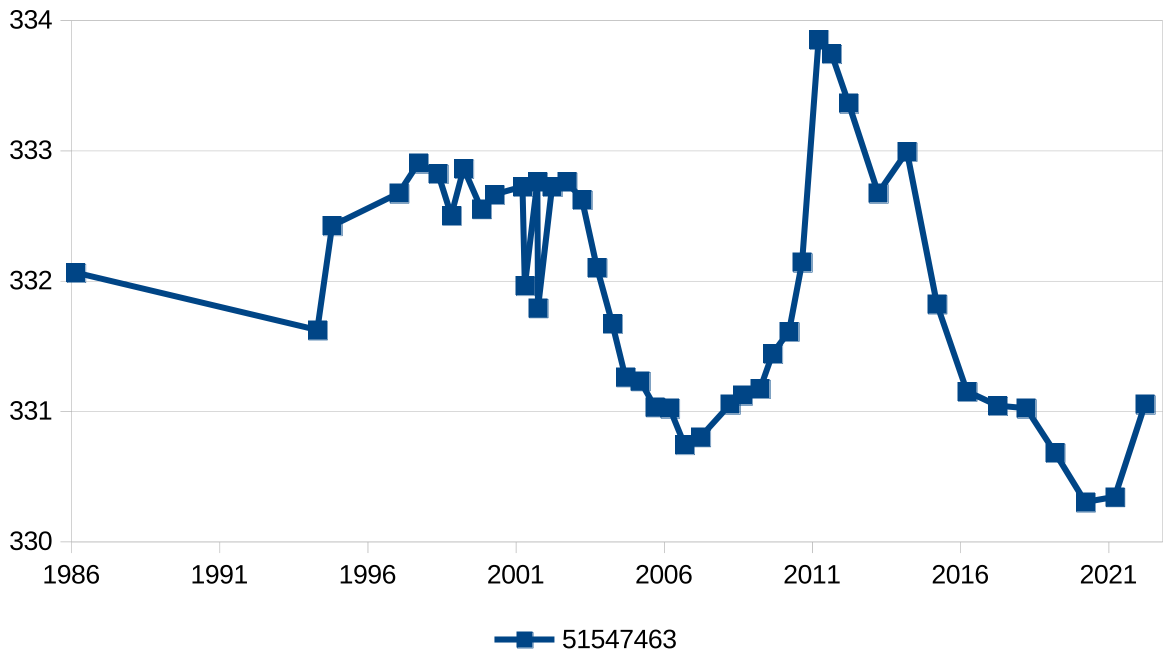

Fig. 120. The water table changes in the monitoring well No. 51547463

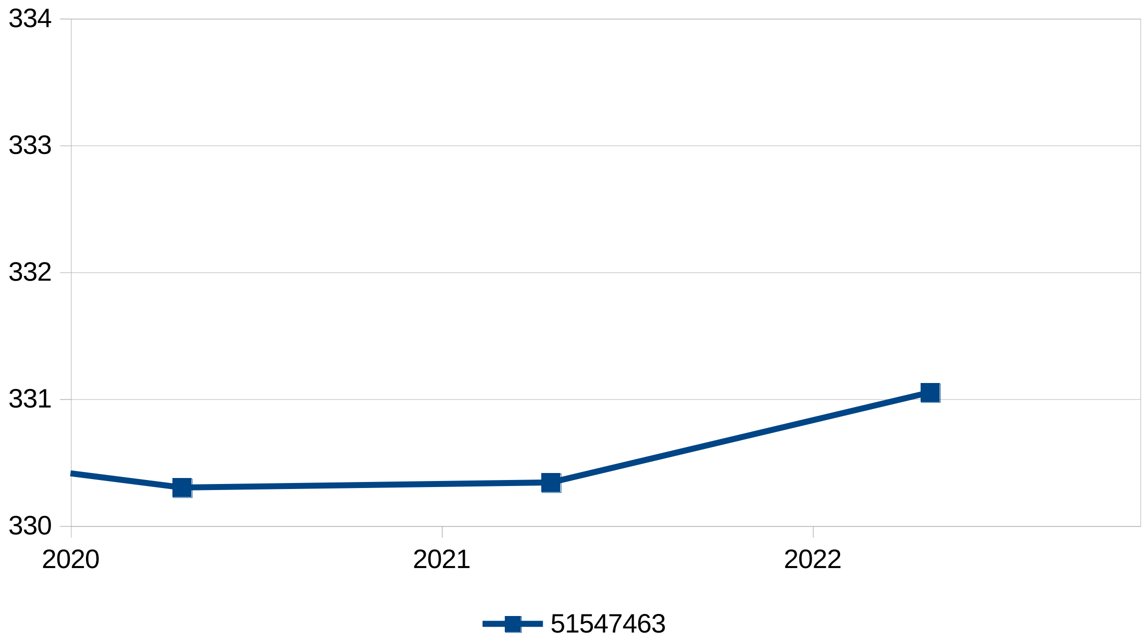

Fig. 121. The water table changes in the monitoring well No. 51547463

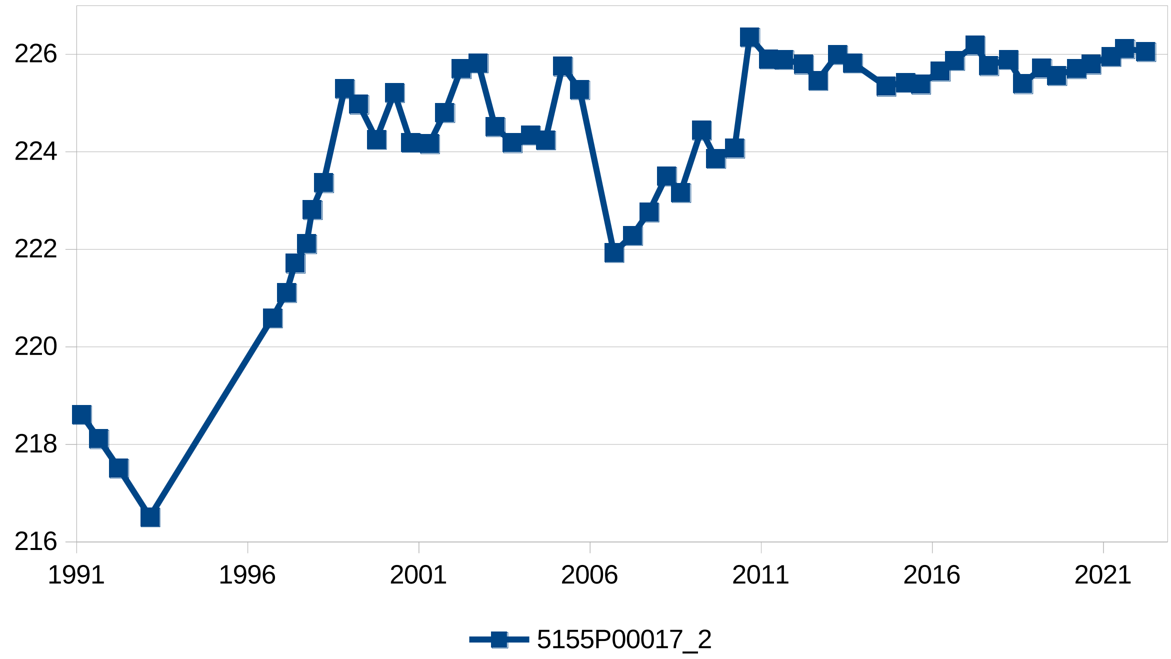

Fig. 122. The water table changes in the monitoring well No. 5155P00017_2

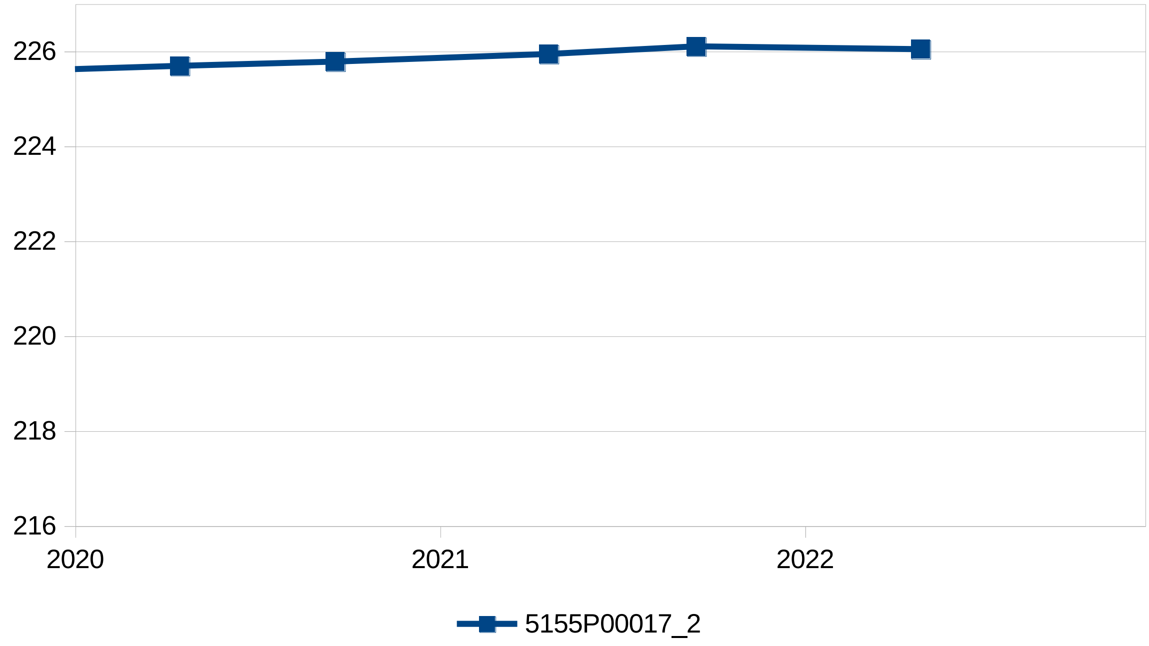

Fig. 123. The water table changes in the monitoring well No. 5155P00017_2

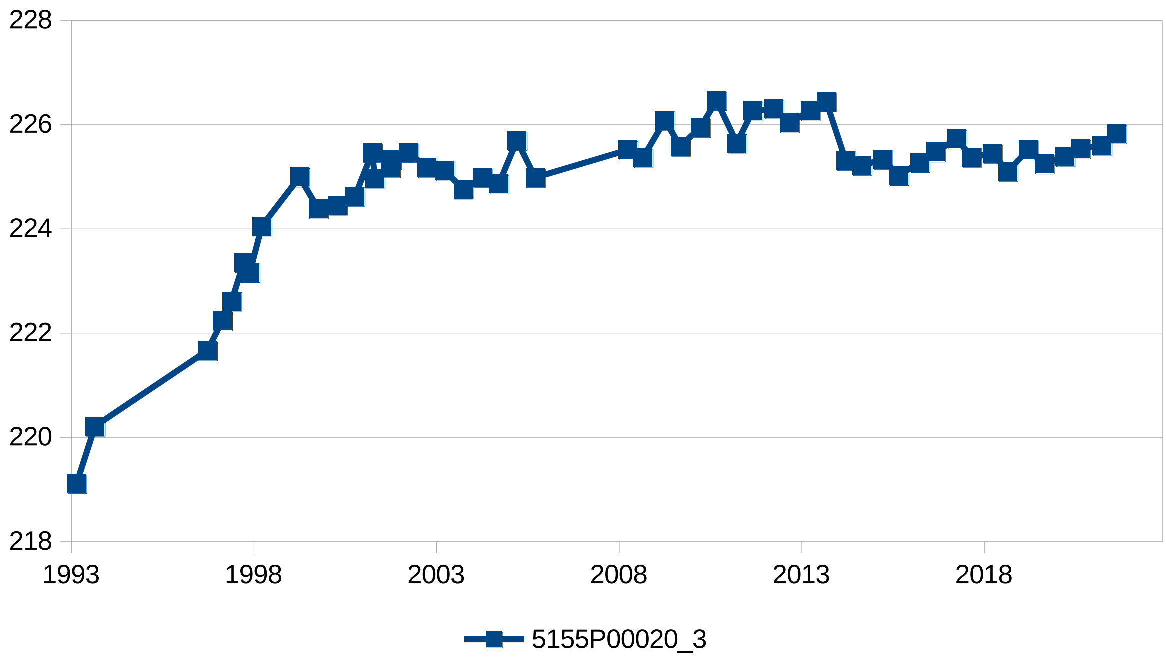

Fig. 124. The water table changes in the monitoring well No. 5155P00020_3

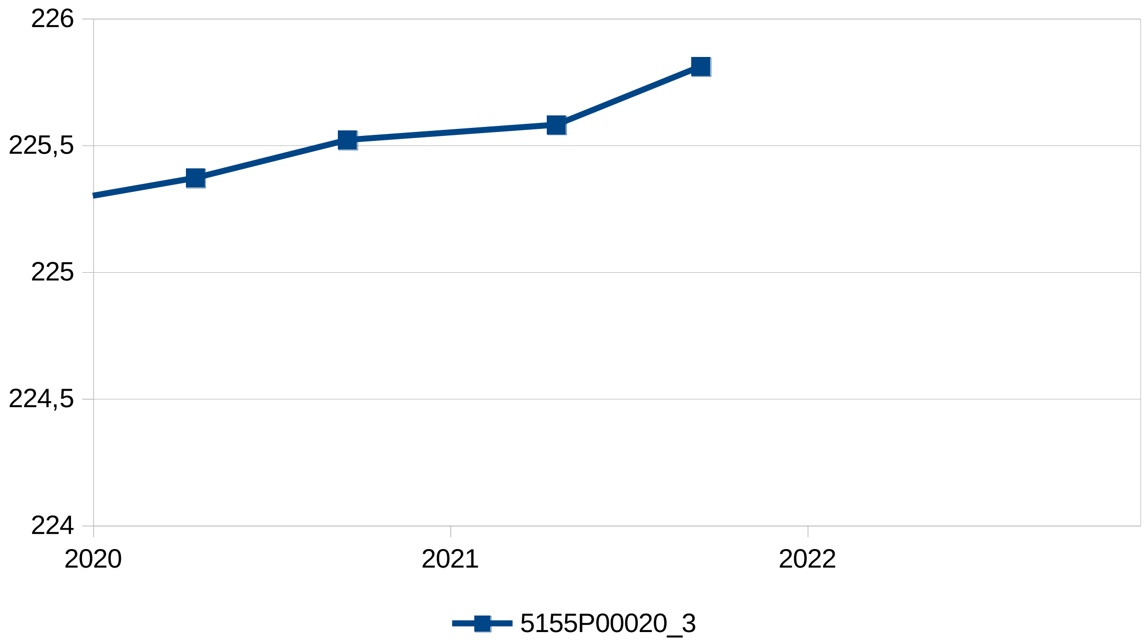

Fig. 125. The water table changes in the monitoring well No. 5155P00020_3

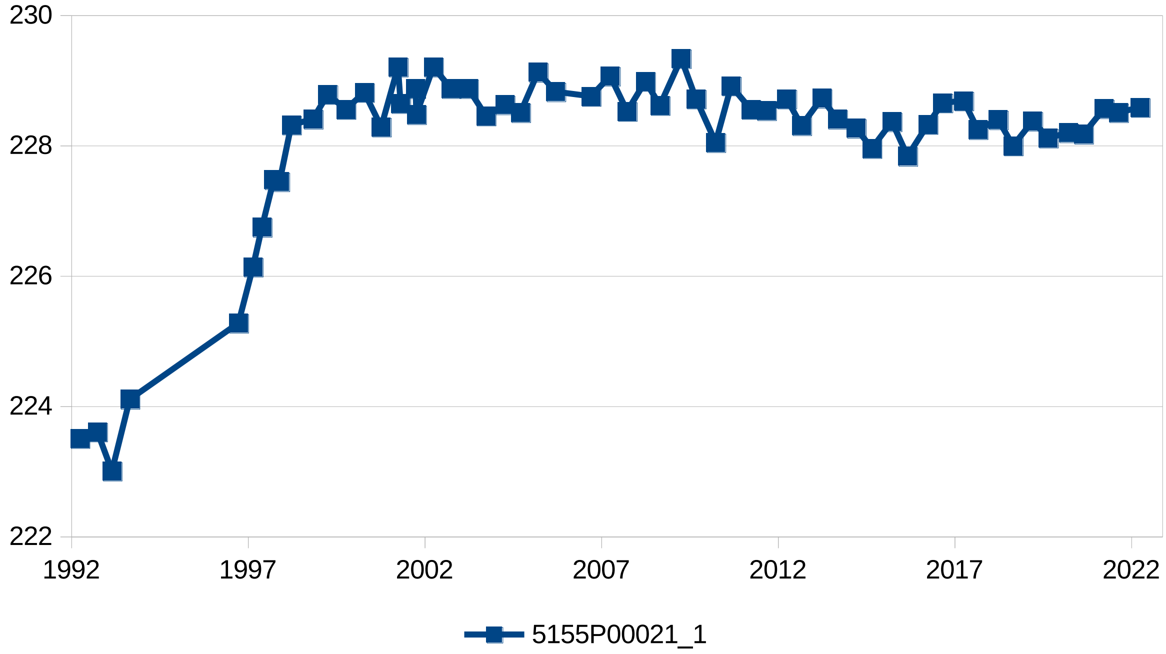

Fig. 126. The water table changes in the monitoring well No. 5155P00021_1

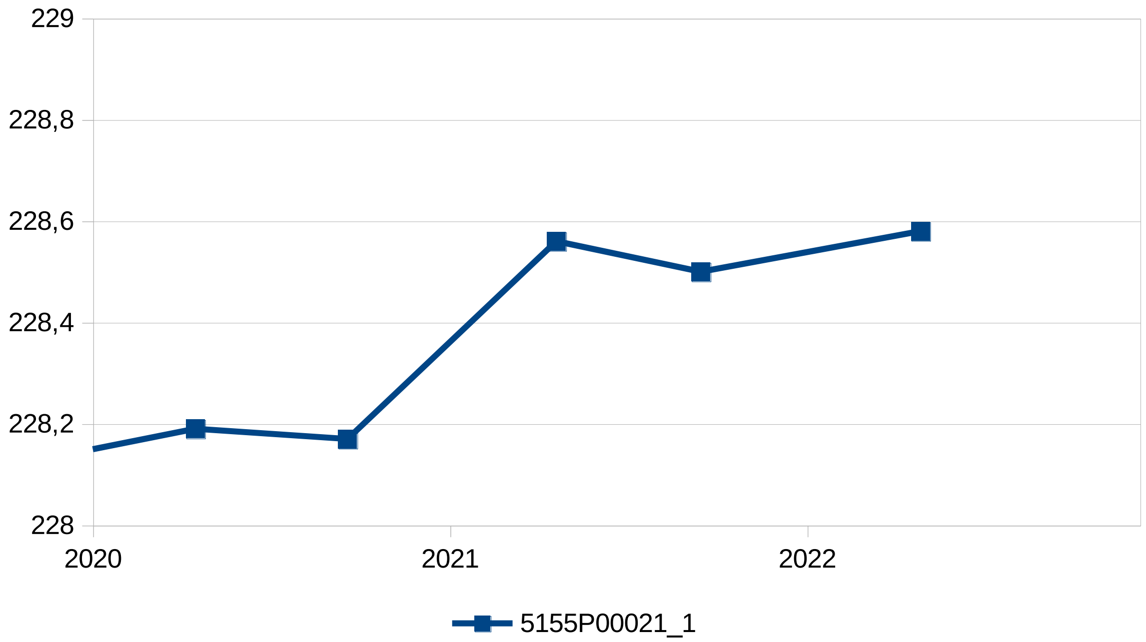

Fig. 127. The water table changes in the monitoring well No. 5155P00021_1

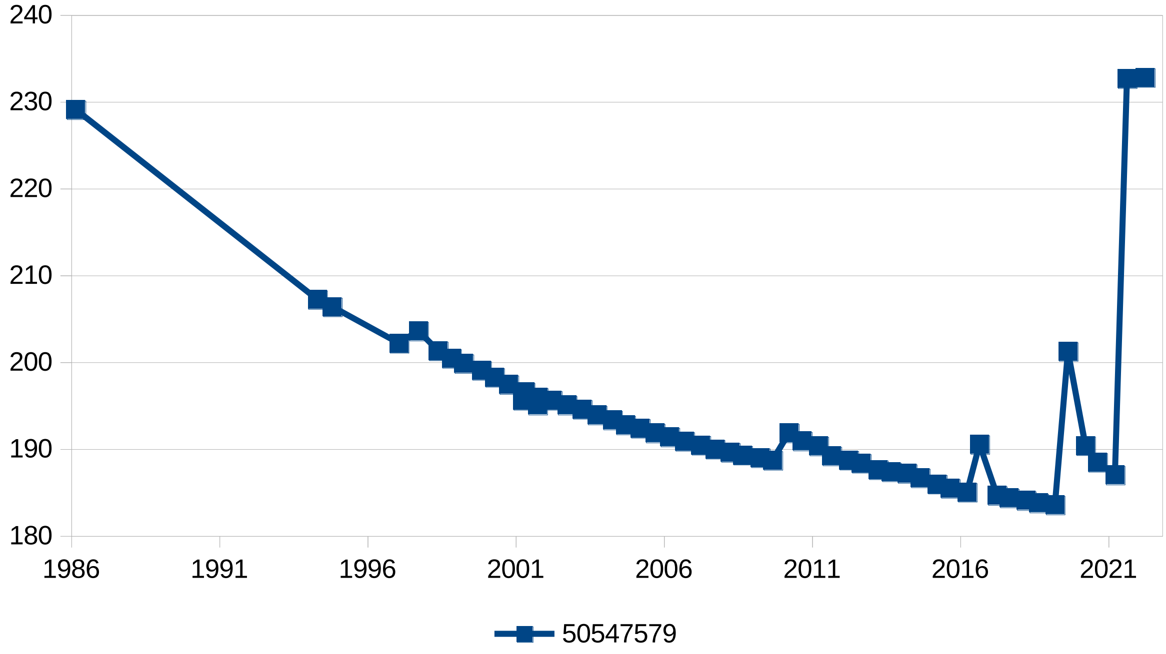

Fig. 128. The water table changes in the monitoring well No. 50547579

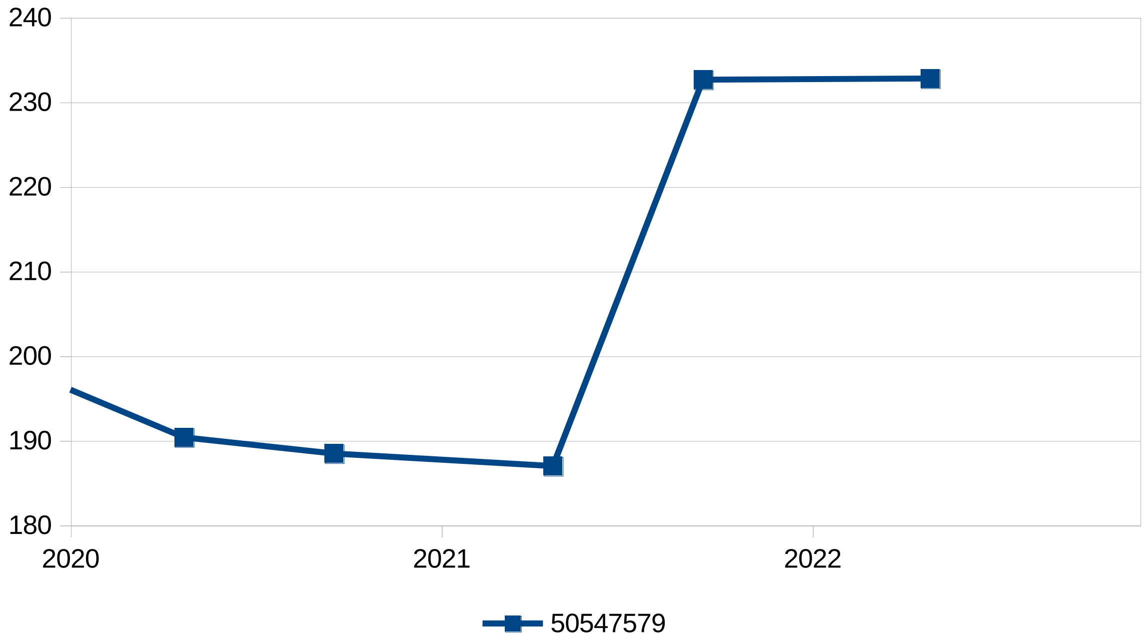

Fig. 129. The water table changes in the monitoring well No. 50547579

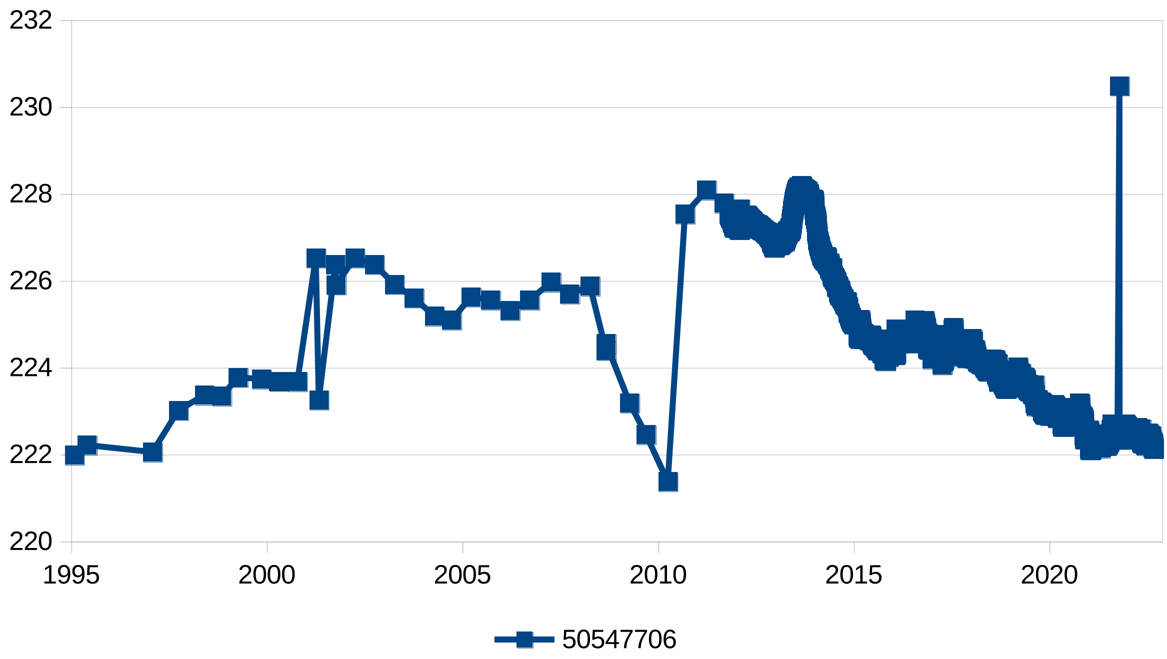

Fig. 131. The water table changes in the monitoring well No. 50547706

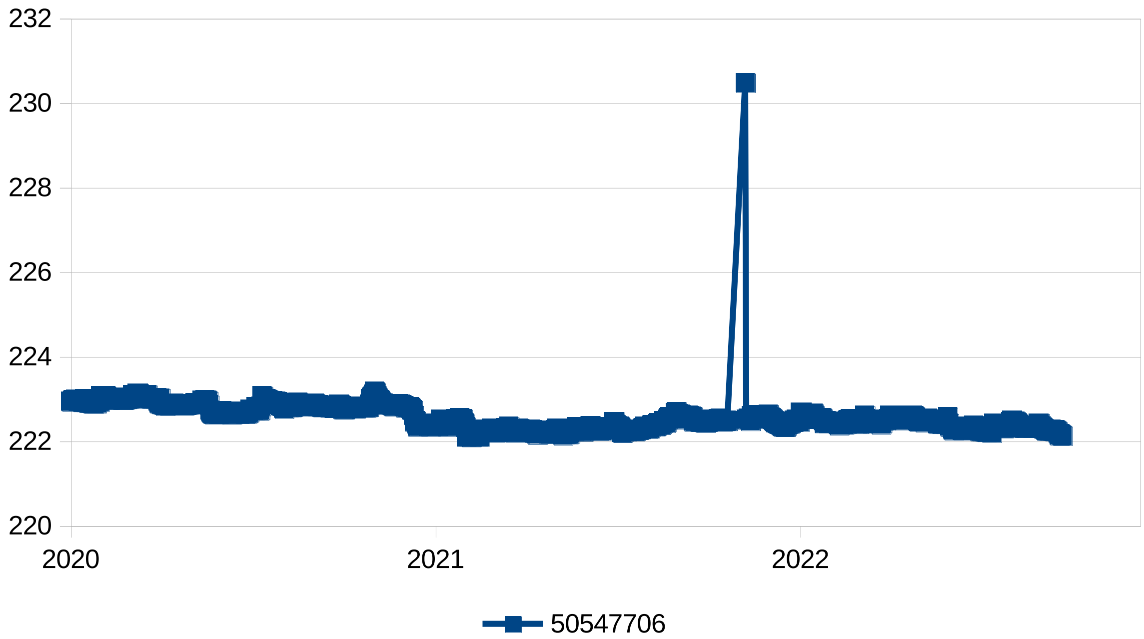

Fig. 132. The water table changes in the monitoring well No. 50547706

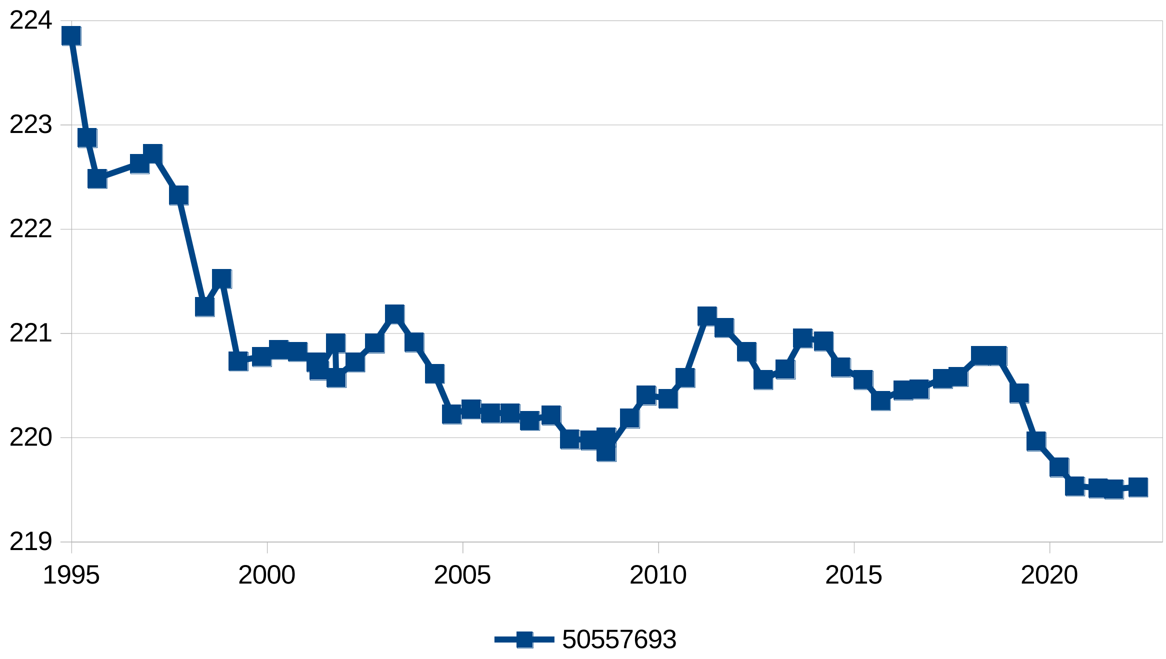

Fig. 133. The water table changes in the monitoring well No. 50557693

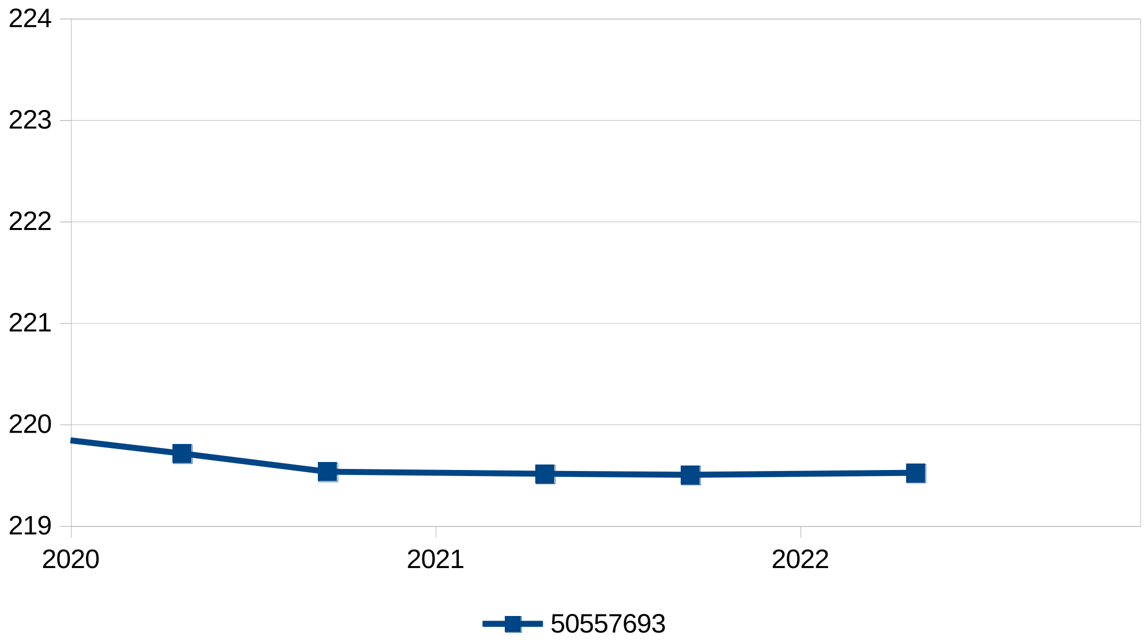

Fig. 134. The water table changes in the monitoring well No. 50557693

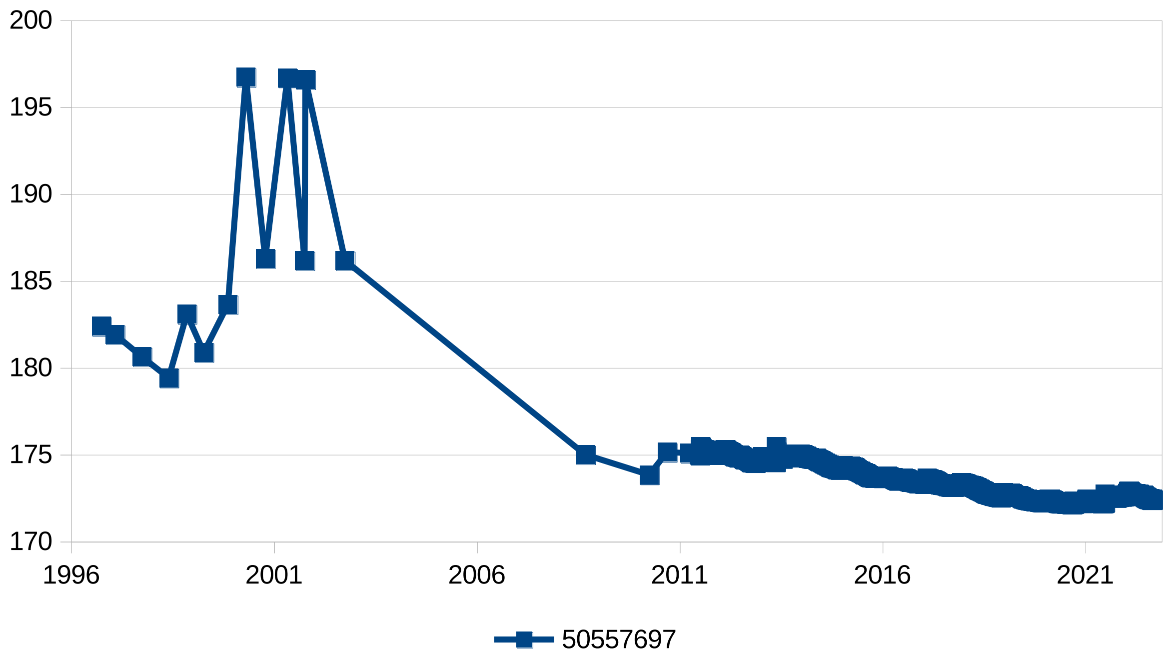

Fig. 135. The water table changes in the monitoring well No. 50557697

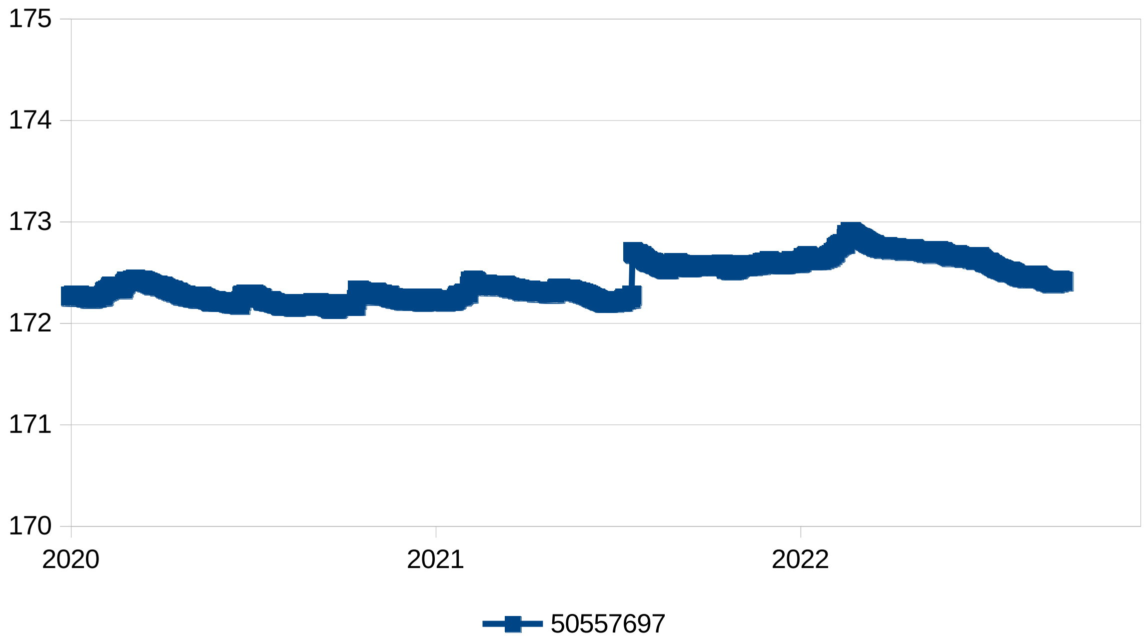

Fig. 136 The water table changes in the monitoring well No. 50557697

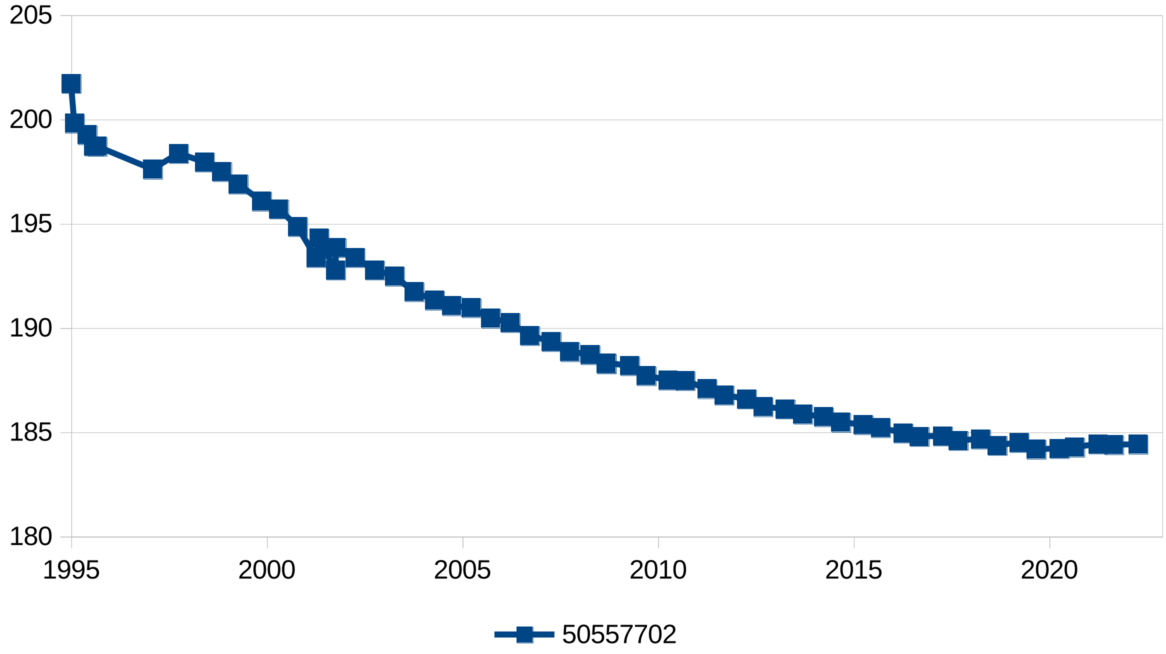

Fig. 137. The water table changes in the monitoring well No. 50557702

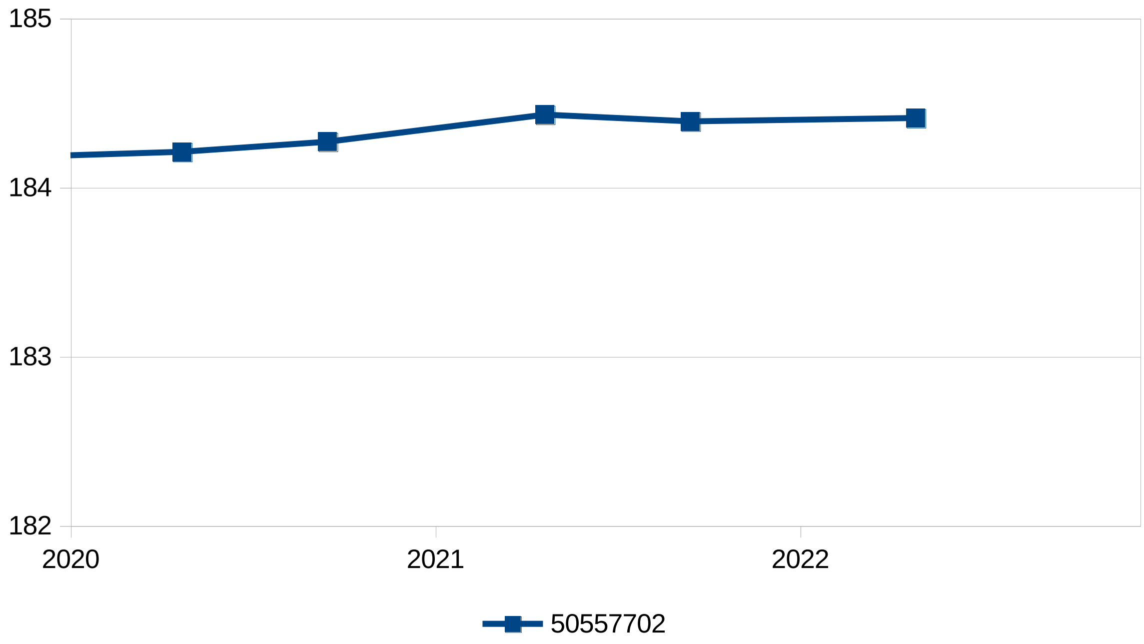

Fig. 138. The water table changes in the monitoring well No. 50557702

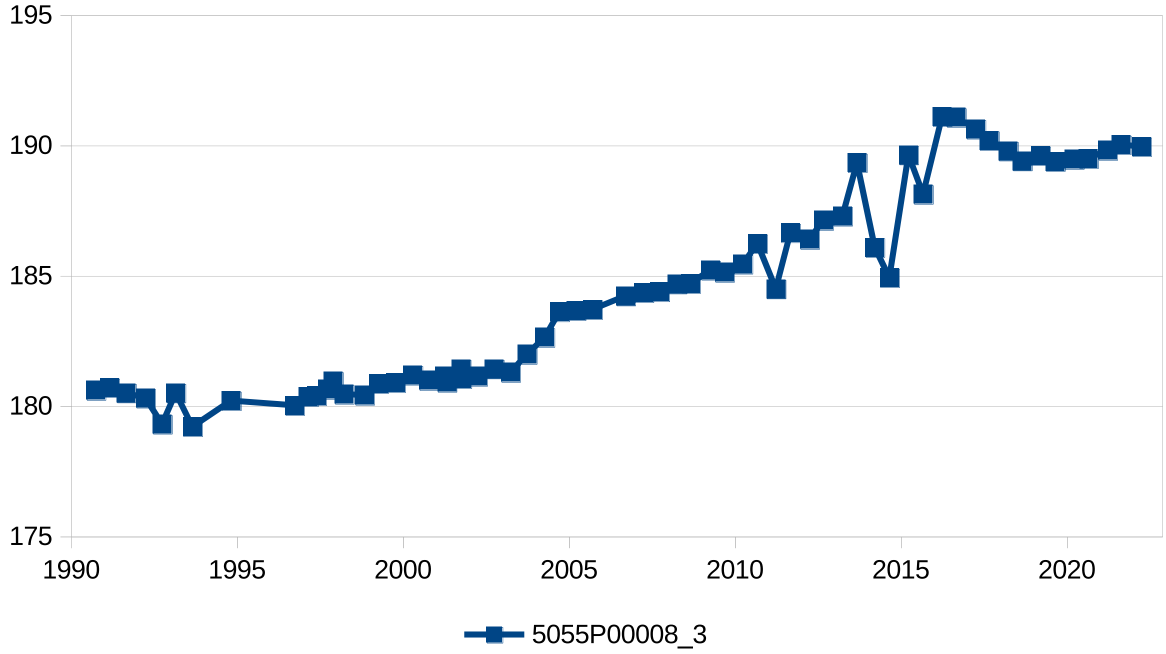

Fig. 139. The water table changes in the monitoring well No. 5055P00008_3

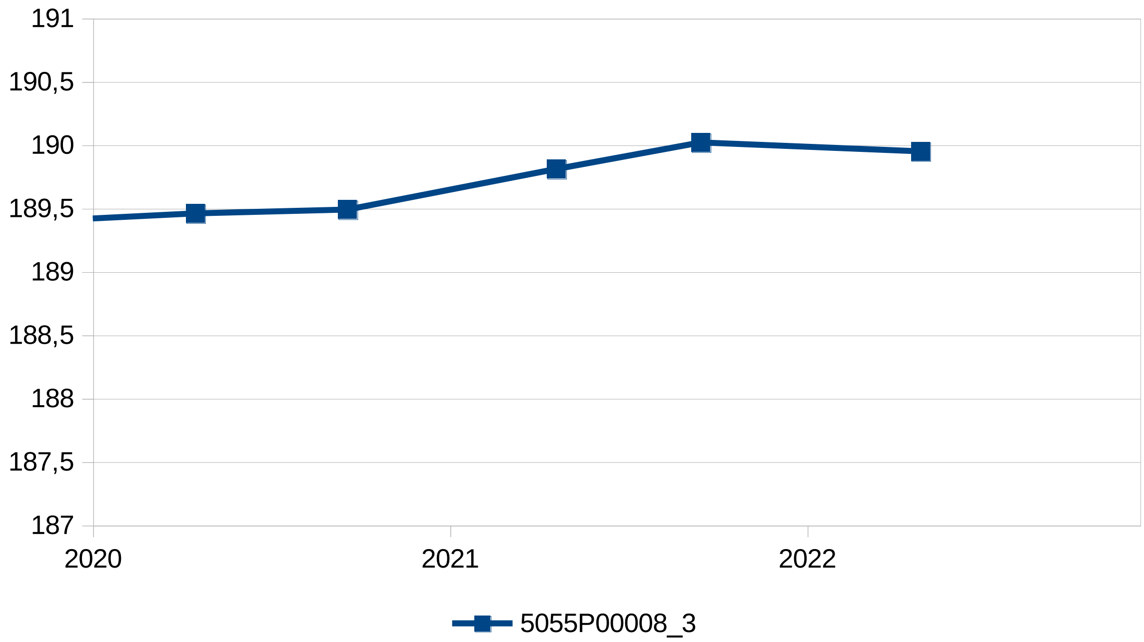

Fig. 140. The water table changes in the monitoring well No. 5055P00008_3

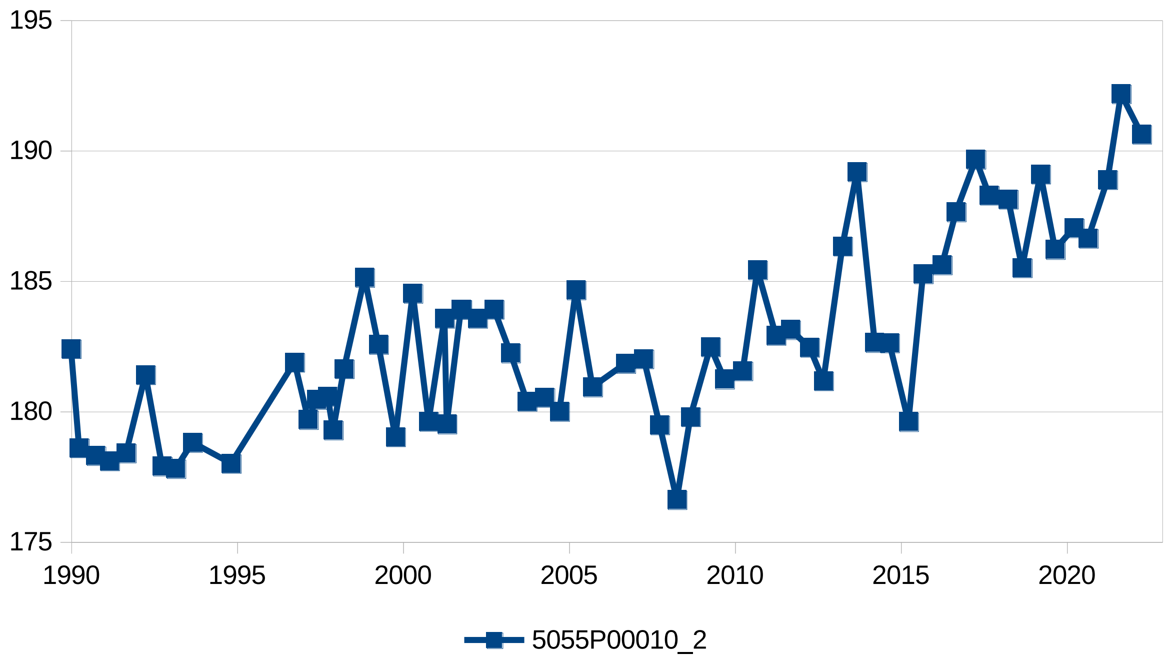

Fig. 141. The water table changes in the monitoring well No. 5055P00010_2

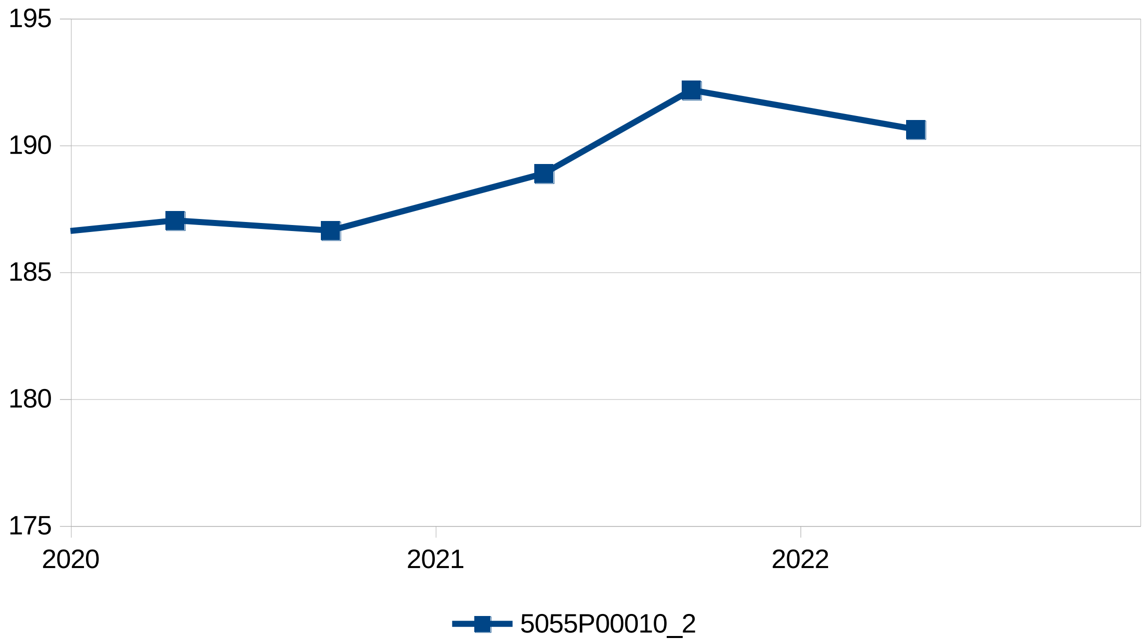

Fig. 142. The water table changes in the monitoring well No. 5055P00010_2

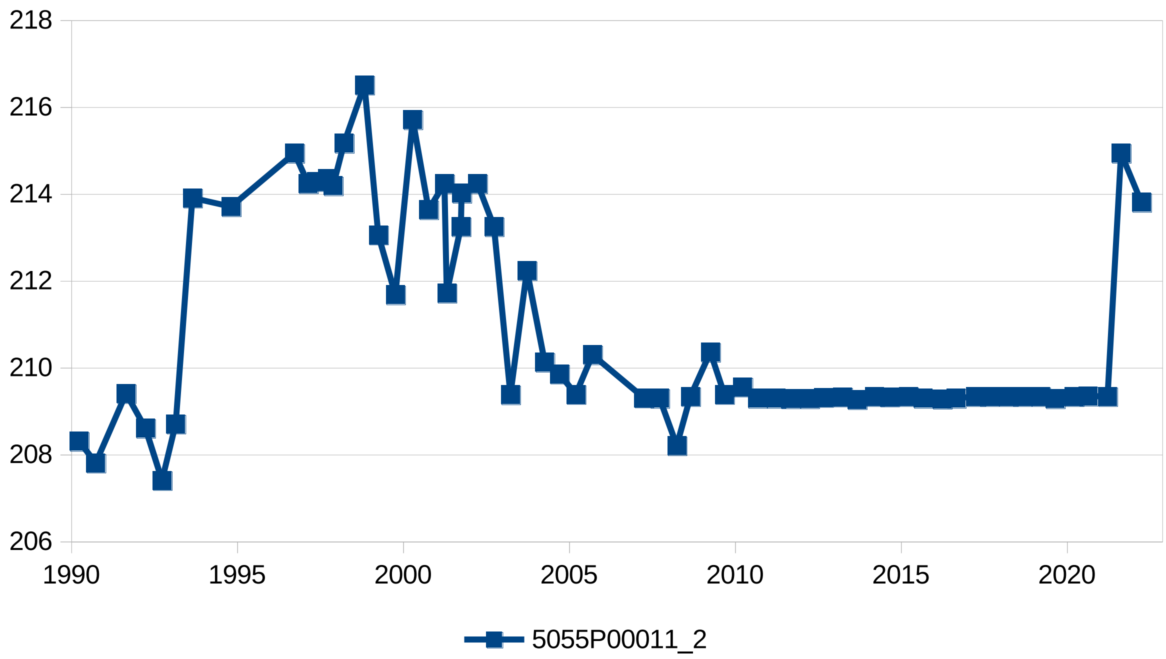

Fig. 143. The water table changes in the monitoring well No. 5055P00011_2

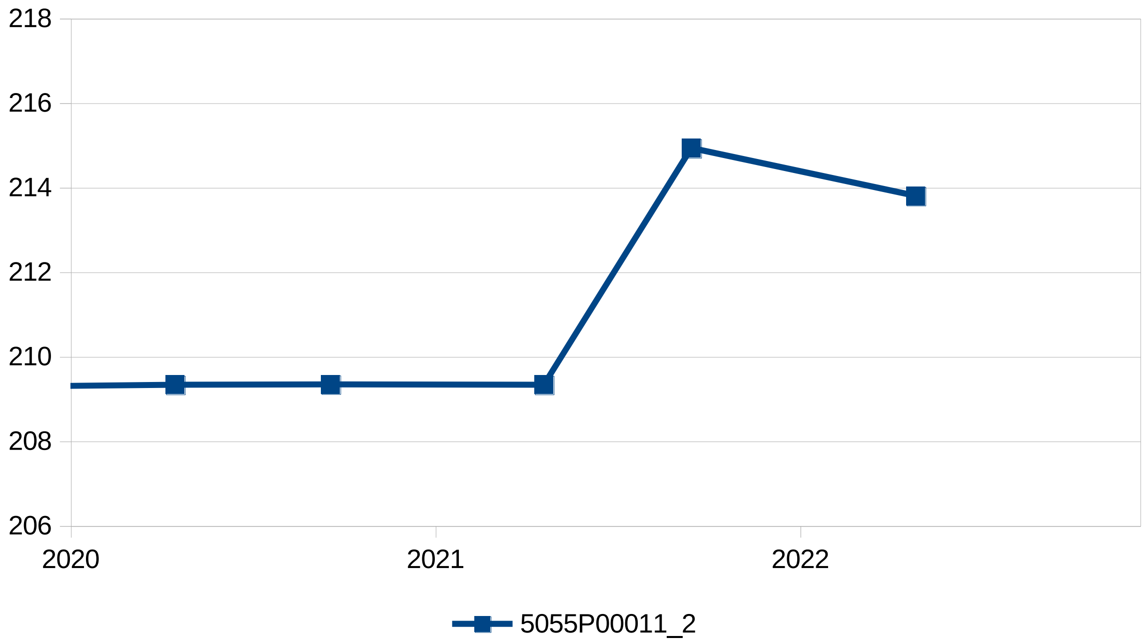

Fig. 144. The water table changes in the monitoring well No. 5055P00011_2

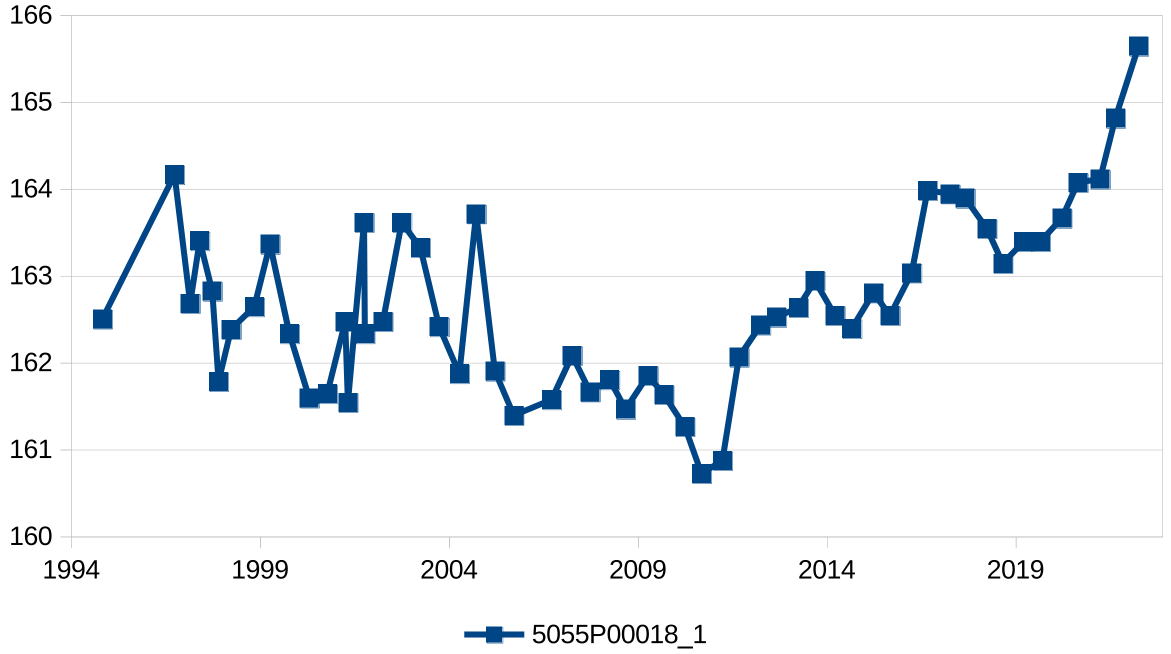

Fig. 145. The water table changes in the monitoring well No. 5055P00018_2

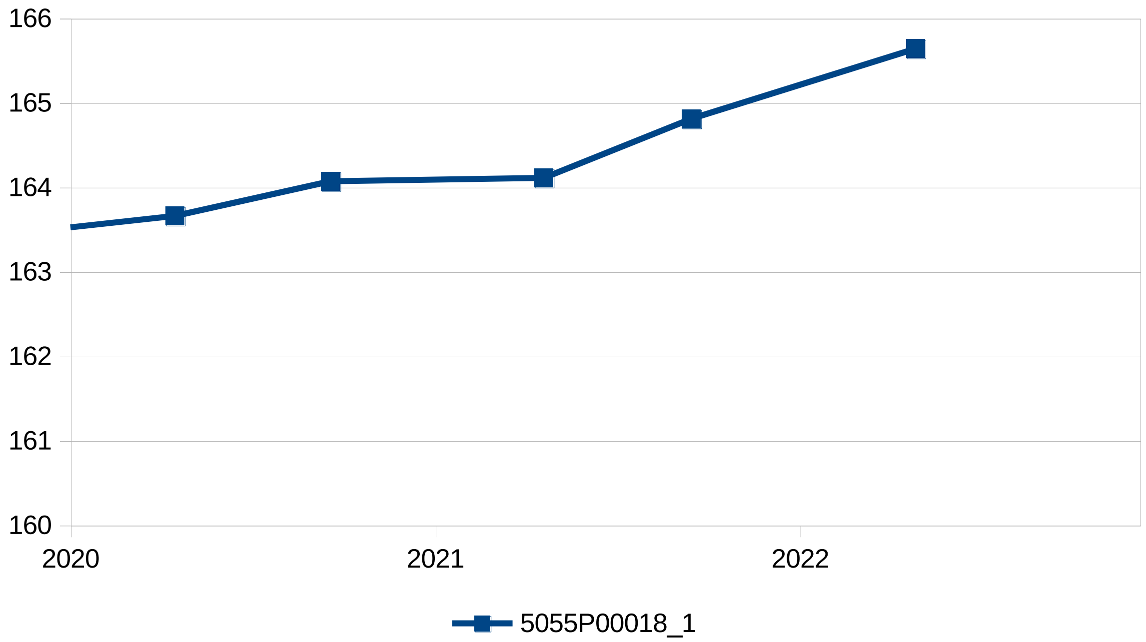

Fig. 146. The water table changes in the monitoring well No. 5055P00018_2

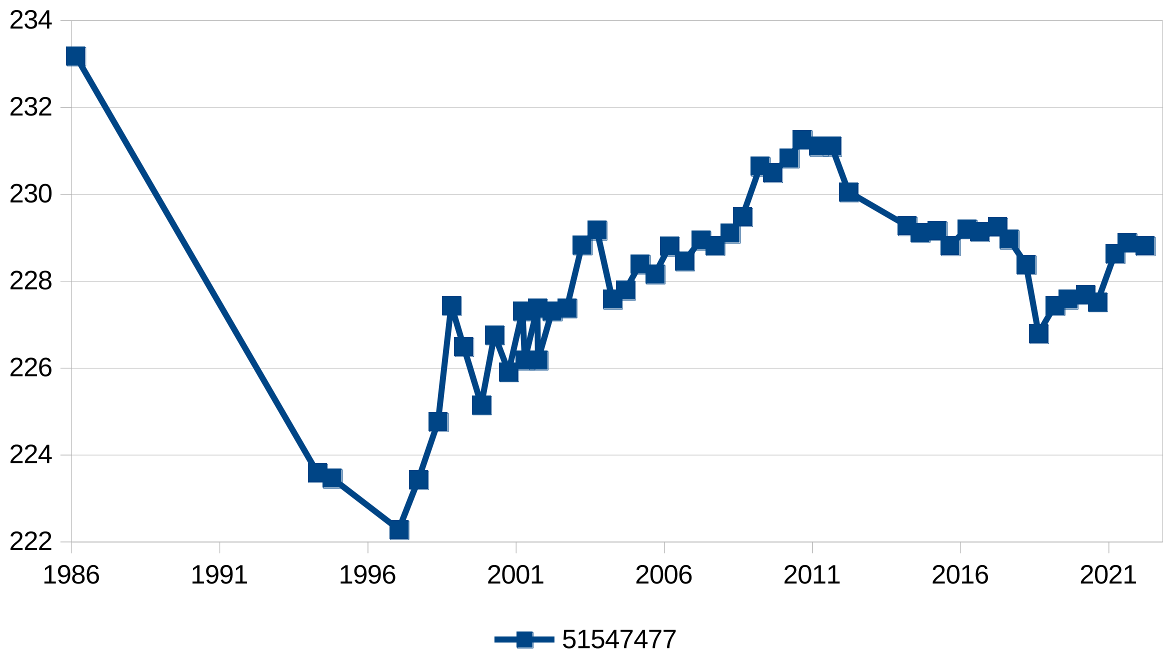

Fig. 147. The water table changes in the monitoring well No. 51547477

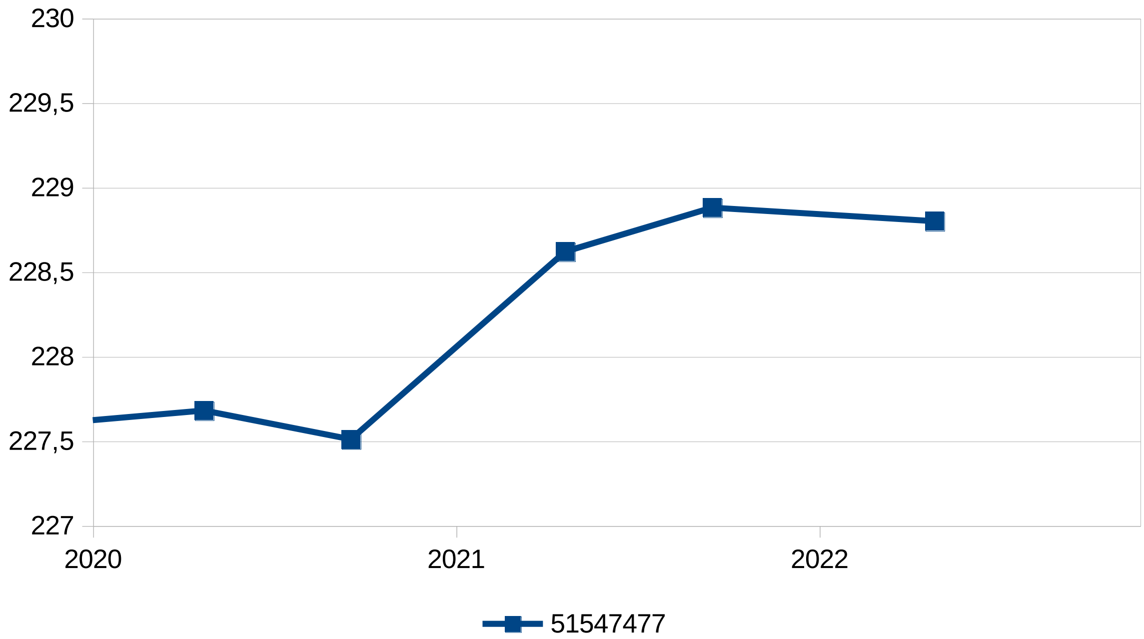

Fig. 148. The water table changes in the monitoring well No. 51547477

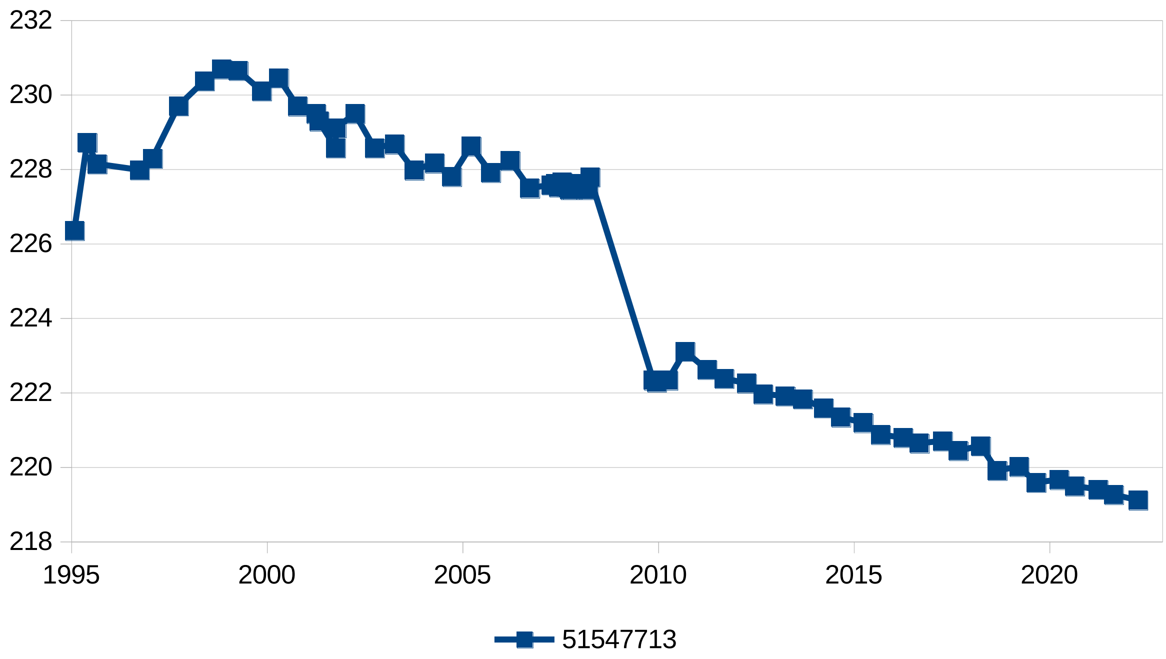

Fig. 149. The water table changes in the monitoring well No. 51547713

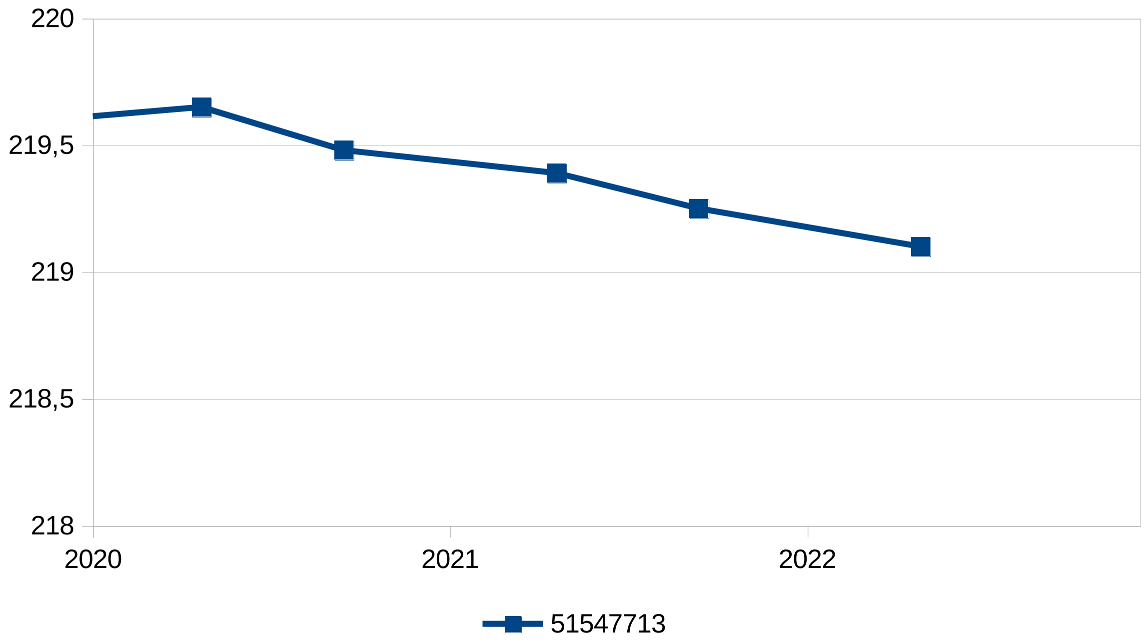

Fig. 150. The water table changes in the monitoring well No. 51547713

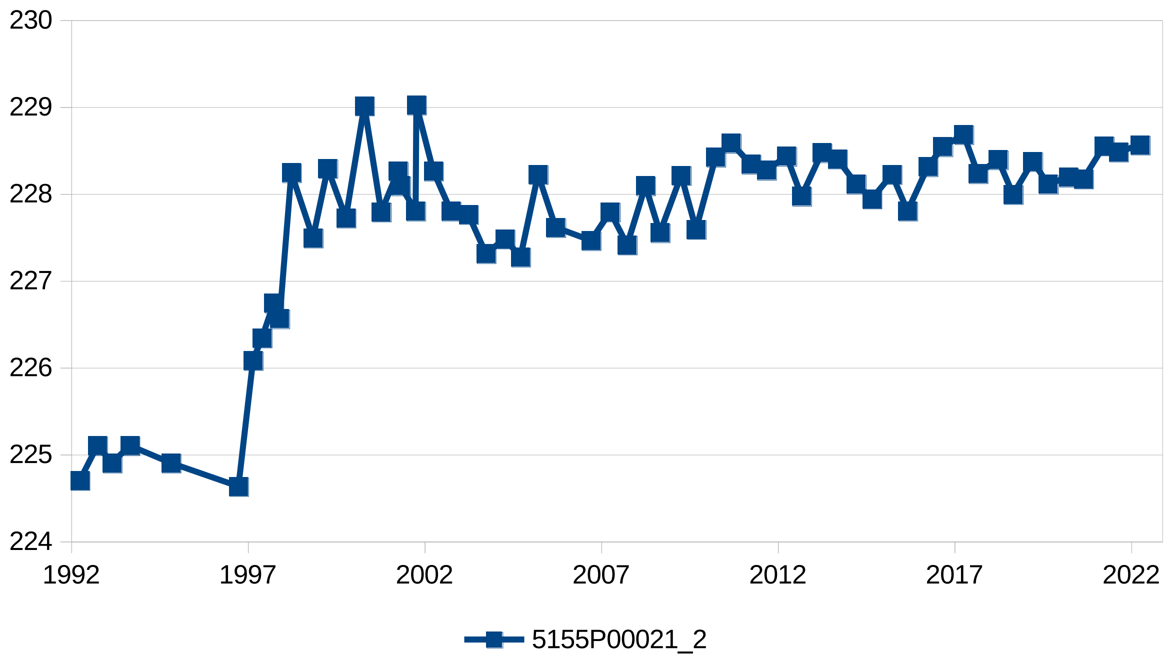

Fig. 151. The water table changes in the monitoring well No. 5155P00021_2

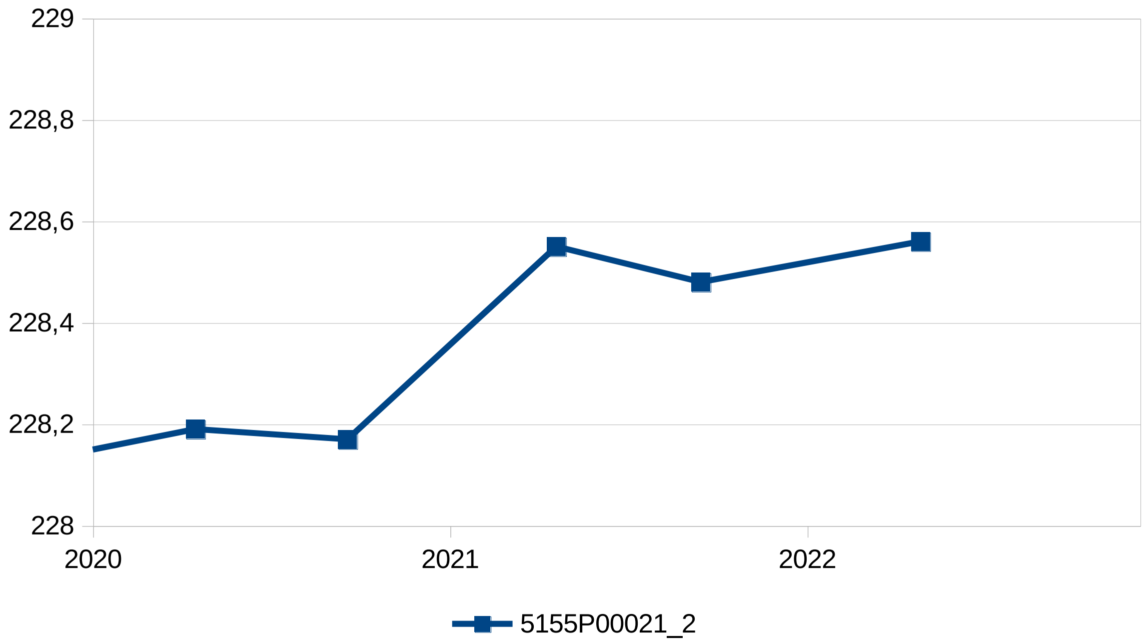

Fig. 152. The water table changes in the monitoring well No. 5155P00021_2

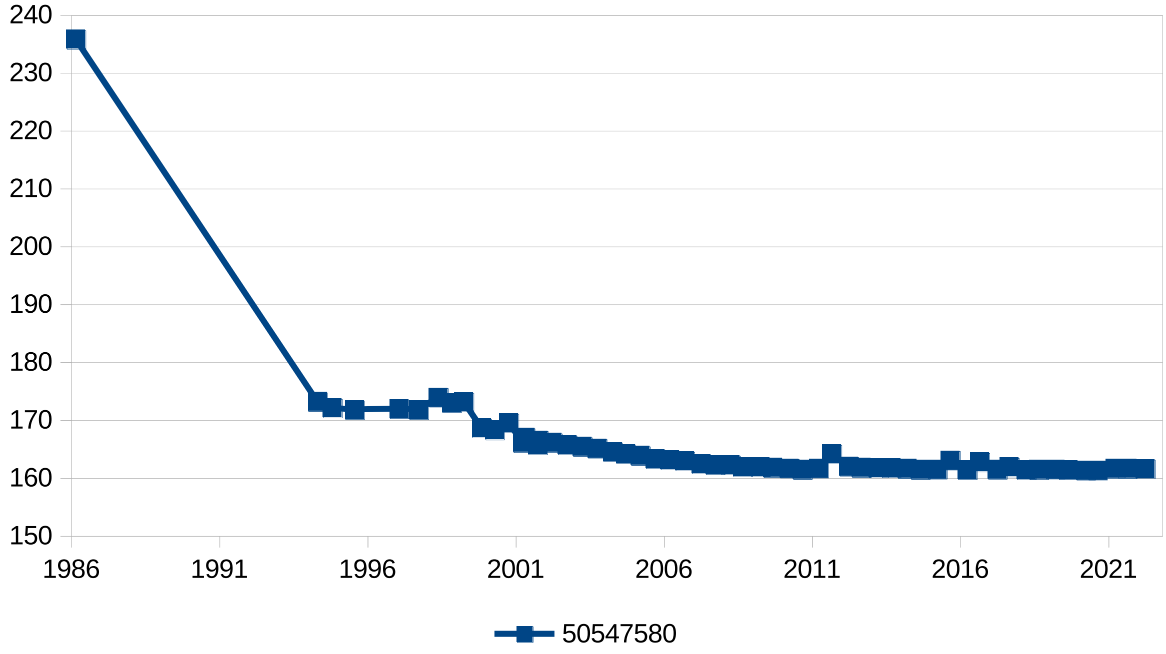

Fig. 153. The water table changes in the monitoring well No. 50547580

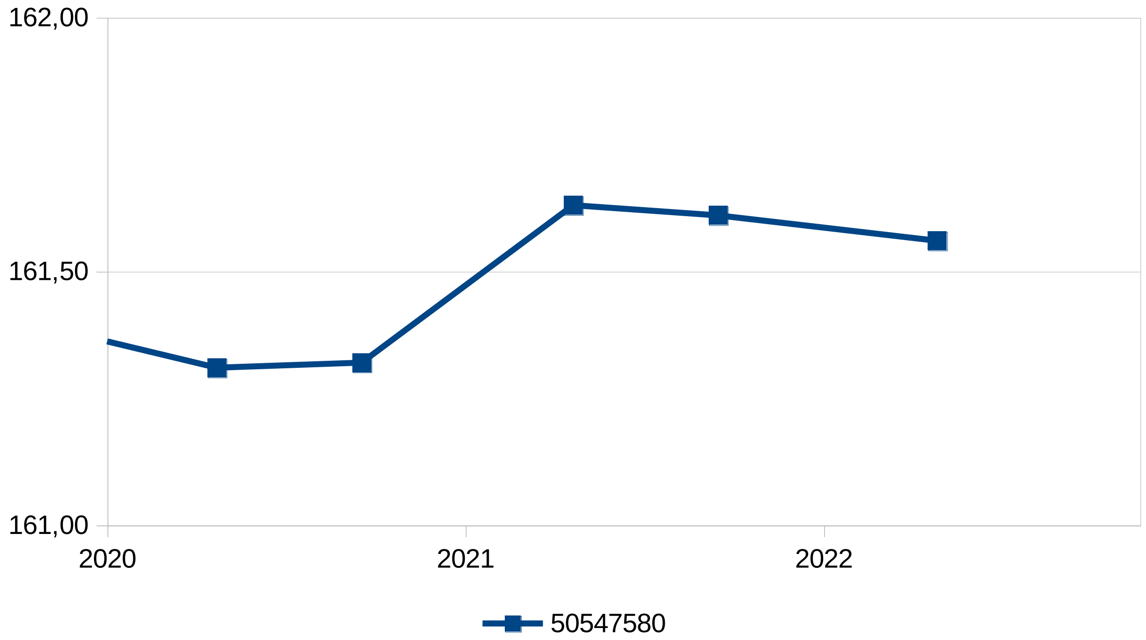

Fig. 154. The water table changes in the monitoring well No. 50547580

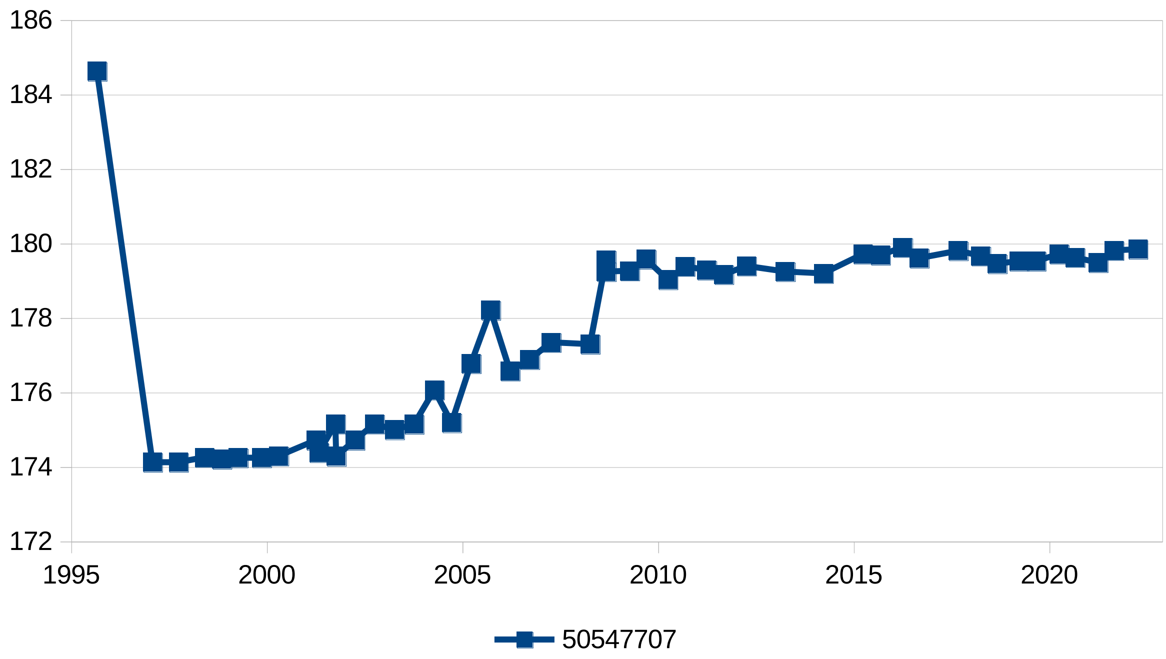

Fig. 155. The water table changes in the monitoring well No. 50547707

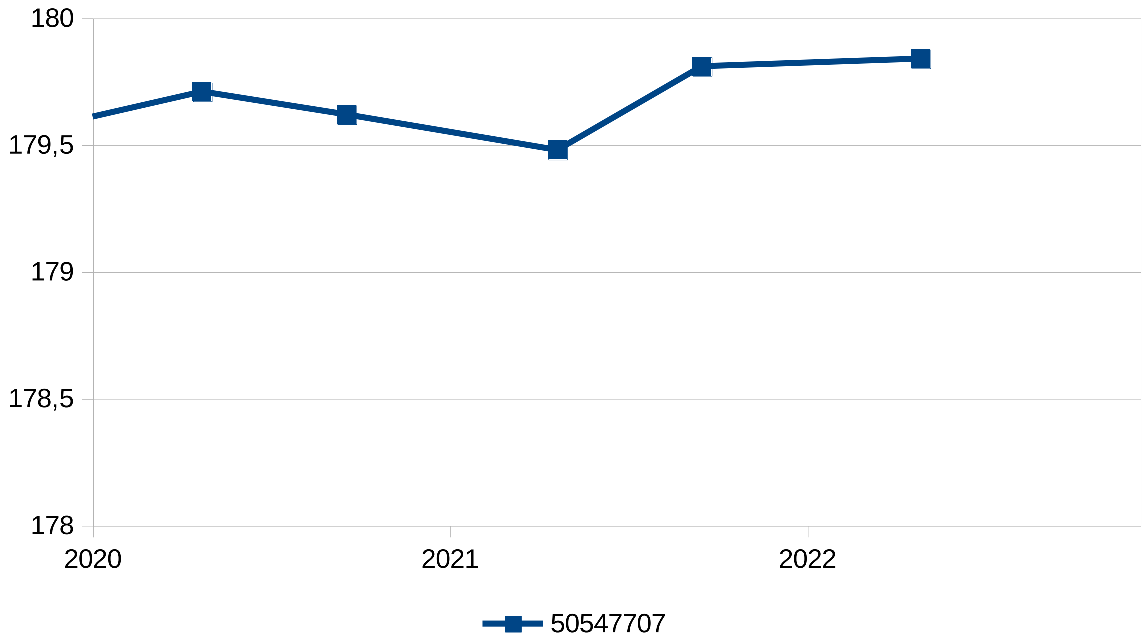

Fig. 156. The water table changes in the monitoring well No. 50547707

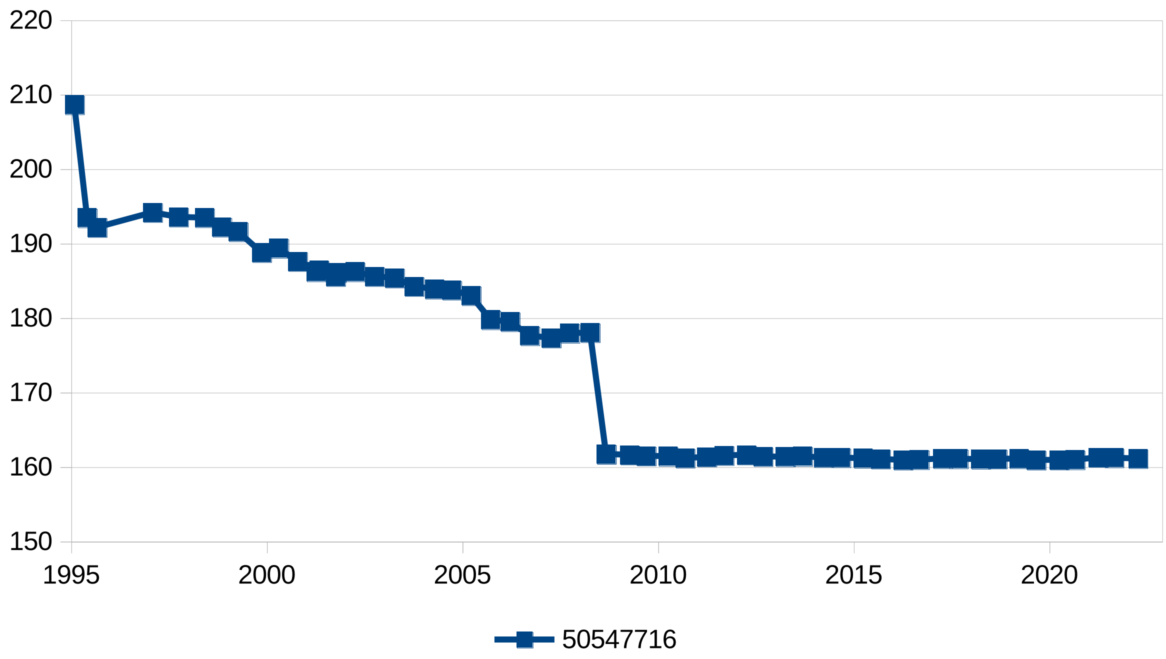

Fig. 157. The water table changes in the monitoring well No. 50547716

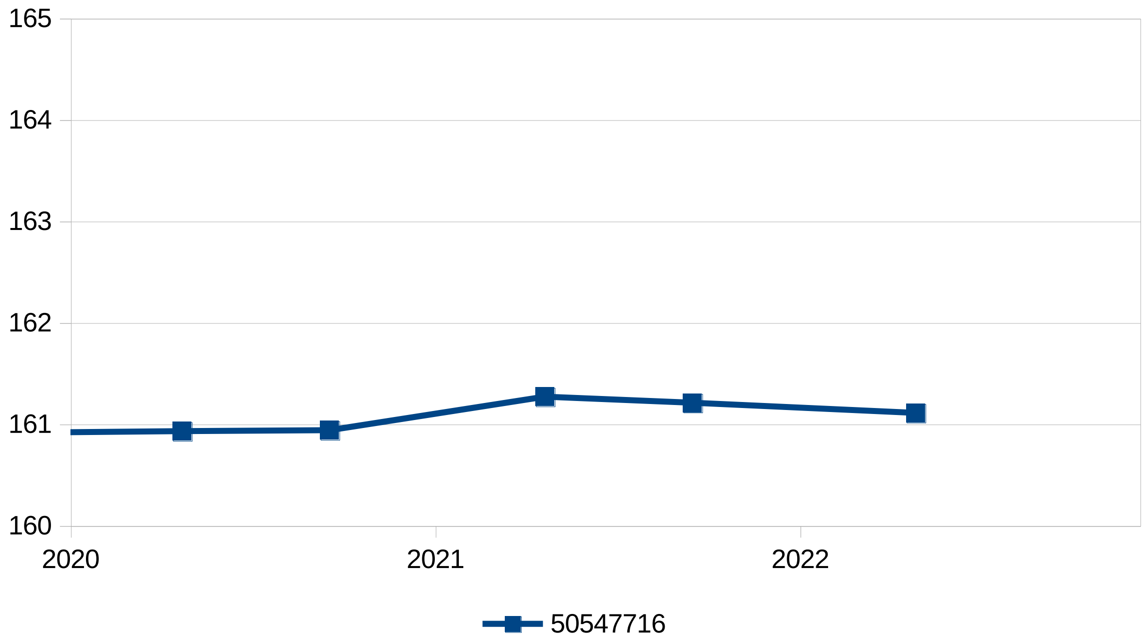

Fig. 158. The water table changes in the monitoring well No. 50547716

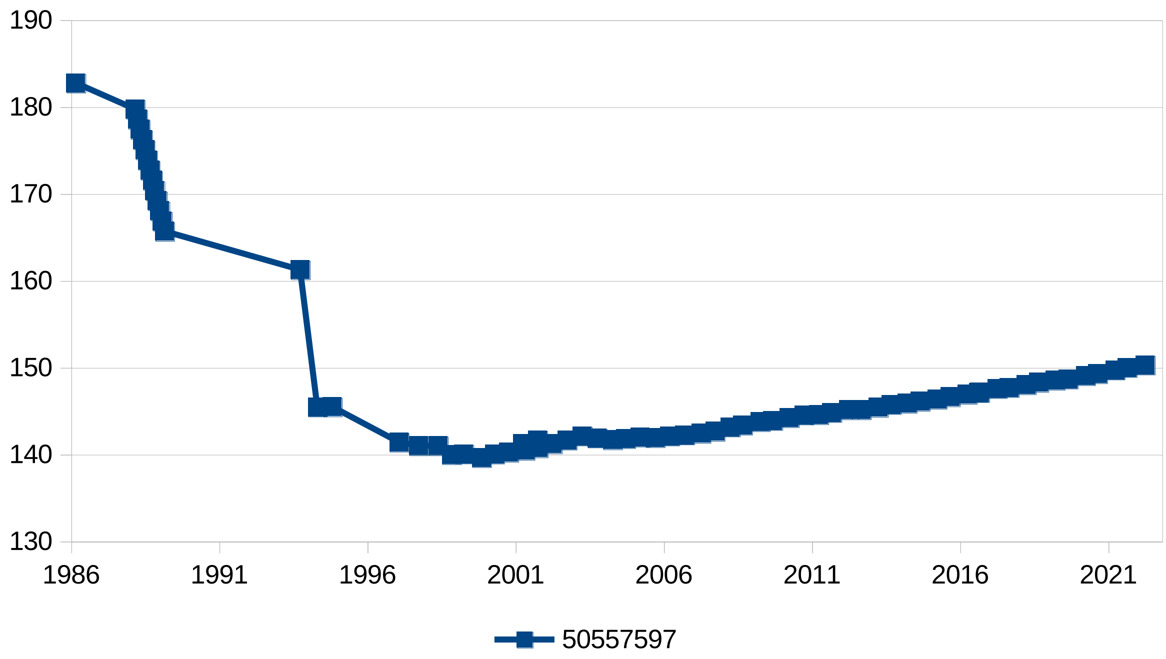

Fig. 159. The water table changes in the monitoring well No. 50557597

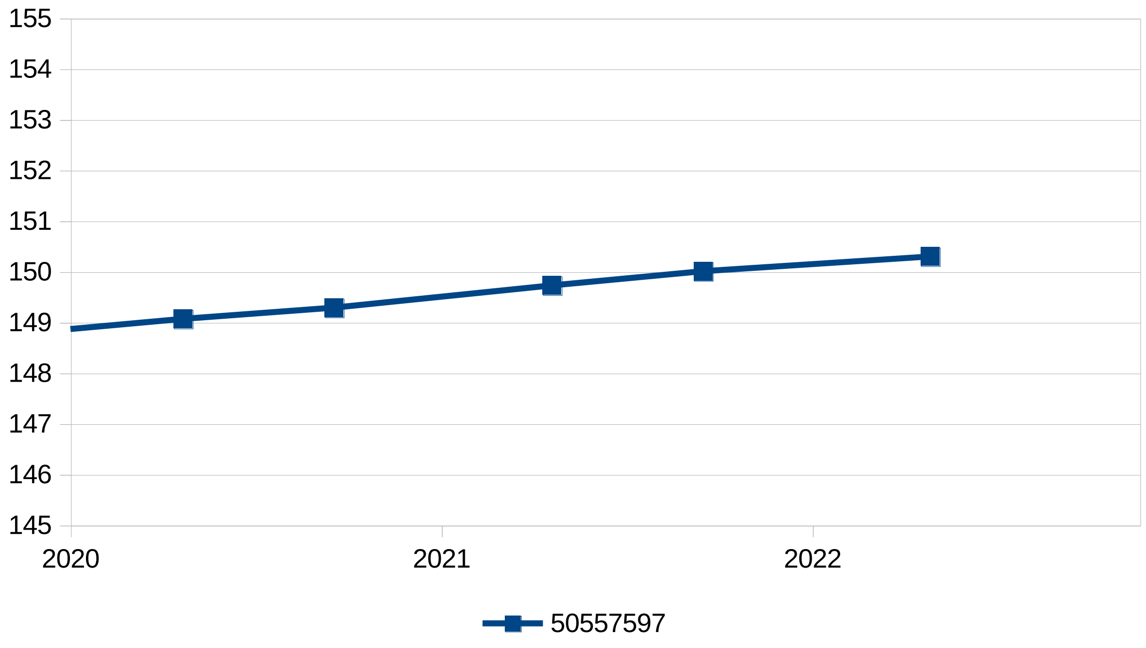

Fig. 160. The water table changes in the monitoring well No. 50557597

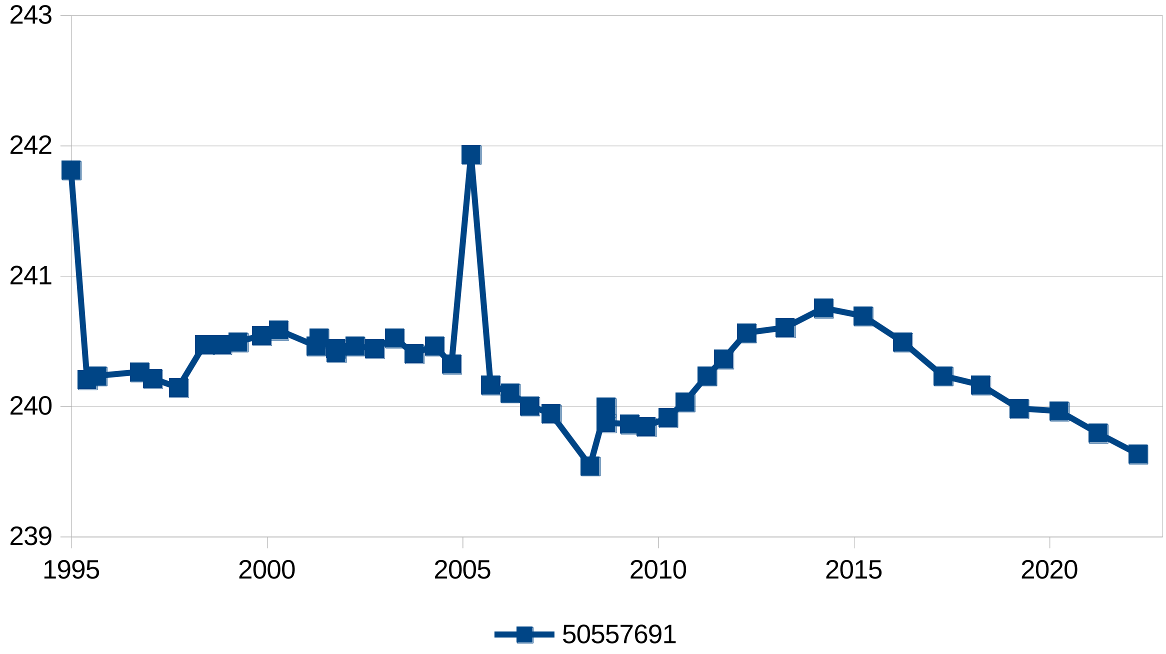

Fig. 161. The water table changes in the monitoring well No. 50557691

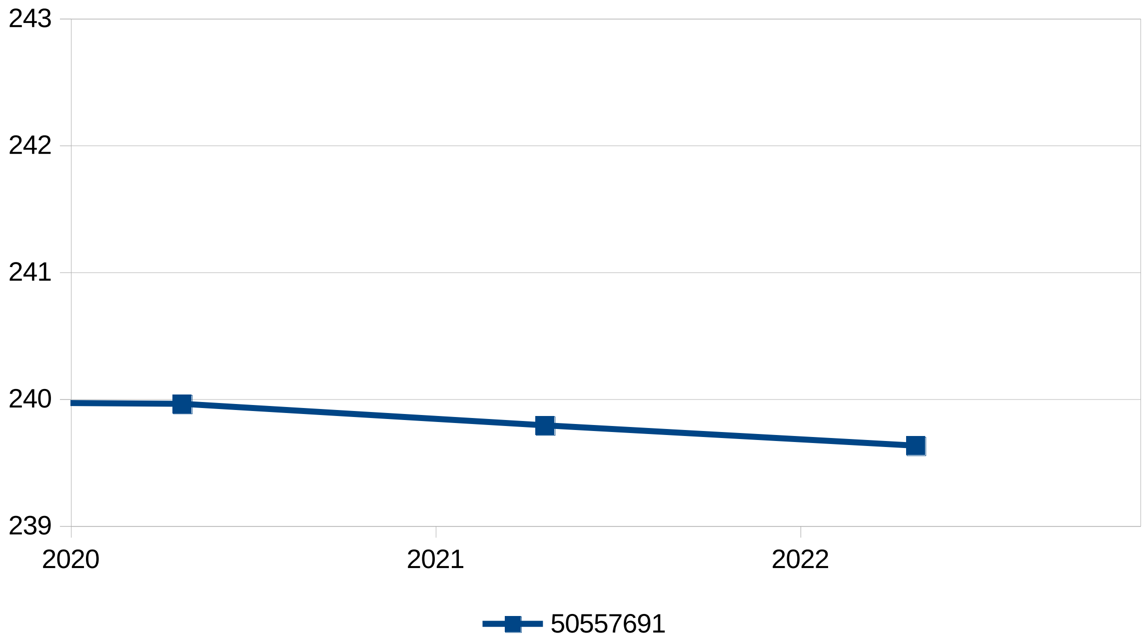

Fig. 162. The water table changes in the monitoring well No. 50557691

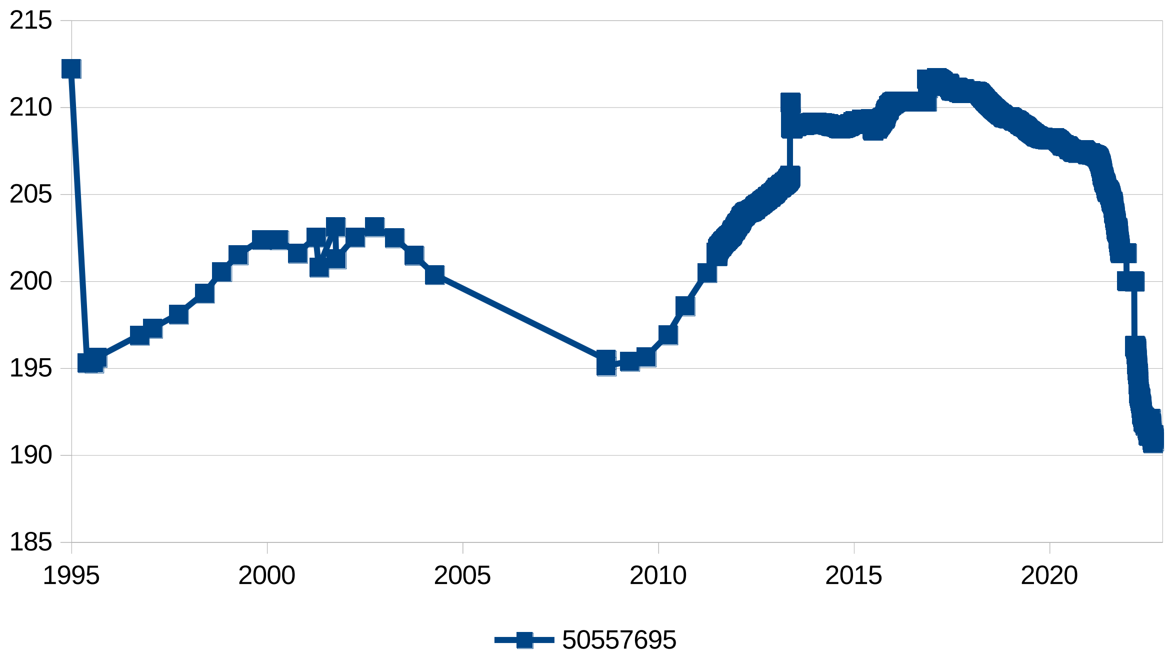

Fig. 163. The water table changes in the monitoring well No. 50557695

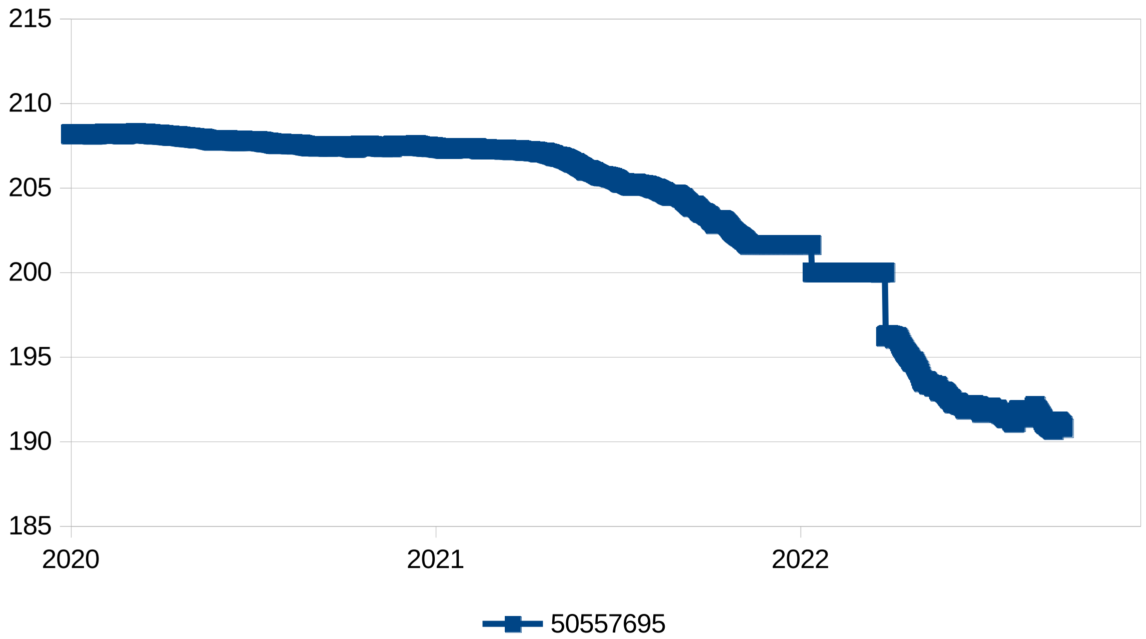

Fig. 164. The water table changes in the monitoring well No. 50557695

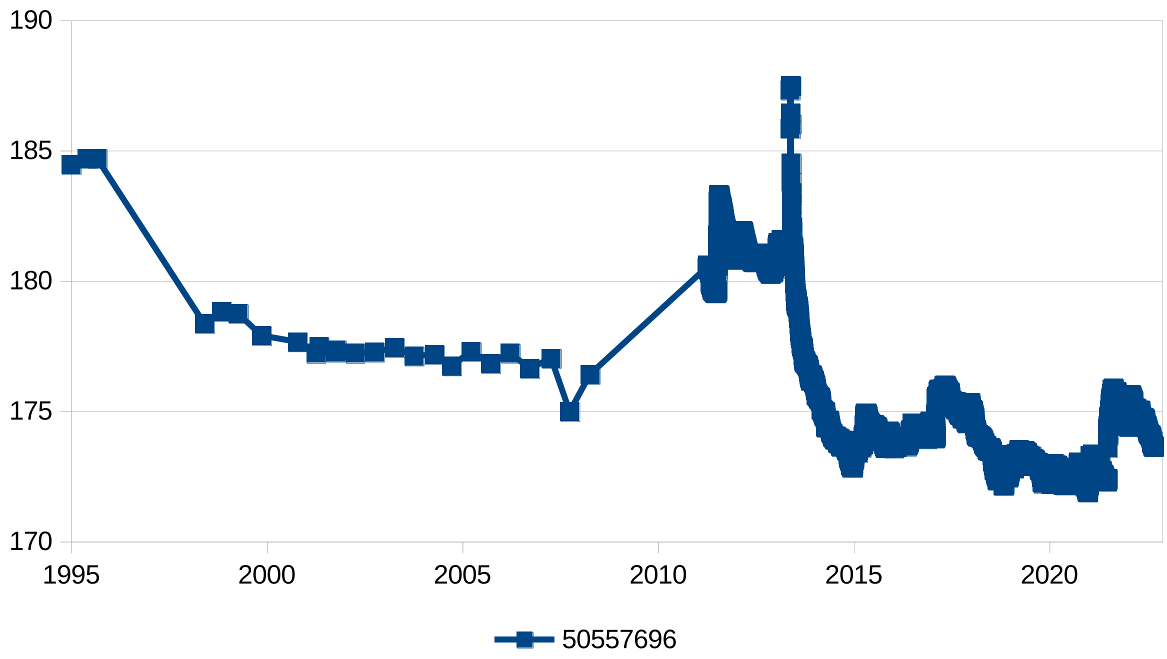

Fig. 165. The water table changes in the monitoring well No. 50557696

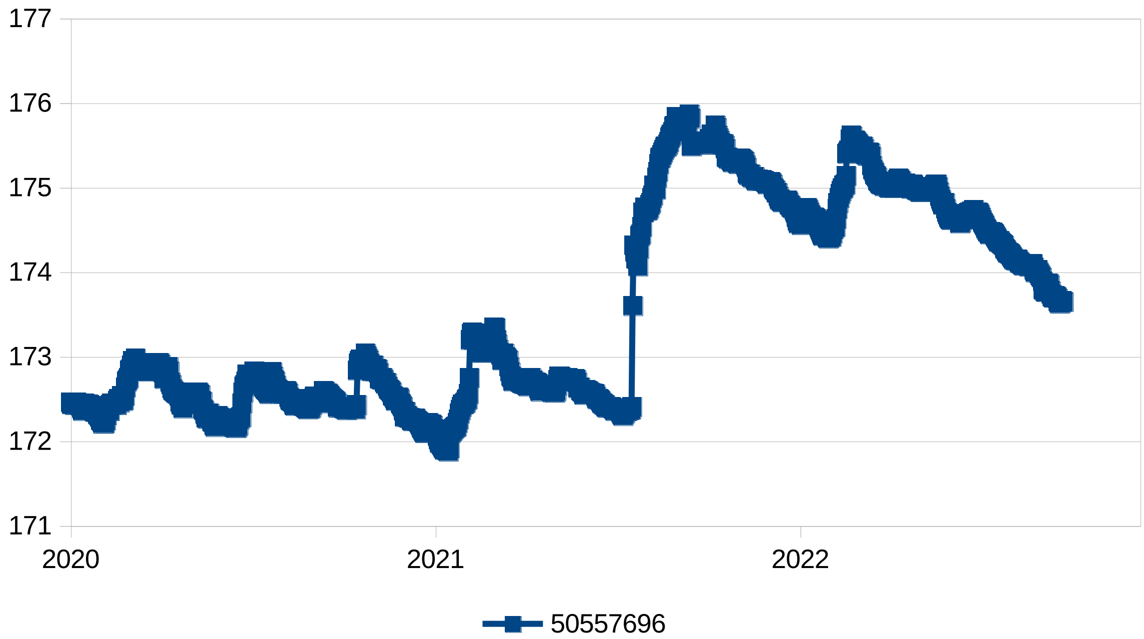

Fig. 166. The water table changes in the monitoring well No. 50557696

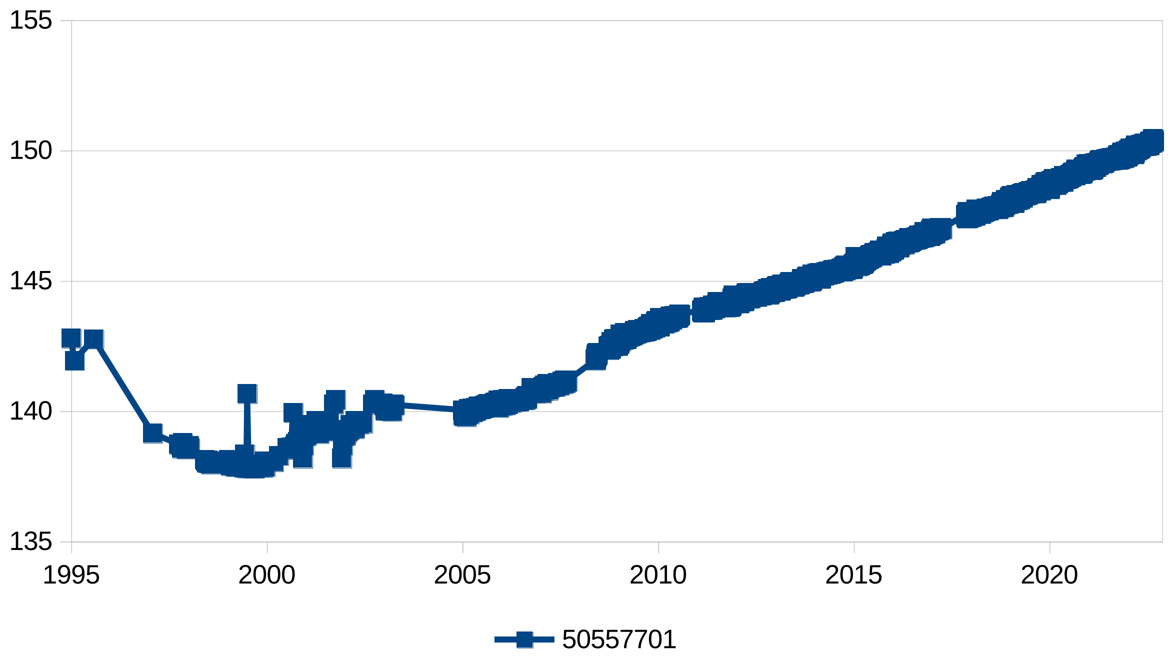

Fig. 167. The water table changes in the monitoring well No. 50557701

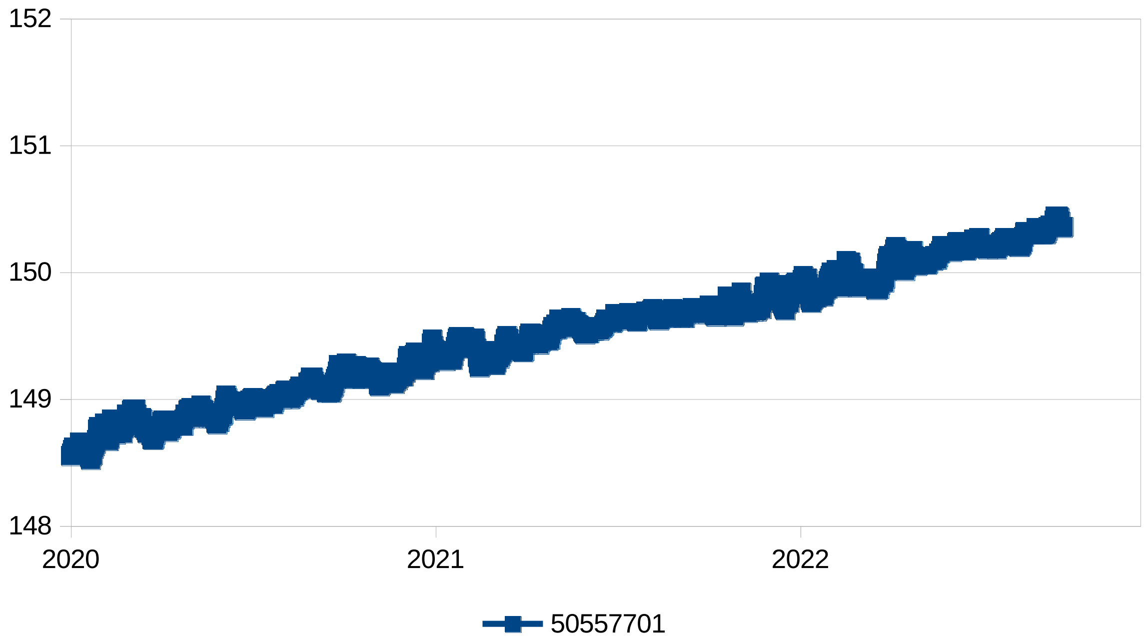

Fig. 168. The water table changes in the monitoring well No. 50557701

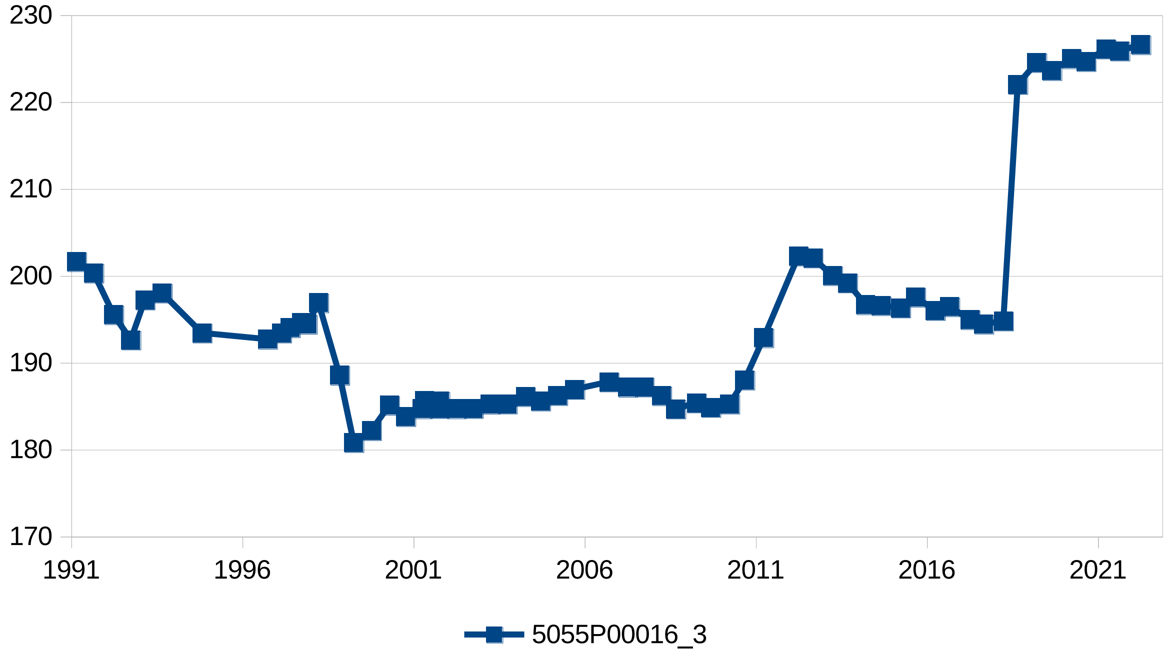

Fig. 169. The water table changes in the monitoring well No. 5055P00016_3

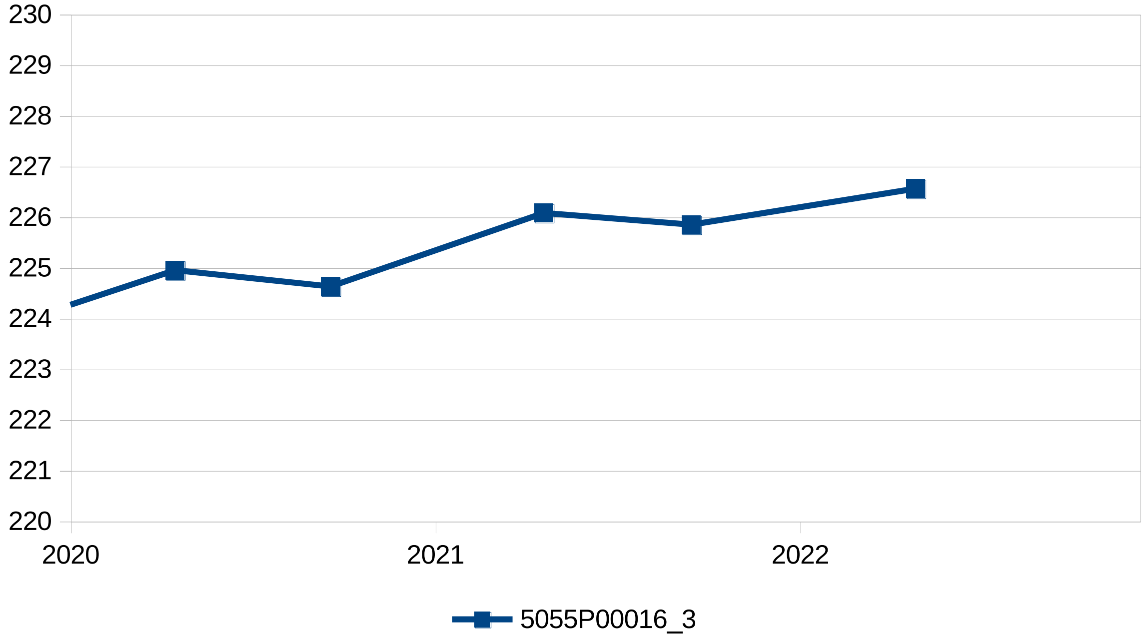

Fig. 170. The water table changes in the monitoring well No. 5055P00016_3

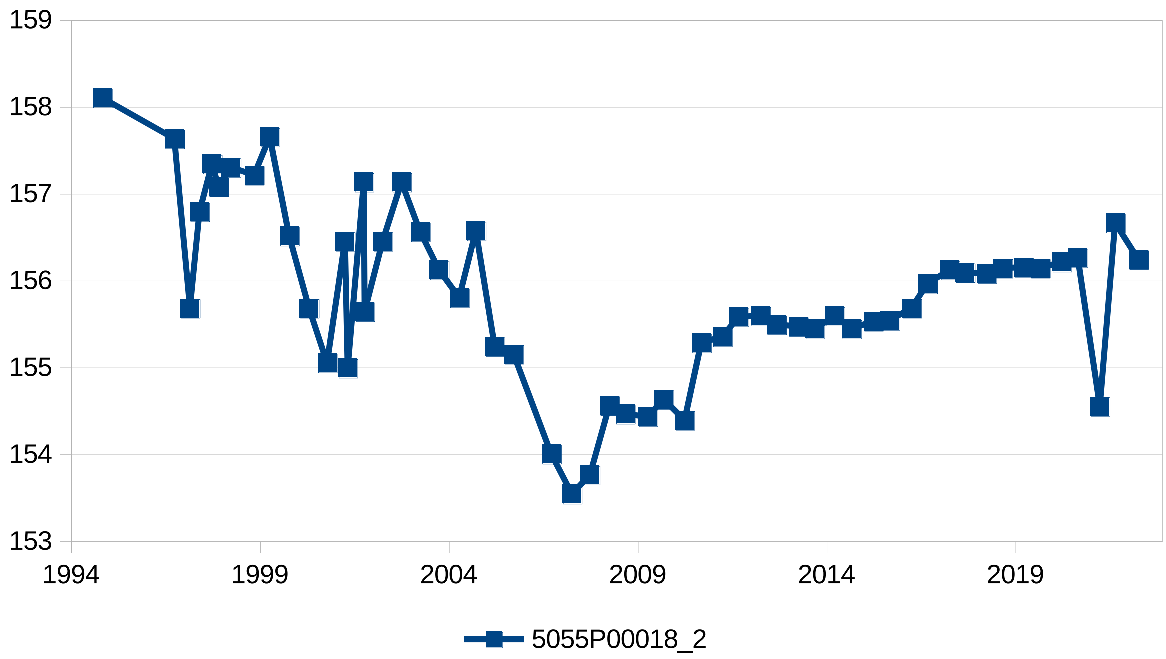

Fig. 171. The water table changes in the monitoring well No. 5055P00018_2

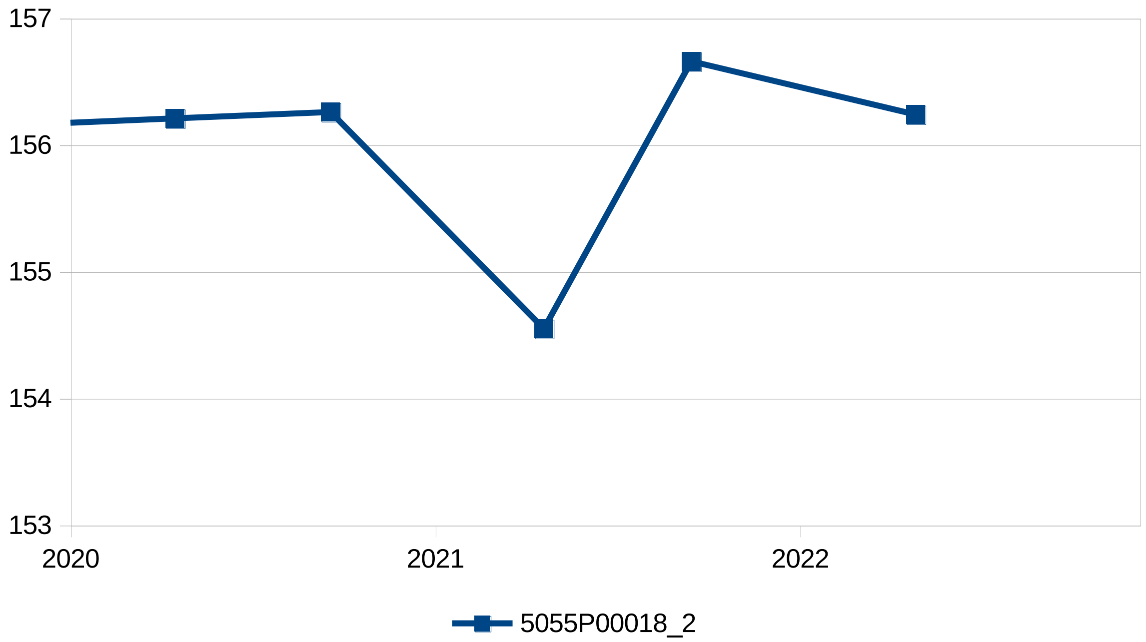

Fig. 172. The water table changes in the monitoring well No. 5055P00018_2

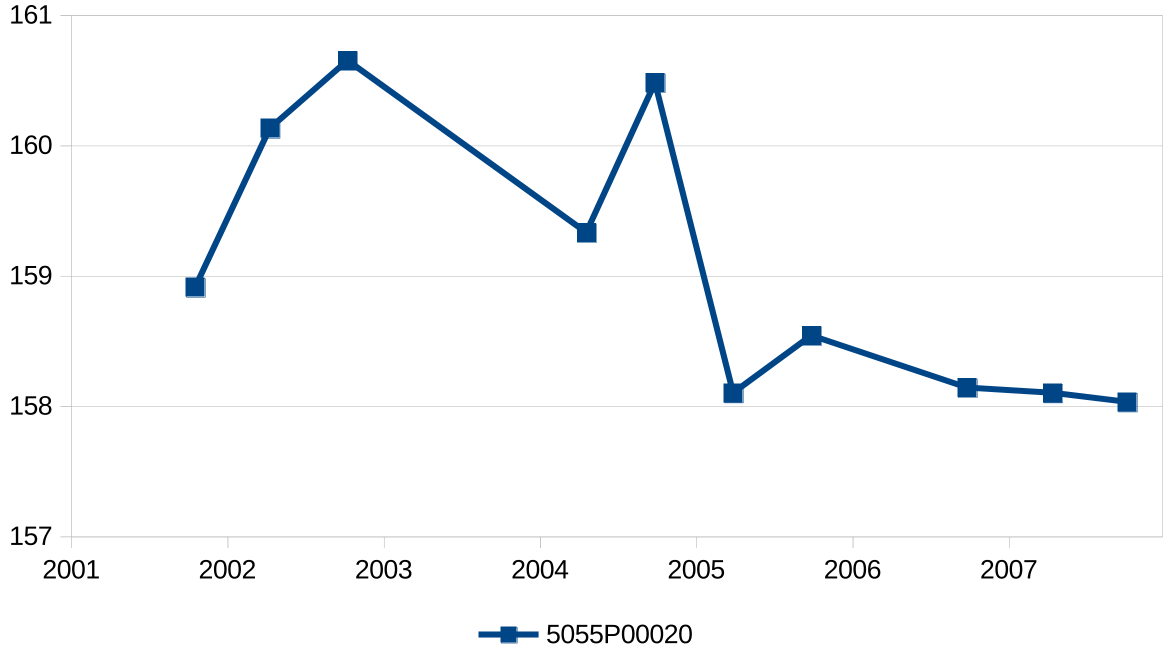

Fig. 173. The water table changes in the monitoring well No. 5055P00020

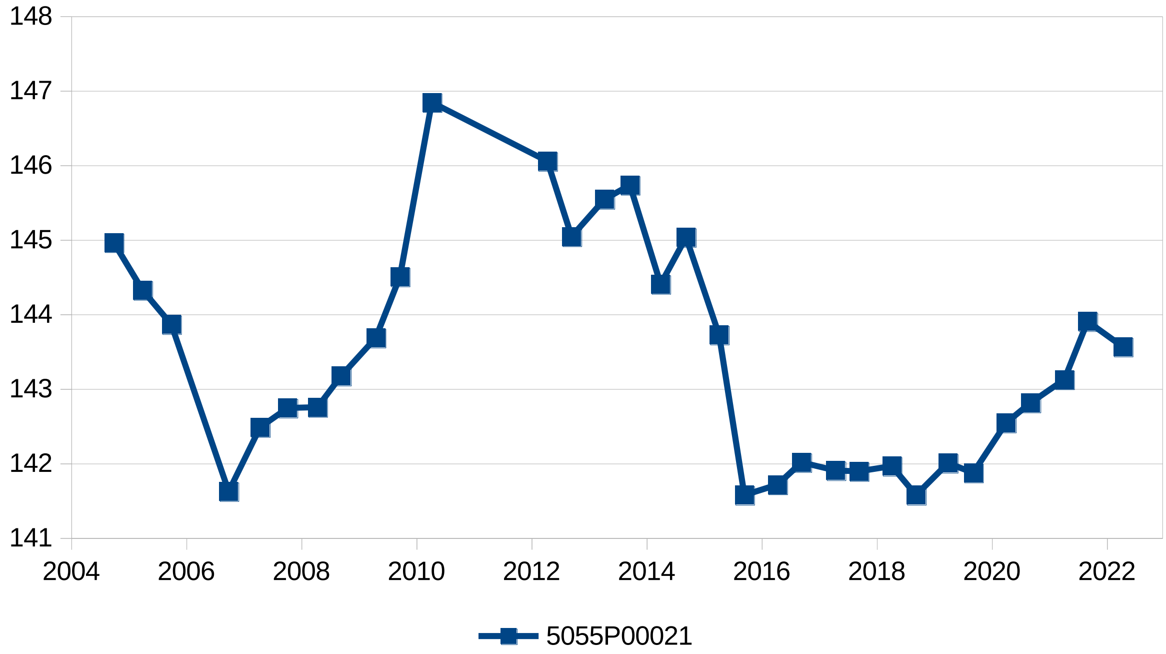

Fig. 174. The water table changes in the monitoring well No. 5055P00021

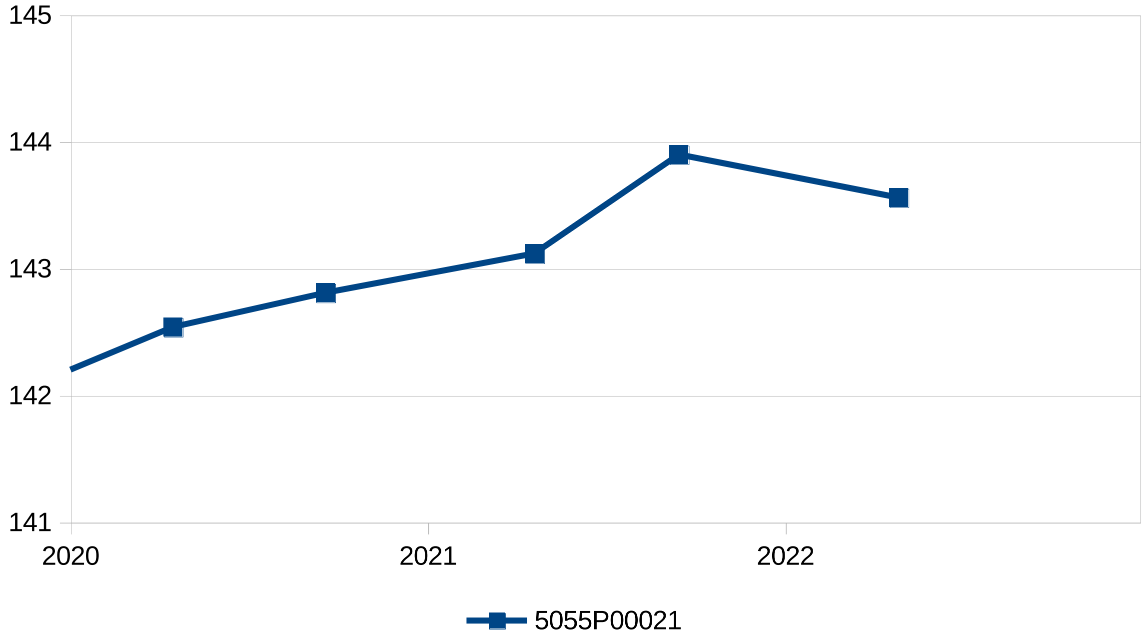

Fig. 175. The water table changes in the monitoring well No. 5055P00021

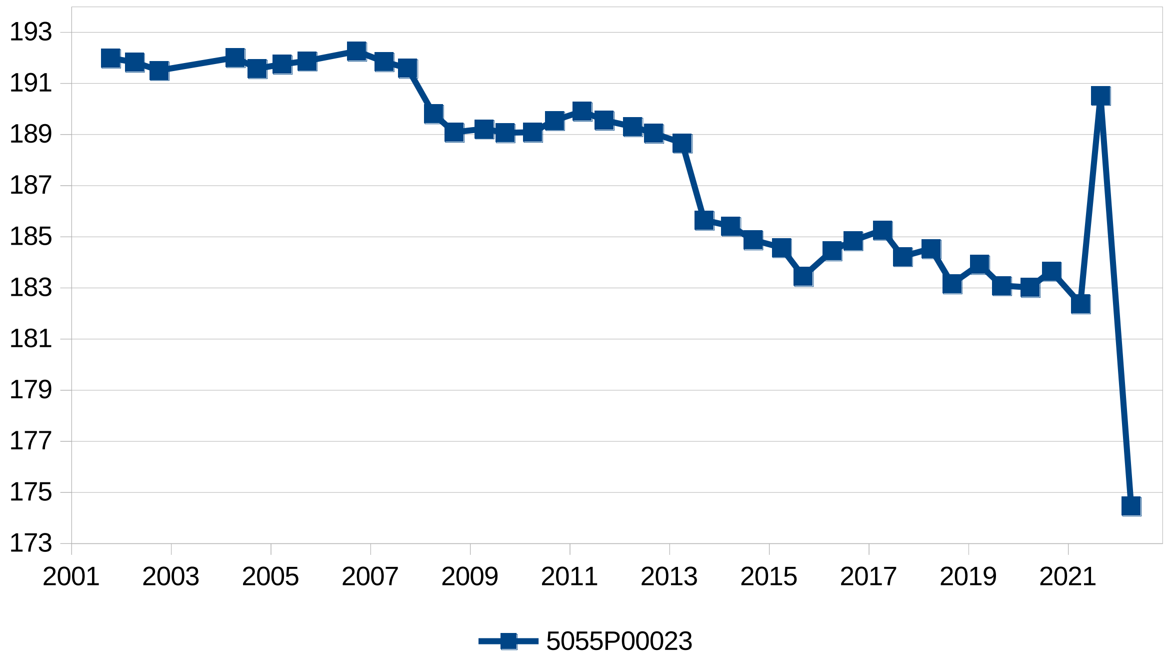

Fig. 176. The water table changes in the monitoring well No. 5055P00023

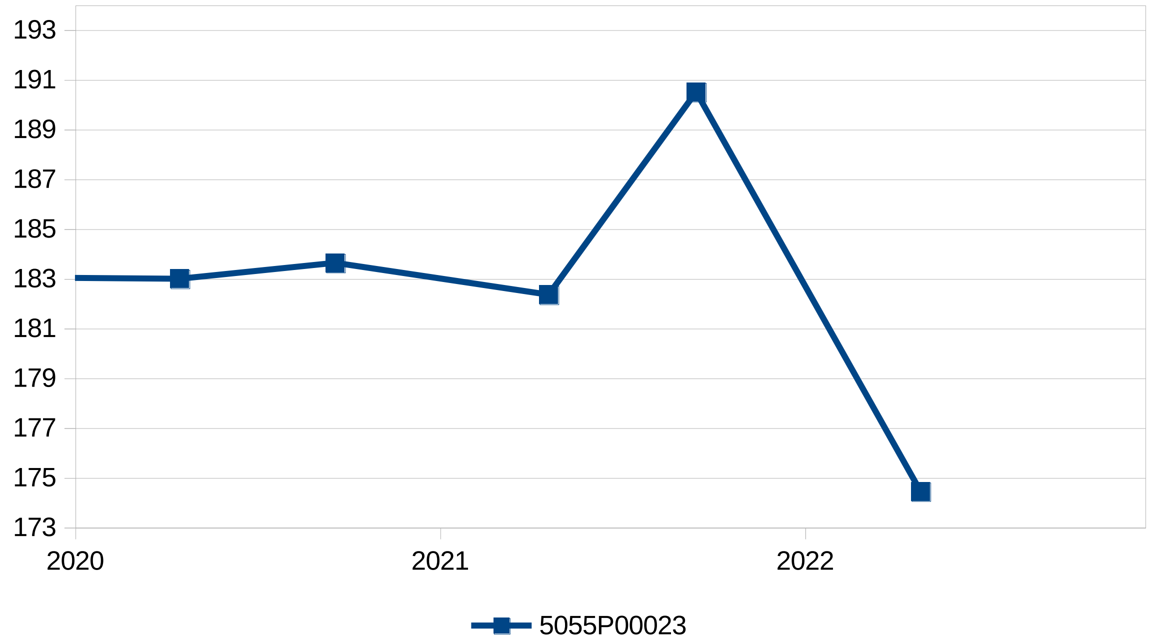

Fig. 177. The water table changes in the monitoring well No. 5055P00023

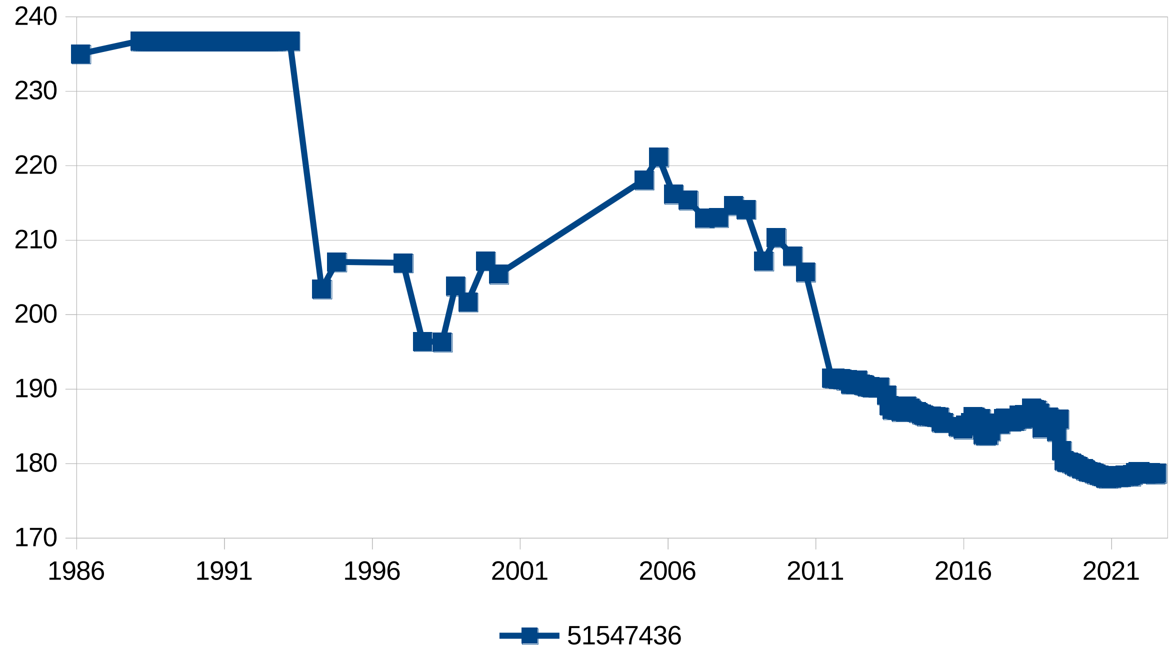

Fig. 178. The water table changes in the monitoring well No. 51547436

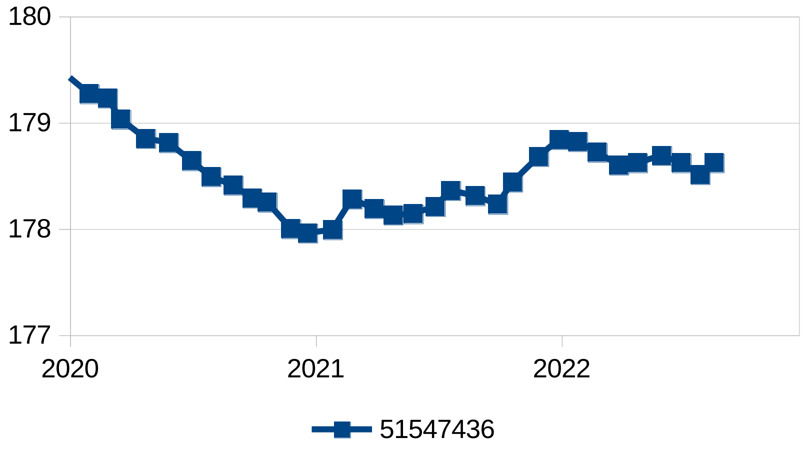

Fig. 179. The water table changes in the monitoring well No. 51547436

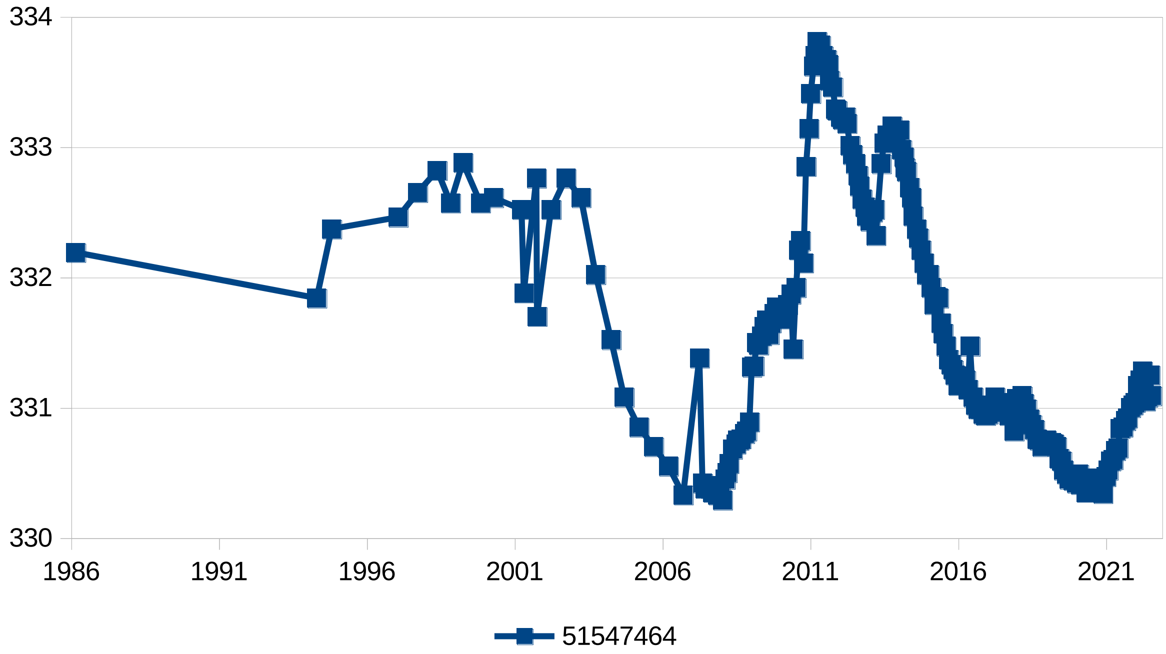

Fig. 180. The water table changes in the monitoring well No. 51547464

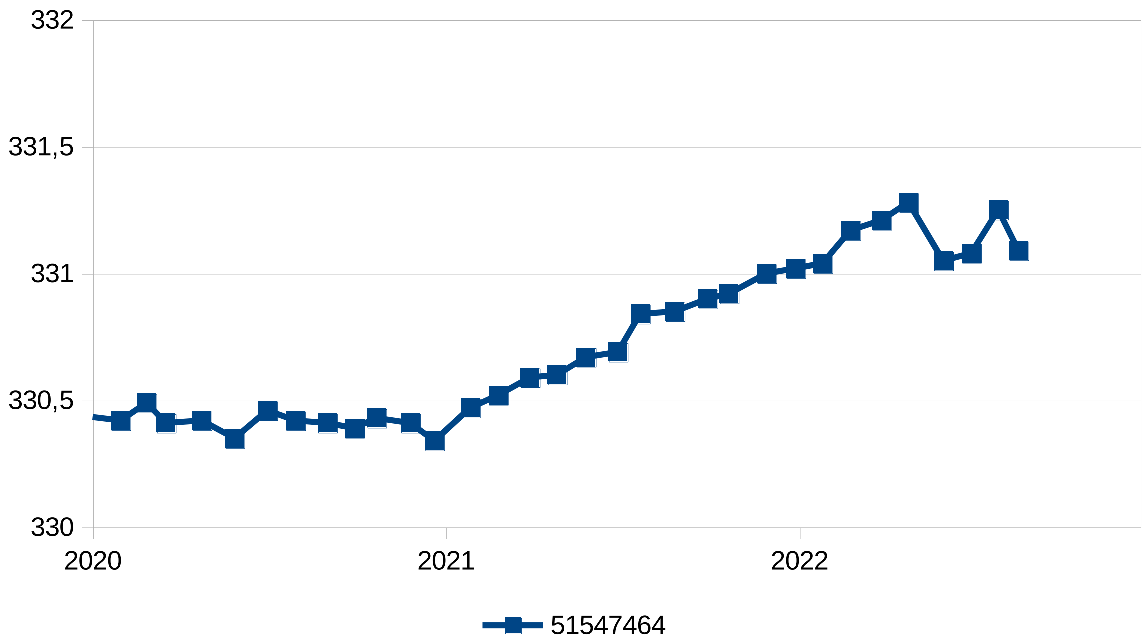

Fig. 181. The water table changes in the monitoring well No. 51547464

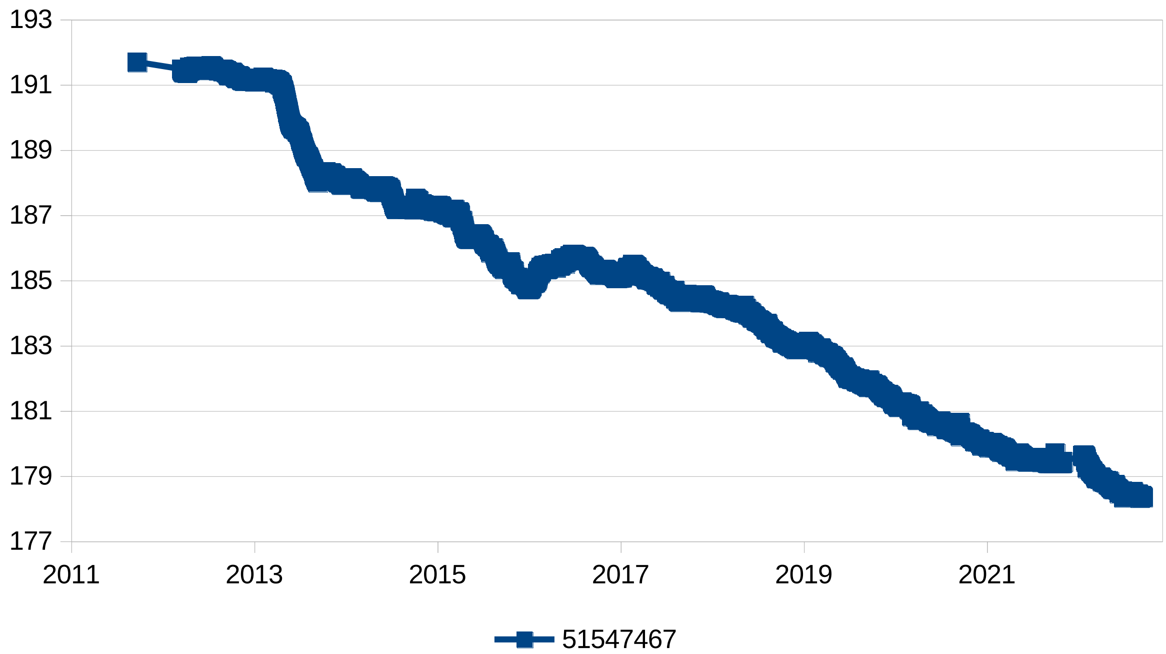

Fig. 182. The water table changes in the monitoring well No. 51547467

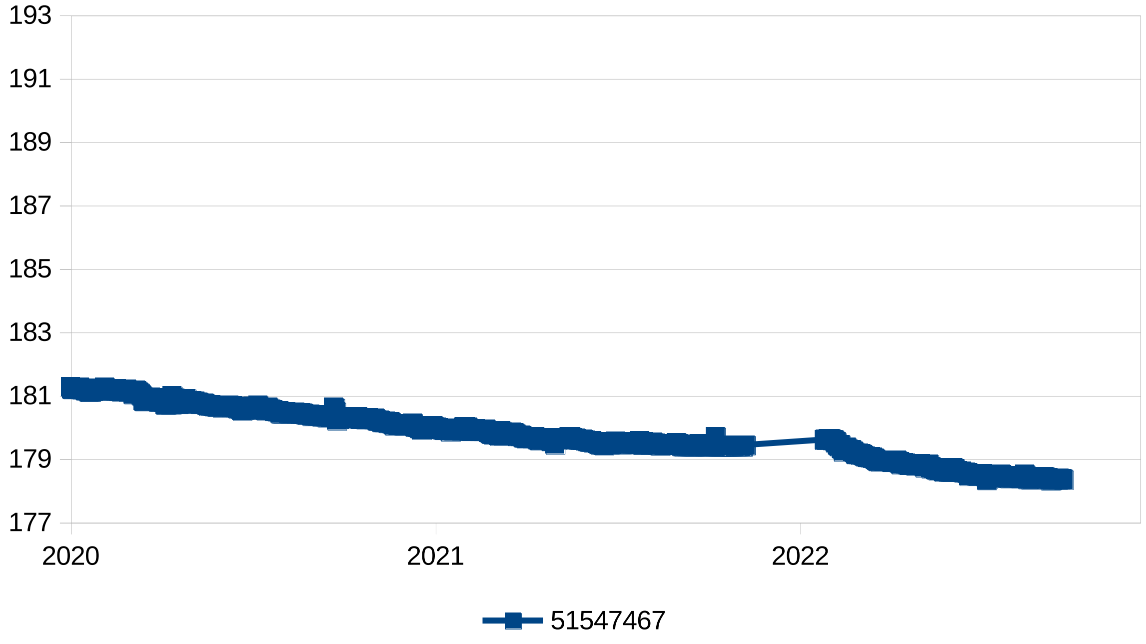

Fig. 183. The water table changes in the monitoring well No. 51547467

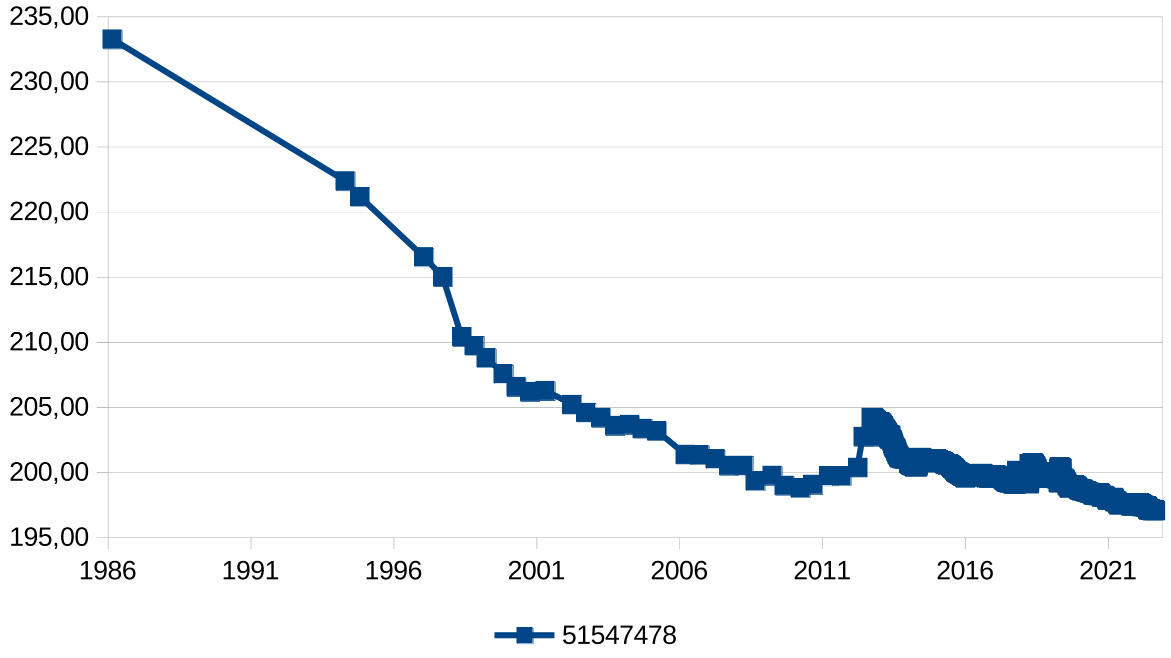

Fig. 184. The water table changes in the monitoring well No. 51547478

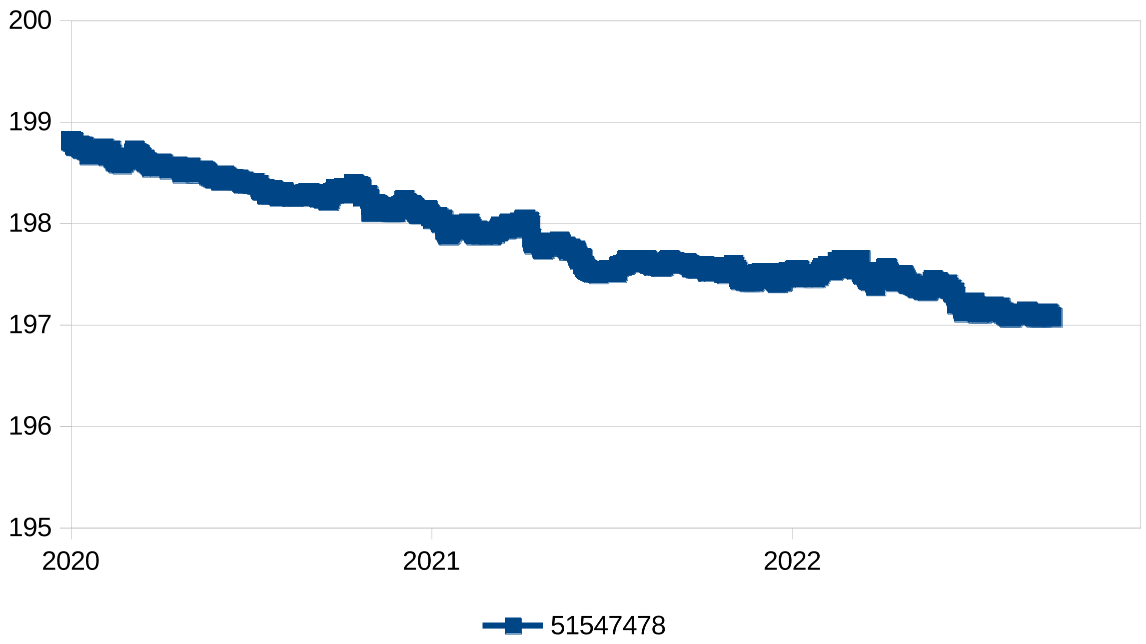

Fig. 185. The water table changes in the monitoring well No. 51547478

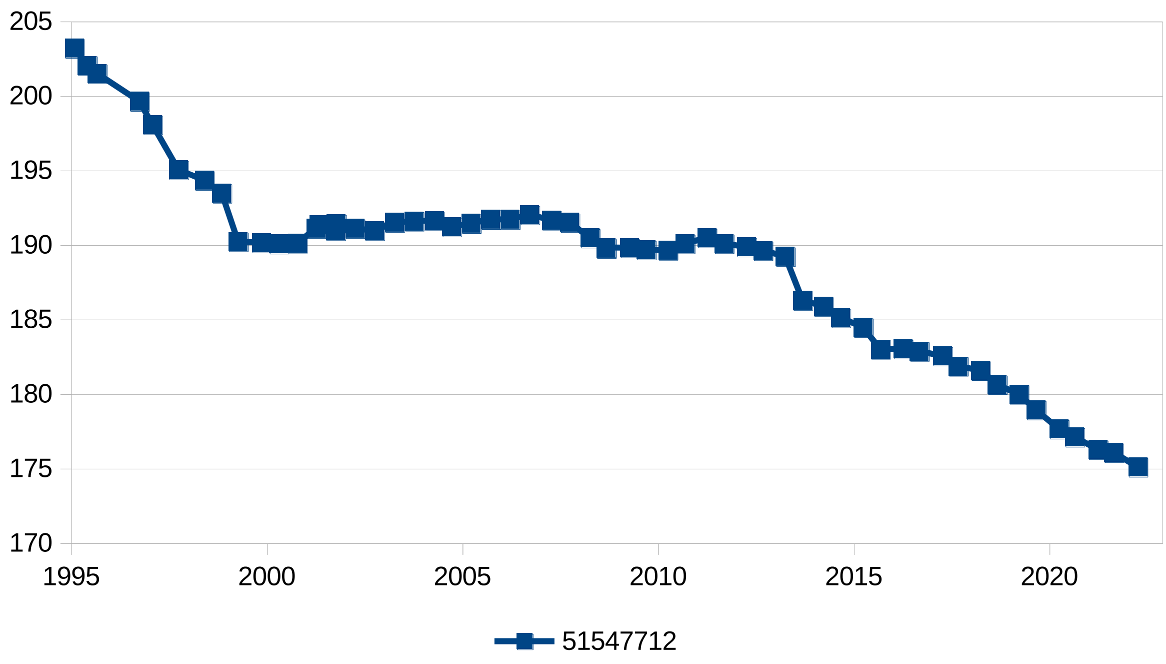

Fig. 186. The water table changes in the monitoring well No. 51547712

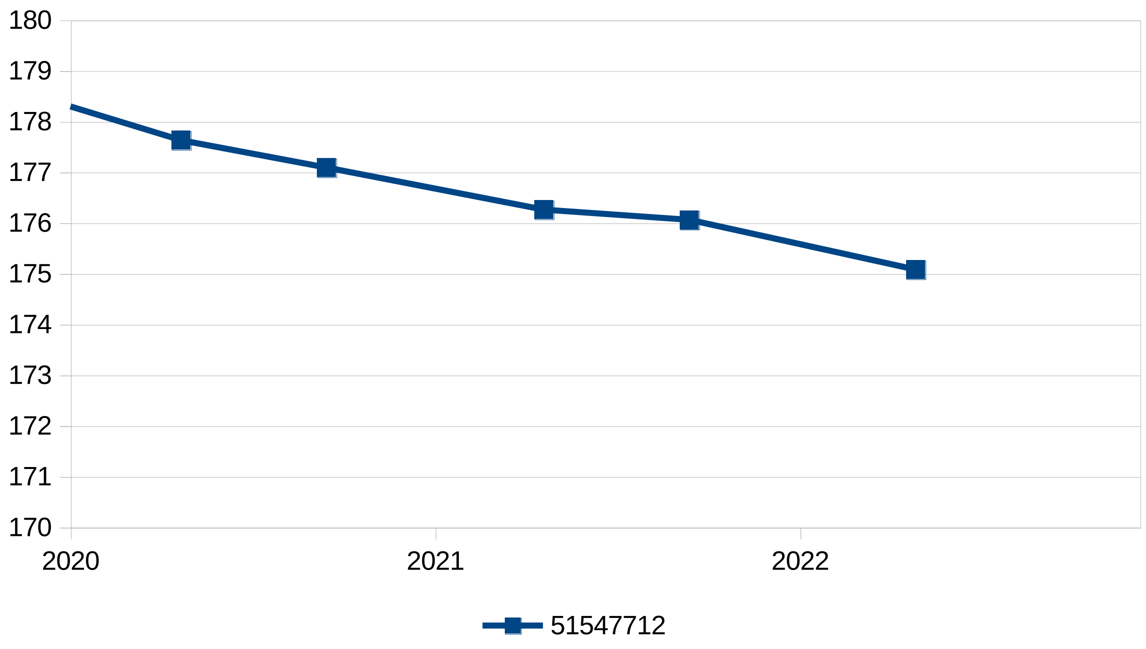

Fig. 187. The water table changes in the monitoring well No. 51547712

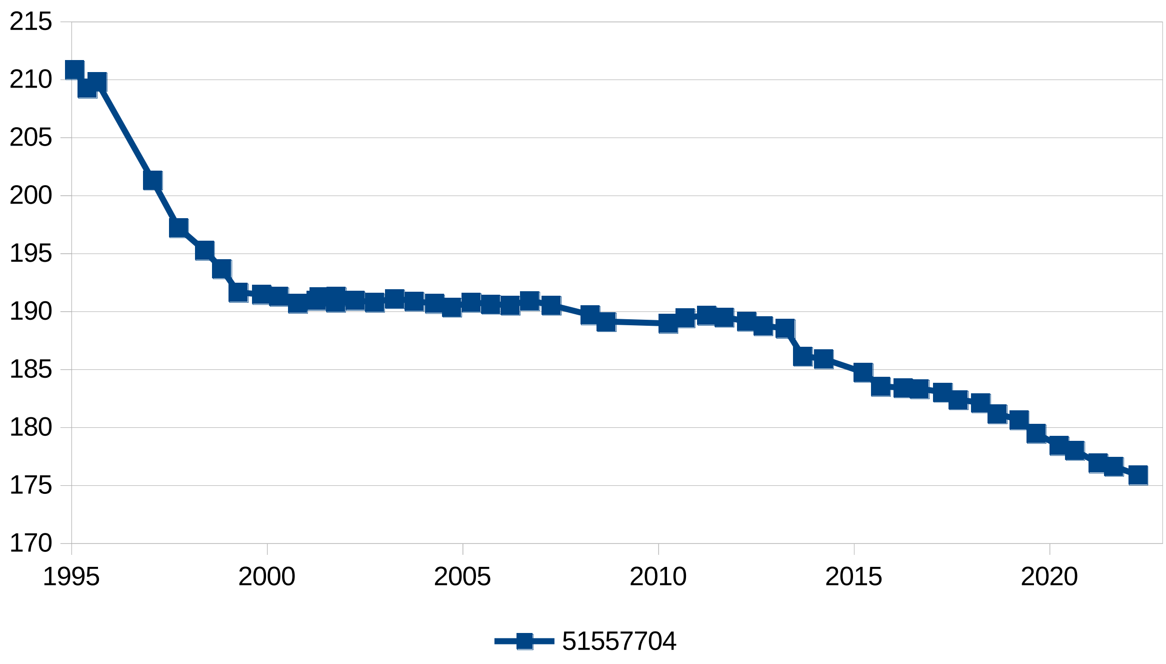

Fig. 188. The water table changes in the monitoring well No. 51557704

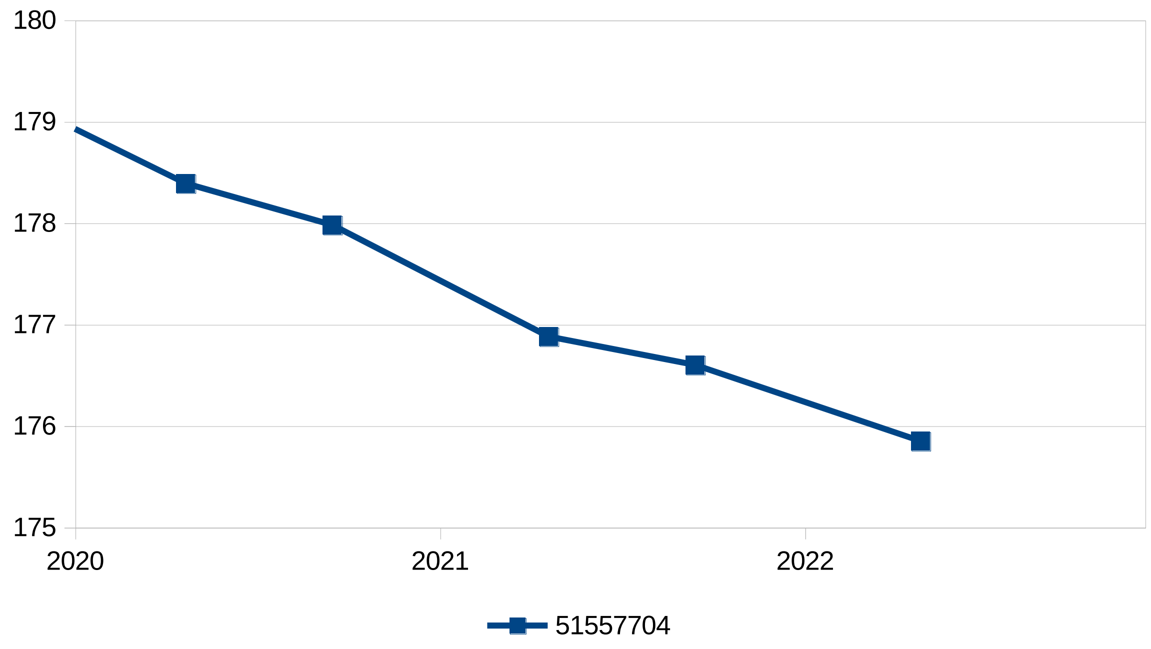

Fig. 189. The water table changes in the monitoring well No. 51557704

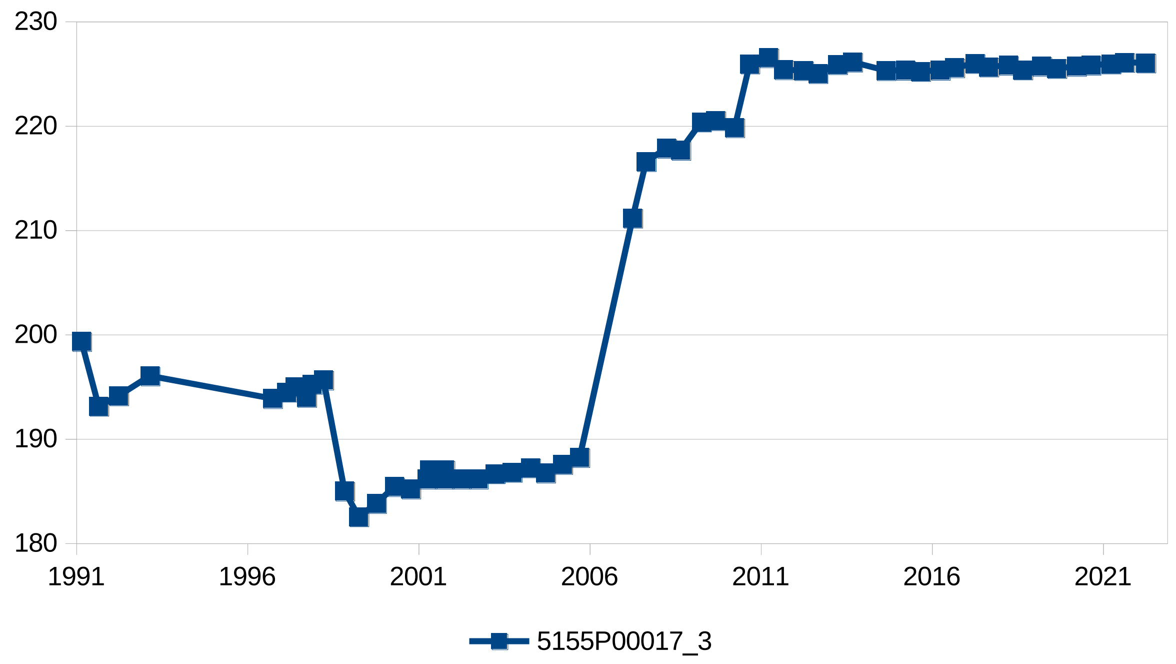

Fig. 190. The water table changes in the monitoring well No. 5155P00017_3

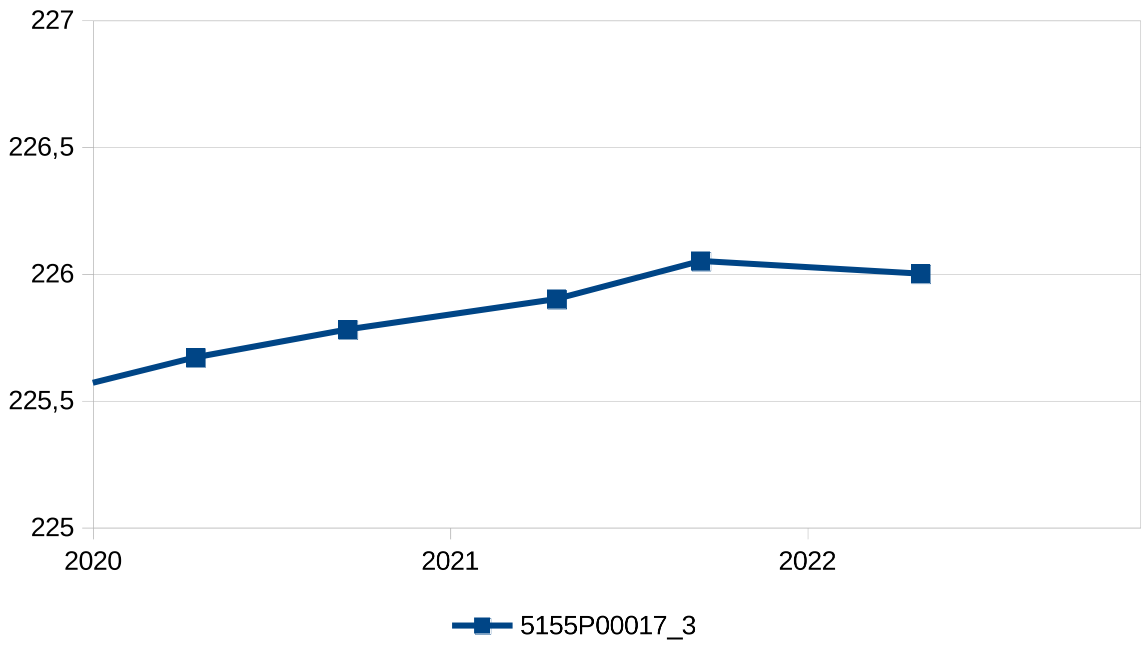

Fig. 191. The water table changes in the monitoring well No. 5155P00017_3

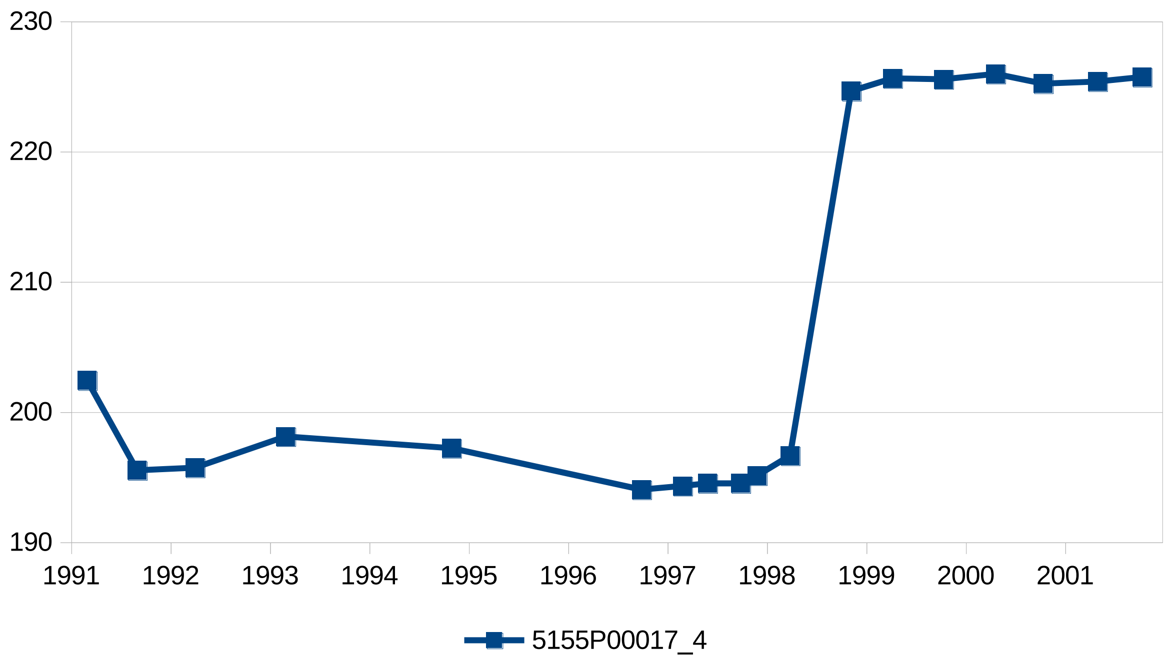

Fig. 192. The water table changes in the monitoring well No. 5155P00017_4

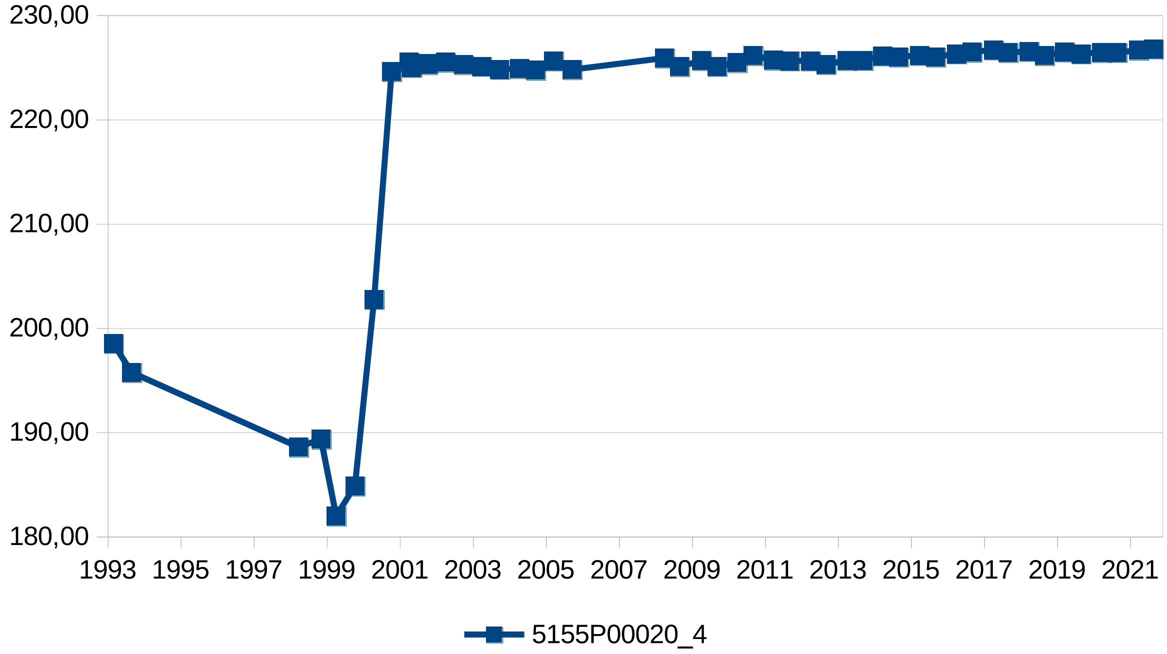

Fig. 193. The water table changes in the monitoring well No. 5155P00020_4

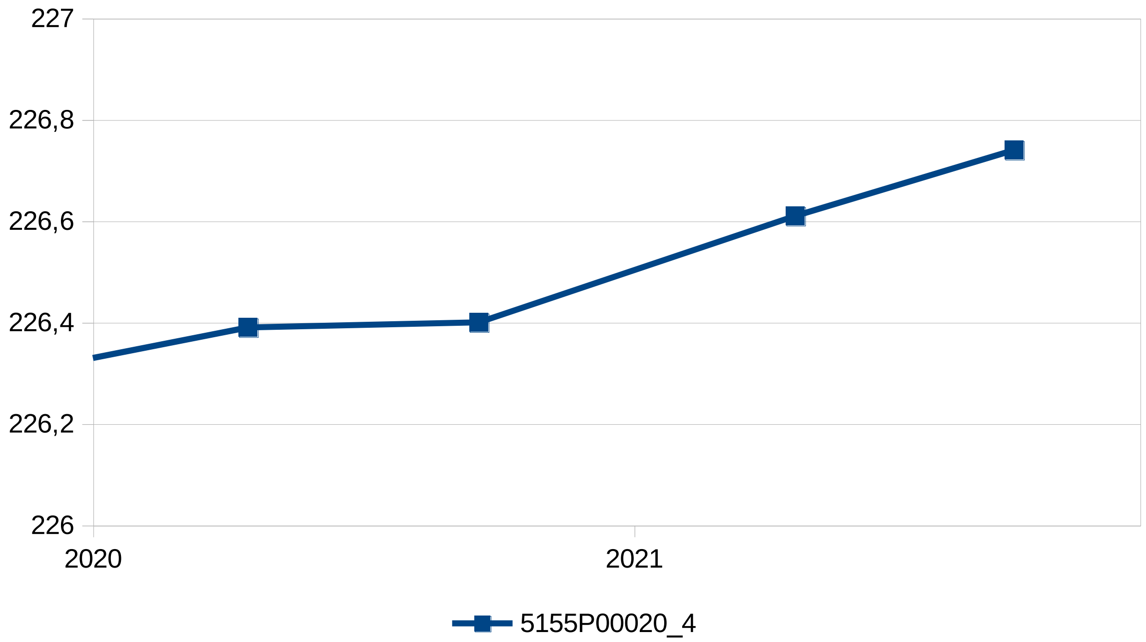

Fig. 194. The water table changes in the monitoring well No. 5155P00020_4

GWL ZU

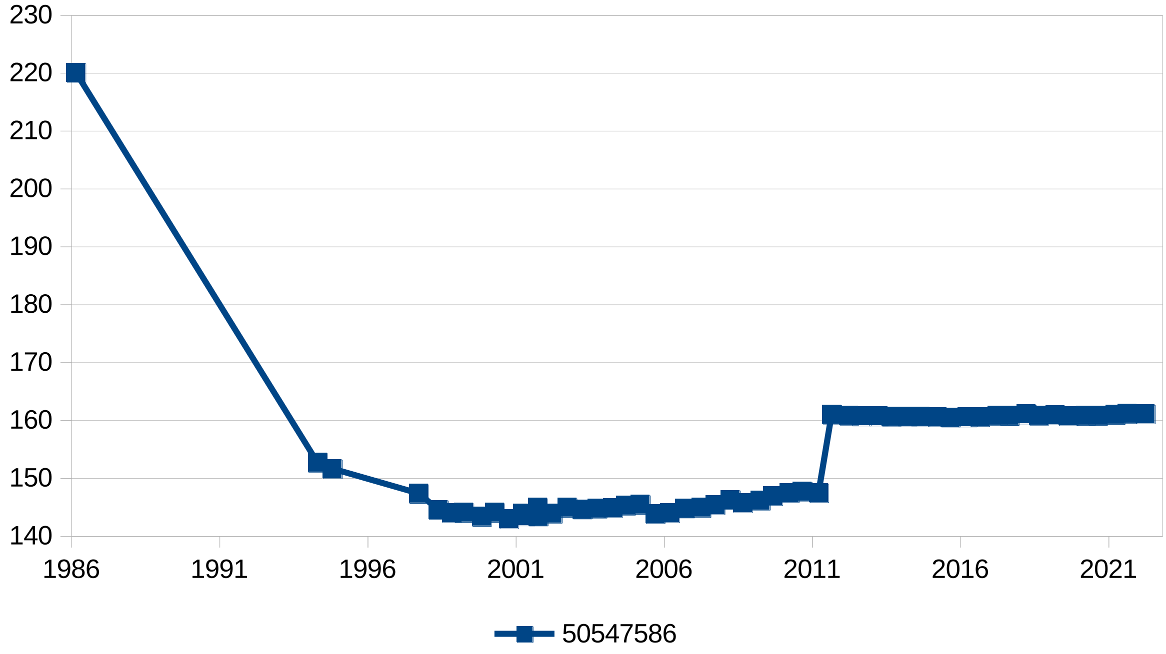

Fig. 195. The water table changes in the monitoring well No. 50547586

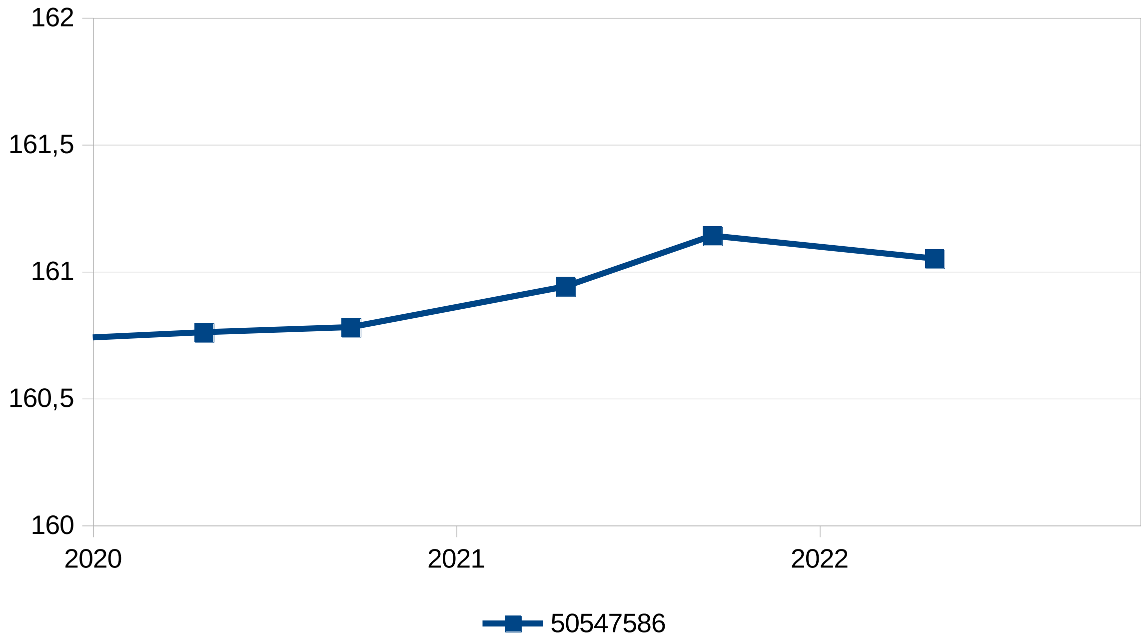

Fig. 196. The water table changes in the monitoring well No. 50547586

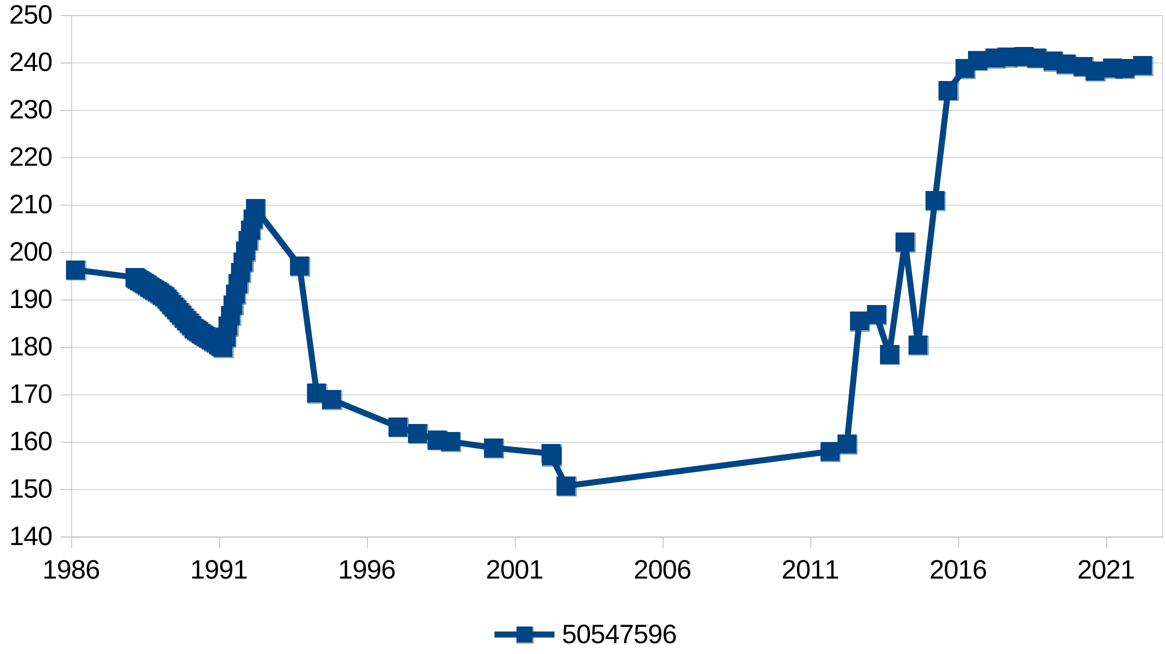

Fig. 197. The water table changes in the monitoring well No. 50547596

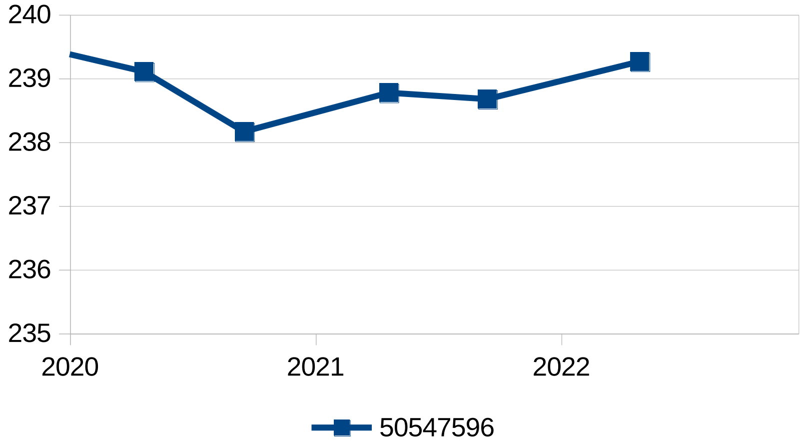

Fig. 198. The water table changes in the monitoring well No. 50547596

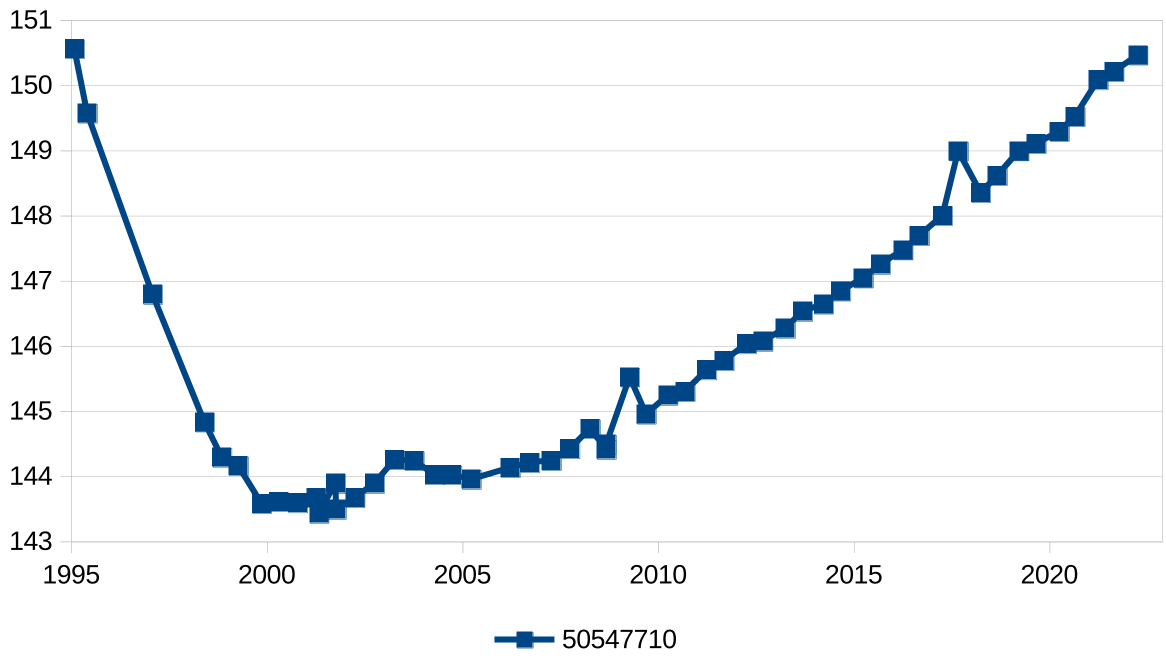

Fig. 199. The water table changes in the monitoring well No. 50547710

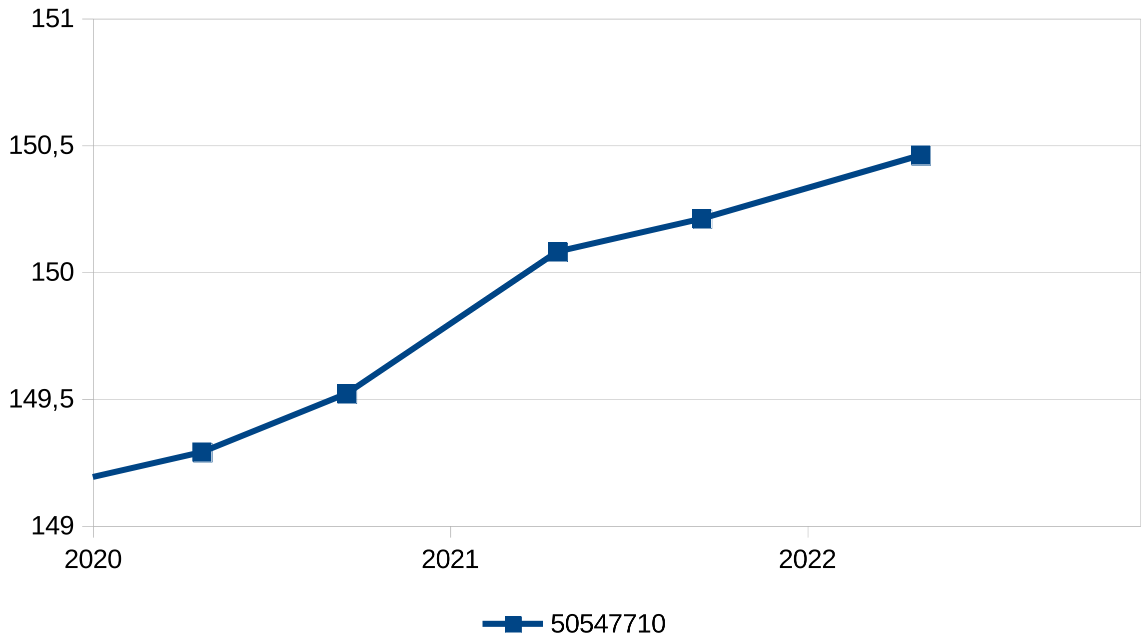

Fig. 200. The water table changes in the monitoring well No. 50547710

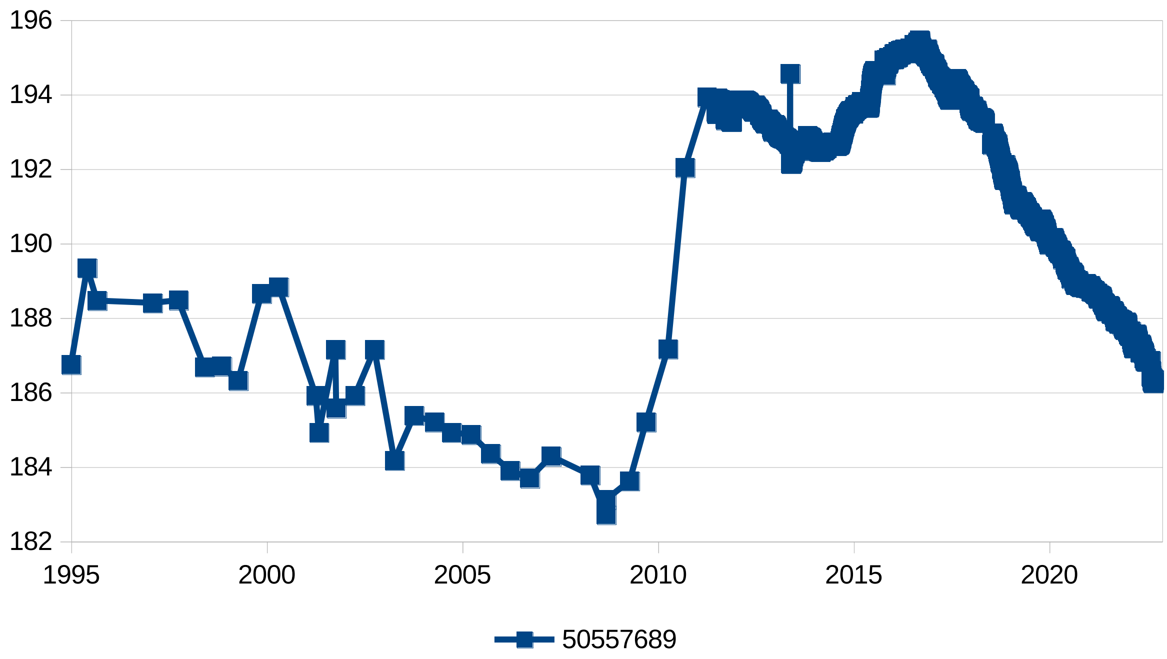

Fig. 201. The water table changes in the monitoring well No. 50557689

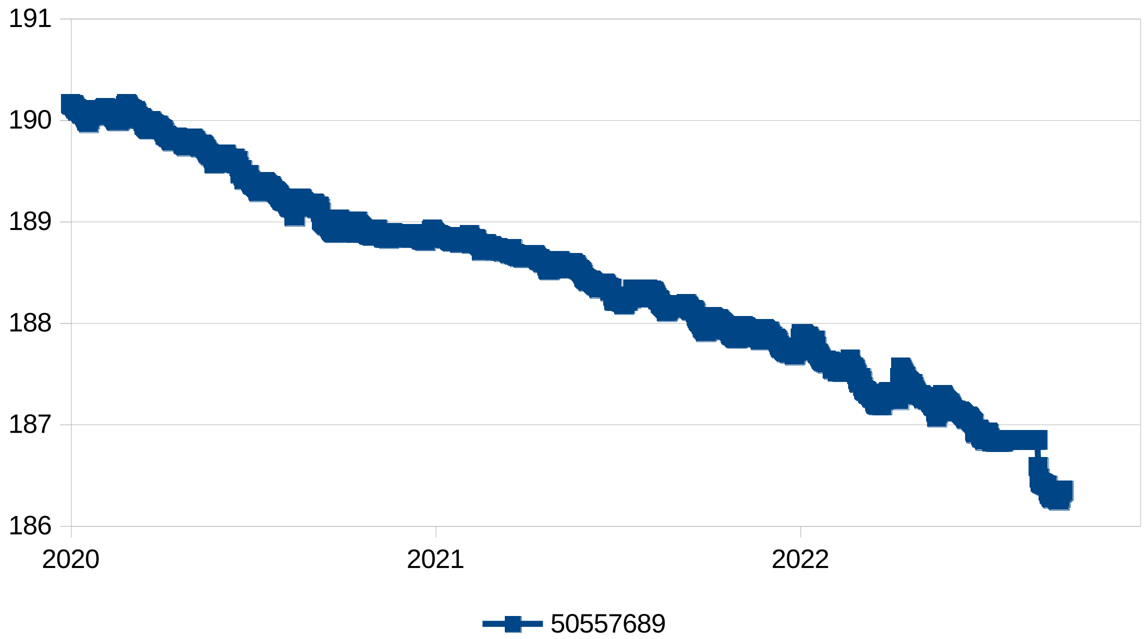

Fig. 202. The water table changes in the monitoring well No. 50557689

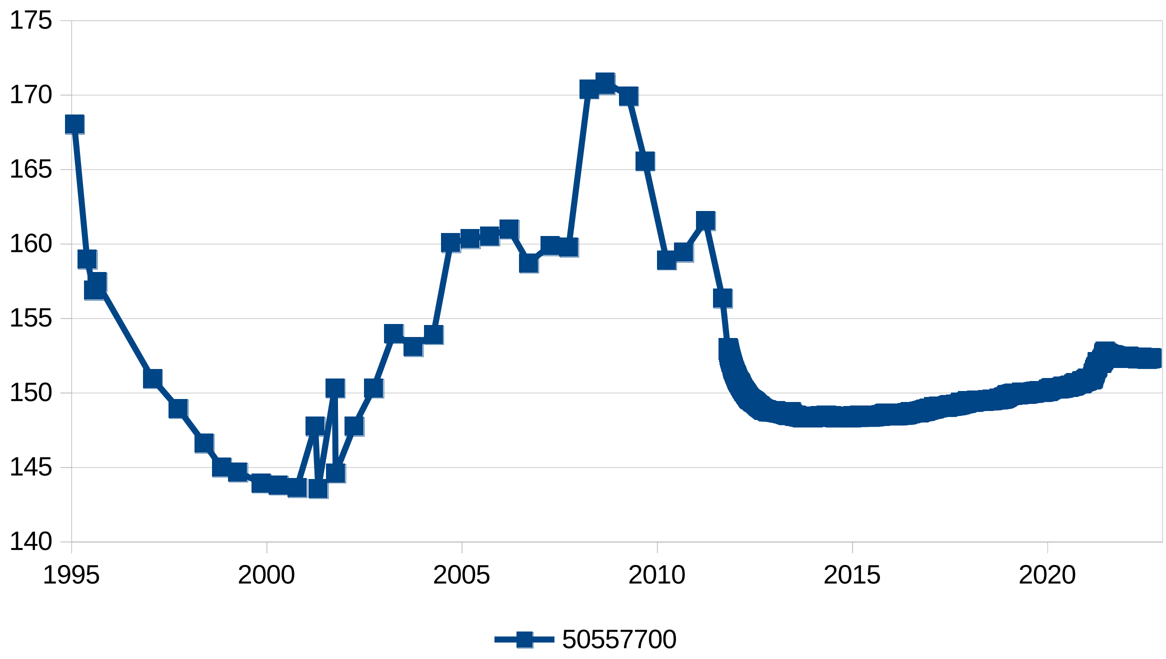

Fig. 203. The water table changes in the monitoring well No. 50557700

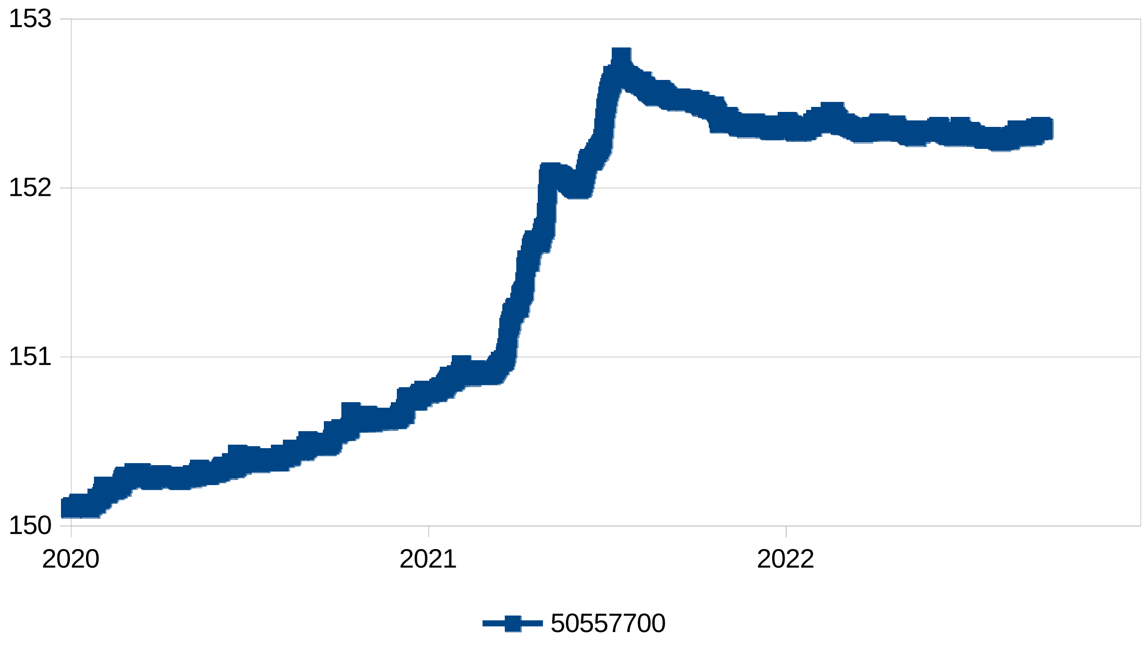

Fig. 204. The water table changes in the monitoring well No. 50557700

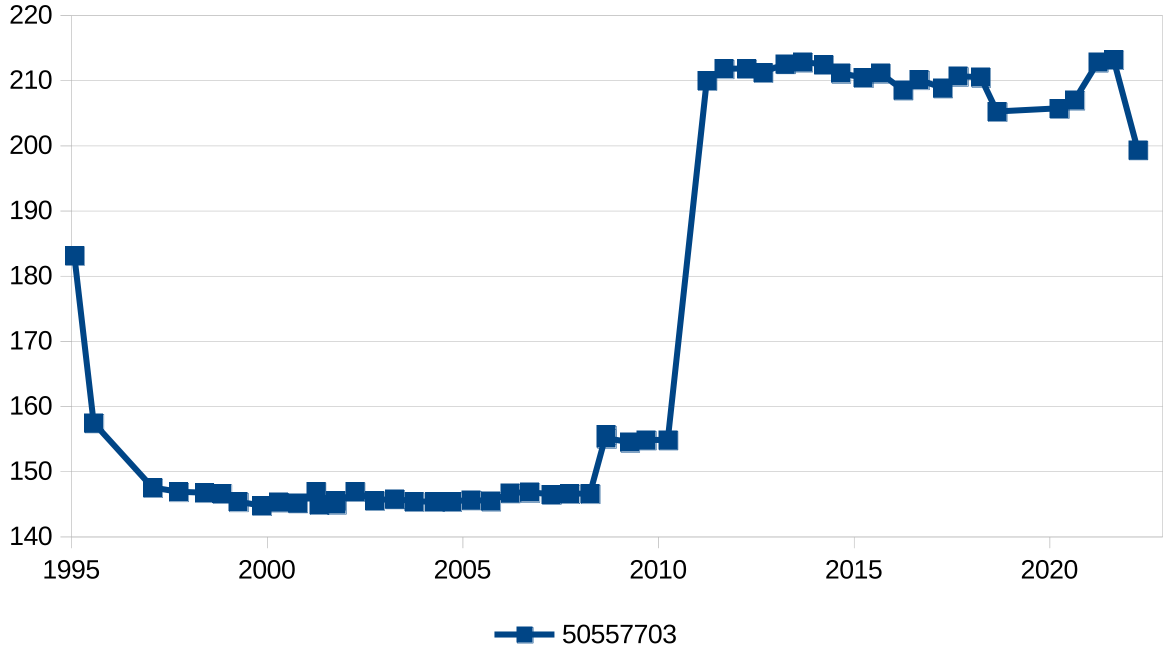

Fig. 205. The water table changes in the monitoring well No. 50557703

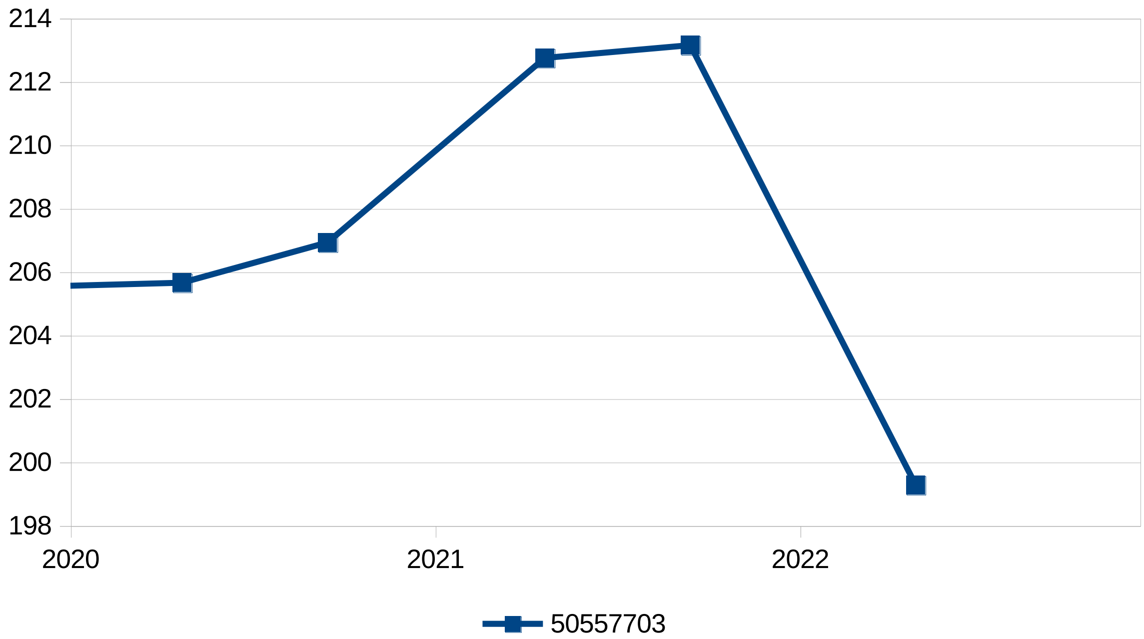

Fig. 206. The water table changes in the monitoring well No. 50557703

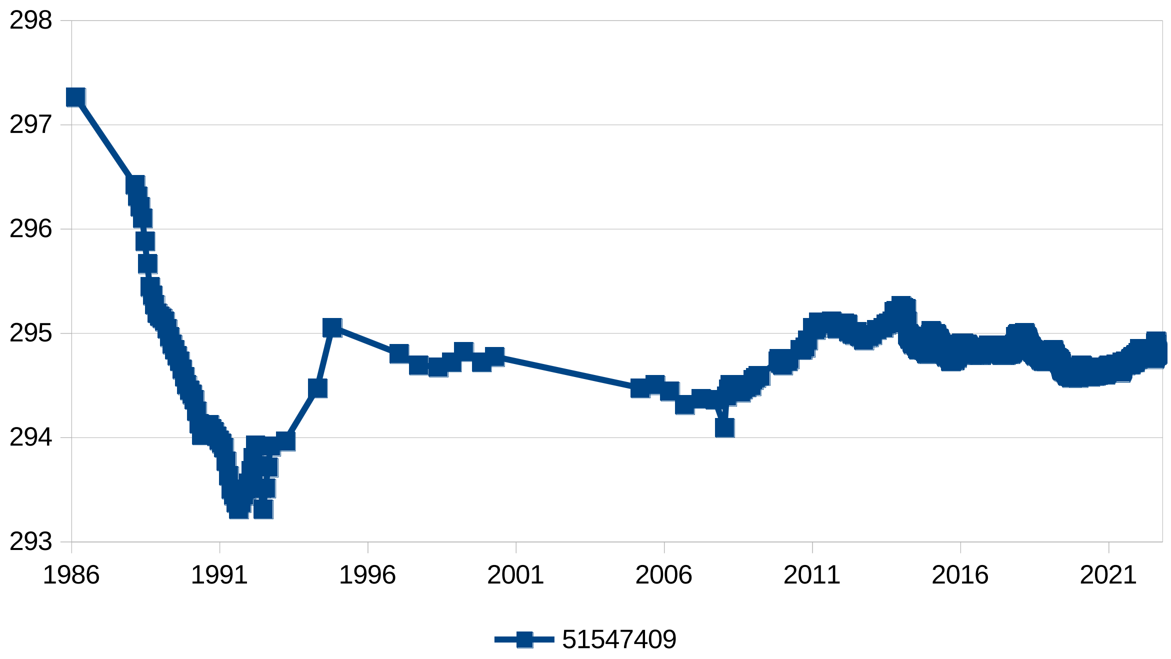

Fig. 207. The water table changes in the monitoring well No. 51547409

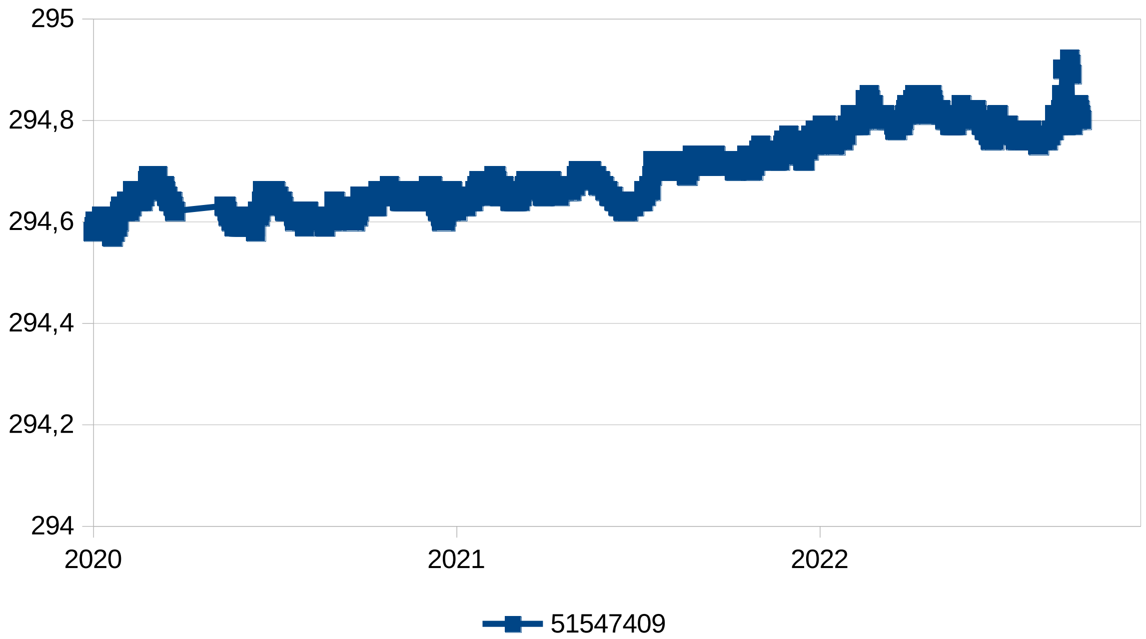

Fig. 208. The water table changes in the monitoring well No. 51547409

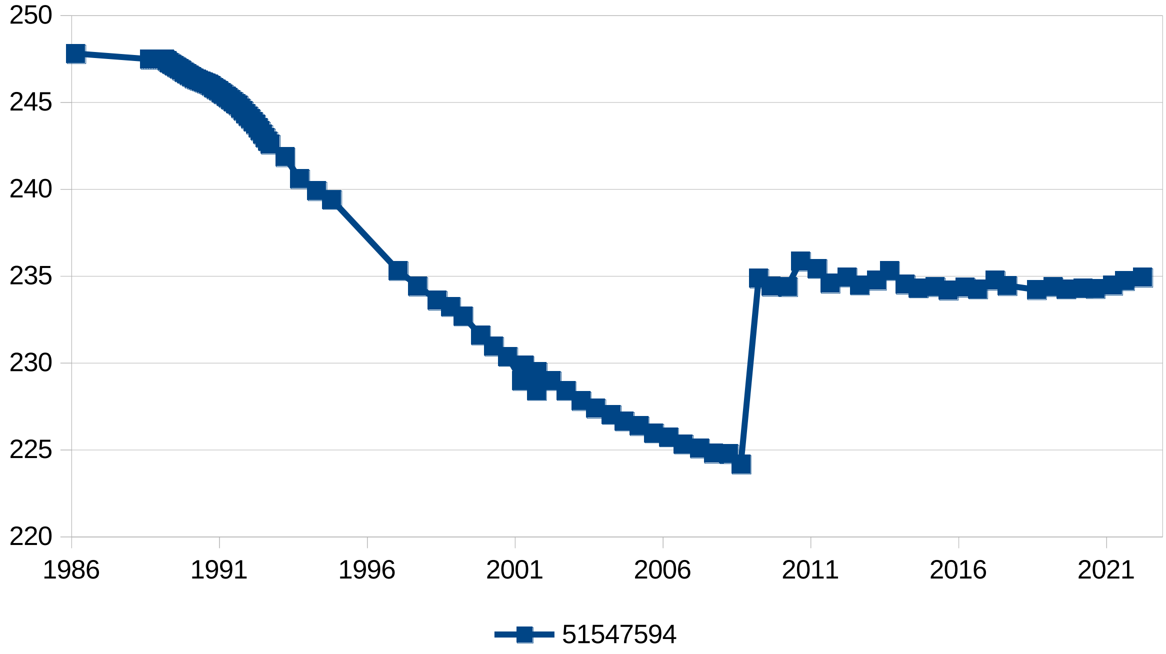

Fig. 209. The water table changes in the monitoring well No. 51547594

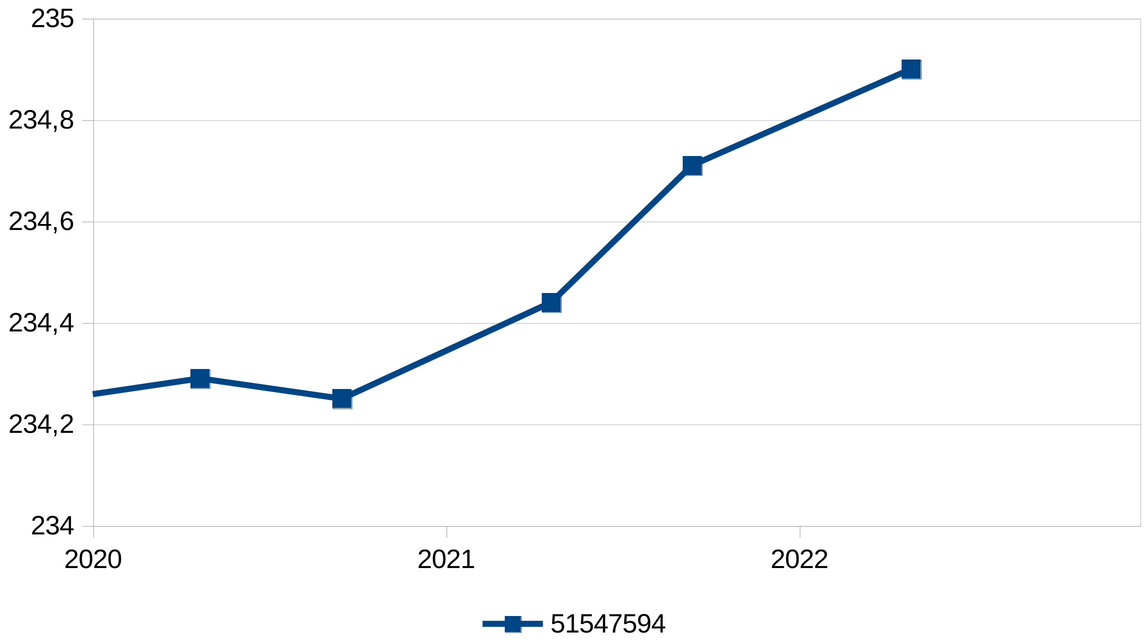

Fig. 210. The water table changes in the monitoring well No. 51547594

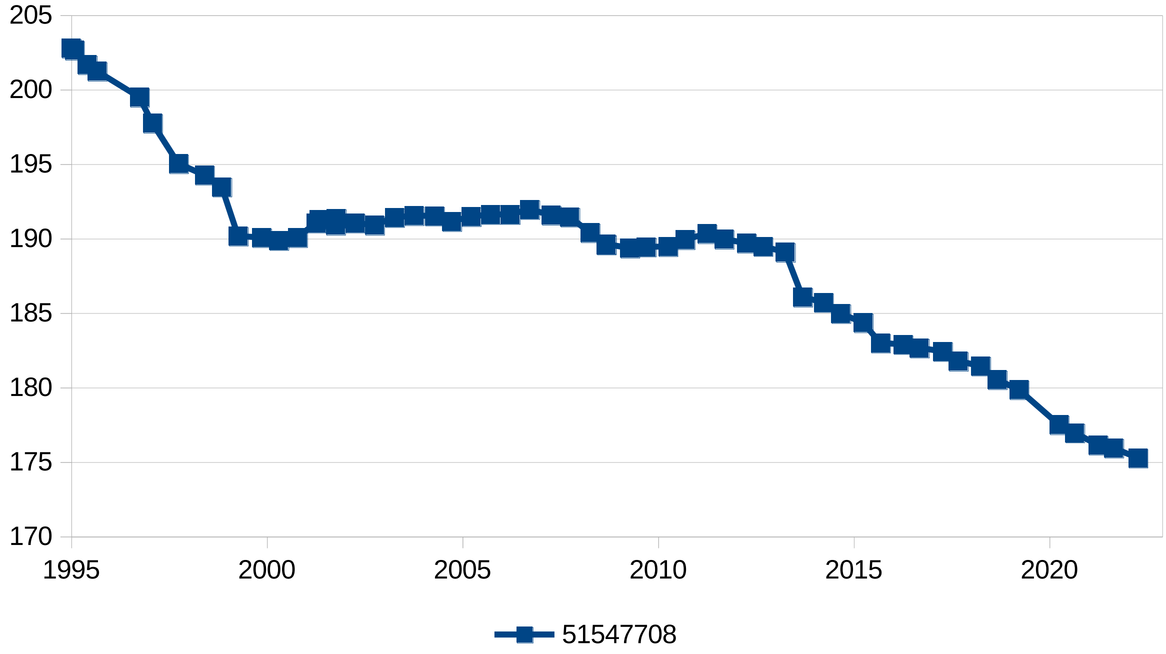

Fig. 211. The water table changes in the monitoring well No. 51547708

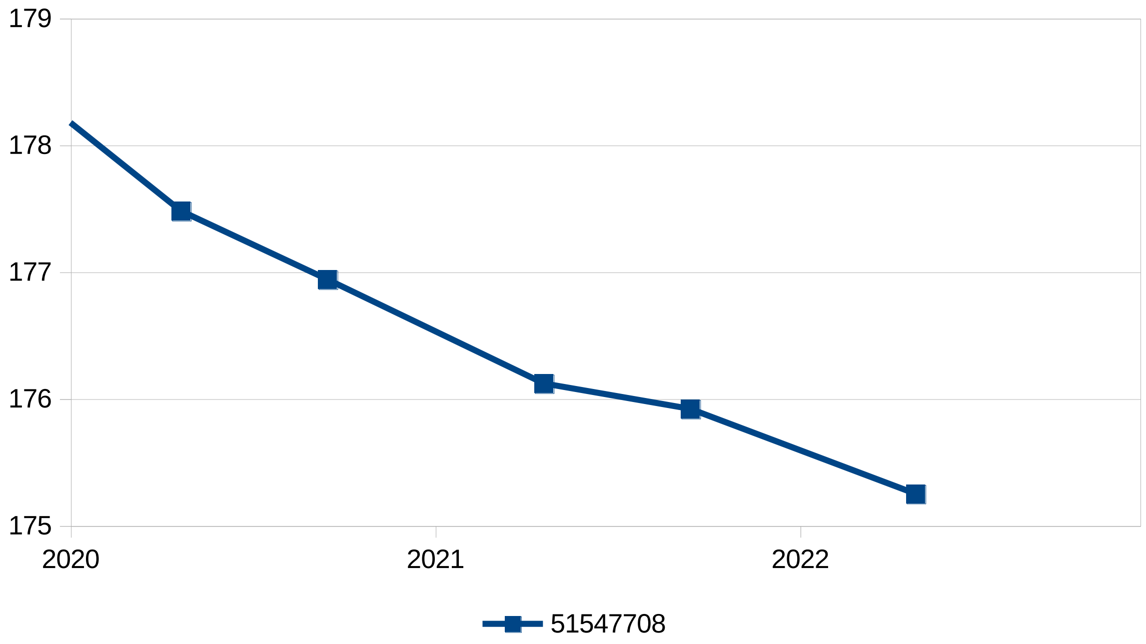

Fig. 212. The water table changes in the monitoring well No. 51547708

Other aquifers

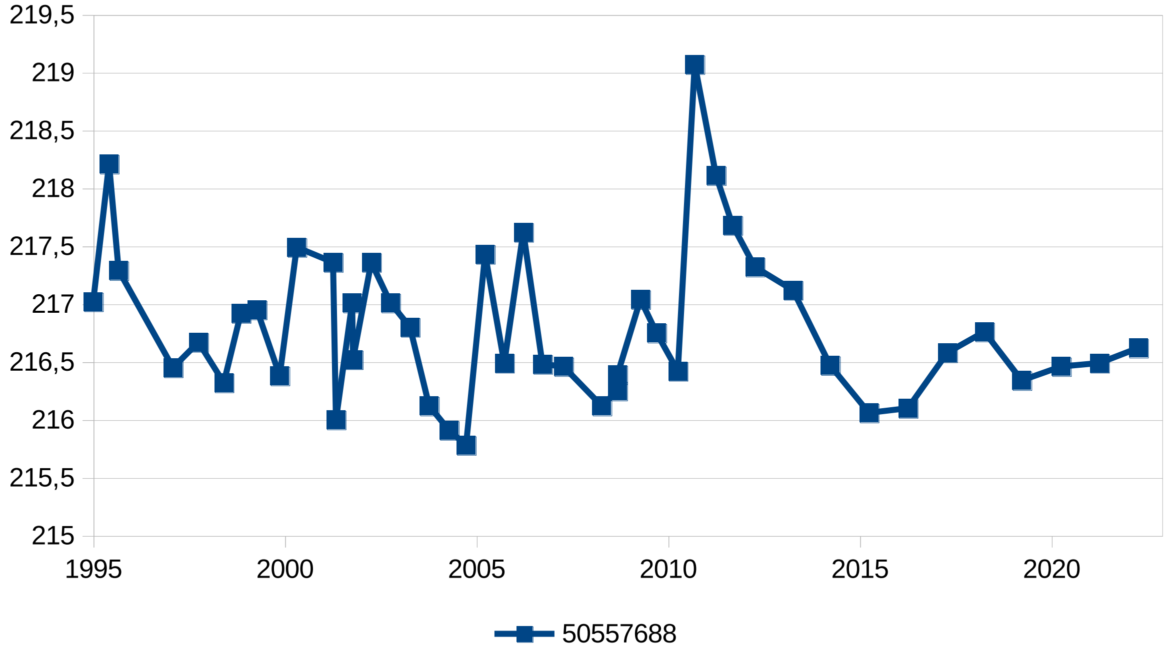

Fig. 213. The water table changes in the monitoring well No. 50557688 (GWL 1e).

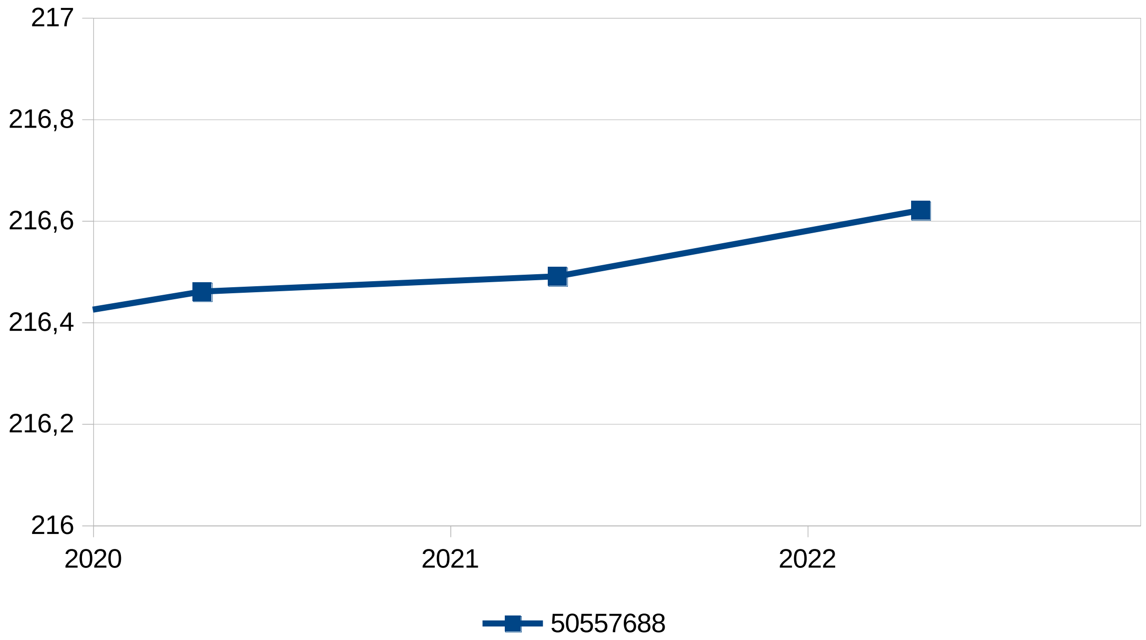

Fig. 214. The water table changes in the monitoring well No. 50557688 (GWL 1e).

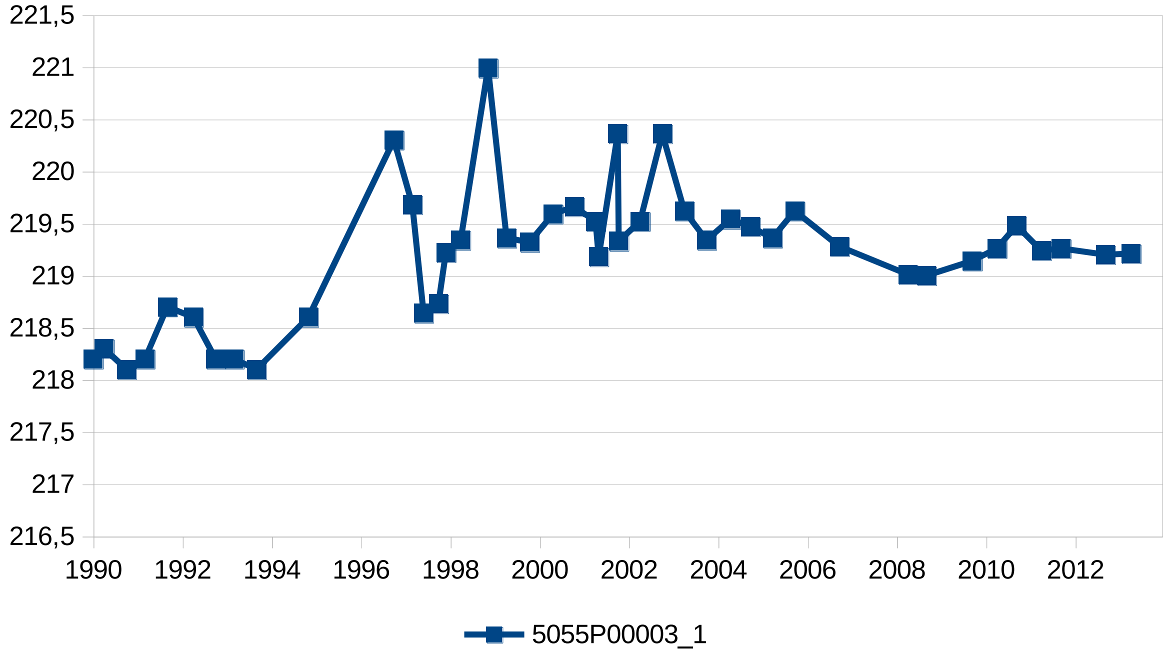

Fig. 215. The water table changes in the monitoring well No. 5055P00003_1 (GWL 1+OO).

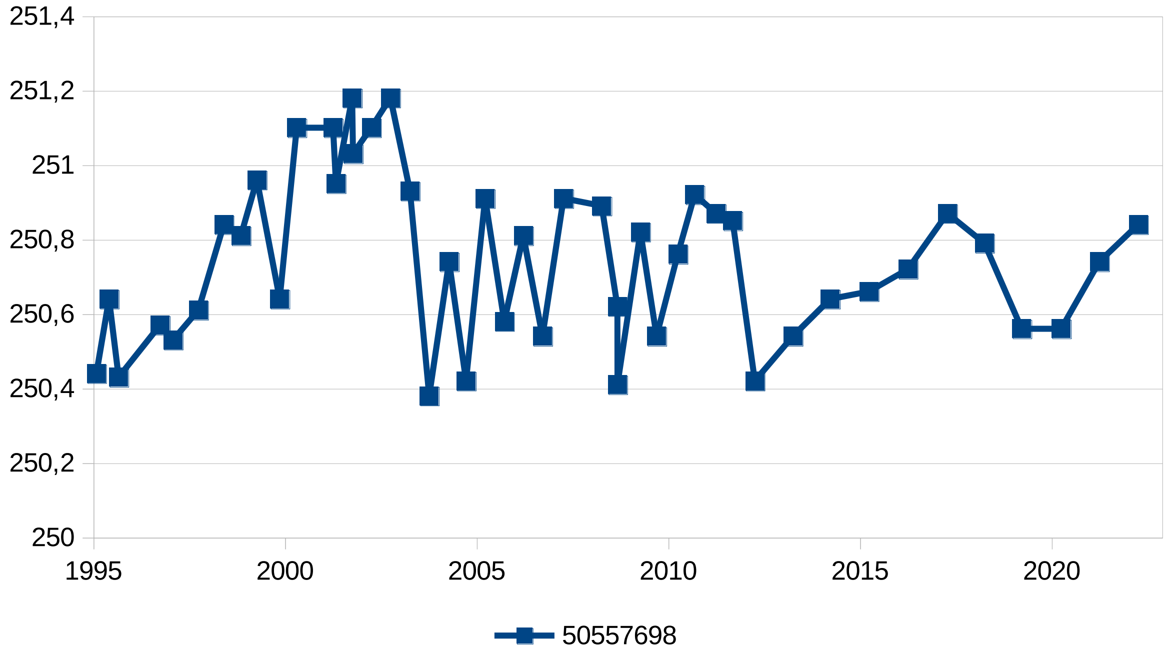

Fig. 216. The water table changes in the monitoring well No. 50557698 (GWL ZiB+VBaZ).

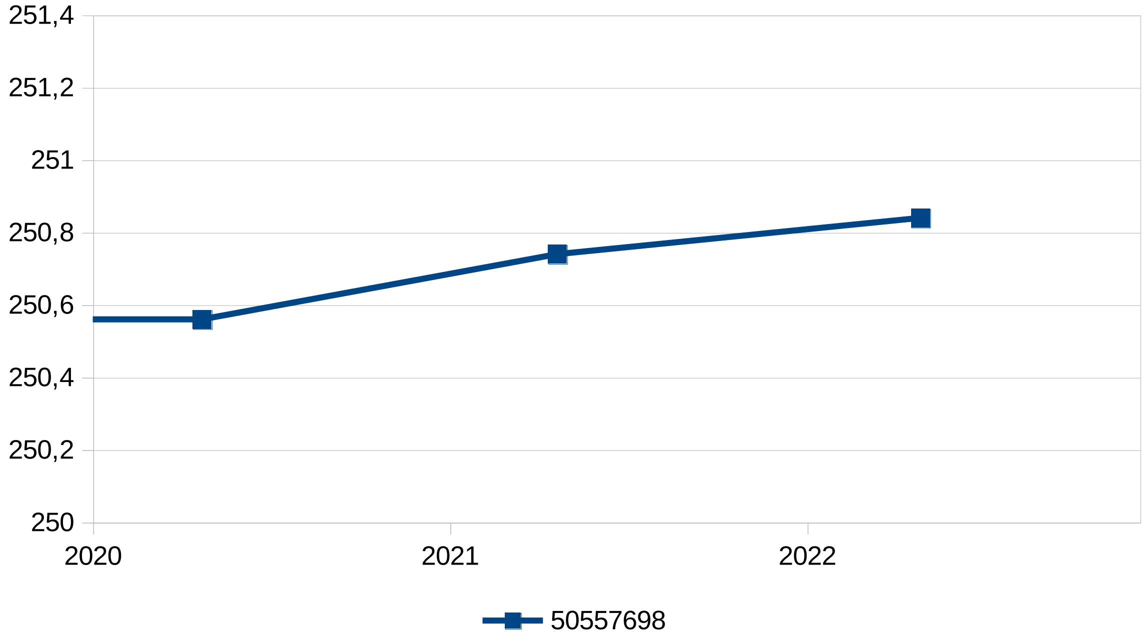

Fig. 217. The water table changes in the monitoring well No. 50557698 (GWL ZiB+VBaZ).

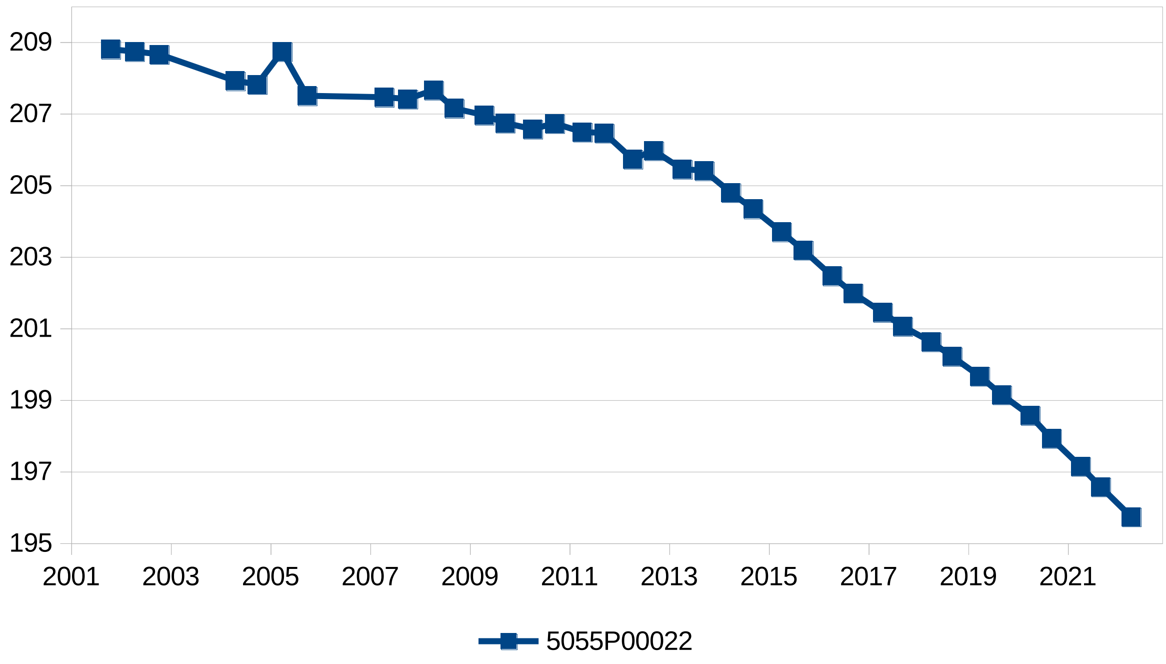

Fig. 218. The water table changes in the monitoring well No. 5055P00022 (GWL VBaZ).

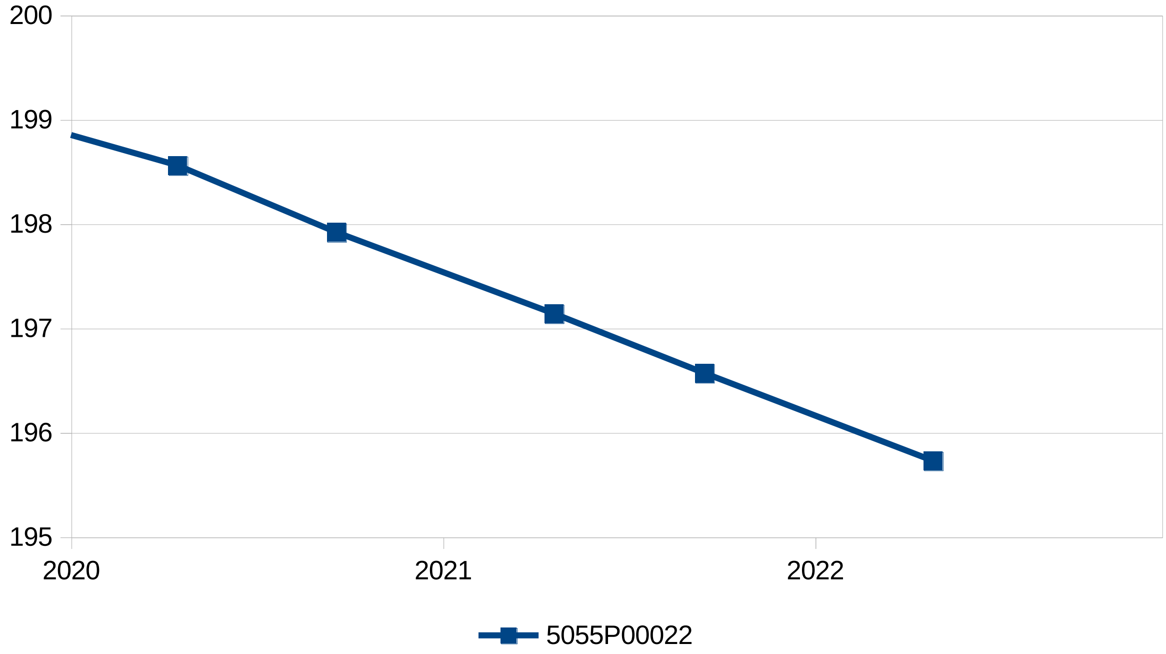

Fig. 219. The water table changes in the monitoring well No. 5055P00022 (GWL VBaZ).

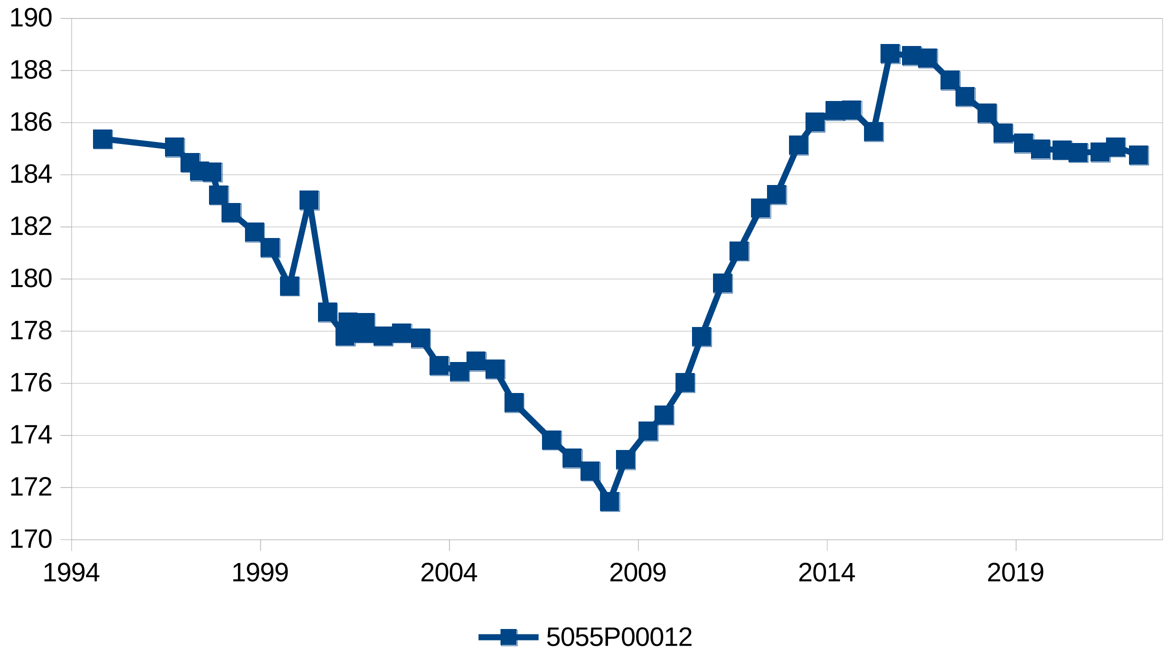

Fig. 220. The water table changes in the monitoring well No. 5055P00012 (GWL ZiA+PGDZ).

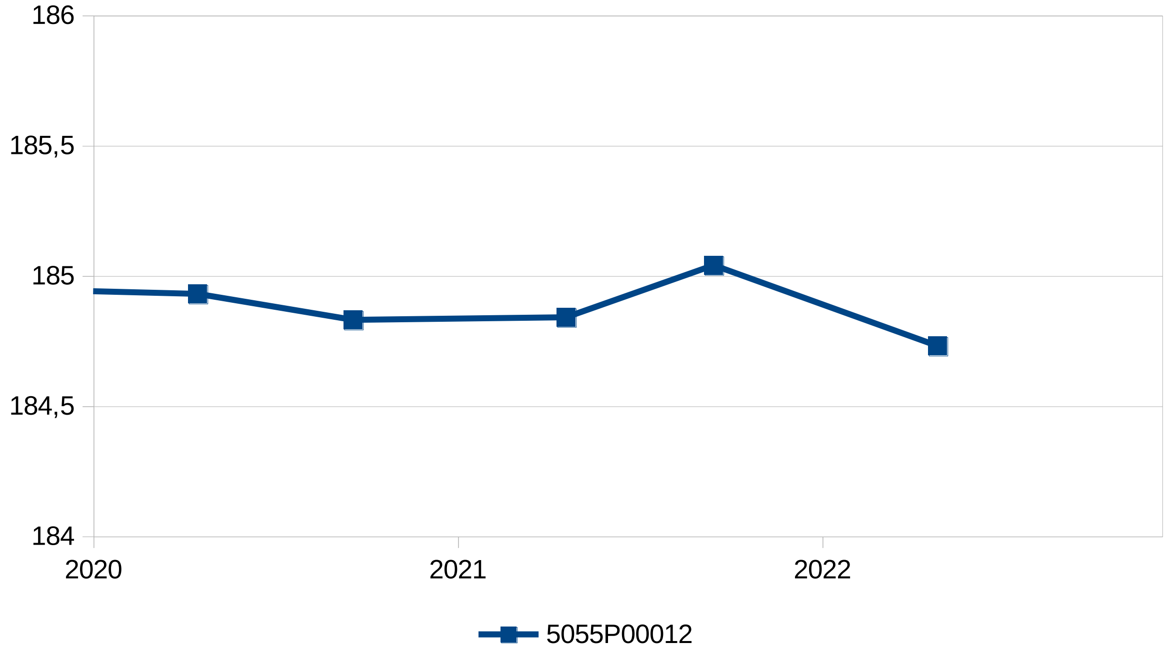

Fig. 221. The water table changes in the monitoring well No. 5055P00012 (GWL ZiA+PGDZ).

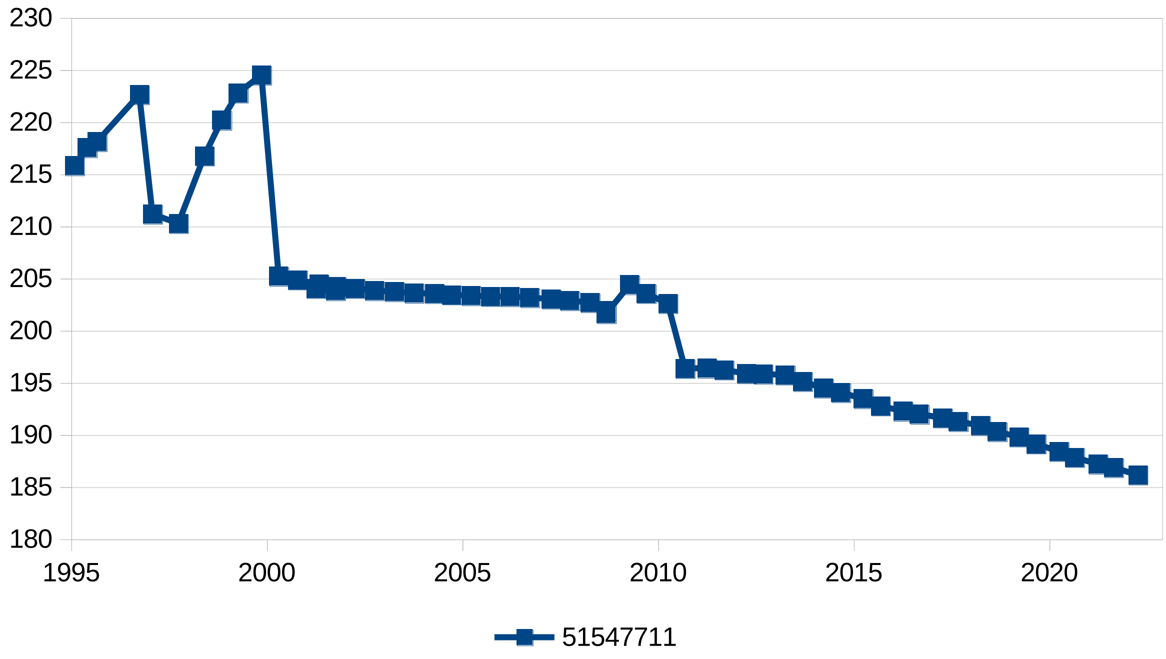

Fig. 222. The water table changes in the monitoring well No. 51547711 (GWL PGDZ).

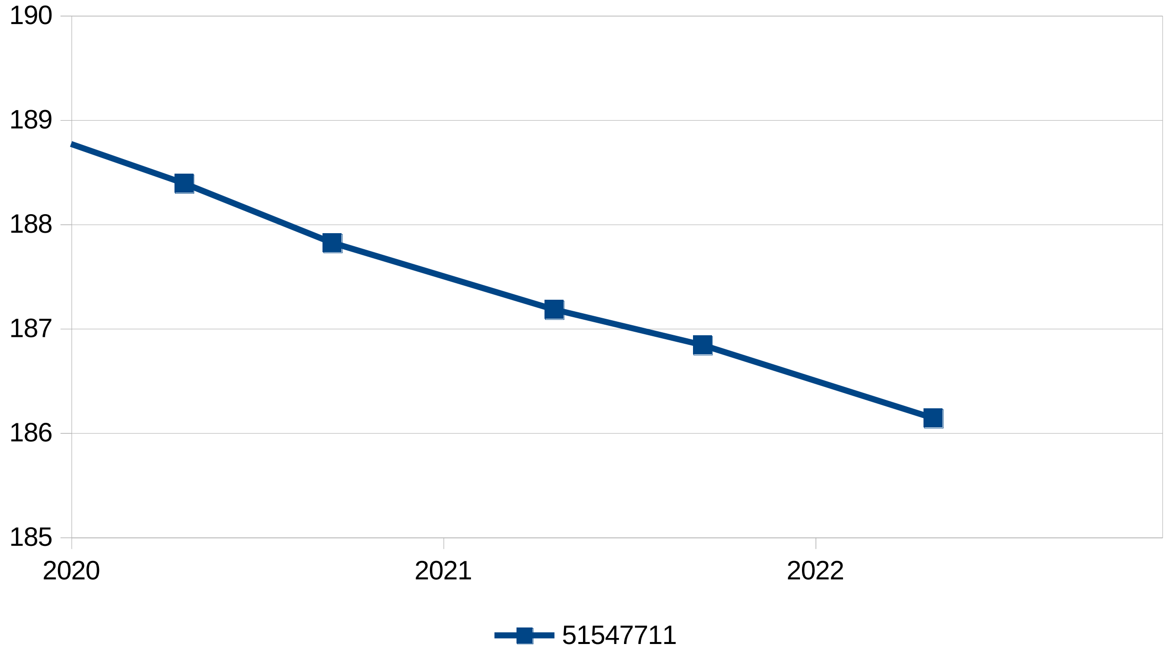

Fig. 223. The water table changes in the monitoring well No. 51547711 (GWL PGDZ).